

**ADVANCED AND
CONTEMPORARY STUDIES
IN NATURAL SCIENCE AND
MATHEMATICS**

Editor

Prof. Dr. N. Gülşah Deniz



**ADVANCED AND CONTEMPORARY STUDIES IN
NATURAL SCIENCE AND MATHEMATICS**

Editor: Prof.Dr. N.Gülşah Deniz

Editor in chief: Berkan Balpetek

Cover and Page Design: Duvar Design

Printing : December -2023

Publisher Certificate No: 49837

ISBN: 978-625-6585-94-2

© Duvar Yayınları

853 Sokak No:13 P.10 Kemeraltı-Konak/İzmir

Tel: 0 232 484 88 68

www.duvar yayinlari.com

duvarkitabevi@gmail.com

TABLE OF CONTENTS

Chapter 1.....5	
Influence of Fungicides on Soil Protease Activity: A Mini-Review	
<i>Burak KOÇAK</i>	
Chapter 2.....18	
Recent Advances Of Fluorescent Detector Molecules For Detection Of Monoamine Oxidase <i>In Vivo</i> And <i>In Vitro</i>	
<i>Emin Ahmet YEŞİL, Mustafa ÖZYÜREK</i>	
Chapter 334	
Semiconductor Material Formation and Properties	
<i>Gizem AYAS, İbrahim BOZ</i>	
Chapter 4.....46	
Jacobsthal 3-Parameter Generalized Quaternions	
<i>Göksal BİLGİCİ</i>	
Chapter 5.....54	
Molecular Scissors Rewriting the Genetic Code: CRISPR-Cas System	
<i>İbrahim DAĞCI, Yağmur ÜNVER</i>	
Chapter 6.....70	
Cytotoxicity effect of cadmium (II) acetate intercalated boron nitride	
<i>Muhammed ÖZ, Büşra MORAN BOZER</i>	
Chapter 7.....82	
A Comparative Study Of The Antimicrobial Activities Of Field-Grown And <i>In Vitro</i> Grown Plants of <i>Verbascum Scamandri</i> Murb.	
<i>Nurşen ÇÖRDÜK, Ebru CAMBAZ, İlke KARAKAŞ, Nurcihan HACIOĞLU DOĞRU</i>	
Chapter 8.....95	
Determination the antimicrobial activities of <i>Verbascum hasbenlii</i> Aytac & H. Duman, an endemic species of Türkiye	
<i>Nurşen ÇÖRDÜK, Ebru CAMBAZ, İlke KARAKAŞ, Nurcihan HACIOĞLU DOĞRU</i>	

Chapter 9.....106

Important Organocatalytic Intramolecular Friedel-Crafts
Alkylation Reactions In The Last Decade

Tülay YILDIZ

Chapter 10.....119

Faunistic and floristic diversity around the marble quarries in the
vicinity of Lake Yarışlı (Burdur, Türkiye)

Ümit KEBAPÇI, Neslihan BALPINAR

Chapter 11.....131

The Role of Supramolecular Design in the Progress of Gas Sensing
Performance with Nano Thin Films by Calix[4]arene Macrocycle: SPR
Detection for the Excellent VOC Molecule Recognition

Erkan HALAY, Yaser AÇIKBAŞ, Rifat ÇAPAN

Chapter 12.....148

A Review Exploring Biological Activities Of N-Sulfonyl Hydrazones
(From 2013 To 2023)

Belma HASDEMİR, Tülay YILDIZ

Chapter 13.....172

Heavy Metal Contamination: Processes, Distribution and
Environmental Impacts

Kadriye URUÇ PARLAK

Chapter 14.....185

Major Members of the Reactive Oxygen Species (ROS):
Formations & Specific Reactions

Mustafa ÖZYÜREK

Chapter 15.....198

Bimultipliers of R-algebroids

Gizem KAHRIMAN

Chapter 1

Influence of Fungicides on Soil Protease Activity: A Mini-Review

Burak KOÇAK¹

1- Doç. Dr.; Çukurova Üniversitesi Fen-Edebiyat Fakültesi Biyoloji Bölümü, Adana, Türkiye. bkocak@cu.edu.tr ORCID No: 0000-0003-4144-6079

INTRODUCTION

Pesticide applications have been one of the main conventional agricultural practices for a very long time and have contributed to increased efficiency in plant production and food yield (Lee, 1985:115). However, most of these chemicals, in addition to their toxic effects on non-target organisms, can also impact organisms benefiting from agricultural ecosystems (Van-Zwieten et al., 2004:6). Pesticides are widely used in agriculture and are defined as bioactive molecules that eliminate various animal, plant, and fungal species (Ozkara et al., 2016:4).

Pesticides are used not only in agricultural fields and private gardens but also by certain industrial companies with the aim of removing weeds and shrubs on roadsides, eradicating invasive species, and controlling the growth of algae in water bodies (Ozkara et al., 2016:4). With regard to safeguarding crop production, it is anticipated that pesticide use will increase due to the rising global population and increased food demand (Roman et al., 2021:1). In 2021, the total pesticide use in agricultural lands reached 3.5 million tons (Mt) of active ingredients, showing an annual increase of 4% since 1990 and a 11% increase every decade up to this point (FAO, 2023:5). Globally, herbicides constitute 40% of pesticide use, followed by insecticides at 17% and fungicides at 10%. In the European Union, the most sold pesticide groups were fungicides and bactericides in 2019 (Roman et al., 2021:1).

Herbicides are chemicals that predominantly control the growth of weeds by killing them. Insecticides are used to control insects on farms, food storage areas, and gardens. Fungicides, on the other hand, are utilized to prevent fungal infections in plants and are often applied to seeds or on plants before or after fungal infection occurs (Mahmood et al., 2016:254).

The number of active ingredients in pesticides used worldwide has exceeded 1000 (Machado & Martins, 2018:277). The emergence of resistant species, the

increase in the world population, and pesticide regulations have caused an increase in the number of new pesticide formulations. More than 98% of sprayed pesticides reach beyond the target organisms and can become pollutants in the water, air and soil (Pérez-Lucas et al., 2019:3). Non-target organisms in areas where pesticides are applied may inadvertently be exposed to these chemicals. Some of the applied pesticides can persist in the soil, while others, through evaporation or through irrigation and rainfall, may leach into underground water sources (Fig 1.) (Doran and Zeiss, 2000:3).

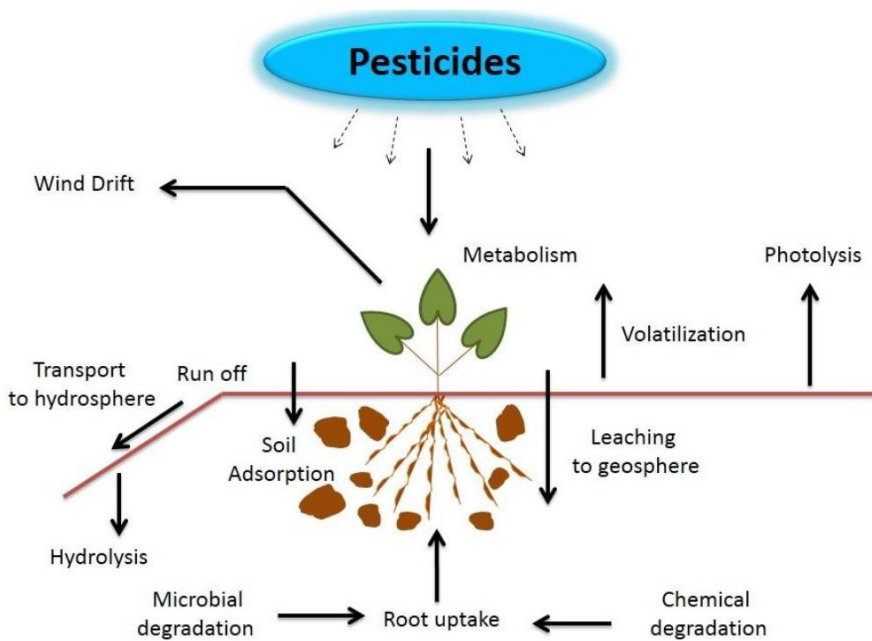


Figure 1: The fate of pesticides in the environment (Ahemad, 2013)

According to pesticide application regulations, it is necessary to determine the effects of pesticides on soil microorganisms and soil productivity. Soil fertility depends not only on the physical and chemical properties of the soil but also on its biological properties. The application of pesticides can alter microbial diversity and activities in the soil (Cenkseven et al. 2019:1140, Koçak and Cenkseven, 2021a:1), and such changes can impact soil fertility and health. Therefore, soil microorganisms play significant roles in soil fertility. Pesticides used for crop protection can directly or indirectly alter the biological activity of the soil, yet information on the roles of soil microorganisms in pesticide degradation and the effects of pesticides on microbial diversity and enzyme activities in the soil remains limited (Lo, 2010:348).

Fungicides are one of the key components in integrated disease management in plant production, notably in open-field agriculture. Despite the various types of fungicides available, the control of significant diseases mainly relies on only a few chemical classes due to their efficacy and residue status (Dowling et al., 2020: 2301; Hawkins and Fraaije, 2018: 339). Pathogenic fungi that settle on commercial products or clandestinely infect plants can easily spread between countries and continents, posing challenges to resistance management (Hu and Chen, 2021:1). Since the 1980s, the emergence rate of fungal populations that show resistance to fungicides has continuously increased globally, posing a serious threat to the sustainability and profitability of agriculture (Fisher et al., 2018:739).

The microorganisms living in the soil produce proteases to regulate the recycling of soil organic matter, thereby generating microbial nutrients (Rahman et al., 2003:199). Proteases have important duties in the interactions between soil organisms by breaking down the proteins of cell wall. These include bacterial-origin anti-fungal proteases and alkaline serine proteases of nematophagous or entomopathogenic bacteria and fungi (Chang et al., 2007:1224; Morton et al., 2003:38; Tian et al., 2007:372). Additionally, serine proteases from different soil bacteria and fungi are important biomolecules in the recycling of keratinaceous residues (Gradisar et al., 2005:3420). Furthermore, proteases have an important role in the survival of microorganisms under unfavorable conditions. For instance, Kim et al. (1999: 1363) identified the proteolytic activities of heat shock proteins in *E. coli*, enabling bacterial survival at high temperatures. There's been a correlation found between the biological control, pathogenicity, and development of microorganisms and serine endopeptidases (Pöll et al., 2009:1366).

Vranova et al. (2013:23) published a review study on proteolytic activity in soils. Roman et al. (2021:1) published a review regarding the effects of triazole fungicides on microbial enzymes and activities in soil. Kenarova and Boteva (2023:1) have published a review on the side effects of fungicides used in agriculture on soil enzyme activities; however, there's no information in this publication regarding the effects on protease activity. Yet, there isn't enough information available about the effects of pesticides on soil protease activity and their responses in different ecosystems. This study assesses interactions between pesticides and soil microorganisms, evaluates fungicides, protease activity, and the impact of fungicides on soil protease activity based on existing literature.

Relationship between pesticides and soil microorganisms

The habitats, activities, and interactions of microorganisms are interconnected, and even over small distances, these microorganisms can exhibit variations. The most important microorganisms living in soil are algae, bacteria, fungi, nematodes and protozoa. Their metabolisms are closely linked to the element cycles and energy flow within ecosystems (Boga et al., 2017:1056, Cenkseven et al., 2017a:378, Cenkseven et al., 2017b:766). Due to their rapid response to natural and anthropogenic changes in soil, the enzymatic activities of soil microorganisms (Koçak, 2020:51) and the quantities of hormones that they produce are considered significant indicators of soil quality and health. Determining the distribution of microorganisms in the soil also plays a vital role in identifying optimal conditions for plant growth and productivity (Hu et al., 2014:110).

An important aspect of pesticide risk assessment involves investigating the effects of pesticides on soil microflora and their beneficial activities. Predicting the relationship between the chemical structure of a pesticide and its effects on various groups of soil microorganisms is quite challenging. When applied at normal doses, some pesticides stimulate the growth of microorganisms, while others either have negative effects on microorganisms or no impact at all (Koçak and Cenkseven 2021b:540, Lo, 2010:348).

In addition to their effects on microorganisms, the accumulation of pesticides has significant impacts on soil enzymes, which act as fundamental catalysts influencing the living habitats of soil microorganisms (Lozowicka et al., 2016:1310). The sources and origins of existing enzymes in the soil can be diverse, including dead prokaryotic or eukaryotic cells. Furthermore, fungi and plant roots can release these enzymes into the soil (Datta et al., 2017:288). Evaluating the enzymatic and microbiological responses of pesticide applications is challenging due to the structural diversity of pesticides and variations in degradation pathways (Gianfreda and Rao, 2008). It's crucial to remember that pesticides applied to the soil may consist of different chemical compounds, making it difficult to determine their effects on the biological activities of the soil (Wolejko et al., 2020:1).

Fungicides

Fungicides are chemical substances or living organisms that inhibit or destroy the growth of fungi or fungal spores (Gullino et al., 2000:1). Their use in agricultural systems has become an effective tool in controlling plant diseases in recent years, as fungal infections globally have reduced plant production by up to 20% (Gullino et al., 2000:2). Due to their low cost, ease of use, and

effectiveness, fungicides have become vital in controlling fungal diseases (Xia et al., 2006:42). However, the widespread use of these compounds to control fungal diseases in plants has led to the emergence of new pathogen strains that can resist existing commercial fungicides (García et al., 2003:162).

The first region-specific fungicides are methyl benzimidazole carbamates (MBC), which have been used for 50 years and have reportedly encountered resistance in approximately 100 plant pathogen species (FRAC, 2020; Hawkins & Fraaije, 2016:2). In some pathogens, resistance has been reported to emerge after two years of fungicide use (Grimmer et al., 2015:207). Azole resistance has been reported in 30 plant pathogens across 60 countries (Fisher et al., 2018:739; FRAC, 2020). The development of resistance has been indicated in all major fungicide classes that affect a single region (Corkley et al., 2022:150).

Due to the development of resistance leading to the loss of effectiveness of fungicides, public concerns regarding the potential environmental and human health impacts of agrochemicals have led to significant interest in developing non-chemical control methods and employing integrated pest management strategies (Birch et al., 2011: 3251; Pertot et al., 2017:70). However, chemical control is anticipated to remain necessary in the production of many crops, and thus, implementing fungicide resistance management strategies is vital to prolong the effective lifespans of current products (Popp, 2011:105).

Soil Protease Activity

Proteases can be classified based on numerous factors, including the type of reaction they catalyze, the functional group of the active site, the molecular structure of proteases, and their evolutionary relationships (Landi et al., 2011:247; Rotanova et al., 2004: 4865). Proteases like exopeptidases hydrolyze the terminal amino acids of a polypeptide chain, while endopeptidases are responsible for hydrolyzing internal peptide bonds. Exopeptidases function at both the C- and N-terminals of peptide chains (Vranova et al., 2013:24). Endopeptidases, on the other hand, are recognized by the chemical structure of catalytic active groups and are divided into four main groups (Table 1): serine, cysteine, aspartic, and metalloendopeptidases (Kalisz, 1988:2; Page and Di Cera, 2008: 1220).

Table 1: Classification of proteases based on the enzyme classification nomenclature (Vranova et al., 2013)

Sub-subclass	Proteases
3.4.11	Aminopeptidases
3.4.13	Dipeptidases
3.4.14	Dipeptidyl-peptidases
3.4.15	Peptidyl-dipeptidases
3.4.16	Serine-type carboxypeptidases
3.4.17	Metallopeptidases
3.4.18	Cysteine-type carboxypeptidases
3.4.19	Omega peptidases
3.4.21	Serine endopeptidases
3.4.22	Cysteine endopeptidases
3.4.23	Aspartic endopeptidases
3.4.24	Metalloendopeptidases
3.4.99	Endopeptidases of unknown type

In soil, proteases originate from various sources including plants, microorganisms, animal feces, decomposition, and both dry and wet deposition. The significance of these sources can vary depending on the ecosystem type and management practices (Vranova et al., 2013:23). Proteolysis is an important process in the nitrogen cycle within many ecosystems. Due to the primary stage of protein mineralization being much slower than amino acid mineralization, proteolysis in soils is considered a limiting step during nitrogen mineralization (Weintraub & Schimel, 2005:1470).

Impacts of Fungicides on Protease activity in the Soil Environment

Roman et al. (2023:199) incubated myclobutanil, a triazole fungicide, at the recommended dose, half that dose, and twice that dose in laboratory conditions ($22^{\circ}\text{C} \pm 2^{\circ}\text{C}$, soil moisture: $19\% \pm 3\%$, for 28 days) after mixing it into the soil. Throughout the entire incubation period, the researchers reported that there was no statistically significant difference between the control group and the three doses of myclobutanil.

Chauhan et al. (2023:1) investigated the effects of different fertilizers, cultivation practices, and plant applications (fallow, farm manure, rice straw with corn and clover) on soil protease activity 30 days after mixing Carbendazim, a systemic fungicide, at a rate 10 times the recommended dose into the soil under field conditions. They reported a significant increase in

protease activity with the corn+carbendazim treatment and observed increased activity across all treatments involving carbendazim.

Jeziarska-Tys et al. (2021:1) reported that the fungicide Caramba 60 SL (applied at 1 dm³ ha⁻¹) reduced soil protease activity in a field planted with rapeseed.

Wang et al. (2018: 2775) mixed different doses of azoxystrobin (Azo) (0, 0.1, 1, 10 mg/kg) with a Cambisol soil, humidified the mixtures to 60% water-holding capacity, and incubated it at 25±2°C for 28 days. They measured the protease activity in the soil on the 7th, 14th, 21st, and 28th days of incubation. The study concluded that Azo did not significantly alter this activity compared to the control across these time points.

Zhang et al. (2017:11340) investigated the effects of 3,4-dimethylpyrazole phosphate (DMPP), a nitrification inhibitor, and iprodione, a fungicide, on neutral protease (NPR) and its functional gene (*nprA*) in the soil. The study found that when applied alone, iprodione reduced NPR activity. It also noted that DMPP mitigated iprodione's inhibitory effect on this enzyme and that both alone and in combination with DMPP, iprodione reduced the abundance of the *nprA* gene.

Guo et al. (2015:1353) measured the protease activity on days 7, 14, 21, and 28 after mixing different doses of azoxystrobin (0, 0.1, 1.0, and 10.0 mg kg⁻¹) in a black soil. They reported that at lower concentrations, Azo had minimal effect on this activity, but as the concentration increased and over time, its impact became more pronounced. They mentioned that the application of 0.1 mg kg⁻¹, when compared to the control, showed no significant effects throughout the entire duration of the experiment. However, they found that applications of 1.0 and 10 mg kg⁻¹ significantly inhibited soil protease activity on days 14, 21, and 28 ($p < 0.05$).

Filimon et al. (2015: 1127) investigated the effects of difenoconazole (DFC) on soil protease activity through three different experiments: 1) under field conditions at different temperatures (10-21°C, variants A1–A3), 2) under constant temperature in laboratory conditions (30°C, variants B1-B3), and soil without any application (variant C). The doses of difenoconazole used in the experiments were 0.037 mg DFC g⁻¹ soil (A1 and B1), 0.075 mg DFC g⁻¹ soil (A2 and B2), and 0.150 mg DFC g⁻¹ soil (A3 and B3). As a result, they found that protease activity decreased in variants A1-A3 compared to variant C, and in variant B3 with the dose of 0.150 mg DFC g⁻¹ soil, the protease activity increased.

CONCLUSIONS

Overall, in this study, it can be concluded that fungicides have both positive, negative, and neutral effects on soil microorganisms' protease activities. However, information regarding proteolysis in soil remains limited. Future studies aimed at identifying new proteolytic genes in soil and investigating how fungicides affect microbial diversity may aid in understanding the effects of these chemicals on protease activity. Although it's known that plant-derived proteases contribute to the total soil protease activity, information on this topic is relatively scarce. It's crucial to consider two significant factors, vegetation, and environmental factors, in understanding the relationship between soil protease activity and fungicides.

REFERENCES

- Ahemad, M. (2013). Pesticides as antagonists of rhizobia and the legume-rhizobium symbiosis: a paradigmatic and mechanistic outlook. *Biochemistry & Molecular Biology*, 1(4), 65-75.
- Birch, A. N. E., Begg, G. S., Squire, G. R. (2011). How agro-ecological research helps to address food security issues under new IPM and pesticide reduction policies for global crop production systems. *Journal of Experimental Botany*, 62(10), 3251-3261.
- Boga, T., Aka Sagliker, H., Cenkseven, S. (2017). The first effect of *Eucalyptus camaldulensis* leaves and eucalyptol additions on soil carbon mineralization. *Fresenius Environmental Bulletin*, 26, 1052-1060.
- Cenkseven, S., Kocak, B., Kuzu, S. B., Korkmaz-Guvenmez, H., Darici, C. (2017a). Response of microbial activity to addition of *Nerium oleander* L. leaves in soil under different moisture conditions. *Fresenius Environmental Bulletin*, 26(12a), 377-385.
- Cenkseven, S., Kizildag, N., Kocak, B., Sagliker, H. A., Darici, C. (2017b). Soil organic matter mineralization under different temperatures and moisture conditions in Kızıldag Plateau, Turkey. *Sains Malaysiana*, 46(5), 763-771.
- Cenkseven, S., Koçak, B., Kizıldag, N., Aka Sagliker, H., Darici, C. (2019). Negative priming effects of emamectin benzoate on soil microbial activity. *Journal of Environmental Protection and Ecology*, 20(3), 1140-1148.
- Chang, W. T., Chen, Y. C., Jao, C. L. (2007). Antifungal activity and enhancement of plant growth by grown on shellfish chitin wastes. *Bioresource Technology*, 98(6), 1224-1230.
- Chauhan, S., Yadav, U., Bano, N., Kumar, S., Fatima, T., Dubey, A., Singh, P. C. (2023). Carbendazim modulates the metabolically active bacterial populations in soil and rhizosphere. *Current Microbiology*, 80(9), 280.
- Corkley, I., Fraaije, B., Hawkins, N. (2022). Fungicide resistance management: Maximizing the effective life of plant protection products. *Plant Pathology*, 71(1), 150-169.
- Datta, R., Anand, S., Moulick, A., Baraniya, D., Pathan, S. I., Rejsek, K., Vranova, V., Sharma, M., Sharma, D., Kelkar, A., Formanek, P. (2017). How enzymes are adsorbed on soil solid phase and factors limiting its activity: A Review. *International Agrophysics*, 31(2), 287-302.
- Doran, J. W., Zeiss, M. R. (2000). Soil health and sustainability: managing the biotic component of soil quality. *Applied Soil Ecology*, 15(1), 3-11.

- Dowling, M., Peres, N., Villani, S., Schnabel, G. (2020). Managing colletotrichum on fruit crops: a "complex" challenge. *Plant Disease*, 104(9), 2301-2316.
- FAO. (2023). *Pesticides use and trade, 1990–2021*.
- Filimon, M. N., Voia, S. O., Vladiou, D. L., Isvoran, A., Ostafe, V. (2015). Temperature dependent effect of difenoconazole on enzymatic activity from soil. *Journal of the Serbian Chemical Society*, 80(9), 1127-1137.
- Fisher, M. C., Hawkins, N. J., Sanglard, D., Gurr, S. J. (2018). Worldwide emergence of resistance to antifungal drugs challenges human health and food security. *Science*, 360(6390), 739-742.
- FRAC. (2020). Fungal control agents sorted by cross resistance pattern and mode of action (including FRAC Code numbering). <https://cpb-us-w2.wpmucdn.com/u.osu.edu/dist/b/28945/files/2020/02/frac-code-list-2020-final.pdf> adresinden 11.12.2023 tarihinde alınmıştır.
- García, P. C., Rivero, R. M., Ruiz, J. M., Romero, L. (2003). The role of fungicides in the physiology of higher plants: Implications for defense responses. *Botanical Review*, 69(2), 162-172.
- Gianfreda, L., Rao, M. A. (2008). Interactions between xenobiotics and microbial and enzymatic soil activity. *Critical Reviews in Environmental Science and Technology*, 38(4), 269-310.
- Gradisar, H., Friedrich, J., Krizaj, I., Jerala, R. (2005). Similarities and specificities of fungal keratinolytic proteases: Comparison of keratinases of and to some known proteases. *Applied and Environmental Microbiology*, 71(7), 3420-3426.
- Grimmer, M. K., van den Bosch, F., Powers, S. J., Paveley, N. D. (2015). Fungicide resistance risk assessment based on traits associated with the rate of pathogen evolution. *Pest Management Science*, 71(2), 207-215.
- Gullino, M. L., Leroux, P., Smith, C. M. (2000). Uses and challenges of novel compounds for plant disease control. *Crop Protection*, 19(1), 1-11.
- Guo, P. P., Zhu, L. S., Wang, J. H., Wang, J., Xie, H., Lv, D. D. (2015). Enzymatic activities and microbial biomass in black soil as affected by azoxystrobin. *Environmental Earth Sciences*, 74(2), 1353-1361.
- Hawkins, N. J., Fraaije, B. A. (2016). Predicting resistance by mutagenesis: lessons from 45 years of MBC resistance. *Frontiers in Microbiology*, 7, 1814.
- Hawkins, N. J., Fraaije, B. A. (2018). Fitness penalties in the evolution of fungicide resistance. *Annual Review of Phytopathology*, 56, 339-360.

- Hu, G. P., Zhao, Y., Song, F. Q., Liu, B., Vasseur, L., Douglas, C., You, M. S. (2014). Isolation, identification and cyfluthrin-degrading potential of a novel strain, FLQ-11-1. *Research in Microbiology*, 165(2), 110-118.
- Hu, M. J., Chen, S. N. (2021). Non-target site mechanisms of fungicide resistance in crop pathogens: a review. *Microorganisms*, 9(3), 502.
- Jeziarska-Tys, S., Joniec, J., Bednarz, J., Kwiatkowska, E. (2021). Microbiological nitrogen transformations in soil treated with pesticides and their impact on soil greenhouse gas emissions. *Agriculture-Basel*, 11(8), 787
- Kalisz, H. M. (1988). Microbial proteinases. *Enzyme Studies. Advances in Biochemical Engineering/Biotechnology*, (p. 1-65) Springer Berlin, Heidelberg.
- Kenarova, A., Boteva, S. (2023). Fungicides in agriculture and their side effects on soil enzyme activities: a review. *Bulgarian Journal of Agricultural Science*, 29(1).
- Kim, K. I., Park, S. C., Kang, S. H., Cheong, G. W., Chung, C. H. (1999). Selective degradation of unfolded proteins by the self-compartmentalizing HtrA protease, a periplasmic heat shock protein in. *Journal of Molecular Biology*, 294(5), 1363-1374.
- Koçak, B. (2020). Importance of urease activity in soil. Presented in V. *International Scientific and Vocational Studies Congress–Science and Health (BILMES SH 2020)*, Edirne.
- Koçak, B., Cenkseven, S. (2021a). Effects of three commonly used herbicides in maize on short-term soil organic carbon mineralization. *Water, Air, & Soil Pollution*, 232(9), 386.
- Koçak, B., Cenkseven, Ş. (2021b). Şeker pancarında kullanılan iki farklı triazol fungisidin toprak mikrobiyal solunumuna etkileri. *Journal of Anatolian Environmental and Animal Sciences*, 6(4), 540-547.
- Landi, L., Renella, G., Giagnoni, L., Nannipieri, P. (2011). Activities of proteolytic enzymes. *Methods of Soil Enzymology*, 9, 247-260.
- Lee, K. E. (1985). *Earthworms: their ecology and relationships with soils and land use*. Academic Press Inc.
- Lo, C. C. (2010). Effect of pesticides on soil microbial community. *Journal of Environmental Science and Health Part B-Pesticides Food Contaminants and Agricultural Wastes*, 45(5), 348-359.
- Lozowicka, B., Kaczynski, P., Wolejko, E., Piekutin, J., Sagitov, A., Toleubayev, K., Isenova, G., Abzeitova, E. (2016). Evaluation of organochlorine pesticide residues in soil and plants from East Europe and Central Asia. *Desalination and Water Treatment*, 57(3), 1310-1321.

- Machado, S. C., Martins, I. (2018). Risk assessment of occupational pesticide exposure: Use of endpoints and surrogates. *Regulatory Toxicology and Pharmacology*, 98, 276-283.
- Mahmood, I., Imadi, S. R., Shazadi, K., Gul, A., Hakeem, K. R. (2016). Effects of Pesticides on Environment. Editors K. R. Hakeem, M. S. Akhtar, S. N. A. Abdullah, *Plant, Soil and Microbes: Volume 1: Implications in Crop Science* (pp. 253-269). Springer International Publishing.
- Morton, C. O., Hirsch, P. R., Peberdy, J. P., Kerry, B. R. (2003). Cloning of and genetic variation in protease VCP1 from the nematophagous fungus. *Mycological Research*, 107, 38-46.
- Ozkara, A., Akil, D., Konuk, M. (2016). Pesticides, environmental pollution, and health. Editors M. L. Larramendy, S. Soloneski *Environmental Health Risk—Hazardous Factors to Living Species* (pp 3-26). IntechOpen.
- Page, M. J., Di Cera, E. (2008). Serine peptidases: Classification, structure and function. *Cellular and Molecular Life Sciences*, 65(7-8), 1220-1236.
- Pérez-Lucas, G., Vela, N., El Aatik, A., Navarro, S. (2019). Environmental risk of groundwater pollution by pesticide leaching through the soil profile. Editors M. L. Larramendy & S. Salonescki, *Pesticides-use and misuse and their impact in the environment* (pp. 1-28). IntechOpen.
- Pertot, I., Caffi, T., Rossi, V., Mugnai, L., Hoffmann, C., Grando, M. S., Gary, C., Lafond, D., Duso, C., Thiery, D., Mazzoni, V., Anfora, G. (2017). A critical review of plant protection tools for reducing pesticide use on grapevine and new perspectives for the implementation of IPM in viticulture. *Crop Protection*, 97, 70-84.
- Popp, J. (2011). Cost-benefit analysis of crop protection measures. *Journal Fur Verbraucherschutz Und Lebensmittelsicherheit-Journal of Consumer Protection and Food Safety*, 6, 105-112.
- Pöll, V., Denk, U., Shen, H. D., Panzani, R. C., Dissertori, O., Lackner, P., Hemmer, W., Mari, A., Cramer, R., Lottspeich, F., Rid, R., Richter, K., Breitenbach, M., Simon-Nobbe, B. (2009). The vacuolar serine protease, a cross-reactive allergen from. *Molecular Immunology*, 46(7), 1360-1373.
- Rahman, R. N. Z. R. A., Basri, M., Salleh, A. B. (2003). Thermostable alkaline protease from F1; nutritional factors affecting protease production. *Annals of Microbiology*, 53(2), 199-210.
- Roman, D. L., Matica, M. A., Ciorsac, A., Boros, B. V., Isvoran, A. (2023). The Effects of the fungicide myclobutanil on soil enzyme activity. *Agriculture-Basel*, 13(10), 1956.

- Roman, D. L., Voiculescu, D. I., Filip, M., Ostafe, V., Isvoran, A. (2021). Effects of triazole fungicides on soil microbiota and on the activities of enzymes found in soil: a review. *Agriculture*, 11(9), 893.
- Rotanova, T. V., Melnikov, E. E., Khalatova, A. G., Makhovskaya, O. V., Botos, I., Wlodawer, A., Gustchina, A. (2004). Classification of ATP-dependent proteases Lon and comparison of the active sites of their proteolytic domains. *European Journal of Biochemistry*, 271(23-24), 4865-4871.
- Tian, B. Y., Yang, J. K., Lian, L. H., Wang, C. Y., Li, N., Zhang, K. Q. (2007). Role of an extracellular neutral protease in infection against nematodes by strain G4. *Applied Microbiology and Biotechnology*, 74(2), 372-380.
- Van-Zwieten, L., Merrington, G., Van-Zwieten, M. (2004). Review of impacts on soil biota caused by copper residues from fungicide application. *Presented in SuperSoil, 2004*, 3rd. Australian New Zealand Soils Conference
- Vranova, V., Rejsek, K., Formanek, P. (2013). Proteolytic activity in soil: A review. *Applied Soil Ecology*, 70, 23-32.
- Wang, F. H., Li, X. Y., Zhu, L. S., Du, Z. K., Zhang, C., Wang, J., Wang, J. H., & Lv, D. D. (2018). Responses of soil microorganisms and enzymatic activities to azoxystrobin in Cambisol. *Polish Journal of Environmental Studies*, 27(6), 2775-2783.
- Weintraub, M. N., Schimel, J. P. (2005). Seasonal protein dynamics in Alaskan arctic tundra soils. *Soil Biology & Biochemistry*, 37(8), 1469-1475.
- Wolejko, E., Jablonska-Trypuc, A., Wydro, U., Butarewicz, A., Lozowicka, B. (2020). Soil biological activity as an indicator of soil pollution with pesticides - A review. *Applied Soil Ecology*, 147.
- Xia, X. H., Huang, Y. Y., Wang, L., Huang, L. F., Yu, Y. L., Zhou, Y. H., Yu, J. Q. (2006). Pesticides-induced depression of photosynthesis was alleviated by 24-epibrassinolide pretreatment in *Cucumis sativus* L. *Pesticide Biochemistry and Physiology*, 86(1), 42-48.
- Zhang, M. Y., Wang, W. J., Wang, J., Teng, Y., Xu, Z. H. (2017). Dynamics of biochemical properties associated with soil nitrogen mineralization following nitrification inhibitor and fungicide applications. *Environmental Science and Pollution Research*, 24(12), 11340-11348.

Chapter 2

RECENT ADVANCES OF FLUORESCENT DETECTOR MOLECULES FOR DETECTION OF MONOAMINE OXIDASE *IN VIVO* AND *IN VITRO*

EMİN AHMET YEŞİL^{1*} and MUSTAFA ÖZYÜREK²

¹ *Istanbul Gedik University, Vocational School, Chemical Technology
Programme, 34906 Pendik - Istanbul, Turkey*
ahmet.yesil@gedik.edu.tr
ORCID No: 0000-0001-8559-1951

² *Istanbul University-Cerrahpaşa, Faculty of Engineering, Department of
Chemistry, Analytical Chemistry Division, 34320 Avcılar - Istanbul, Turkey*
mozyurek@iuc.edu.tr
ORCID No: 0000-0001-5426-9775

MONOAMINE OXIDASE ENZYME

Monoamine oxidase enzyme (EC 1.4.3.4) is a flavin adenine dinucleotide (FAD) enzyme that plays an important role in the homeostasis and protection of neurotransmitters against toxic biogenic amine compounds. It exists in the form of two types of isoforms, MAO-A and MAO-B [1]. They are generally found in the outer membrane of mitochondria and are involved in the metabolism of amine compounds in the human body [2]. Although both enzyme isoforms are structurally very similar, they differ from each other in many ways, such as pKa values, biological activity&function, and distribution in cells and tissues [3].

MAO plays an important role in regulating the metabolism of exogenous amines, such as the level of intracellular amines and neurotransmitters (dopamine, norepinephrine, serotonin, etc.). As a result of some medical studies, it has been observed that the concentrations of dopamine, which are among these neurotransmitters, are significantly reduced in Parkinson's patients, serotonin and norepinephrine (noradrenaline) in depression patients. The increase in the level of these amines, which are the substrate of MAO, occurs with the inhibition of MAO. MAO is responsible for raising amine concentrations in neurons in many diseases such as depression, dementia, schizophrenia, Parkinson's and Alzheimer's disease. Since MAO plays an important role in the diagnosis and treatment of the above-mentioned diseases,

it is of great importance to design/identify new substances that can inhibit the MAO enzyme and to develop appropriate methods to determine the MAO inhibition activity.

THE IMPORTANCE OF MONOAMINE OXIDASE ENZYME IN TERMS OF HEALTH AND ITS RELATIONSHIP WITH DISEASES

MAO isoforms directly affect the vital process in human cells and tissues. It is closely related to many types of cancer, especially neurological diseases such as Parkinson's, Alzheimer's, depression, and other systemic diseases [1] (Fig. 1). While MAO-A isoform is mostly active in nasopharyngeal epithelial cells, it causes diseases in the upper and lower respiratory tract and chest-abdomen regions; MAO-B isoform triggers the formation of neurological diseases such as Alzheimer's, Parkinson's and depression by showing high activity especially in the brain region. Therefore, the detection of enzyme activity plays an important role in revealing the pathogenesis of MAO isoforms and diagnosing different diseases [4].

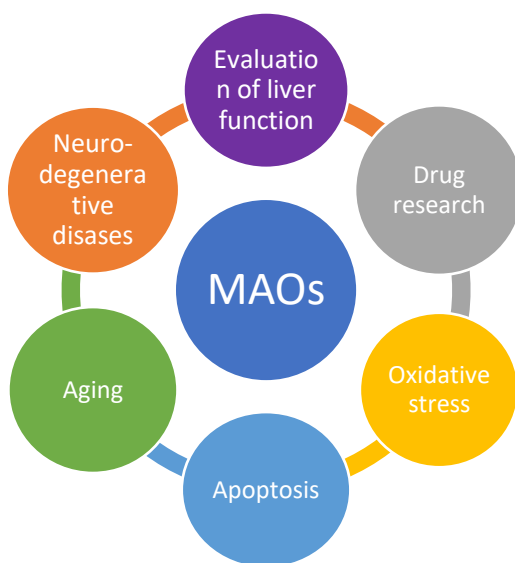


Fig. 1. Some diseases closely related to MAO isoforms.

MEASUREMENT AND VISUALIZATION OF MAO ACTIVITY

In a study conducted by Warshel et al. in 1976 investigating the effect of electrostatic field on lysosome activity, it was observed that the charge transfer caused some compounds to protonate and fluorescence [5]. With this study, it was concluded that there is a relationship between enzymes and fluorescence

and that it should be investigated in depth. Due to their small molecular structure, biocompatibility, easy synthesis, rapid response, *etc.*, the development of fluorogenic probes and the usage of these probes in measurement of MAO isoforms activity have gained great momentum/attention. Imaging using non-invasive fluorogenic probes is preferred over other techniques to visualize the distribution of MAO isoforms in cells and tissues in real time and at high resolution. In particular, the development of fluorogenic probes that allow the measurement and visualization of enzyme activity based on a specific reaction mechanism has paved the way for the formation of an important research area [6].

Some Selected Functional Groups of Fluorogenic MAO Probes and Their Reaction Mechanisms

Synthesis of a fluorogenic probes that will interact specifically with the target biomolecule is very difficult, and the analyte-specific functional groups to be preferred in the molecular structure of the probe are of great importance. Characteristic groups such as 3-aminopropanol, N-substituted tetrahydropyridine and piperazine are generally used in the molecular structure of fluorogenic probes synthesized for the determination of activity of MAO isoforms (**Fig. 2**). These specific diagnostic groups react with MAO isoforms and detach from the probe structure as a result of β -elimination, resulting in a change in fluorescence intensity [7].

A large number of fluorogenic probes that respond to MAO enzyme isoforms have been synthesized via 3-aminopropanol and N-substituted tetrahydropyridine analogues, which are ethereal bonded to fluorophores with free hydroxyl groups at certain sites on the molecular structure. Although these probes can selectively detect MAO-A and MAO-B isoforms, they are adversely affected by the concentration of H_2O_2 present in the analysis medium and the variable pH range of the analysis medium. The piperazine ring, on the other hand, has become more preferred in new generation MAO probes due to its advantages such as accelerating intramolecular charge transfer (ICT) by providing strong electron flow to the fluorophore molecule, increasing solubility and allowing total MAO activity determination [8]. The derivation of fluorophores, whose molecular structure is rich in conjugated bonds, with electron-rich functional groups from suitable sites causes more dipole moment change and Stoke shift in the molecule after excitation by radiation. Based on this interaction, photophysical changes in the form of increased or decreased fluorescence occur in the molecular structure of the fluorogenic probe. As a result, the analysis data are interpreted based on the change in fluorescence

intensity value depending on the reaction between the fluorogenic probe and the related analyte [9].

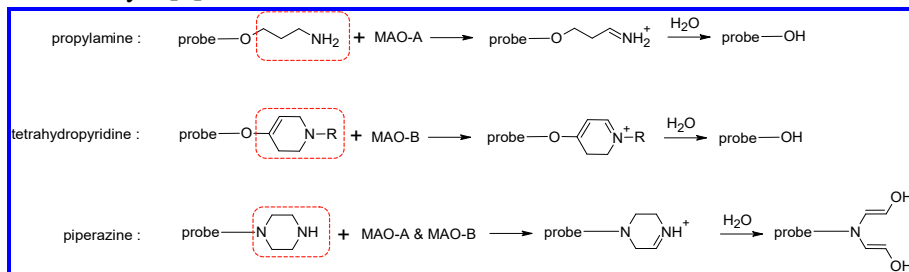


Fig. 2. Some specific MAO analogues used in the molecular structures of fluorogenic probes.

Fluorogenic Probes Developed for MAO Isoforms

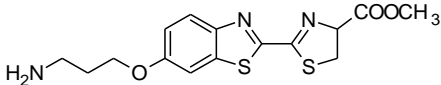
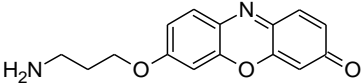
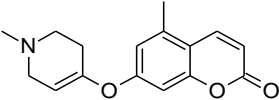
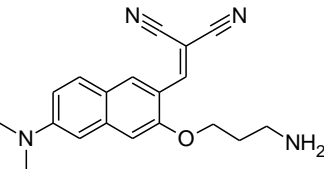
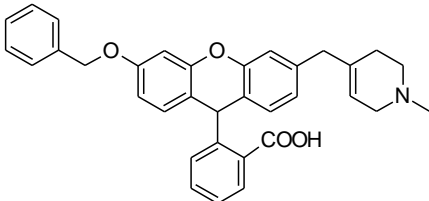
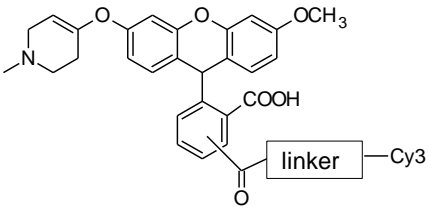
Currently, a limited number of fluorogenic probes have been synthesized/designed for use in the determination of activity of MAO isoforms. When the existing fluorogenic probes are examined;

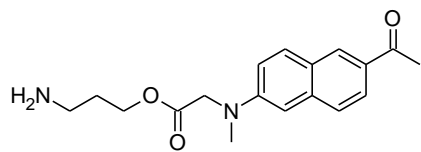
- a.) Specific activity determination of MAO-A
- b.) Specific activity determination of MAO-B
- c.) Determination of total MAO activity

MAO isoforms appear to have been developed based on differences in molecular structure and active sites (**Table 1**).

The reaction mechanisms of fluorogenic probes synthesized for the measurement of the activity of MAO isoforms have been investigated and it has been observed that a large number of probes are not sufficiently specific or sensitive for these enzyme isoforms.

Table 1. Fluorogenic probes synthesized for the measurement of activity of MAO isoforms.

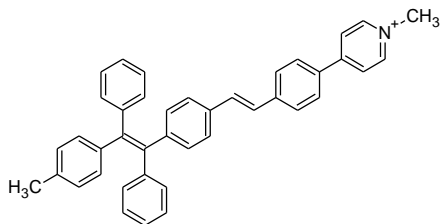
Molecule Structure	Excitation Wavelength (lex)	Broadcast Dalgaboyu (λem)	Literature
	-	-	[10]
	544	590	[11]
	360	460	[7]
	448	600	[12]
	470	515	[13]
	475	570	[14]



304

449

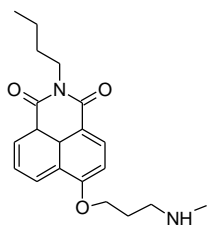
[15]



360

530

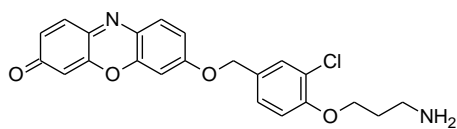
[16]



454

550

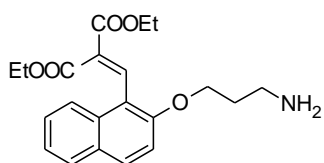
[17]



550

586

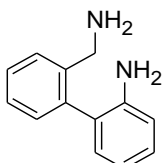
[18]



360

456

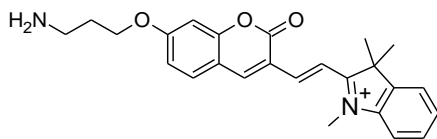
[19]



490

520

[20]



540

626

[21]

NIR Fluorogenic Probes Developed for MAO Isoforms

NIR fluorogenic probes, which have excitation and emission values in the near-infrared region of the electromagnetic spectrum, allow real-time and *in vivo* examination of biological processes, especially in living metabolisms with fluorescence imaging technique [22].

The NIR fluorescence imaging technique have some advantages over traditional methods using fluorogenic probes with shorter wavelengths for the following reasons:

- a.) The wavelength of the light source used in the NIR region is longer than the wavelength of the light source in the visible (Vis) region. Therefore, the damage caused by the light source to living cells and tissues is significantly reduced; imaging is performed without deteriorating the structure of biological samples [23].
- b.) NIR fluorogenic probes have generally deep penetration. Since water and lipids, which are the main components in the structure of living things, have a permeable structure, they absorb short-wavelength radiation in the Vis region, causing a decrease in imaging efficiency. However, NIR fluorogenic probes penetrate cells and tissues that remain in the background of water and lipids, allowing in-depth imaging of biological samples [24].
- c.) It makes it suitable for taking images *in vivo* regardless of the autofluorescence produced by highly structured biomolecules. Autofluorescence, which occurs due to the chemical structures of many tissues and biomolecules, especially cytochrome, myoglobin, hemoglobin, and the emission wavelength of fluorogenic probes with short wavelengths preferred for imaging, may overlap. In such a case, the imaging performance is reduced. On the other hand, NIR fluorogenic probes, generate a high rate of signal-noise and provide images without being affected by autofluorescence [25].

d.) NIR fluorogenic probes have high fluorescence efficiency and stability.

For this reason, it makes it possible to perform high-resolution and simultaneous sensitive imaging of the treated biological samples [26].

Imaging using NIR fluorogenic probes has become a popular method for detecting active molecules/analytes in biological samples. In this context, NIR fluorogenic probes have been designed and synthesized, which provide specific interaction with the target biomolecule in a short time, have high resolution, and allow in situ imaging and diagnosis. Especially for the early detection of neurodegenerative diseases such as Alzheimer's and Parkinson's, precise determination of the activity of MAO enzyme isoforms *in vivo* using such probes has become an imperative strategy.

BODIPY, fluorophores are frequently used in the development of NIR fluorogenic probes, as the dyes fluorescein, rhodamine, coumarin, and cyanine make it possible to analyze biomolecules in real time thanks to their deep penetration and non-cytotoxic properties [27] (Fig.3.). However, cyanine derivatives with improved photooxidation stability are preferred in the vast majority of NIR fluorogenic probes used in *in vivo* imaging procedures.

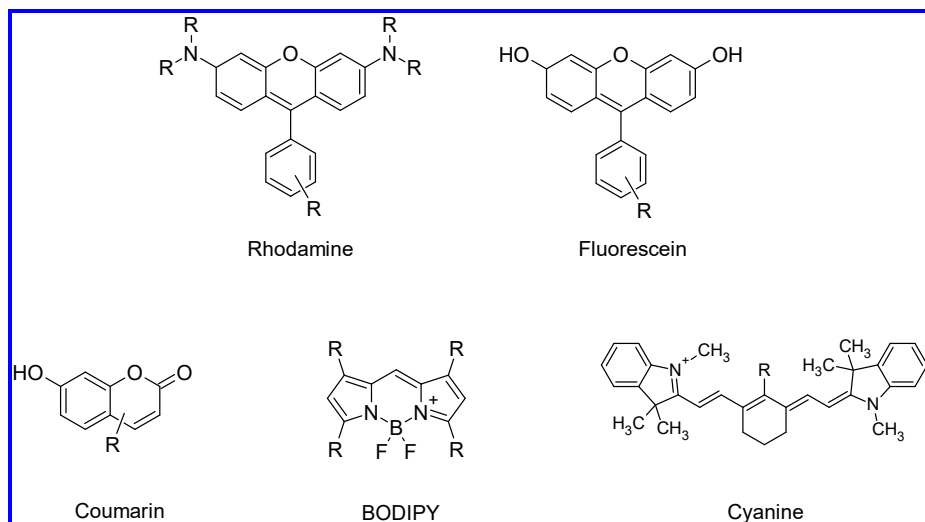


Fig. 3. Fluorophore structures used in the synthesis of NIR fluorogenic probes.

It has been seen that there are only 5 NIR fluorogenic probes developed for the measurement of the activity of MAO isoforms in the literature (Fig. 4). When the molecular structures are examined, it is seen that these fluorogenic

probes are derived with the 3-aminopropanol group and selectivity is given to MAO isoforms.

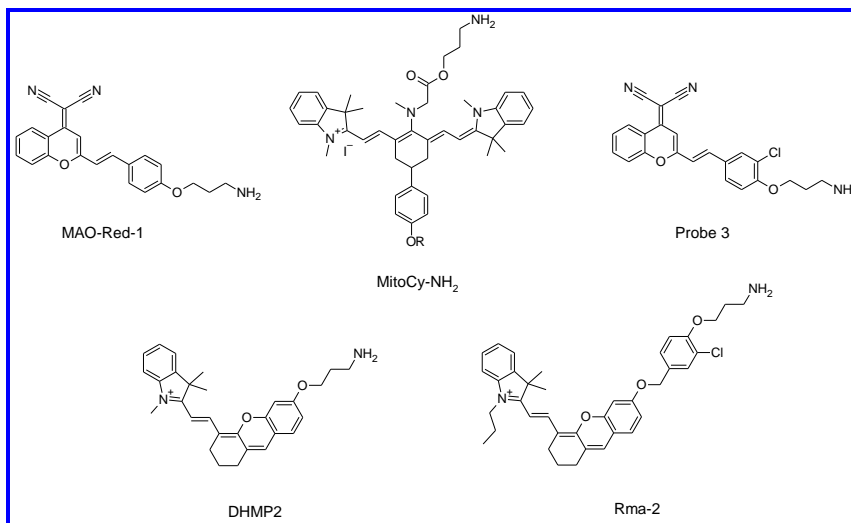


Fig. 4. NIR-capable fluorogenic probes with selectivity to MAO isoforms.

In the study carried out by Li *et al.*, a fluorogenic probe (MAO-Red-1) was developed. When the chemical structure of this compound was examined, the NIR fluorogenic probe was developed for the activity measurement of MAO isoforms by etherically binding the 3-aminopropanol structure over the free OH group on the fluorophore, which has an emission wavelength of 664 nm. An increase in fluorescence intensity was observed as a result of 1-hour incubation of the probe at 37 °C with enzyme solutions (**Fig.5**). When the findings were evaluated, it was seen that the MAO-Red-1 probe responded selectively to the MAO-B isoform; The LOD value was calculated as 1.2 µg/mL [28].

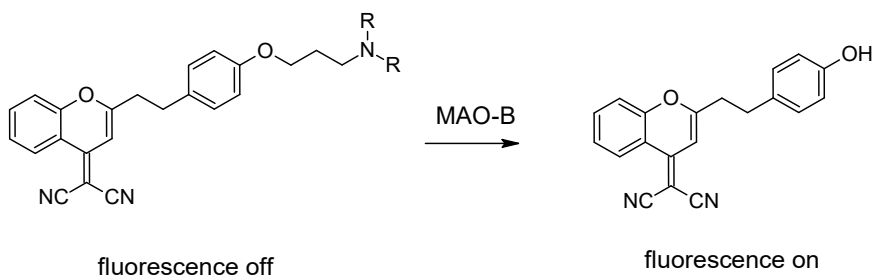


Fig. 5. Reaction mechanism of MAO-Red-1 [28].

The probe structure developed by Wang *et al.*, by derivatizing the cyanine fluorophore of heptametin was named Mito-CyNH₂. When the probe structure

was examined, the 3-aminopropanol group was used to create selectivity for MAO isoforms. As a result of 120-minute incubation of the probe at 37 °C with enzyme solutions, an increase in fluorescence was observed at 750 nm and a decrease in fluorescence at 791 nm (**Fig.6**). While the LOD value was not specified for the method, it was stated that the developed probe responded selectively to the MAO-B isoform [**29**].

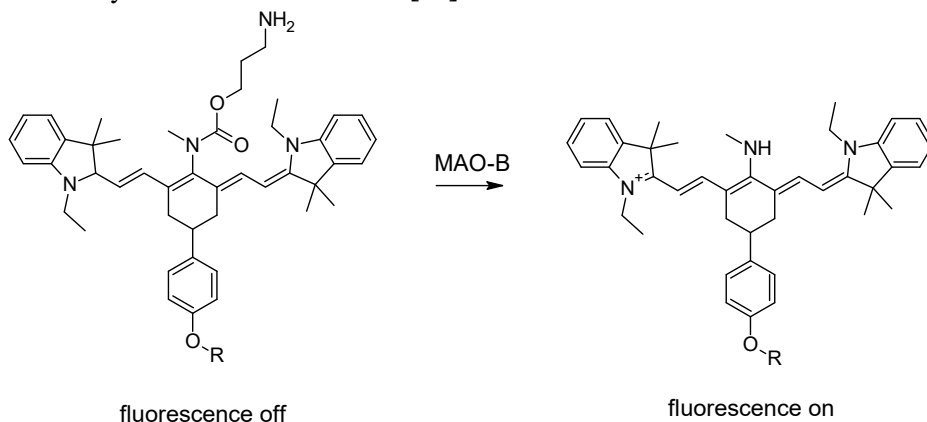


Fig. 6. Reaction mechanism of MitoCy-NH₂ probe [**29**].

In the study carried out by Yang *et al.*, a fluorogenic probe called Probe 3, which contains chlorine atoms in its molecular structure, was synthesized from the molecular structure of the inhibitory compound chlorgyline. When the chemical structure of the compound was examined, the NIR fluorogenic probe was developed for the activity measurement of MAO isoforms by etherically binding the 3-aminopropanol structure over the free OH group on the fluorophore, which has an emission wavelength of 675 nm. An increase in fluorescence intensity was observed as a result of 1-hour incubation of the probe at 37 °C with enzyme solutions (**Fig.7**). When the findings were evaluated, it was seen that the Probe 3 probe responded selectively to the MAO-A isoform; The LOD value was calculated as 2.6 ng/mL [**30**].

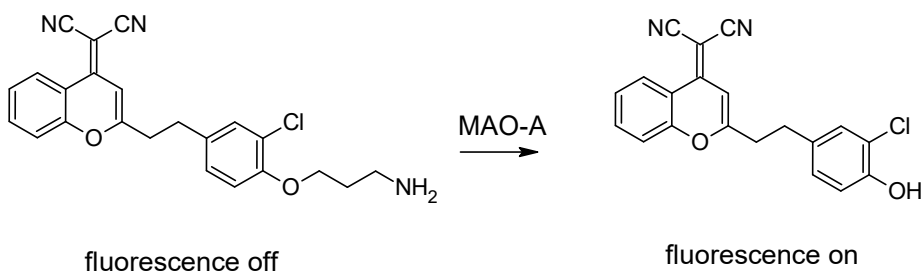


Fig. 7. Reaction mechanism of Probe 3 [**30**].

In the fluorogenic probe structure called DHMP2, which was synthesized by Yang *et al.*, using a new generation cyanin fluorophore, 3-aminopropanol was etherically bound over the free OH group and selectivity against MAO isoforms was achieved. As a result of 12-hour incubation of the probe at 37 °C with enzyme solutions, an increase in fluorescence intensity was observed at a wavelength of 710 nm (**Fig. 8**). When the findings were evaluated, it was seen that the DHMP2 probe responded selectively to the MAO-A isoform; The LOD value was calculated as 13 ng/mL [31].

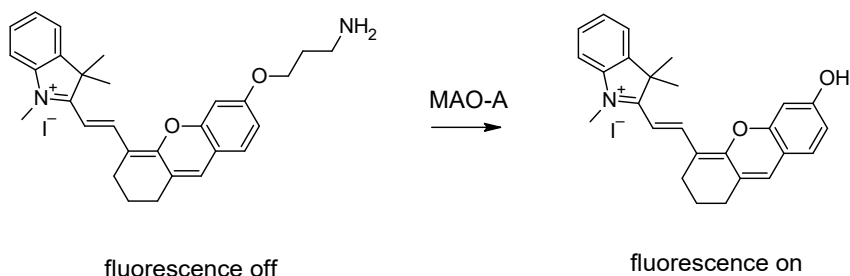


Fig. 8. Reaction mechanism of DHMP2 probe [31].

A similar study using a new generation of cyanine fluorophore was carried out by Shang *et al.*, The fluorogenic probe, called Rma-2, contains chlorine atoms in its molecular structure. When the chemical structure of the compound was examined, the NIR fluorogenic probe was developed for the activity measurement of MAO isoforms by etherically binding the 3-aminopropanol structure over the free OH group on the fluorophore, which has an emission wavelength of 708 nm. An increase in fluorescence intensity was observed as a result of 1-hour incubation of the probe at 37 °C with enzyme solutions (**Fig.9**). When the findings were evaluated, it was seen that the Rma-2 probe responded selectively to the MAO-A isoform; The LOD value was calculated as 4.5 ng/mL [32].

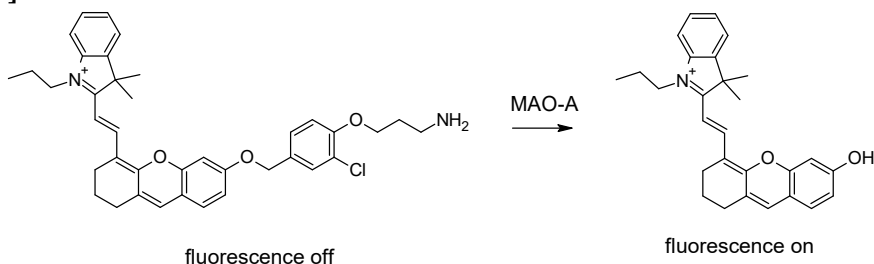


Fig. 9. Reaction mechanism of RMA-2 probe [32].

Fluorogenic probes developed for the measurement of total MAO activity

In addition to fluorogenic probes that allow the specific measurement of activity of MAO isoforms, there are a limited number of probes developed for the detection of total MAO, which are more preferred in clinical applications and have a higher potential for commercialization.

In 2012, it was reported that the coumarin-derived fluorogenic probe synthesized by Zhang *et al.*, and named CR1 responded additively to both MAO-A and MAO-B isoforms. The 3-aminopropanol structure was made selective to MAO isoforms by etherically binding to the molecule over the free OH group on the coumarin fluorophore, and an increase in fluorescence intensity at a wavelength of 465 nm was observed as a result of 1-min incubation at 37 °C with enzyme solutions (**Fig. 10**) [33].

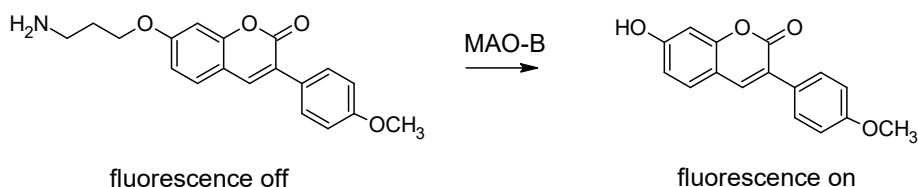


Fig. 10. Reaction mechanism of CR1 probe [33].

In a study carried out by Li *et al.*, in 2013, the 3-aminopropanol structure was made selective to MAO isoforms by etherically binding to the molecule over the free OH group on the fluorophore, a fluorosin derivative. According to the R group in the molecular structure, an increase in fluorescence intensity was observed at a wavelength of 535 nm as a result of 1-hour incubation of compounds called Probe 1-4 at 37 °C with enzyme solutions (**Fig.11**). When the findings were evaluated, it was seen that the Probe-1 probe responded to MAO-A and MAO-B isoforms in total; The LOD value was 3.5 µg/mL for MAO-A; It was calculated as 6 µg/mL for MAO-B [34].

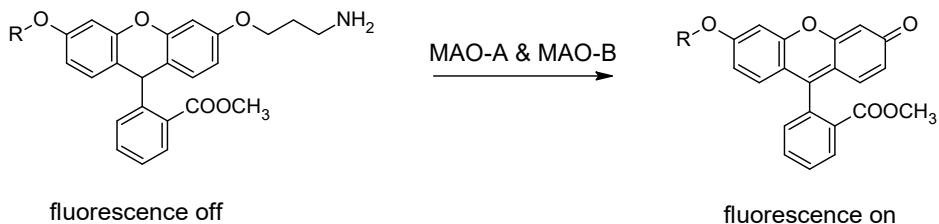


Fig. 11. Reaction mechanism of Probe-1 probe [34].

In the study carried out by Zhang *et al.*, the triarylphosphine structure was used in the synthesis of a new type of fluorophore. When the chemical structure of the fluorogenic probe called OTNP-3-Piperazine, which allows total MAO activity measurement in accordance with the electron attractive properties of the phosphorus and oxygen groups in the center and the ICT mechanism realized by the effect of conjugated π bonds in aromatic rings, is examined, it is seen that the piperazine ring is used to create MAO selectivity. As a result of 1-min incubation at 37 °C with enzyme solutions, an increase in fluorescence intensity was detected at a wavelength of 415 nm (**Fig.12**) [8].

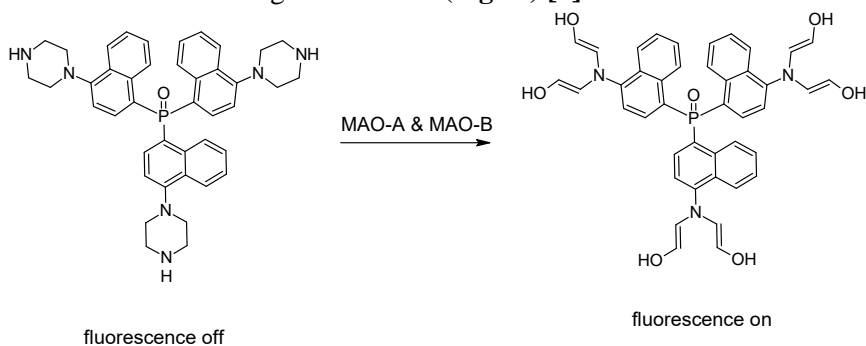


Fig.12. Reaction mechanism of OTNP-3-Piperazine probe [8].

CONCLUSIONS

Among the various standard methods used for the determination of MAO enzyme activity, advanced fluorescence-based methods are preferred due to their practicality, high sensitivity and the convenience of biological imaging in tissues. Fluorometric determination for MAO enzyme has recently been investigated as a new topic. In the developed fluorescence-based studies, MAO-A/MAO-B selectivity was also achieved. In addition, some probes have been developed for the determination of total MAO activity. On the other hand, fluorogenic probes of different molecular sizes are synthesized due to their excellent properties in living cell/tissue imaging. However, the response times and sensitivities of known probes need to be improved for their medical applications.

REFERENCES

- A. Draoui, O. Hiba, A. Aimrane, A. Khiat, H. Gamrani, 2020. Parkinson's disease: from bench to bedside, *Rev. Neurol.* 176, 543–559.
- M. Mladenovi, A. Patsilnakos, A.M. Pirolli, R. Ragno, 2017. Understanding the molecular determinant of reversible human monoamine oxidase B inhibitors containing 2h-chromen-2-one core: structure-based and ligand-based derived 3-d qsar predictive models, *J. Chem. Inf. Model.* 57, 787.
- R. Matej, P. Miha, V. Robert, M. Janez, 2014. Examining electrostatic preorganization in monoamine oxidases A and B by structural comparison and pKa calculations, *J. Phys. Chem. B*, 118, 4326–4332.
- S. Kakinuma, M. Beppu, S. Sawai, A. Nakayama, S. Hirano, et al., 2020. Monoamine oxidase B rs1799836 g allele polymorphism is a risk factor for early development of levodopa-induced dyskinesia in Parkinson's disease, *eNeurologicalSci*, 19, 100239.
- A. Warshel, M. Levitt, 1976. Theoretical studies of enzymic reactions: dielectric, electrostatic and steric stabilization of the carbonium ion in the reaction of lysozyme, *J. Mol. Biol.* 103, 227–249.
- J. Huang, D. Hong, W. Lang, J. Liu, J. Dong, C. Yuan, J. Luo, J. Ge, Q. Zhu, 2019. Recent advances in reaction-based fluorescent probes for detecting monoamine oxidases in living systems, *Analyst*, 144, 3703–3709.
- S. Long, L. Chen, Y. Xiang, M. Song, Y. Zheng, Q. Zhu, 2012. An activity-based fluorogenic probe for sensitive and selective monoamine oxidase-B detection, *Chem. Commun.*, 48, 7164.
- S. Zhang, B. Zhao, L. Yu, J. Liu, X. Zhang, 2020. Piperazine multi-substituted triarylphosphine oxide compound as an instant light-up fluorescent probe for monoamine oxidase, *Talanta*, 209, 120559.
- B. Valeur, I. Leray, 2000, Design principles of fluorescent molecular sensors for cation recognition, *Coord. Chem. Rev.*, 205, 3-40.
- W. Zhou, M. P. Valley, J. Shultz, E. M. Hawkins, L. Bernad, T. Good, D. Good, T.L. Riss, D. H. Klaubert, K. V. Wood, 2006. New bioluminescent substrates for monoamine oxidase assays, *J. Am. Chem. Soc.*, 128, 3122-3123.
- E. Albers, K. A. Rawls, C. J. Chang, 2007. Activity-based fluorescent reporters for monoamine oxidase in living cells, *Chem. Commun.*, 44, 4647-4649.
- D. Kim, S. Sambasivan, H. Nam, K. H. Kim, J. Y. Kim, T. Joo, K. H. Lee, K. T. Kim, K. H. Ahn, 2012. Reaction-based two-photon probes for in vitro

- analysis and cellular imaging of monoamine oxidase activity, *Chem. Commun.*, 48, 6833-6835.
- Y. Xiang, B. He, X. Li, Q. Zhu, 2013. The design and synthesis of novel turn-on fluorescent probes to visualize monoamine oxidase-B in living cells, *Rsc. Adv.*, 3, 4876.
- X. Li, J. Yu, Q. Zhu, L. Qian, L. Li, Y. Zheng, S. Q. Yao, 2014. Visualization of monoamine oxidases in living cells using turn-on fluorescence resonance energy transfer probes, *Analyst*, 139, 6092-6095.
- L. Li, C. W. Zhang, G. Y. J. Chen, B. W. Zhu, C. Chai, Q. H. Xu, E. K. Tan, Q. Zhu, K. L. Lim, S. Q. Yao, 2014. A role for sorting nexin 27 in AMPA receptor trafficking, *Nat. Commun.* 5, 3176.
- W. Shen, J. Yu, J. Ge, R. Zhang, F. Cheng, X. Li, Y. Fan, S. Yu, B. Liu, Q. Zhu, 2016. Light-up probes based on fluorogens with aggregation-induced emission characteristics for monoamine oxidase-A activity study in solution and in living cells, *ACS Appl. Mater. Inter.*, 8, 927-935.
- X. Wu, L. Li, W. Shi, Q. Gong, X. Li, H. Ma, 2016. Sensitive and selective ratiometric fluorescence probes for detection of intracellular endogenous monoamine oxidase A, *Anal. Chem.*, 88, 1440-1446.
- X. Wu, S. Wen, X. H. Li, H. M. Ma, 2017. A-strategy for specific fluorescence imaging of monoamine oxidase A in living cells, *Angew. Chem. Int. Ed.*, 56, 15319.
- H. Qin, L. Li, K. Li and X. Yu, 2019. Novel strategy of constructing fluorescent probe for MAO-B via cascade reaction and its application in imaging MAO-B in human astrocyte, *Chin. Chem. Lett.*, 30, 71.
- N. Fan, C. Wu, Y. Zhou, X. Wang, P. Li, Z. Liu, B. Tang, 2021. Rapid two-photon fluorescence imaging of monoamine oxidase B for diagnosis of early-stage liver fibrosis in mice, *Anal. Chem.*, 93, 7110-7117.
- J. Wu, C. Han, X. Cao, Z. Lv, C. Wang, X. Huo, L. Feng, B. Zhang, X. Tian, X. Ma, 2022. Mitochondria targeting fluorescent probe for MAO-A and for application in the development of drug candidate for neuroinflammation, *Anal. Chem. Acta*, 1199, 339573.
- C. Ding, T. Ren, 2023. Near infrared fluorescent probes for detecting and imaging active small molecules, *Coord. Chem. Rev.* 482, 215080.
- J. Li, Z. Feng, X. Yu, D. Wu, T. Wu, J. Qian, 2022. Aggregation-induced emission fluorophores towards the second near-infrared optical windows with suppressed imaging background *Coord. Chem. Rev.* 472, 214792.

- R. Wang, J. Chen, J. Gao, J.A. Chen, G. Xu, T. Zhu, X. Gu, Z. Guo, W.H. Zhu, C. Zhao, 2019. A molecular design strategy toward enzyme-activated probes with near-infrared I and II fluorescence for targeted cancer imaging, *Chem. Sci.* 10, 7222–7227.
- N. Billinton, A.W. Knight, 2001. Seeing the wood through the trees: A review of techniques for distinguishing green fluorescent protein from endogenous autofluorescence, *Anal. Biochem.* 291, 175–197.
- M. Gao, F. Yu, C. Lv, J. Choo, L. Chen, 2017. Fluorescent Chemical probes for accurate tumor diagnosis and targeting therapy, *Chem. Soc. Rev.* 46, 2237–2271.
- F. Liu, X. Shi, X. Liu, F. Wang, H.B. Yi, J.H. Jiang, 2019. Engineering an NIR rhodol derivative with spirocyclic ring-opening activation for high-contrast photoacoustic imaging, *Chem. Sci.*, 10, 9257–9264.
- L.L. Li, K. Li, Y. H. Liu, H. R. Xu, X. Q. Yu, 2016. Red emission fluorescent probes for visualization of monoamine oxidase in living cells, *Sci. Rep.*, 6, 31217.
- R. Wang, X. Han, J. You, F. Yu, L. Chen, 2018. Ratiometric near-infrared fluorescent probe for synergistic detection of monoamine oxidase B and its contribution to oxidative stress in cell and mice aging models, *Anal. Chem.*, 90, 4054-4061.
- Z. Yang, W. Li, H. Chen, Q. Mo, J. Li, S. Zhao, C. Hou, J. Qin, G. Su, 2019. Inhibitor structure-guided design and synthesis of near-infrared fluorescent probes for monoamine oxidase A and its application in living cells and in vivo, *Chem. Commun.*, 55, 2477.
- Z.M., Yang, Q.Y., Mo, J.M., He, D.L., Mo, J., Li, H., Chen, S.L., Zhao, J.K., Qin, 2020. Mitochondrial-targeted and near-infrared fluorescence probe for bioimaging and evaluating monoamine oxidase A activity in hepatic fibrosis, *ACS Sens.* 5, 943-951.
- J. Shang, W. Shi, X. Li, H. Ma, 2021. Water-soluble near-infrared fluorescent probes for specific detection of monoamine oxidase A in living biosystems, *Anal. Chem.*, 93, 4285-4290.
- Y. Zhang, Y. Xu, S. Tan, L. Xu, X. Qian, 2012. Rapid and sensitive fluorescent probes for monoamine oxidases B to A at low concentrations, *Tetrahedron Lett.*, 53, 6881-6884.
- X. Li, H. Zhang, Y. S. Xie, Y. Hu, H. Sun, Q. Zhu, 2014. Fluorescent probes for detecting monoamine oxidase activity and cell imaging, *Org. Biomol. Chem.*, 12, 2033-2036.

Chapter 3

SEMICONDUCTOR MATERIAL FORMATION AND PROPERTIES

Gizem AYAS¹

İbrahim BOZ²

*1-Lecture. Gizem AYAS, gizemayas@artuklu.edu.tr, Mardin Artuklu
University,*

Orcid no: 0000-0002-7683-4285

*2-Lecture. İbrahim BOZ, ibrahimboz@artuklu.edu.tr, Mardin Artuklu
University*

Orcid no: 0000-0002-2719-4197

INTRODUCTION

With technological developments, the importance of materials in daily life is increasing. Precisely determining the thermodynamic and transport properties of conductor, semiconductor and insulator materials plays an important role in scientific and technological studies (Bounab et al., 2021; Garrido et al., 2021; Singh et al., 2021; Zidani et al., 2021). To date, many theoretical and experimental studies have been proposed to examine these features (Gisbergen et al., 1990; Coronado and Mascarós, 2005; Liu et al., 2006). Materials are classified as insulators, conductors and semiconductors according to their conductivity properties. This classification is made according to the energy difference between the valence band and conduction band. Insulators do not conduct electric current under normal conditions and have large resistances. Insulators have more than 4 electrons in the valence orbit. Since these electrons are tightly bound to the atom, there are very few free electrons in this orbit. They do not exchange electrons. When insulators are placed in an electric field, unlike metals, since they do not have weakly bound or free electrons that can drift within the material, no current flows through them and electric polarization occurs (Fu et al., 2008). Those found between conductor and insulator materials that have the ability to conduct electric current are called semiconductors. A pure semiconductor material is neither a good conductor nor a good insulator. To list semiconductor materials with a single element; arsenic, boron, antimony, astatine, tellurium, polonium, germanium and silicon. Some

compounds are widely used in making semiconductor materials. These can be listed as indium phosphide, silicon germanium, gallium arsenide, gallium nitride, silicon carbide, silicon germanium. Semiconductor materials containing a single element are characterized by atoms having four valence electrons. The most commonly used semiconductor material is silicon. (Balkanski et al., 2000; Mishra and Singh,2007; Fraser, 1986; Roy 2004).

GENERAL PROPERTIES OF SEMICONDUCTORS

According to the classification made considering their electrical and optical properties, solids are; They are divided into three groups: conductors, insulators and semiconductors. The reasons for these different features are; The number of electrons in the outer orbits of the atoms forming the solid, the periodicity coming from the crystal structure and the Pauli Principle. With the most general definitions; conductive materials that conduct electricity well; Insulators are materials that do not conduct electricity well. Semiconductors are; They are substances whose resistivity decreases rapidly with temperature and which conduct electricity less than conductors but more than insulators. Semiconductors constitute the most interesting and important class of solids. They exhibit a wide range of events spanning the region from metals to insulators and have wide application areas. Resistivities of semiconductors span the range of 10^{-2} - 10^9 ohm.cm at room temperature. This range; It falls in the region between good conductors (10^{-6} ohm.cm) and insulators (10^{14} - 10^{20} ohm.cm). At absolute zero temperature (0 K), pure and perfect crystals of semiconductors show insulating properties. The conductivity of semiconductors is generally sensitive to temperature, light, magnetic field and the amount of foreign atoms in their structure. This feature of their conductivity has made semiconductors an important material in electronic applications. Some elemental and compound semiconductors are given in Table 1.1As in other solids, electrons in semiconductors can only have energies in certain bands. Each of the energy bands relates to different quantum states, and most of the lower energy (closer to the nucleus) states are occupied. These states are called valence bands. The band consisting of the excitation levels of valence electrons in atoms is called the free or conduction band. There is a forbidden band between the conduction and valence bands. E_c is the smallest energy of electrons in the conduction band. This energy level is called the bottom of the conduction band.

E_v is the largest energy of the electrons in the valence band, and this energy level is called the ceiling of the valence band. The difference between the bottom energy of the conduction band and the top energy of the valence band E_c .

– $E_v = E_g$ characterizes the band gap of the semiconductor. In perfect and pure semiconductors, the energy of electrons cannot be within the band band energies. The forbidden bandwidth is determined by the type of chemical bonds and the type of atoms in the semiconductors. The gap bandwidth of different semiconductors can vary from 0.1eV to 5eV. In semiconductors and insulators, unlike metals, the valence band is generally almost completely filled.

Çizelge 1.1. Some elemental and compound semiconductors ((Sze,1985))

Element	IV-IV compounds	III-V compounds	II-VI compounds	IV-VI compounds
Si	SiC	AlAs	CdS	PbS
Ge		AlSb	CdSe	PbTe
		BN	CdTe	
		GaAs	ZnS	
		GaP	ZnSe	
		GaSb	ZnTe	
		InAs		
		InP		
		InSb		

Electrons in semiconductors can be excited from the valence band depending on the bandwidth. The difference between insulators and semiconductors is due to the width of the band gap. When the temperature of a semiconductor is raised above absolute zero, some of the electrons reach the energy to move from the valence band to the conduction band. Electrons moving to the conduction band leave unoccupied electron holes in the valence band. Both electrons in the conduction band and holes in the valence band contribute to electrical conductivity. Holes cannot move on their own, but neighboring electrons fill these holes and create a new hole behind. In this way, the holes behave like positively charged particles. Figure 1.1 shows the energy band diagrams of conductors, semiconductors and insulators.

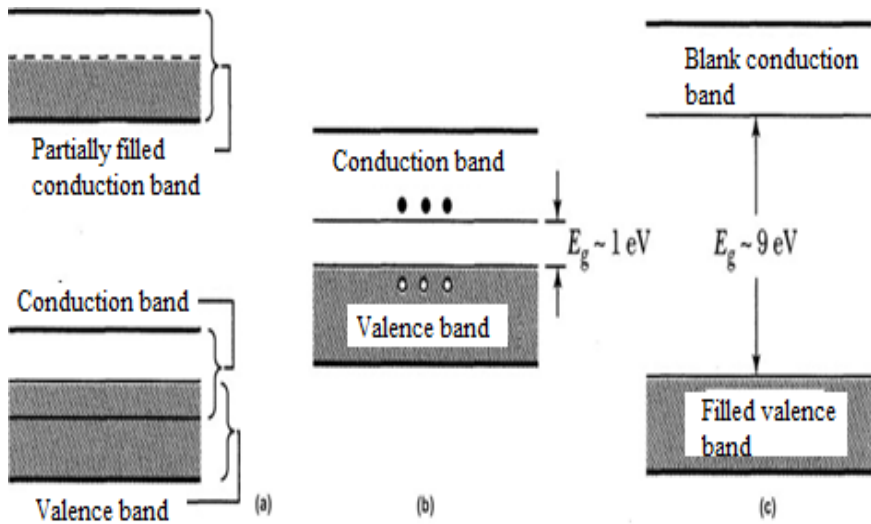


Figure 1.1. Metal (a) semiconductor (b) or insulator (c) band diagram

In semiconductors, the bonds between atoms are relatively strong. So thermal vibration can break some bonds. When a bond is broken, a free hole is formed along with a free electron. As seen in Figure 3.1b, the band gap of the semiconductor is not as wide as that of the insulator (for example, the band gap for silicon is 1.12 eV). Therefore, some electrons can move from the valence band to the conduction band, leaving holes behind. When an electric field is applied, electrons and holes gain kinetic energy and enable electrical conduction. In conductors, the valence band and conduction band overlap each other. Therefore, conductors do not have a band gap and conduct electricity quickly under an electric field.

ELECTRICAL PROPERTIES OF SEMICONDUCTORS

Electrical conductivity is the reciprocal of electrical resistivity. Electrical conductivity defined as current density per unit electric field.

$$\sigma = \frac{|J|}{|\bar{E}|} = \frac{J}{E} \quad (3.1)$$

It is given by the relation . Here, J indicates the current density and E indicates the value of the electric field.

Since conductivity is a measure of the movement of free charges within matter; The mobility of free charges, that is, their mobility, is a parameter that affects the resistivity. Mobility is the speed a charged particle gains per unit electric field. If a particle with speed v is under the influence of an electric field with intensity E; mobility

$$\mu = \frac{|\vec{v}|}{|\vec{E}|} = \frac{v}{E} \quad (3.2)$$

The relation is expressed. The unit of mobility is m²/Vs. According to this definition, it is possible to write the mobilities of electrons and holes separately. According to the definition of mobility, μ_e is the mobility of electrons,

$$\mu_e = \frac{|\vec{v}_e|}{|\vec{E}|} = \frac{v_e}{E} \quad (3.3)$$

And the mobility of the holes μ_h ,

$$\mu_h = \frac{|\vec{v}_h|}{|\vec{E}|} = \frac{v_h}{E} \quad (3.4)$$

It is given by the relation. \vec{v}_e in the equation (3.3) shows the speed of the electrons, and \vec{v}_h in the equation (3.4) shows the speed of the holes. Since the total mobility is equal to the sum of the mobilities of electrons and holes,

$$\mu = \mu_e + \mu_h = \frac{v_e}{E} + \frac{v_h}{E} \quad (3.5)$$

It is equal to the relation.

When an electric field is applied to a semiconductor, free charges begin to drift at certain speeds. Thus, a drift current occurs in the semiconductor. If the electric field applied to the semiconductor is \vec{E} ; Total current expressed in \vec{J} density is the sum of the current density \vec{J}_e formed by electrons and the current density \vec{J}_h formed by holes. Accordingly, the total current density is;

$$\vec{J} = \vec{J}_e + \vec{J}_h = -qn\vec{v}_e + qp\vec{v}_h \quad (3.6)$$

It is given by the relation. Here ; $-q$, n and \vec{v}_e are the charges, densities and drift speeds of the electrons, respectively. Similarly; q , p , \vec{v}_h are the loads, densities and drift speeds of the holes, respectively.

Based on the mobility relations of electrons and holes, it is possible to reach the relations giving the drift velocities of electrons and holes. Accordingly, the drift speed of electrons is;

$$\mu_e = \frac{v_e}{E} \Rightarrow v_e = \mu_e E \quad (3.7)$$

and the drift speed of the halls,

$$\mu_h = \frac{v_h}{E} \Rightarrow v_h = \mu_h E \quad (3.8)$$

It is given by the relation. If equations (3.7) and (3.8) are substituted for \vec{v}_e and \vec{v}_h in equation (3.6), the current density becomes,

$$\vec{J} = \vec{J}_e + \vec{J}_h = q(n\mu_e + p\mu_h)\vec{E} \quad (3.9)$$

It is expressed by the relation. If this relation is substituted for J in equation (3.1), for the conductivity of the semiconductor,

$$\sigma = q(n\mu_e + p\mu_h) \quad (3.10)$$

The relation is reached. As can be seen, the conductivity of a semiconductor depends on the density and mobility of the charge carriers.

In a pure semiconductor, since the electron density is equal to the hole density, the electrical conductivity σ_i is,

$$\sigma_i = qn_i (\mu_e + \mu_h) \quad (3.11)$$

It is equal to the relation. The total carrier density n_i in a specific semiconductor is as a function of temperature;

$$n_i(T) = 2 \left(\frac{2\pi (\mu_e^* + \mu_h^*)^{1/2} kT}{h^2} \right)^{3/2} e^{-E_g/2kT} \quad (3.12)$$

It is given by the relation. Here μ_e^* and μ_h^* respectively; active electrons and holes masses, k is the Boltzmann constant, h is the Planck constant, and E_g is the forbidden energy range of the semiconductor. (3.11) equation, (3.12) for the conductivity of n_i semiconductors;

$$\sigma_i = 2q(\mu_e + \mu_h) \cdot \left(\frac{2\pi (\mu_e^* + \mu_h^*)^{1/2} kT}{h^2} \right)^{3/2} e^{-E_g/2kT} \quad (3.13)$$

The relation is obtained. According to the equation (3.10), for the resistivity ρ of a semiconductor;

$$\rho = \frac{1}{\sigma} = \frac{1}{q(n\mu_e + p\mu_p)} \quad (3.14)$$

There is a relation. If the semiconductor is n-type, since the electron density will be much larger than the hole density ($n \gg p$), the expression $p\mu_p$ in the equation (3.10) is ignored. Thus, the resistivity relation for an n-type semiconductor is,

$$\rho = \frac{1}{qn\mu_h} \quad (3.15)$$

is given as.

OPTICAL PROPERTIES OF SEMICONDUCTORS **OPTICAL ABSORPTION IN SEMICONDUCTORS**

The most common and perhaps the simplest method to determine the band structures of semiconductors is the optical absorption method. Absorption is the energy loss phenomenon that occurs as a result of the interaction of the electromagnetic wave arriving at the semiconductor and the electrical charges in the material. In the absorption process, a photon of a certain energy excites an electron from a lower energy level to a higher energy level. Therefore, all possible transitions from this spectrum can provide information about the forbidden energy and band type of the semiconductor. When an electromagnetic wave acts on a material with thickness x , absorption;

$$(4.1)$$

$$I = I_0 e^{-\alpha x}$$

It is given by the relation. Here;

I_0 is the intensity of the electromagnetic wave incident on the material

I is the intensity of the electromagnetic wave passing through the material of thickness x

α indicates the linear absorption coefficient.

If the absorption $L(h\nu)$ is defined according to the rate of decrease in light intensity, the coefficient $\alpha(h\nu)$ is calculated as follows.

$$(4.2)$$

$$\alpha(h\nu) = \frac{1}{L(h\nu)} \frac{d[L(h\nu)]}{dx}$$

It is expressed with . As can be seen from Equation (3.25), as the linear

absorption coefficient increases, the intensity of the light passing through the material will decrease (Pankove, 1971).

REFERENCES

- Balkanski, M., Wallis, R. F., & Wallis, R. F. (2000). Semiconductor physics and applications (Vol. 8). Oxford University Press
- Bounab, S., Bentabet, A., Bouahadda, Y. 2021 Study of the Structural, Dynamic and Thermodynamic Properties of the III-Antimonides Semiconductors. Defect and Diffusion Forum. 250-255.
- Coronado, E., and Galán-Mascarós, J. R., 2005. Hybrid molecular conductors. J. Mater. Chem., 15, 66-74. Guseinov I.I., Mehmetoğlu B., 2007. Calculation of Integer and Non-integer n-Dimensional Debye Functions Using Binomial Coefficients and Incomplete Gamma Functions. Int. J. Thermophys, 28(), 1420-1426
- Garrido, L. C., et al. 2021. First-principles calculation to investigate elastic, electronic and thermophysical properties of the Dy₂Bi₂Fe₄O₁₂ ferromagnetic semiconductor. Semiconductor Science and Technology, 36 (9) 095015.
- Gisbergen, S. J. C. H. M., Godlewski, M., Gregorkiewicz, T., Ammerlaan, C. A. J. 1990. Magnetic-resonance studies of interstitial Mn in GaP and GaAs. Phys. Rev. B, 44, 3012-3019.
- Fu, M., Dissado, L. A., Chen, G., Fothergill, J. C. (2008). Space charge formation and its modified electric field under applied voltage reversal and temperature gradient in XLPE cable. IEEE Transactions on Dielectrics and Electrical Insulation. 15 (3).
- Liu, M., Lu, Y., Xie, Z. B., Chow, G. M., 2011. Enhancing near-infrared solar cell response using up converting transparent ceramics. Solar Energy Materials and Solar Cells. 95, 800-803.
- Mishra, U., & Singh, J. (2007). Semiconductor device physics and design. Springer Science & Business Media.
- Fraser, D. A. (1986). The physics of semiconductor devices. Clarendon Press.
- Roy, D. K. (2004). Physics of semiconductor devices. Universities Press
- PANKOVE, J.J. 1971. Optical processes in semiconductors, Solid State Physical Electronics Series, Princeton Press, New Jersey.
- Singh, J., Verma, C., 2021. Modeling methods for nanoscale semiconductor devices Silicon. <https://doi.org/10.1007/s12633-021-01323-w>
- SZE, SIMON M., Physics of Semiconductor Devices (Wiley-Interscience, New York, NY) 1981.
- Zidani, M., Farh, H., 2021 Study of the Structural, Dynamic and Thermodynamic Properties of the III-

Antimonides Semiconductors. Defect and Diffusion Forum. 250-255.

Chapter 4

Jacobsthal 3-Parameter Generalized Quaternions

Göksal BİLGİCİ¹

1- Prof. Dr.; Kastamonu Üniversitesi Eğitim Fakültesi Matematik Eğitimi
Anabilim Dalı. gbilgici@kastamonu.edu.tr ORCID No: 0000-0001-9964-5578

INTRODUCTION

Jacobsthal (Jc) and Jacobsthal-Lucas (JcL) numbers form well-known integer sequences. These numbers satisfy the following second-order recurrence relation.

$$A_n = A_{n-1} + 2A_{n-2}.$$

The difference between the definitions of these two sequences is the initial conditions. The first two terms of Jc numbers are $J_0 = 0$ and $J_1 = 1$, whereas the first two terms of JcL numbers are $j_0 = 2$ and $j_1 = 1$. Binet-like formulas for Jc and JcL numbers are, respectively,

$$J_n = \frac{2^n - (-1)^n}{3} \text{ and } JL_n = 2^n + (-1)^n$$

where 2 and -1 are the roots of the characteristic equations $x^2 - x - 2 = 0$.

There are many studies in literature about Jc numbers and their generalizations. Horadam (1996) studied Jc and JcL numbers and gave many properties of these sequences. Falcon (2014) introduced k-Jc numbers similar to k-Fibonacci numbers. Djordevic and Srivastasa (2005) defined incomplete generalized Jc and JcL numbers. Uygun and Owusu (2016) studied the bi-periodic Jc sequence. Torunbalci Aydin (2018a) defined another generalization of Jc and JcLucas sequence by changing the initial conditions with two parameters.

Hamilton first introduced quaternions in 1843. These hyper-complex numbers play some important roles in modern physics. One parameter and two-parameter generalizations appear in literature. Senturk and Unal (2022) defined 3-parameter generalized quaternions. The set of these hyper-complex numbers is

$$\mathbb{Q} = \{q_0 + iq_1 + jq_2 + kq_3 : q_0, q_1, q_2, q_3 \in \mathbb{R}\}.$$

Multiplication rules of the versors $\{i, j, k\}$ are given in Table 1.

Table 1: Multiplication rules of $\{i, j, k\}$

	i	j	k
i	$-\gamma_1\gamma_2$	γ_1k	$-\gamma_2j$
j	$-\gamma_1k$	$-\gamma_1\gamma_3$	γ_3i
k	γ_2j	$-\gamma_3i$	$-\gamma_2\gamma_3$

Here γ_1 and γ_2 are any arbitrary real numbers. The norm of a 3-parameter generalized quaternion $r = a_0 + ia_1 + ja_2 + ka_3$ is

$$N(r) = r\bar{r} = a_0^2 + \gamma_1\gamma_2a_1^2 + \gamma_1\gamma_3a_2^2 + \gamma_2\gamma_3a_3^2.$$

Many authors studied hyper-complex numbers whose coefficients are Jc and JcL numbers. For example, quaternions with Jc numbers coefficients (Szynal-Liana and Wloch, 2016; Torunbalci Aydin and Yuce, 2017; Cerda-Morales, 2017; Cerda-Morales, 2018; Tasci, 2017; Yasarsoy and Acikgoz, 2018; Ozkan, Uysal and Godase, 2022; Gul, 2019; Brod and Szynal-Liana, 2019; Brod, 2020; Antriello and Vincenzi, 2019; Torunbalci Aydin, 2018b; Torunbalci Aydin, 2020; Dasdemir, 2020; Halici, 2020), octonions with Jacobsthal numbers coefficients (Cimen and Ipek, 2017; Ozkan and Uysal, 2022; Mert, Unal, Tokeser and Bilgici, 2022) and sedenions with Jacobsthal numbers coefficients (Cimen, 2019; Cimen and Ipek, 2017; Yasarsoy and Acikgoz, 2018).

Definitions, Generating Functions and Binet-like Formulas

In this section, we introduce Jacobsthal 3-parameter generalized quaternions (J3GQ) and Jacobsthal-Lucas 3-parameter generalized quaternions (JL3GQ).

Definition 1. For any non-negative integer r , Jacobsthal 3-parameter generalized quaternion is

$$\chi_r = J_r + iJ_{r+1} + jJ_{r+2} + kJ_{r+3}$$

and Jacobsthal-Lucas 3-parameter generalized quaternion is

$$\psi_r = JL_r + iJL_{r+1} + jJL_{r+2} + kJL_{r+3}$$

where J_r and JL_r is the r th Jc and JcL number, respectively.

It is easy to see that the numbers J3GQ and JL3GQ satisfy the following recursive relations

$$\chi_r = \chi_{r-1} + 2\chi_{r-2} \tag{1}$$

and

$$\psi_r = \psi_{r-1} + 2\psi_{r-2}. \tag{2}$$

The following theorem gives generating functions for the sequences $\{\chi_r\}_{r=0}^{\infty}$ and $\{\psi_r\}_{r=0}^{\infty}$.

Theorem 2. The sequences $\{\chi_r\}_{r=0}^{\infty}$ and $\{\psi_r\}_{r=0}^{\infty}$ satisfy

$$\sum_{r=0}^{\infty} \chi_r x^r = \frac{\chi_0 + (1-x)\chi_1}{1-x-2x^2}$$

and

$$\sum_{r=0}^{\infty} \psi_r x^r = \frac{\psi_0 + (1-x)\psi_1}{1-x-2x^2}$$

respectively.

We do not give the proof of this theorem because it's so simple. Next theorem gives the Binet-like formulas for the numbers J3G and JL3G quaternions.

Theorem 3. For any nonnegative integer r , the r th J3G and JL3G quaternions are, respectively

$$\chi_r = \frac{\tau 2^r - v(-1)^r}{3}$$

and

$$\psi_r = \tau 2^r + v(-1)^r$$

where $\tau = 1 + 2i + 4j + 8k$ and $v = 1 - i + j - k$.

Proof. From the first equations in Theorem 3, we have

$$\begin{aligned} \chi_r &= J_r + iJ_{r+1} + jJ_{r+2} + kJ_{r+3} \\ &= \frac{2^r - (-1)^r}{3} + i \left[\frac{2^{r+1} - (-1)^{r+1}}{3} \right] + j \left[\frac{2^{r+2} - (-1)^{r+2}}{3} \right] \\ &\quad + k \left[\frac{2^{r+3} - (-1)^{r+3}}{3} \right] \\ &= \frac{2^r(1 + 2i + 4j + 8k) + (-1)^r(1 - i + j - k)}{3}. \end{aligned}$$

The final equation gives the first Binet-like formula. The second equation can be found similarly. ■

From the equation $J_{-r} = (-1)^{r+1}J_r/2^r$ and $JL_{-r} = (-1)^rJL_r/2^r$, we can obtain J3G and JL3G quaternions for negative indices as follows

$$\chi_{-r} = \frac{(-1)^r}{2^r} [-J_r + 2iJ_{r-1} - 4jJ_{r-2} + 8kJ_{r-3}]$$

and

$$\psi_{-r} = \frac{(-1)^{r+1}}{2^r} [-JL_r + 2iJL_{r-1} - 4jJL_{r-2} + 8kJL_{r-3}].$$

We note that

$$\tau v = M + 6N \quad (3)$$

and

$$v\tau = M - 6N \quad (4)$$

where $M = \psi_0 - 1 + 2\gamma_1\gamma_2 - 4\gamma_1\gamma_3 + 8\gamma_2\gamma_3$ and $N = -2\gamma_3i - \gamma_2j + \gamma_1k$.

We easily see that.

$$\tau v + v\tau = 2M. \quad (5)$$

Some Properties of J3G and JL3G Quaternions

We obtain some generalizations of well-known identities. One of them is Vajda's identities and its generalizations for J3G and JL3G quaternions can be found in the next theorem.

Theorem 4. For $r, s, t \in \mathbb{Z}$, we have

$$\chi_{r+s}\chi_{r+t} - \chi_r\chi_{r+s+t} = (-2)^r J_s(MJ_t - 2N JL_t)$$

and

$$\psi_{r+s}\psi_{r+t} - \psi_r\psi_{r+s+t} = -9(-2)^r J_s(MJ_t - 2N JL_t).$$

Proof. From the Binet-like formula for J3G quaternions, we have

$$\begin{aligned} & \chi_{r+s}\chi_{r+t} - \chi_r\chi_{r+s+t} \\ &= \frac{1}{9} [(\tau 2^{r+s} - v(-1)^{r+s})(\tau 2^{r+t} - v(-1)^{r+t}) \\ & - (\tau 2^r - v(-1)^r)(\tau 2^{r+s+t} - v(-1)^{r+s+t})] \end{aligned}$$

$$\begin{aligned}
&= \frac{1}{9} [\tau v(-2^{r+s}(-1)^{r+t} + 2^r(-1)^{r+s+t}) + v\tau(2^{r+s+t}(-1)^r - 2^{r+t}(-1)^{r+s})] \\
&= \frac{(-2)^r}{9} [\tau v(-2^s(-1)^t + (-1)^{s+t}) + v\tau(2^{s+t} - 2^t(-1)^s)] \\
&= \frac{(-2)^r}{9} [\tau v(-1)^t(-2^s + (-1)^s) + v\tau 2^t(2^s - (-1)^s)] \\
&= \frac{(-2)^r}{3} [\tau v(-1)^t(-J_s) + v\tau 2^t J_s] \\
&= \frac{(-2)^r J_s}{3} [-\tau v(-1)^t + v\tau 2^t] \\
&= \frac{(-2)^r J_s}{3} [-(M + 6N)(-1)^t + (M - 6N)2^t] \\
&= \frac{(-2)^r J_s}{3} [M(2^t - (-1)^t) - 6N(2^t + (-1)^t)].
\end{aligned}$$

The last equation gives the first identity in the theorem. The second identity can be proved similarly. ■

Vajda's identities give Catalan's identities for $t \rightarrow -s$.

Theorem 5. For $r, s \in \mathbb{Z}$, we have

$$\chi_{r+s}\chi_{r-s} - \chi_r^2 = (2)^{r-s}(-1)^{r+s+1}J_s(MJ_s + 2N JL_s)$$

and

$$\psi_{r+s}\psi_{r-s} - \psi_r^2 = 9(2)^{r-s}(-1)^{r+s}J_s(MJ_s + 2N JL_s).$$

Catalan's identities give Cassini's identities for $s \rightarrow 1$ given in the next theorem.

Theorem 6. For $r \in \mathbb{Z}$, we have

$$\chi_{r+1}\chi_{r-1} - \chi_r^2 = (-1)^r(2)^{r-1}(M + 2N)$$

and

$$\psi_{r+1}\psi_{r-1} - \psi_r^2 = 9(-1)^{r-1}(2)^{r-1}(M + 2N).$$

Another important identity is d'Ocagne's identity. The identity for J3G and JL3G quaternions can be found by substituting $s \rightarrow 1$ and $t \rightarrow k - r$ into Vajda's identity.

Theorem 7. For $r, k \in \mathbb{Z}$, we have

$$\chi_{r+1}\chi_k - \chi_r\chi_{k+1} = (-2)^r(MJ_{k-r} - 2N JL_{k-r})$$

and

$$\psi_{r+1}\psi_k - \psi_r\psi_{k+1} = -9(-2)^r(MJ_{k-r} - 2N JL_{k-r}).$$

We give more relations for J3G and JL3G quaternions in the following theorem without proofs. They can be proved by using Binet-like formulas and recursive relations for J3G and JL3G quaternions.

Theorem 8. For $r \in \mathbb{Z}$, we have

$$\begin{aligned} \psi_r &= \chi_{r+1} + 2\chi_{r-1}, \\ 9\chi_r &= \psi_{r+1} + 2\psi_{r-1}, \\ \chi_r + \psi_r &= 2\chi_{r+1}, \\ 3\chi_r + \psi_r &= 2^{n+1}(1 + 2i + 4j + 8k), \\ \psi_{r+1} + \psi_r &= 3(\chi_{r+1} + \chi_r) = 2^n(1 + 2i + 4j + 8k), \\ \chi_{r+1} - 2\chi_r &= 3(\psi_{r+1} - 2\psi_r) = (-1)^n(1 - i + j - k), \\ \sum_{i=0}^r \chi_i &= \frac{\chi_{r+2} - \chi_1}{2}, \\ \sum_{i=0}^r \psi_i &= \frac{\psi_{r+2} - \psi_1}{2}. \end{aligned}$$

RESULTS

There is a huge interest in hyper-complex numbers whose coefficients are integer sequences. Two well-known integer sequences are Jacobsthal and Jacobsthal-Lucas numbers among integer sequences. Many authors have studied Jacobsthal quaternions, and the current study is one of them. There are some kinds of quaternions and recently Senturk and Unal (2022) have introduced a new type of quaternions, namely 3-parameter quaternions. In this study, it is aimed to introduce Jacobsthal and Jacobsthal 3-parameter generalized quaternions. For this purpose, Binet-like formulas and generating functions for these new hyper-complex numbers are obtained. Also, generalizations of some well-known identities are obtained.

REFERANSLAR

- Anatriello, G., & Vincenzi, G. (2019). On h-Jacobsthal and h-Jacobsthal–Lucas sequences, and related quaternions. *Analele științifice ale Universității "Ovidius" Constanta. Seria Matematica*, 27(3), 5-23.
- Brod, D. (2020). On split r-Jacobsthal quaternions. *Annales Universitatis Mariae Curie-Sklodowska, Sectio A–Mathematica*, 74(1), 1-14.
- Brod, D., & Szynal-Liana, A. (2019). On a new generalization of Jacobsthal quaternions and several identities involving these numbers. *Commentationes Mathematicae*, 59(1-2), 33-45.
- Cerda-Morales, G. (2017). Identities for third order Jacobsthal quaternions. *Advances in Applied Clifford Algebras*, 27(2), 1043-1053.
- Cerda-Morales, G. (2018). On fourth order Jacobsthal quaternions. *Journal of Mathematical Sciences and Modelling*, 1(2), 73-79.
- Cimen, C. (2019). On the dual Jacobsthal and dual Jacobsthal-Lucas sedenions. *Erzincan University Journal of Science and Technology*, 12(3), 1759-1766.
- Cimen, C. B., & Ipek, A. (2017). On Jacobsthal and Jacobsthal–lucas octonions. *Mediterranean Journal of Mathematics*, 14, 1-13.
- Cimen, C., & Ipek, A. (2017). On Jacobsthal and Jacobsthal-Lucas sedenions and several identities involving these numbers. *Mathematica Aeterna*, 7(4), 447-454.
- Dasdemir, A. (2020). On hyperbolic Lucas quaternions. *Ars Combinatoria*, 150, 77-84.
- Djordjević, G. B., & Srivastava, H. M. (2005). Incomplete generalized Jacobsthal and Jacobsthal-Lucas numbers. *Mathematical and Computer Modelling*, 42(9-10), 1049-1056.
- Falcon, S. (2014). On the k-Jacobsthal numbers. *American Review of Mathematics and Statistics*, 2(1), 67-77.
- Gul, K. (2019). On bi-periodic Jacobsthal and Jacobsthal-Lucas quaternions. *Journal of Mathematics Research*, 11(2), 44-52.
- Halici, S. (2020). On bicomplex Jacobsthal-Lucas numbers. *Journal of Mathematical Sciences and Modelling*, 3(3), 139-143.
- Horadam, A. F. (1996). Jacobsthal representation numbers. *Fibonacci Quarterly*, 34(1), 40-54.
- Mert, T., Unal, Z., Tokeser, U., & Bilgici, G. (2022). Some special identities for Jacobsthal and Jacobsthal-Lucas generalized octonions. *Caspian Journal of Mathematical Sciences (CJMS)*, 11(1), 15-25.
- Ozkan, E., & Uysal, M. (2022). On hyperbolic k-Jacobsthal and k-Jacobsthal–Lucas octonions. *Notes Number Theory Discrete Math*, 28(2), 318-330.

- Ozkan, E., Uysal, M., & Godase, A. D. (2022). Hyperbolic k-Jacobsthal and k-Jacobsthal-Lucas quaternions. *Indian Journal of Pure and Applied Mathematics*, 53(4), 956-967.
- Sentürk, T.D., & Unal, Z. (2022). 3-parameter generalized quaternions. *Computational Methods and Function Theory*, 22(3), 575-608.
- Szynał-Liana, A., & Wloch, I. (2016). A note on Jacobsthal quaternions. *Advances in Applied Clifford Algebras*, 26, 441-447.
- Tasci, D. (2017). On k-jacobsthal and k-jacobsthal-lucas quaternions. *Journal of Science & Arts*, 17(3), 469-476.
- Torunbalci Aydin, F. (2020). Dual-complex Jacobsthal quaternions. *Mathematical Sciences and Applications E-Notes*, 8(2), 145-156.
- Torunbalci Aydın, F. (2018a). On generalizations of the Jacobsthal sequence. *Notes on Number Theory and Discrete Mathematics*, 24(1), 120-135.
- Torunbalci Aydin, F. (2018b). Dual Jacobsthal quaternions. *Communications in Advanced Mathematical Sciences*, 3(3), 130-142.
- Torunbalci Aydin, F., & Yuce, S. (2017). A new approach to Jacobsthal quaternions. *Filomat*, 31(18), 5567-5579.
- Uygun, S., & Owusu, E. (2016). A new generalization of Jacobsthal numbers (bi-periodic Jacobsthal sequences). *Journal of Mathematical Analysis*, 7(5), 28-39.
- Uysal, M., & Özkan, E. (2022). Higher-Order Jacobsthal–Lucas Quaternions. *Axioms*, 11, 671.
- Yasarsoy, S., Acikgoz, M., & Duran, U. (2018). A Study on the k-Jacobsthal and k-Jacobsthal-Lucas quaternions and octonions. *Journal of Analysis and Number Theory*, 6(2), 1-7.

Chapter 5

Molecular Scissors Rewriting the Genetic Code: CRISPR-Cas System

İbrahim DAĞCI¹

Yağmur ÜNVER²

1- İbrahim DAĞCI; Atatürk University, Institute of Science, Department of Molecular Biology and Genetics. ibrahim.dagci16@ogr.atauni.edu.tr ORCID No: 0000-0002-6354-2654

2- Assoc. Prof. Yağmur ÜNVER; Atatürk University, Faculty of Science, Department of Molecular Biology and Genetics. yunver@atauni.edu.tr ORCID No: 0000-0003-1497-081X

THE FUNDAMENTALS AND DISCOVERY OF CRISPR-CAS SYSTEMS

Basically, CRISPR-Cas (clustered regularly interspaced short palindromic repeats and associated proteins) system has been discovered as an adaptive immune defense system found in bacteria and archaea. These systems consist of a memory storage locus called a CRISPR array and Cas genes that encode the immune mechanism. The information stored in CRISPR arrays serves to direct array-specific-based destruction of invading genetic elements, including viruses and plasmids (Jackson et al. 2017).

The discovery of CRISPR began in 1987 when unusual repeat sequences were observed in the genome of the bacterium *Escherichia coli* (Ishino et al. 1987). These repeat sequences were later found in other microbial species and were eventually named "CRISPR" (Mojica, Juez, and Rodriguez-Valera 1993). However, the function of these sequences was not yet known.

By 2002, a set of genes adjacent to the CRISPR locus was discovered and these systems were named "Cas (CRISPR-associated system)" (Jansen et al. 2002). This new discovery paved the way for new research in understanding the CRISPR system. Further independent research in the following years revealed that these repeat sequences were interrupted by short, dissimilar "spacer" sequences, and that the CRISPR spacer sequences were derived from foreign chromosomal DNA, in particular from bacteriophages (viruses that infect bacteria) (Bolotin et al. 2005; Mojica et al. 2005; Pourcel, Salvignol, and

Vergnaud 2005). This led to the hypothesis that the CRISPR system serves as an adaptive immune system in prokaryotes, helping to defend against viral infections.

The breakthrough in understanding the biological function of CRISPR came in 2007 with the discovery of "CRISPR-associated RNA (crRNA)" molecules (Brouns et al. 2008). These short RNA molecules were found to be the processed products of transcription from the CRISPR locus and play an important role in guiding the Cas9 protein to target foreign DNA. These developments have been published experimentally supporting the adaptive immune system function of CRISPR.

In 2012, Jennifer Doudna and Emmanuelle Charpentier published their groundbreaking study on the CRISPR-Cas9 system, which they termed "Dual-RNA-Guided". In this study, they showed that they can specifically guide Cas9 with RNA molecules (tracrRNA and crRNA) and that the Cas9 protein can be used to target and modify specific DNA sequences. Doudna and Charpentier's studies on CRISPR-Cas9 has earned them the Nobel Prize in Chemistry in 2020.

A year after Doudna and Charpentier's revolutionary studies in the field of genetic engineering, Church et al. published another paper in which they successfully created crRNA-tracrRNA fusion transcripts that become single guide RNAs (sgRNAs) and shrink crRNAs to 20 base pairs (Mali et al. 2013). The important results of this study not only confirmed that CRISPR motifs function efficiently in mammalian cells, but also significantly simplified the CRISPR gene editing system, opening up further possibilities in the use of CRISPR technology.

This study by Church et al. represents a significant advance in gene editing and makes genetic interventions more accessible. The use of single guide RNAs has the potential to optimize gene editing processes, making them more specific and effective. Furthermore, the use of crRNA-tracrRNA fusion transcripts has allowed gene editing systems to become simpler and more user-friendly.

These milestones in CRISPR history have led to its widespread use as a powerful tool for genome editing (Fig.1).

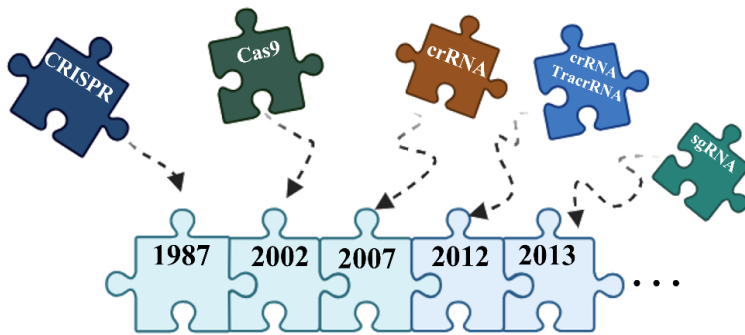


Figure 1 Key developments in the history of CRISPR. (Created with BioRender.com)

THE BIOLOGICAL MECHANISM OF CRISPR-CAS SYSTEMS

The biological mechanism of CRISPR involves the use of Cas proteins to target and edit specific DNA sequences. The CRISPR system functions as the genomic memory of invading pathogens, allowing Cas proteins to screen and deactivate foreign DNA by creating a double-strand break (DSB). This system basically consists of three main phases: adaptation, biogenesis and target interference (Fig.2) (Hille and Charpentier 2016).

Adaptation: When a bacterium encounters a viral infection, it captures a small piece of viral DNA through Cas proteins, in particular with the participation of Cas1 and Cas2, and inserts this genetic material into its own genome, the CRISPR locus, as a new spacer sequence. This important process allows the bacterium to efficiently remember the viral DNA and recognize it in future encounters with the virus (Gostimskaya 2022). Cas proteins, especially Cas1 and Cas2, play a key role in the efficient functioning of this adaptive immunity mechanism, and the CRISPR sequence functions as a kind of genetic memory bank of previous infections. In this way, the bacterium can recognize viruses to which it has been previously exposed and thus develop a more effective defense strategy against future infections (Hille and Charpentier 2016).

Biogenesis: The CRISPR sequence is transcribed into precursor CRISPR RNA (pre-crRNA), a long RNA molecule. The pre-crRNA is then processed into smaller "CRISPR RNAs" (crRNA), each containing specific spacer sequences that are unique to a piece of viral DNA. Each crRNA contains a spacer sequence that is complementary to the target DNA or RNA sequence. In type II CRISPR systems, an additional RNA molecule "tracrRNA (trans activating crRNA)" is required for crRNA processing (Hille and Charpentier 2016).

Target Interference: crRNA associates with a specific Cas protein (such as Cas9) to form a complex that can recognize and bind to a complementary target DNA or RNA sequence. This binding triggers a double-stranded break in the target DNA or RNA by the Cas protein, which leads to inactivation or modification of the target gene (Hille and Charpentier 2016). The Cas protein acts as a molecular scissors guided by crRNA to precisely cut the target sequence. In type II systems, the hybrid RNA formed when crRNA fuses with tracrRNA to form a complex that guides the Cas protein to the target DNA sequence is called "sgRNA (single-guide RNA)". This complex directs Cas to the target DNA sequence and the crRNA acts as a guide to the complementary sequence in the viral DNA. When the Cas protein binds to the target DNA, it cuts both strands, effectively deactivating the viral DNA, which prevents further infection (Gostimskaya 2022). This complex and precise mechanism allows bacteria and archaea to develop a powerful defense against viruses.

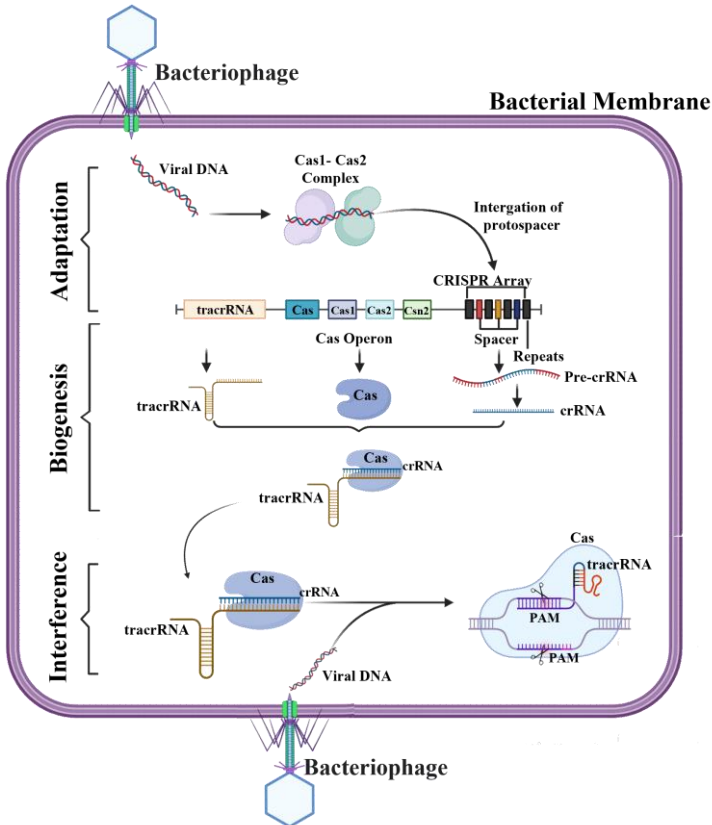


Figure 2 The biological mechanism of the CRISPR-CAS system and the stages of adaptation, biogenesis and target interference. (Created with BioRender.com)

CLASSIFICATION OF CRISPR-CAS SYSTEMS

CRISPR-Cas system is divided into two main classes as Class 1 and Class 2, depending on the composition of the effector module (Fig.3) (Makarova et al. 2020).

Class 1 systems in CRISPR are characterized by a multiprotein complex in the effector module. They are classified into three types: Type I, Type III and Type IV. Type I systems are the most complex, consisting of multiple protein subunits. (Gostimskaya 2022). CRISPR-associated complex for antiviral defense (Cascade) is used by these systems to target and cleave DNA. In this system, a pre-crRNA molecule, previously transcriptionally produced, is targeted and cut by Cas endoribonuclease 6 (Cas6) to form short RNA molecules called mature crRNA. The mature crRNA interacts with Cascade, a Cas protein complex composed of Cse1, Cse2, Cas7, Cas5e and Cas6e subunits. The Cascade complex circulates in the cell containing the mature crRNA and is programmed to screen for potential foreign genetic material (Nishimasu and Nureki 2017). Cascade changes its conformation when it binds to a region compatible with the target DNA. This binding event leads to the activation of Cas3, a Cas nuclease. Cas3 recognizes and cuts the target DNA, which enables the cell's ability to eliminate foreign genetic material. In this way, the type I CRISPR-Cas system prevents the foreign genetic material from damaging the cell, effectively realizing the immune defense of prokaryotes.

Type III systems also have multiple protein subunits and use a complex called Csm to target and cleave DNA. The Type III CRISPR-Cas system, like the Type I and Type II systems, requires pre-crRNA cleavage to generate mature crRNA. The Type III system has two subtypes, Type III-A and Type III-B. In Type III-A, targeting of invading DNA requires directional transcription to produce an RNA transcript complementary to the crRNA (Zhang and An 2022). During transcription, denaturation of the target DNA occurs and crRNA binds to the RNA transcript, leading to activation of the protein complex required to cut the target nucleic acid. An ssRNA that is complementary to the CRISPR RNA can be cleaved by the Type III-B system (Samai et al. 2015). Thus, while the target nucleic acid in Type I, Type II and Type III-A systems is usually dsDNA, the Type III-B system targets single-stranded RNA or ssDNA.

Type IV systems are the least characterized and have a different composition compared to Type I and Type III systems. They use a complex called C2c to target and cleave DNA (Gostimskaya 2022). This system includes Cas proteins such as Cas7, Cas5 and Cas8, as well as a smaller version, Cas8, called Csf1. In addition, this system also encodes a DinG helicase called Csf4 and a type IV-specific Cas6-like protein, Csf5 (Taylor et al. 2021). Biochemical and structural

analysis of organisms with a type IV CRISPR-Cas system suggests that the Cas6-like protein is involved in the maturation of crRNAs and the formation of the effector complex driven by a Cascade-like crRNA. This system, like other CRISPR-Cas systems, has ability to probe the cellular environment by recognizing matching nucleic acid targets.

Class 2 systems use single protein effectors (Cas9, Cas12 or Cas13). Class 2 systems are classified into three types: Type II, Type V, and Type VI.

Type II systems are the best known and most widely used and are represented by the CRISPR-Cas9 system from *Streptococcus pyogenes* (Gostimskaya 2022). Cas9 is the effector protein that binds to a guide RNA molecule and cleaves DNA at a specific target site. The type I system carries out pre-crRNA cleavage with the help of Cas6 endoribonuclease, while the type II system carries out pre-crRNA cleavage with the expression of tracrRNA. The duplex formed as a result of this process is cleaved in repeat sequences by RNase III (Mir et al. 2018). Then, crRNA and tracrRNA form a search complex by complexing with the Cas9 protein. Cas9 is a programmable protein defined by the crRNA guide sequence. This guide sequence directs the Cas9 protein to recognize viral DNA. If the crRNA sequence matches the DNA of the virus, Cas9 cuts the viral DNA, creating a break in the double helix. The Cas9 protein has two lobes; one for target recognition and one for nuclease activity. The recognition lobe is required to bind target DNA and crRNA. The nuclease lobe cuts the target DNA. HNH and RuvC nuclease domains that cause double-stranded breaks in target DNA are located in the Nuclease lobe (Chylinski et al. 2014). The DNA strand complementary to the crRNA guide is broken by the HNH domain, while the non-complementary or coding strand of the target DNA is broken by the RuvC domain.

Type V systems are represented by the CRISPR-Cas12 (previously known as Cpf1) protein family. Cas12 also binds to a guide RNA molecule and cuts DNA. However, it has different properties compared to Cas9 (Gao et al. 2016). Highlights of Cas12 include its 'stepwise' cutting of double-stranded DNA and, unlike Cas9, its ability to produce single-stranded overhangs. Furthermore, Cas12 requires only one crRNA for successful targeting, whereas Cas9 requires the cooperation of both crRNA and an rRNA for transactivation. Cas12's 'stepped' cut in double-stranded DNA provides a more pronounced effect at the targeted site. This differs from the 'blunt' cut applied by Cas9, which leads to the formation of single-stranded overhangs (Hillary and Ceasar 2023). Furthermore, Cas12's ability to successfully target with a single crRNA increases its ease in the system. This ensures that, unlike Cas9, no additional

rRNA is required for transactivation. These differences enable the Type V CRISPR-Cas system to work effectively through the Cas12 enzyme.

The type VI CRISPR-Cas system works using the Cas13 enzyme. The Cas13 enzyme is an RNA-directed endonuclease and cuts only single-stranded RNA (Hillary and Ceasar 2023). A notable feature of the Cas12 and Cas13 enzymes is that they have trans or collateral cutting activity (Bot, van der Oost, and Geijsen 2022). That is, these enzymes not only cut the targeted DNA or RNA, but can also cut surrounding non-single-stranded nucleic acid molecules. This DNAase and RNase activity may be a disadvantage in terms of specific gene editing, but it has become a powerful tool for the development of CRISPR-based diagnostics.

In summary, the CRISPR-Cas system is divided into two classes, each containing multiple types. Class 1 systems have multiple proteins in the effector module, while Class 2 systems have a single protein as the effector module. The types in each class have different compositions and mechanisms of action. The best known and widely used type is Type II, represented by the CRISPR-Cas9 system. Other types, such as Type V (Cas12) and Type VI (Cas13), have unique properties and applications in genome editing and diagnostics.

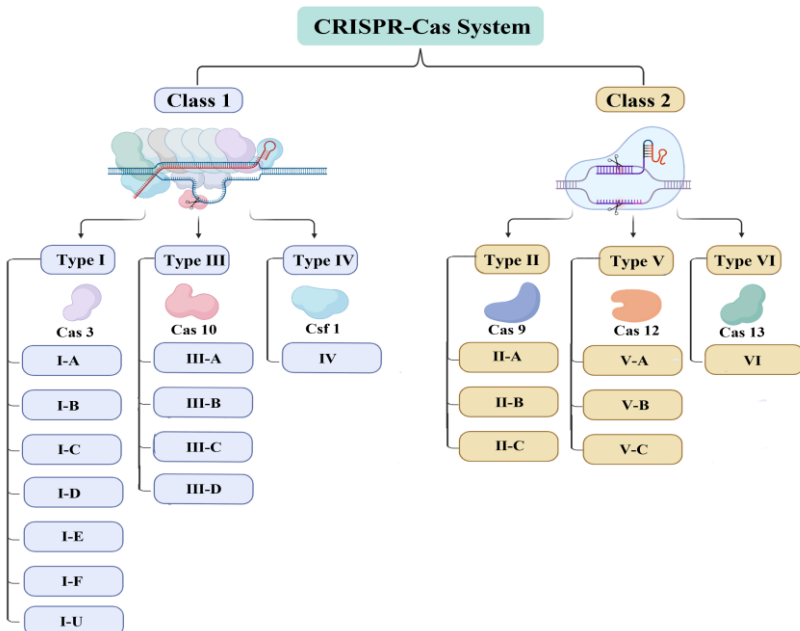


Figure 3 CRISPR-Cas Systems Classification. The CRISPR-Cas systems are classified based on the crRNA-effector protein complex. Additionally, they are differentiated by the presence of six types of Cas proteins and their corresponding subtypes. (Created with BioRender.com)

STUDIES USING THE CRISPR-CAS SYSTEM

Since CRISPR-Cas9 technology proved effective in mammalian cells, scientists have achieved rapid gene editing in a variety of plant species and animal, from mice and fruit flies to rats, rice and wheat (Bassett and Liu 2014; Bassett et al. 2013; Chen et al. 2019; Jiang et al. 2013; Kondo and Ueda 2013; Ma et al. 2014; Ren et al. 2013; Wang et al. 2013; Xie and Yang 2013). However, the main promise of CRISPR technology lies in treating genetic diseases. In this context, in December 2013, Wu et al. published an important study using CRISPR-Cas9 to treat cataracts in mice with cataract-causing base deletions (Wu et al. 2013). In this study, they combined the mRNA encoding Cas9 with an sgRNA and injected it into fertilized mouse eggs. Of the 22 mouse offspring obtained, 10 had mutant alleles, including insertions and deletions via NHEJ (Non-homologous end joining). Four mice repaired via HDR (Homology Directed Repair) successfully cured cataracts, and two of the mice created via NHEJ were also successfully treated. In conclusion, it was reported that these findings offer a promising perspective that CRISPR-Cas9 can modify the genome to treat genetic diseases.

Around the same time, intestinal stem cells were isolated from two patients with cystic fibrosis transmembrane conductance receptor (CFTR) mutations and these mutations were successfully corrected using CRISPR-Cas9 technology (Schwank et al. 2013). They also proposed a protocol for the in vitro assembly and subsequent delivery of genetically modified stem cells into the body. This protocol was successfully applied for clinical use a few years later (Frangoul et al. 2021). These findings suggest that CRISPR-Cas9 could be effective as a potential tool to treat genetic diseases.

Apart from these studies, CRISPR, a gene editing tool, has been used to study and develop treatments for hereditary and developmental neurological disorders (HNDs and DNDs) such as fragile X syndrome, Down syndrome, Tay-Sachs and Sandhoff (Lee et al. 2018; Levy et al. 2020; Ou et al. 2020; Zuo et al. 2017). In the field of gene therapy, CRISPR-Cas9 has been used to treat a wide range of genetic disorders, including neurological diseases such as Parkinson's (Lee et al. 2019) , Alzheimer's (György et al. 2018; Ortiz-Virumbrales et al. 2017; Park et al. 2019) and rare diseases such as amyotrophic lateral sclerosis (ALS) (Duan et al. 2020; Wang et al. 2017) and spinal muscular atrophy (SMA) (Li et al. 2020; Zhou et al. 2018). Chimeric antigen receptor (CAR) T cell therapy for cancer treatment has also been developed by CRISPR-Cas9 (Mollanoori et al. 2018). The development and clinical translation of approved gene therapy products for genetic disorders has also been a focus of research, with more than two thousand human gene therapy

clinical trials reported worldwide (Shahryari et al. 2019). These developments hold great promise for the treatment of devastating rare and inherited diseases as well as incurable diseases. However, there are still challenges to overcome, such as the vulnerability of neuronal cells to the negative impact of gene editing and the inefficiency of delivering CRISPR to the brain (Wong et al. 2021). Despite these challenges, the use of CRISPR and gene therapies in the treatment of genetic disorders is a rapidly growing field with great potential to improve human health.

CRISPR-CAS CHALLENGES AND LIMITATIONS

CRISPR-Cas gene editing technology has revolutionized the field of genetic engineering by offering unprecedented precision and efficiency in altering DNA sequences. However, like any powerful tool, CRISPR-Cas is not without its challenges and limitations.

The potential for off-target effects is one of the main concerns of CRISPR-Cas technology. In this case, incorrect cutting of DNA from unwanted locations by the Cas9 enzyme leads to undesirable genetic changes. While significant progress has been made in improving the specificity of CRISPR-Cas systems, the risk of off-target effects remains an issue that needs to be addressed. Detection of off-target effects have been carried out by developed methods such as whole genome sequencing and GUIDE-Seq (Li et al. 2023).

Efficient and targeted delivery of CRISPR components to the desired cells or tissues in the body is another major challenge. Current delivery methods, such as viral vectors or nanoparticles, can have limitations in terms of specificity, efficiency and safety (Li et al. 2023). The development of efficient delivery systems that can precisely deliver CRISPR components to the intended target cells is crucial for the success of CRISPR-based therapies.

While CRISPR-Cas technology is highly efficient in gene editing, its efficiency and specificity can vary depending on the target site and specific genetic sequence. Achieving high editing efficiency and specificity across different cell types and genetic contexts is an ongoing challenge. Researchers are continuously working to improve the efficiency and specificity of CRISPR-Cas systems to increase their applicability in various genetic editing scenarios.

The use of CRISPR-Cas gene editing technology raises important ethical issues. The ability to alter the human germline to cause heritable changes that can be passed on to future generations raises concerns about the potential for unintended consequences and the potential for misuse. The ethical implications of using CRISPR-Cas technology in human embryos or reproductive cells are still under debate.

In conclusion, while CRISPR-Cas gene editing technology holds great promise for the treatment of diseases, it also faces several challenges and limitations. Overcoming these challenges, such as off-target effects, delivery to target cells and tissues, efficiency and specificity, and ethical considerations, will be crucial for the successful implementation of CRISPR-Cas technology into clinical applications. Further research and development are necessary to overcome the challenges and fully realize the potential of CRISPR-Cas gene editing technology for disease treatment.

REFERENCES

- Bassett, Andrew R., and Ji Long Liu. 2014. "CRISPR/Cas9 and Genome Editing in *Drosophila*." *Journal of Genetics and Genomics* 41(1):7–19.
- Bassett, Andrew R., Charlotte Tibbit, Chris P. Ponting, and Ji Long Liu. 2013. "Highly Efficient Targeted Mutagenesis of *Drosophila* with the CRISPR/Cas9 System." *Cell Reports* 4(1):220–28. doi: 10.1016/j.celrep.2013.06.020.
- Bolotin, Alexander, Benoit Quinquis, Alexei Sorokin, and S. Dusko Ehrlich. 2005. "Clustered Regularly Interspaced Short Palindrome Repeats (CRISPRs) Have Spacers of Extrachromosomal Origin." *Microbiology* 151(8):2551–61. doi: 10.1099/mic.0.28048-0.
- Bot, Jorik F., John van der Oost, and Niels Geijsen. 2022. "The Double Life of CRISPR–Cas13." *Current Opinion in Biotechnology* 78.
- Brouns, Stan J. J., Matthijs M. Jore, Magnus Lundgren, Edze R. Westra, Rik J. H. Slijkhuis, Ambrosius P. L. Snijders, Mark J. Dickman, Kira S. Makarova, Eugene V. Koonin, and John Van Der Oost. 2008. "Small CRISPR RNAs Guide Antiviral Defense in Prokaryotes." *Science* 321(5891):960–64. doi: 10.1126/science.1159689.
- Chen, Kunling, Yanpeng Wang, Rui Zhang, Huawei Zhang, and Caixia Gao. 2019. "CRISPR/Cas Genome Editing and Precision Plant Breeding in Agriculture." *Annual Review of Plant Biology* 70:667–97.
- Chylinski, Krzysztof, Kira S. Makarova, Emmanuelle Charpentier, and Eugene V. Koonin. 2014. "Classification and Evolution of Type II CRISPR-Cas Systems." *Nucleic Acids Research* 42(10):6091–6105.
- Duan, Weisong, Moran Guo, Le Yi, Yakun Liu, Zhongyao Li, Yanqin Ma, Guisen Zhang, Yaling Liu, Hui Bu, Xueqin Song, and Chunyan Li. 2020. "The Deletion of Mutant SOD1 via CRISPR/Cas9/sgRNA Prolongs Survival in an Amyotrophic Lateral Sclerosis Mouse Model." *Gene Therapy* 27(3-4):157–69. doi: 10.1038/s41434-019-0116-1.
- Frangoul, Haydar, David Altshuler, M. Domenica Cappellini, Yi-Shan Chen, Jennifer Domm, Brenda K. Eustace, Juergen Foell, Josu de la Fuente, Stephan Grupp, Rupert Handgretinger, Tony W. Ho, Antonis Kattamis, Andrew Kernytsky, Julie Lekstrom-Himes, Amanda M. Li, Franco Locatelli, Markus Y. Mapara, Mariane de Montalembert, Damiano Rondelli, Akshay Sharma, Sujit Sheth, Sandeep Soni, Martin H. Steinberg, Donna Wall, Angela Yen, and Selim Corbacioglu. 2021. "CRISPR-Cas9 Gene Editing for Sickle Cell Disease and β -Thalassemia." *New England Journal of Medicine* 384(3):252–60. doi: 10.1056/nejmoa2031054.

- Gao, Pu, Hui Yang, Kanagalaghatta R. Rajashankar, Zhiwei Huang, and Dinshaw J. Patel. 2016. "Type v CRISPR-Cas Cpf1 Endonuclease Employs a Unique Mechanism for crRNA-Mediated Target DNA Recognition." *Cell Research* 26(8):901–13. doi: 10.1038/cr.2016.88.
- Gostimskaya, Irina. 2022. "CRISPR–Cas9: A History of Its Discovery and Ethical Considerations of Its Use in Genome Editing." *Biochemistry (Moscow)* 87(8):777–88.
- György, Bence, Camilla Lööv, Mikołaj P. Zaborowski, Shuko Takeda, Benjamin P. Kleinstiver, Caitlin Commins, Ksenia Kastanenka, Dakai Mu, Adrienn Volak, Vilmantas Giedraitis, Lars Lannfelt, Casey A. Maguire, J. Keith Joung, Bradley T. Hyman, Xandra O. Breakefield, and Martin Ingelsson. 2018. "CRISPR/Cas9 Mediated Disruption of the Swedish APP Allele as a Therapeutic Approach for Early-Onset Alzheimer's Disease." *Molecular Therapy - Nucleic Acids* 11:429–40. doi: 10.1016/j.omtn.2018.03.007.
- Hillary, V. Edwin, and S. Antony Ceasar. 2023. "A Review on the Mechanism and Applications of CRISPR/Cas9/Cas12/Cas13/Cas14 Proteins Utilized for Genome Engineering." *Molecular Biotechnology* 65(3):311–25.
- Hille, Frank, and Emmanuelle Charpentier. 2016. "CRISPR-Cas: Biology, Mechanisms and Relevance." *Philosophical Transactions of the Royal Society B: Biological Sciences* 371(1707).
- Ishino, Y., H. Shinagawa, K. Makino, M. Amemura, and A. Nakamura. 1987. "Nucleotide Sequence of the Iap Gene, Responsible for Alkaline Phosphatase Isoenzyme Conversion in Escherichia Coli, and Identification of the Gene Product." *Journal of Bacteriology* 169(12):5429–33. doi: 10.1128/jb.169.12.5429-5433.1987.
- Jackson, Simon A., Rebecca E. McKenzie, Robert D. Fagerlund, Sebastian N. Kieper, Peter C. Finan, and Stan J. J. Brouns. 2017. "CRISPR-Cas: Adapting to Change." *Science* 356(6333). doi: 10.1126/science.aal5056.
- Jansen, Ruud, Jan D. A. Van Embden, Wim Gaastra, and Leo M. Schouls. 2002. "Identification of Genes That Are Associated with DNA Repeats in Prokaryotes." *Molecular Microbiology* 43(6):1565–75. doi: 10.1046/j.1365-2958.2002.02839.x.
- Jiang, Wenzhi, Huanbin Zhou, Honghao Bi, Michael Fromm, Bing Yang, and Donald P. Weeks. 2013. "Demonstration of CRISPR/Cas9/sgRNA-Mediated Targeted Gene Modification in Arabidopsis, Tobacco, Sorghum and Rice." *Nucleic Acids Research* 41(20). doi: 10.1093/nar/gkt780.
- Kondo, Shu, and Ryu Ueda. 2013. "Highly Improved Gene Targeting by Germline-Specific Cas9 Expression in Drosophila." *Genetics*

195(3):715–21. doi: 10.1534/genetics.113.156737.

- Lee, Bumwhee, Kunwoo Lee, Shree Panda, Rodrigo Gonzales-Rojas, Anthony Chong, Vladislav Bugay, Hyo Min Park, Robert Brenner, Niren Murthy, and Hye Young Lee. 2018. “Nanoparticle Delivery of CRISPR into the Brain Rescues a Mouse Model of Fragile X Syndrome from Exaggerated Repetitive Behaviours.” *Nature Biomedical Engineering* 2(7):497–507. doi: 10.1038/s41551-018-0252-8.
- Lee, Jaesuk, Delger Bayarsaikhan, Roshini Arivazhagan, Hyejung Park, Byungyoon Lim, Peter Gwak, Goo-Bo Jeong, Jaewon Lee, Kyunghye Byun, and Bonghee Lee. 2019. “CRISPR/Cas9 Edited sRAGE-MSCs Protect Neuronal Death in Parkinson Disease Model.” *International Journal of Stem Cells* 12(1):114–24. doi: 10.15283/ijsc18110.
- Levy, Jonathan M., Wei Hsi Yeh, Nachiket Pendse, Jessie R. Davis, Erin Hennessey, Rossano Butcher, Luke W. Koblan, Jason Comander, Qin Liu, and David R. Liu. 2020. “Cytosine and Adenine Base Editing of the Brain, Liver, Retina, Heart and Skeletal Muscle of Mice via Adeno-Associated Viruses.” *Nature Biomedical Engineering* 4(1):97–110. doi: 10.1038/s41551-019-0501-5.
- Li, Jin Jing, Xiang Lin, Cheng Tang, Ying Qian Lu, Xinde Hu, Erwei Zuo, He Li, Wenqin Ying, Yidi Sun, Lu Lu Lai, Hai Zhu Chen, Xin Xin Guo, Qi Jie Zhang, Shuang Wu, Changyang Zhou, Xiaowen Shen, Qifang Wang, Min Ting Lin, Li Xiang Ma, Ning Wang, Adrian R. Krainer, Linyu Shi, Hui Yang, and Wan Jin Chen. 2020. “Disruption of Splicing-Regulatory Elements Using CRISPR/Cas9 to Rescue Spinal Muscular Atrophy in Human iPSCs and Mice.” *National Science Review* 7(1):92–101. doi: 10.1093/nsr/nwz131.
- Li, Tianxiang, Yanyan Yang, Hongzhao Qi, Weigang Cui, Lin Zhang, Xiuxiu Fu, Xiangqin He, Meixin Liu, Pei feng Li, and Tao Yu. 2023. “CRISPR/Cas9 Therapeutics: Progress and Prospects.” *Signal Transduction and Targeted Therapy* 8(1).
- Ma, Yuanwu, Xu Zhang, Bin Shen, Yingdong Lu, Wei Chen, Jing Ma, Lin Bai, Xingxu Huang, and Lianfeng Zhang. 2014. “Generating Rats with Conditional Alleles Using CRISPR/Cas9.” *Cell Research* 24(1):122–25.
- Makarova, Kira S., Yuri I. Wolf, Jaime Iranzo, Sergey A. Shmakov, Omer S. Alkhnbashi, Stan J. J. Brouns, Emmanuelle Charpentier, David Cheng, Daniel H. Haft, Philippe Horvath, Sylvain Moineau, Francisco J. M. Mojica, David Scott, Shiraz A. Shah, Virginijus Siksnys, Michael P. Terns, Česlovas Venclovas, Malcolm F. White, Alexander F. Yakunin, Winston Yan, Feng Zhang, Roger A. Garrett, Rolf Backofen, John van

- der Oost, Rodolphe Barrangou, and Eugene V. Koonin. 2020. “Evolutionary Classification of CRISPR–Cas Systems: A Burst of Class 2 and Derived Variants.” *Nature Reviews Microbiology* 18(2):67–83.
- Mali, Prashant, Luhan Yang, Kevin M. Esvelt, John Aach, Marc Guell, James E. DiCarlo, Julie E. Norville, and George M. Church. 2013. “RNA-Guided Human Genome Engineering via Cas9.” *Science* 339(6121):823–26. doi: 10.1126/science.1232033.
- Mir, Aamir, Alireza Edraki, Jooyoung Lee, and Erik J. Sontheimer. 2018. “Type II-C CRISPR-Cas9 Biology, Mechanism, and Application.” *ACS Chemical Biology* 13(2):357–65.
- Mojica, F. J. M., G. Juez, and F. Rodriguez-Valera. 1993. “Transcription at Different Salinities of *Haloflex* *Mediterranei* Sequences Adjacent to Partially Modified PstI Sites.” *Molecular Microbiology* 9(3):613–21. doi: 10.1111/j.1365-2958.1993.tb01721.x.
- Mojica, Francisco J. M., César Díez-Villaseñor, Jesús García-Martínez, and Elena Soria. 2005. “Intervening Sequences of Regularly Spaced Prokaryotic Repeats Derive from Foreign Genetic Elements.” *Journal of Molecular Evolution* 60(2):174–82. doi: 10.1007/s00239-004-0046-3.
- Mollanoori, Hasan, Hojat Shahraki, Yazdan Rahmati, and Shahram Teimourian. 2018. “CRISPR/Cas9 and CAR-T Cell, Collaboration of Two Revolutionary Technologies in Cancer Immunotherapy, an Instruction for Successful Cancer Treatment.” *Human Immunology* 79(12):876–82.
- Nishimasu, Hiroshi, and Osamu Nureki. 2017. “Structures and Mechanisms of CRISPR RNA-Guided Effector Nucleases.” *Current Opinion in Structural Biology* 43:68–78.
- Ortiz-Virumbrales, Maitane, Cesar L. Moreno, Ilya Kruglikov, Paula Marazuela, Andrew Sproul, Samson Jacob, Matthew Zimmer, Daniel Paull, Bin Zhang, Eric E. Schadt, Michelle E. Ehrlich, Rudolph E. Tanzi, Ottavio Arancio, Scott Noggle, and Sam Gandy. 2017. “CRISPR/Cas9-Correctable Mutation-Related Molecular and Physiological Phenotypes in iPSC-Derived Alzheimer’s PSEN2N141I Neurons.” *Acta Neuropathologica Communications* 5(1). doi: 10.1186/s40478-017-0475-z.
- Ou, Li, Michael J. Przybilla, Alexandru Flaviu Tăbăran, Paula Overn, M. Gerard O’Sullivan, Xuntian Jiang, Rohini Sidhu, Pamela J. Kell, Daniel S. Ory, and Chester B. Whitley. 2020. “A Novel Gene Editing System to Treat Both Tay–Sachs and Sandhoff Diseases.” *Gene Therapy* 27(5):226–36. doi: 10.1038/s41434-019-0120-5.
- Park, Hanseul, Jungju Oh, Gayong Shim, Byounggook Cho, Yujung Chang,

- Siyong Kim, Soonbong Baek, Hongwon Kim, Jeain Shin, Hwan Choi, Junsang Yoo, Junyeop Kim, Won Jun, Minhyung Lee, Christopher J. Lengner, Yu Kyoung Oh, and Jongpil Kim. 2019. “In Vivo Neuronal Gene Editing via CRISPR–Cas9 Amphiphilic Nanocomplexes Alleviates Deficits in Mouse Models of Alzheimer’s Disease.” *Nature Neuroscience* 22(4):524–28. doi: 10.1038/s41593-019-0352-0.
- Pourcel, C., G. Salvignol, and Gilles Vergnaud. 2005. “CRISPR Elements in *Yersinia Pestis* Acquire New Repeats by Preferential Uptake of Bacteriophage DNA, and Provide Additional Tools for Evolutionary Studies.” *Microbiology* 151(3):653–63. doi: 10.1099/mic.0.27437-0.
- Ren, Xingjie, Jin Sun, Benjamin E. Housden, Yanhui Hu, Charles Roesel, Shuailiang Lin, Lu Ping Liu, Zhihao Yang, Decai Mao, Lingzhu Sun, Qujie Wu, Jun Yuan Ji, Jianzhong Xi, Stephanie E. Mohr, Jiang Xu, Norbert Perrimon, and Jian Quan Ni. 2013. “Optimized Gene Editing Technology for *Drosophila Melanogaster* Using Germ Line-Specific Cas9.” *Proceedings of the National Academy of Sciences of the United States of America* 110(47):19012–17. doi: 10.1073/pnas.1318481110.
- Samai, Poulami, Nora Pyenson, Wenyan Jiang, Gregory W. Goldberg, Asma Hatoum-Aslan, and Luciano A. Marraffini. 2015. “Co-Transcriptional DNA and RNA Cleavage during Type III CRISPR-Cas Immunity.” *Cell* 161(5):1164–74. doi: 10.1016/j.cell.2015.04.027.
- Schwank, Gerald, Bon Kyoung Koo, Valentina Sasselli, Johanna F. Dekkers, Inha Heo, Turan Demircan, Nobuo Sasaki, Sander Boymans, Edwin Cuppen, Cornelis K. Van Der Ent, Edward E. S. Nieuwenhuis, Jeffrey M. Beekman, and Hans Clevers. 2013. “Functional Repair of CFTR by CRISPR/Cas9 in Intestinal Stem Cell Organoids of Cystic Fibrosis Patients.” *Cell Stem Cell* 13(6):653–58. doi: 10.1016/j.stem.2013.11.002.
- Shahryari, Alireza, Marie Saghaeian Jazi, Saeed Mohammadi, Hadi Razavi Nikoo, Zahra Nazari, Elaheh Sadat Hosseini, Ingo Bartscher, Seyed Javad Mowla, and Heiko Lickert. 2019. “Development and Clinical Translation of Approved Gene Therapy Products for Genetic Disorders.” *Frontiers in Genetics* 10(SEP).
- Taylor, Hannah N., Eric Laderman, Matt Armbrust, Thomson Hallmark, Dylan Keiser, Joseph Bondy-Denomy, and Ryan N. Jackson. 2021. “Positioning Diverse Type IV Structures and Functions Within Class 1 CRISPR-Cas Systems.” *Frontiers in Microbiology* 12. doi: 10.3389/fmicb.2021.671522.
- Wang, Haoyi, Hui Yang, Chikdu S. Shivalila, Meelad M. Dawlaty, Albert W. Cheng, Feng Zhang, and Rudolf Jaenisch. 2013. “One-Step Generation of

- Mice Carrying Mutations in Multiple Genes by CRISPR/cas-Mediated Genome Engineering.” *Cell* 153(4):910–18. doi: 10.1016/j.cell.2013.04.025.
- Wang, Lixia, Fei Yi, Lina Fu, Jiping Yang, Si Wang, Zhaoxia Wang, Keiichiro Suzuki, Liang Sun, Xiuling Xu, Yang Yu, Jie Qiao, Juan Carlos Izpisua Belmonte, Ze Yang, Yun Yuan, Jing Qu, and Guang Hui Liu. 2017. “CRISPR/Cas9-Mediated Targeted Gene Correction in Amyotrophic Lateral Sclerosis Patient iPSCs.” *Protein and Cell* 8(5):365–78. doi: 10.1007/s13238-017-0397-3.
- Wong, Poh Kuan, Fook Choe Cheah, Saiful Effendi Syafruddin, M. Aiman Mohtar, Norazrina Azmi, Pei Yuen Ng, and Eng Wee Chua. 2021. “CRISPR Gene-Editing Models Geared Toward Therapy for Hereditary and Developmental Neurological Disorders.” *Frontiers in Pediatrics* 9.
- Wu, Yuxuan, Dan Liang, Yinghua Wang, Meizhu Bai, Wei Tang, Shiming Bao, Zhiqiang Yan, Dangsheng Li, and Jinsong Li. 2013. “Correction of a Genetic Disease in Mouse via Use of CRISPR-Cas9.” *Cell Stem Cell* 13(6):659–62. doi: 10.1016/j.stem.2013.10.016.
- Xie, Kabin, and Yinong Yang. 2013. “RNA-Guided Genome Editing in Plants Using a CRISPR-Cas System.” *Molecular Plant* 6(6):1975–83. doi: 10.1093/mp/sst119.
- Zhang, Xinfu, and Xinmin An. 2022. “Adaptation by Type III CRISPR-Cas Systems: Breakthrough Findings and Open Questions.” *Frontiers in Microbiology* 13.
- Zhou, Miaojin, Zhiqing Hu, Liyan Qiu, Tao Zhou, Mai Feng, Qian Hu, Baitao Zeng, Zhuo Li, Qianru Sun, Yong Wu, Xionghao Liu, Lingqian Wu, and Desheng Liang. 2018. “Seamless Genetic Conversion of SMN2 to SMN1 via CRISPR/Cpf1 and Single-Stranded Oligodeoxynucleotides in Spinal Muscular Atrophy Patient-Specific Induced Pluripotent Stem Cells.” *Human Gene Therapy* 29(11):1252–63. doi: 10.1089/hum.2017.255.
- Zuo, Erwei, Xiaona Huo, Xuan Yao, Xinde Hu, Yidi Sun, Jianhang Yin, Bingbing He, Xing Wang, Linyu Shi, Jie Ping, Yu Wei, Wenqin Ying, Wei Wei, Wenjia Liu, Cheng Tang, Yixue Li, Jiazhi Hu, and Hui Yang. 2017. “CRISPR/Cas9-Mediated Targeted Chromosome Elimination.” *Genome Biology* 18(1). doi: 10.1186/s13059-017-1354-4.

Chapter 6

Cytotoxicity effect of cadmium (II) acetate intercalated boron nitride

Muhammed ÖZ¹

Büşra MORAN BOZER²

1- Assoc. Prof. Dr.; Bolu Abant İzzet Baysal University, Gerede Vocational School, oz_m@ibu.edu.tr, ORCID: 0000-0003-0049-0161

2- Lecturer Dr. Büşra MORAN BOZER; Hitit University, Scientific Technical Application and Research Center, busrabozer@hitit.edu.tr, ORCID No: 0000-0002-7280-4417

ABSTRACT

In this study, the effect of cadmium (II) acetate on the morphology, crystallinity, and cytotoxicity effect boron nitride is discussed in detail. The mass of cadmium (II) acetate in mixture has been adjusted in the range from 0.03 to 1.2 g at the definite amount of urea and B₂O₃ in a mixture of 2 g and 1 g, respectively. The products have been characterized different kind of instrumental methods that they include Fourier Transform-infrared spectroscopy (FTIR), powder X-ray diffraction analysis (XRD), scanning electron microscopy (SEM), and energy-dispersive X-ray spectroscopy (EDS). Boron nitride structure measured by XRD analysis was increased and enhanced ordered lateral morphology with the intercalation of cadmium (II) acetate as for 0.3 dopant level and then the turbostratic boron nitride formation existed at the increase in the amount of additive. The lateral structure of the samples has been evaluated by the SEM as well. The EDS results conducted that the compounds used for the preparation of samples allocated homogeneously and 1.2 g additive amount intercalation of cadmium ion enter into the crystal structure. It was understood from the biological experiments that Cadmium dopation into crystal structure of BN had positive contribution on the cytotoxicity of in vitro applications.

Keywords: Boron Nitride, Intercalation, Cytotoxicity, Crystal Nature

INTRODUCTION

In the ever-evolving landscape of materials science, the interplay between diverse elements and compounds continues to unveil novel materials with unique properties and applications. Current studies on boron focus mostly on the field of health after the impressive findings of boron on health (Rocca et al., 2016). Boric acid found in the eye solution is an example of the biological aspects of boron compound. Boron nitride (BN), an important boron chemical, is produced synthetically which means that there is no possibility to find it in natural. Therefore, the synthetic nature of this chemical allows it to be produced by many different methods such as carbothermic, chemical vapor deposition, physical vapor deposition, catalytic, etc. (Thomas, Weston, & O'connor, 1962; Suri, Subramanian, Sonber, & Murthy, 2010). Most of these methods requires high temperature annealing medium for synthesis of BN (Yoo, et al., 1997). Even though BN has not encountered in daily life, it has applications in many areas of science and industry (Malmqvist, & Tegman, 1997; Kimura, et al., 1999; Haubner, Wilhelm, Weissenbacher, & Lux, 2002; Tabbakh, et al., 2022; Deng, et al., 2023). BN has great variety of morphologies as well as carbon. One of its important crystal structures is a hexagonal morphology not only exhibits similar properties to graphite but also it stands out graphite with its high thermal conductivity (Öz & Ülgen. 2021). Another crystal structure looks like amorphous BN called generally turbostratic indicating irregular and incomplete planar nature (Thomas, Weston, & O'connor, 1962; Hagio, Nonaka, & Sato, 1997; Jähnichen et al., 2022).

An intriguing intersection lies between the exploration of boron nitride (BN) and cadmium (Cd), where the intercalation of Cd within the BN lattice introduces a promising avenue for research (Budak, 2018; Kovtyukhova, et al., 2013; Kim et al., 2017). This article delves into the emergent field of bioactivity associated with Cd intercalated boron nitride, a synthesis that transcends traditional material boundaries and promises exciting implications in the realms of biotechnology and medical science. As researchers embark on this exploration, the questions that arise are manifold. How does the introduction of Cd alter the surface properties of BN? What impact does this intercalation have on the material's interaction with biological entities? Are there potential biomedical applications for Cd-BN composites? These questions form the crux of our investigation, as we navigate the intricate interplay between Cd and BN, aiming to unravel the bioactive potential that lies within this unconventional synthesis.

The integration of Cd, a metal known for its diverse coordination chemistry, into the boron nitride lattice introduces a dynamic component that could be

harnessed for targeted biomedical functionalities. Whether it be through interactions with biomolecules or the modulation of cellular responses, the bioactivity of Cd intercalated BN opens avenues that extend beyond the conventional properties of either component alone.

In the subsequent sections of this article, we will delve into the synthesis methods employed for Cd intercalation, explore the structural implications on boron nitride, and scrutinize the emerging bioactivity that renders this composite material promising for applications in medicine, sensing technologies, and beyond (Merlo, Mokkaḡati, Pandit, & Mijakovic, 2018; Mukheem et al., 2019). This exploration into the bioactivity of Cd intercalated boron nitride exemplifies the interdisciplinary nature of contemporary materials science, where the fusion of seemingly disparate elements holds the key to unlocking unprecedented functionalities with profound implications for human health and technological advancement.

2. EXPERIMENTAL

2.1. BN Synthesis

BN samples are obtained by mixing with boron oxide, urea and different amount range of cadmium (II) acetate (from 0.03 g to 1.2 g). The mixture was annealed at elevated temperature (at 1450 °C) in ammonia atmosphere with the 120 ml/minute (Linde Co. 99.9%) (Öz et. al., 2016). Samples were purified with an acid solution and dried in oven at 100 °C for each process after the cooling to the room temperature gradually. Those detailed studies on the production method can be found in the article published by Öz et al. in 2016.

2.2. Chemicals and Sample Preparation

L929 fibroblast cells served as the foundation for this study. The culture medium for the cells comprised 89 % DMEM (Biological Industries), 10 % Fetal Bovine Serum (FBS; Biological Industries), 1 % L-glutamine (Biological Industries), and 1 % Penicillin/Streptomycin (Capricorn) antibiotic. The culture flasks were treated with 0.05 % Trypsin–EDTA solution to detach the cells, and 1X Calcium/Magnesium-free phosphate buffer (PBS) facilitated for bleaching of apparatus that was utilized during the experiment. Trypan blue, in a 1:1 ratio, was employed for cell counting. Cell viability in cytotoxicity assessments was gauged using MTT tetrazolium salt (serva, Israel). The cell culture procedures were conducted using serological pipettes, culture dishes, and multi-well plates (Corning, USA).

Refrigerated cells were rapidly thawed at 37 °C, and within Class II Laminar flow cabinet, they were put into a 15 mL falcon tube. A 5-minute centrifugation at 250 G in a Falcon tube was performed, and 3 mL of entire culture was poured to the falcon. For the well mixing, flasks were utilized for cultivation, with incubation at 37 °C in a 5% CO₂ incubator. Cell passaging from refrigeration continued until cell proliferation cycle become constant.

In situations where straight application of corresponding Cd-BN samples and used goods was impractical, material extracts were prepared according to the guidelines outlined in TS EN ISO 10993-12:2021. The resulting extract underwent sterilization along a sterile 0.2 µm filter before being incorporated into the process that will be applied to the samples.

2.3. Cytotoxicity Analysis (MTT)

In this testing procedure, utilized for assessing cell viability and investigating the impact of materials on cell health, the reference standard employed was the EN ISO 10993-5. The prescribed MTT method outlined in this standard was executed for the experiment, employing 96-well plates. Following cell enumeration, a density of 10x10³ cells per well was established based on viable cell counts.

The experimental setup involved placing cells in 100 µl of whole composition within each well of 96-well plate, followed by a 24-hour incubation period. Subsequently, an assessment was conducted to verify cell adherence to the well plate surface, scrutinizing morphological features and overall cell viability. Wells meeting the specified criteria had their contents emptied.

Extracts of materials labeled as BN-1.2Cd; 2, BN-0.9Cd; 3, BN-0.6Cd; 4, BN-0.3Cd; 5, BN-0.03Cd. were then administered at five different concentrations (ranging from 1:1 to 1:16) through one after another dilution, commencing fully concentration (1:1). The negative control group received only complete culture medium. The cells were subjected to a 24-hour incubation with the applied materials. After incubation, the medium in the well plates was aspirated, and 50 µl of a 1mg/mL MTT solution was added to each well. Following a 2-2.5 hour incubation at 37 °C, the MTT solution was removed, and 100 µl of MTT solvent (isopropanol) was introduced.

To ascertain cell viability, absorbance density values of the 96-well plate were measured at 570 nm using a multiplate reader. The percentage of cell viability for each group was then computed, assuming 100% viability for the control cell group, as per the equation outlined as followings.

$$\% \text{ Viability of cell} = \frac{\text{optical density of sample}}{\text{optical density of the reference}} \times 100 \quad (1)$$

RESULT AND DISCUSSION

In the present study, it has been intended to examine the in vitro cytotoxicity properties of BN formed with the addition of cadmium (II) acetate, since studies on BN have become widespread in last two decades. At first the first step the intercalated boron nitride synthesis has been carried out by the conventional O'Connor method (O'Connor, 1962). Boric acid and the urea were put into the high temperature furnace under the nitrogen atmosphere in this method. However, that procedure was applied with after some modifications. This study we used boron oxide and ammonia gas instead of the boric acid and nitrogen gas, respectively. Secondly the samples were analyzed for determination of boron nitride formation and cadmium intercalation. The samples were qualitatively investigated by FTIR, XRD, SEM, and EDS analysis that are used to show the BN formation in the specific crystal nature. Instrumental methods show that the resulting samples shift towards a more ordered structure in the presence of cadmium (II) acetate with respect to the rising amount of the cadmium (II) acetate up to 0.3 g. However, we observe that when cadmium acetate concentration is increased the structure of the samples turns into a turbostratic structure as a general trend. Lastly, the biocompatibility of the samples was analyzed by international standard methods such as EN ISO 10993-5, and TS EN ISO 10993-12:202.

The samples produced after cadmium intercalation of h-BN synthesis were analyzed with FTIR spectrometer device that the main peaks showing the formation of the h-BN compound are given in the Figure 1 below. In the figure, the vibration bands of the bonds between boron and nitrogen atoms and the vibration bands of the end groups are observed for the h-BN. 1400 wavenumber indicates the intra-layer vibration frequency, 800 wavenumber indicates the inter-layer vibration frequency, and 4450 wavenumber indicates the end bond vibration frequency.

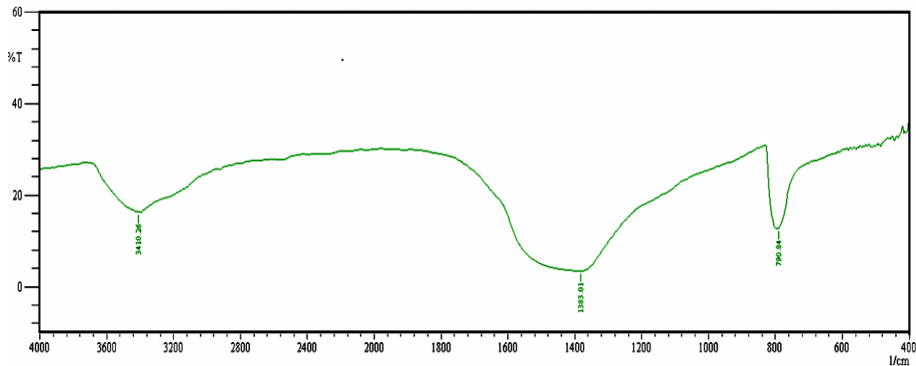


Figure 1. One of the optimum FTIR spectra of the cadmium intercalated BN samples.

XRD analysis is a powerful technique used to study the crystal structure of materials and enhances valuable information about phases, peak broadening, and orientation. XRD patterns of the cadmium doped BN are collected by a Rigaku Multiflex+XRD 2kW diffractometer with providing a monochromatic beam (wavelength of 1.54 Å) obtained from CuK α target in room conditions. The steps were chosen as 0.02° and scan speed is adjusted as 5°/min in the range of 2 θ angle from 10 to 90°. In the context of cadmium intercalated boron nitride (Cd-BN), XRD could provide valuable information about the structural changes induced by the incorporation of cadmium into the boron nitride lattice. By analyzing the positions and intensities of diffraction peaks in Figure 2, phases, peak broadening, and orientation of crystals within the sample could be inferred. The main BN peaks were clearly detected in the entire sample as given in Figure 2. The peaks formed in the diffractograms gives us information about the crystallinity as either turbostratic or hexagonal. In hexagonal form sharp peaks are persists while in turbostratic form wide peaks are prevalent or common. However, there is a peak broadening with the increase the amount of the cadmium because of unregulated BN (turbostratic) or nano structured medium (Balint, & Petrescu, 2009). Those broadening of XRD peaks could provide information about the size and strain of crystallites in the sample indicating the intercalation of cadmium by the distortion at the planar nature. The presence of cadmium strongly influenced the crystallinity and introduce strain into the boron nitride lattice. This situation also determined by the decrease in the sharpness of the 002, 10X, 004 and 11X planes as given in the Figure 2.

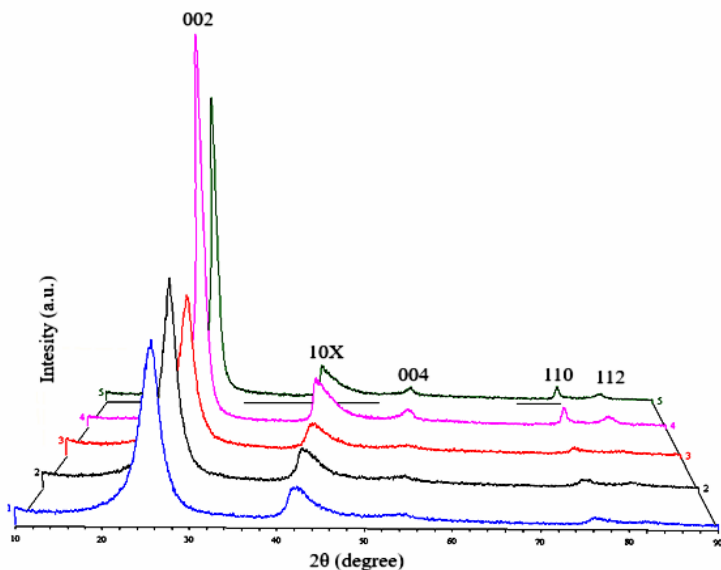


Figure 2. The XRD diffractograms of whole cadmium (II) acetate intercalated h-BN samples. 1, BN-1.2Cd; 2, BN-0.9Cd; 3, BN-0.6Cd; 4, BN-0.3Cd; 5, BN-0.03Cd.

Both SEM images and EDS analysis may reveal the interfaces between cadmium and boron nitride. Examining these interfaces can provide insights into the nature of the interaction, whether it is a physical adsorption or a chemical bonding process. SEM images of cadmium-intercalated boron nitride involves analyzing the microstructural features and morphological changes induced by the introduction of cadmium into the boron nitride lattice. The SEM images may reveal the grain structure of the boron nitride material, showing the arrangement of individual grains or crystals. Cadmium intercalation might influence the grain boundaries and layered structure, resulting in alterations to the overall surface morphology. While surface analysis can be done with the SEM imaging method, it is seen that the cadmium intercalated BN samples in Fig. 3 and 4. Also, the uniformity of the boron nitride surface is observed in the 6000-fold magnification of surface in Fig. 3. The contrast difference in this magnification is evidence of the cadmium which was successfully intercalated into the boron nitride lattice.

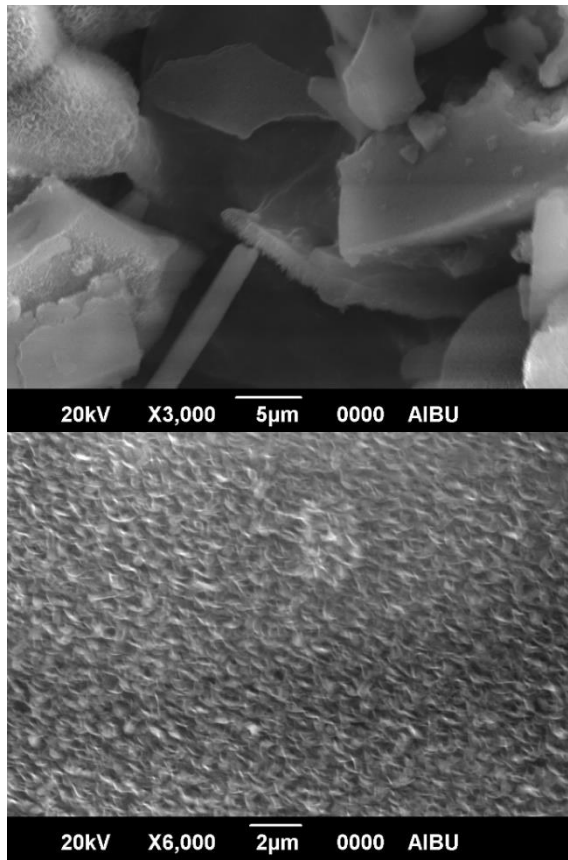


Figure 3. The 3000-fold and 6000-fold magnified SEM images of Cadmium intercalated BN

EDS analysis can be employed to quantitatively assess the elemental composition to complement SEM imaging. This helps confirm the presence of cadmium and provides information on its distribution within the boron nitride structure. In the EDS analysis, boron nitrogen, cadmium and gold are observed in the samples. The high levels of boron and nitrogen found in the EDS analysis indicate that the sample is in the form of BN. It also shows that the cadmium is intercalated in the layers of BN at a weight percentage 1,12 % in Table 1. The gold presence in the EDS is the material on which the surfaces of the samples are coated in order to eliminate BN insulating properties and unsure the visualization of surface of BN. In summary, interpreting SEM images and EDS analysis of cadmium-intercalated boron nitride involves a comprehensive analysis of surface morphology, cadmium distribution, structural changes, and interface characteristics. Combining SEM with other techniques like EDS

allows for a more thorough understanding of the material's microstructure and the effects of cadmium intercalation.

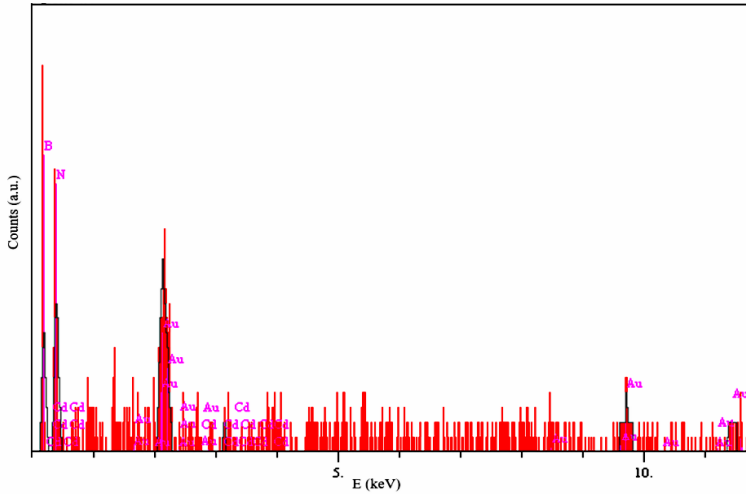


Figure 4. The EDS measurement of Cd intercalated BN

Table 1. Elemental composition of Cd intercalated BN obtained from EDS analysis

Element	Intensity (c/s)	Concentration (wt%)
B	3.17	41.486
N	4.46	30.887
Cd	0.75	1.122
Au	3.10	26.505

The material is evaluated as biocompatible when the vitality values of the materials tested with the MTT method which is commonly utilized for in vitro cytotoxicity are above 70 % (Aydın, et al., 2016). The viability values obtained from BN-1.2Cd were determined as 97.19 ± 1.92 that is in vitro biocompatible according to EN ISO 10993-5. BN-0.03Cd, BN-0.3Cd, BN-0.6Cd and BN-0.9Cd showed cytotoxic effects in vitro since their viability values were below 70 % as given in Figure 5 which illustrates a comprehensive overview of all applied amounts in BN matrix. After assessing the in vitro biocompatibility of the materials post-application, BN-1.2Cd material was confirmed to be biocompatible. The study revealed that the use of the 1.2 g of cadmium resulted in an enhancement of cell viability. As the concentration of cadmium in BN crystal matrix decreased, cell viability exhibited a diminishing trend.

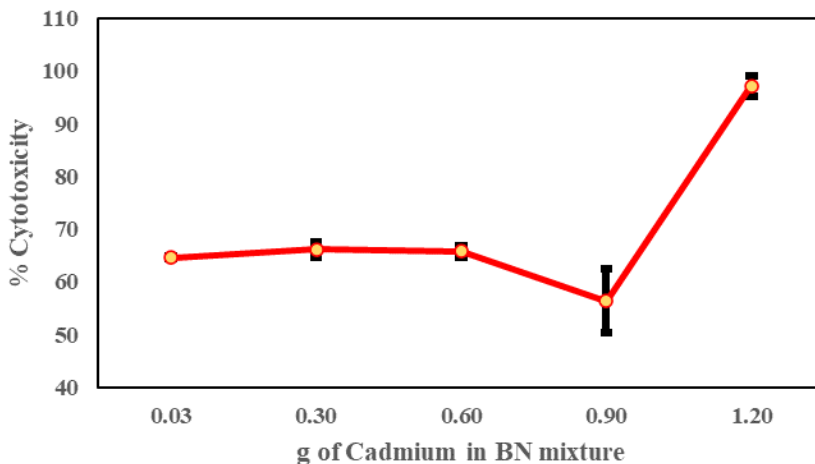


Figure 5. The viability values of Cd intercalated the BN samples

CONCLUSION

In this study, BN was produced by the traditional solid-state method and after characterization of Cd-BN, a detailed study was carried out on its bioactivity. Instrumental measurements proved the formation of BN and the intercalation of Cadmium into the lateral structure. XRD analysis was mainly indicated BN formation in the turbostratic crystal structure with increase amount of cadmium that was intercalated in the stratified nature of the BN. FTIR also included the main BN peaks and broadening nature of these main peaks were detected with the rise at the concentration of Cadmium in mixture. SEM images and EDS measurements supported both XRD and FTIR results in the view of surface analysis and sample contents.

In other goal of this study, while cadmium was intercalated into the BN, it was concluded that it was bound to B and N atoms with different coordination numbers via the pi bonds, and thus, a certain reduction in its harmful effects on health occurred and successively achieved. To validate the efficacy of this decrease on health, cytotoxicity assessments were conducted, simulating the intended applications of biomaterials primarily designed for bone repair. These biomaterials could be created by blending boron nitride samples with cadmium (II) acetate, boron oxide, and urea. The MTT test revealed a notable enhancement in cell viability induced by these materials. The findings indicate that the synthesized biomaterials exhibit potential for use within the body and demonstrate favorable characteristics when the cadmium ratio is elevated in boron nitride.

REFERENCES

- Aydin, A., Erenler, R., Yılmaz, B., & Tekin, Ş. (2016). Antiproliferative effect of Cherry laurel. *Journal of the Turkish Chemical Society Section A: Chemistry*, 3(3), 217-228.
- Balint, M. G., & Petrescu, M. I. (2009). An attempt to identify the presence of polytype stacking faults in hBN powders by means of X-ray diffraction. *Diamond and related materials*, 18(9), 1157-1162.
- Budak, E. (2018). Incorporation of Cadmium into Hexagonal Boron Nitride by Solid State Reaction. *Sakarya University Journal of Science*, 22(6), 1947-1950.
- Deng, T., Lin, J., Yu, C., Liu, Z., Guo, Z., Liu, Y., Tang, C., & Huang, Y. (2023). Boron Nitride Nanofibers as Catalysts for High-Efficiency Aerobic Oxidative Desulfurization. *ACS Applied Nano Materials*.
- Hagio, T., Nonaka, K., & Sato, T. (1997). Microstructural development with crystallization of hexagonal boron nitride. *Journal of materials science letters*, 16, 795-798.
- Haubner, R., Wilhelm, M., Weissenbacher, R., Lux, B. (2002). Boron nitrides—properties, synthesis and applications (pp. 1-45). Springer Berlin Heidelberg.
- Jähnichen, T., Hojak, J., Bläker, C., Pasel, C., Mauer, V., Zittel, V., Deneche, R., Bathen, D., & Enke, D. (2022). Synthesis of Turbostratic Boron Nitride: Effect of Urea Decomposition. *ACS omega*, 7(37), 33375-33384.
- Kim, J., Yamasue, E., Okumura, H., Michioka, C., & Ishihara, K. N. (2017). Intercalation of hexagonal boron nitride and graphite with lithium by sequential process of ball milling and heat treatment. *Journal of Alloys and Compounds*, 707, 172-177.
- Kimura, Y., Wakabayashi, T., Okada, K., Wada, T., & Nishikawa, H. (1999). Boron nitride as a lubricant additive. *Wear*, 232(2), 199-206.
- Kovtyukhova, N. I., Wang, Y., Lv, R., Terrones, M., Crespi, V. H., & Mallouk, T. E. (2013). Reversible intercalation of hexagonal boron nitride with Brønsted acids. *Journal of the American Chemical Society*, 135(22), 8372-8381.
- Merlo, A., Mokkalapati, V. R. S. S., Pandit, S., & Mijakovic, I. (2018). Boron nitride nanomaterials: biocompatibility and bio-applications. *Biomaterials science*, 6(9), 2298-2311.
- Malmqvist, J., & Tegman, R. (1997). Boron nitride coated ceramic crucible with a hole in the bottom—a new device replacing expensive crucibles for the preparation of fusion bead samples for X-ray fluorescence analysis. *Analytical Communications*, 34(11), 343-350.

- Mukheem, A., Shahabuddin, S., Akbar, N., Miskon, A., Muhamad Sarih, N., Sudesh, K., Khan, N. A., Saidur, R., & Sridewi, N. (2019). Boron nitride doped polyhydroxyalkanoate/chitosan nanocomposite for antibacterial and biological applications. *Nanomaterials*, 9(4), 645.
- O'connor, T. E. (1962). Synthesis of boron nitride. *Journal of the American Chemical Society*, 84(9), 1753-1754.
- Öz M., Saritekin N. K., Bozkurt Ç., Yildirim G., (2016). Synthesis of highly ordered hBN in presence of group I/IIA carbonates by solid state reaction, *Crystal Research and Technology*, 51(6), 380-392.
- Öz, M., & Ulgen, A. T. (2021). Synthesis of boron nitride by solid state reactions: designation of barium salts effect, Editors: Hasan Akgül, Alparslan Dayangaç *Research & Reviews in Science and Mathematics-I*, (pp. 105-119)
- Rocca, A., Marino, A., Del Turco, S., Cappello, V., Parlanti, P., Pellegrino, M., Golberg, D., Mattoli, G., Ciofani, V. (2016). Peptin-coated boron nitride nanotubes: in vitro cyto-immune - compatibility on raw 264.7 macrophages, *Biochim. Biophys. Acta*, 1860, 775– 784.
- Suri, A. K., Subramanian, C., Sonber, J. K., & Murthy, T. C. (2010). Synthesis and consolidation of boron carbide: a review. *International Materials Reviews*, 55(1), 4-40.
- Tabbakh, T. A., Tyagi, P., Anandan, D., Sheldon, M. J., & Alshihri, S. (2022). Boron Nitride Fabrication Techniques and Physical Properties. *Characteristics and Applications of Boron*. IntechOpen.
- Thomas, J. R., Weston, N. E., & O'connor, T. E. (1962). Turbostratic boron nitride, thermal transformation to ordered-layer-lattice boron nitride. *Journal of the American Chemical Society*, 84(24), 4619-4622.
- Yoo, C. S., Akella, J., Cynn, H., & Nicol, M. (1997). Direct elementary reactions of boron and nitrogen at high pressures and temperatures. *Physical Review B*, 56(1), 140.

Chapter 7

A comparative study of the antimicrobial activities of field-grown and *in vitro* grown plants of *Verbascum scamandri* Murb.

Nurşen ÇÖRDÜK¹

Ebru CAMBAZ²

İlke KARAKAŞ³

Nurcihan HACIOĞLU DOĞRU⁴

1- Assoc. Prof. Dr.; Çanakkale Onsekiz Mart University, Faculty of Sciences, Department of Biology. nursencorduk@comu.edu.tr ORCID: 0000-0001-8499-4847

2- Çanakkale Onsekiz Mart University, School of Graduate Studies, Department of Biology. ebrucmbzz@gmail.com ORCID: 0000-0001-7301-9288

3- Lect.; Çanakkale Onsekiz Mart University, Vocational School of Health Services, Pharmacy Services Program. ilke.karakas@comu.edu.tr ORCID:0000-0001-6596-0879

4- Prof. Dr.; Çanakkale Onsekiz Mart University, Faculty of Sciences, Department of Biology. nurcihan.n@gmail.com ORCID: 0000-0002-5812-9398

INTRODUCTION

In the universe, all living organisms, especially plant, animal, and human, possess an important balance with each other. Mythological knowledge particularly reveals that especially plants are the most precious reward of the gods for human beings. The relationship established between human and plant species for centuries has led to the emergence of a science called ethnobotany. Today, natural products produced by plants as defense mechanisms, namely primary and secondary metabolites, have become the raw materials for many medicinal products (Faydaoğlu and Sürücüoğlu, 2011). Plants, through their metabolic activities necessary for their survival, generate important compounds that the human body can utilize. Among these metabolic products are essential oils (volatile oils, essences), alkaloids, tannins, bitter substances, and similar components, which have also served as natural sources for the treatment of

numerous diseases throughout human history. According to the World Health Organization (WHO), approximately 80% of the world's population (about 4 billion) has used herbal drugs as the primary step in the treatment of diseases and health problems. About 25% of the prescription drugs used today contain active ingredients derived from plants (Farnsworth et al., 1985).

Antibiotics are substances derived from microorganisms or chemically synthesized. They are effective against pathogenic microorganism species even in highly diluted concentrations, stopping their development or killing them completely. Since the discovery of the first antibiotic, Penicillin, thousands of antibiotics used in treatment or in clinical settings have been discovered. However, the discovery of new antibiotic derivatives has brought about one of the most significant health problems in all countries today: antibiotic resistance, along with side effects such as allergic reactions, teratogenic effects, accumulation of drug residues in food, endotoxic shock, and disruption of the natural flora (Alsan, 1999).

The genus *Verbascum* L. (Scrophulariaceae), commonly known as mullein and represented 459 species (natural and hybrid) worldwide (POWO, 2023). Taxa of this genus in Türkiye belong to the *Bothrospermae* section, comprising 130 hybrids and circa 250 natural species, with 80% of them being endemic (Murbeck, 1925; 1933; Huber-Morath, 1971; Karavelioğulları et al., 2014). Species within the *Verbascum* genus, a significant botanical asset in our country, have been traditionally utilized in treating various ailments. Numerous phytochemical and bioactivity studies have been conducted on *Verbascum* species. Consequently, the *Verbascum* genus stands as a group of plants that find significant application across diverse industrial sectors such as agriculture, medicine, pharmacy, and cosmetics. Through classes of secondary metabolites such as iridoids (Arrif et al., 2008), phenylethanoids (Brownstein et al., 2017), flavonoids (Nykmuhanova et al., 2019), neolignan glycosides (Akdemir et al., 2004), saponins (Kahraman et al., 2018), spermine alkaloids (Halimi and Nasrabadi, 2018), mucilage (Saeidi and Lorigooini, 2017), essential oils, and fatty acids (Boğa et al., 2016), this genus has potential for various properties such as antimicrobial effects (Hacıoğlu Dođru et al., 2021), anticancer activities (Zhao et al., 2013), antioxidant benefits (Mihailović et al., 2016), and antimutagenic potential (Erdođan, 2014). Additionally, it has been reported that the secondary metabolites of *Verbascum* species are used in traditional medicine for the treatment of diseases such as sore throat, lung diseases, and whooping cough (Prakash et al., 2016). Furthermore, they have been indicated for use in conditions like fever, snakebites, migraines, and intestinal diseases (Turker and Camper, 2002; Shinwari and Gilani, 2003; Ghorbani, 2005;

Georgiev et al., 2011; Sher, 2011). *Verbascum scamandri* Murb., commonly known as Kazdağı mullein, distributed in Kazdağı, Türkiye. This species is a biennial plant that can grow up to 50-80 cm tall, with a cylindrical and simple stem, short and dense tomentose or glabrous hairs (Huber-Morath, 1978). *V. scamandri* is an endemic species to Türkiye and is classified as endangered (EN, B1-B2a) according to IUCN criteria (IUCN, 2012).

The aim of this study was to determine the comparative antimicrobial activities of plants samples collected from different localities of Çanakkale, Türkiye and *in vitro* grown plants of *V. scamandri*.

MATERIAL AND METHODS

Plant materials

Plant samples of *Verbascum scamandri* were collected from different localities and altitudes of Bayramiç, Çanakkale, Türkiye during the flowering period in August and September of 2021. (Figure 1a and Table 1). The collected field-grown plant samples were washed with distilled water to eliminate any dust or dirt, and then left to dry at room temperature.

V. scamandri seeds were also collected from in Çanakkale-Bayramiç, Türkiye. The seeds were treated with 5% sodium hypochlorite solution for 20 minutes for surface sterilization, then rinsed four times with sterile distilled water. Following this, they were aseptically placed onto Murashige & Skoog (MS: Murashige and Skoog, 1962) basal medium containing 3% sucrose and 0.7% phytoagar for *in vitro* germination. These seeds were left to germinate in darkness at 25 ± 2 °C and $50\pm 5\%$ humidity in a plant growth chamber. Growth and development of germinated plants were continued in *in vitro* culture vessels under aseptic conditions. Germinated plants were transferred to MS medium with 3% sucrose and 0.7% phytoagar once every 4 weeks. All plants were kept in the growth chamber at 25 ± 2 °C under 16 h light/8 h dark photoperiod at a light intensity of $72 \mu\text{mol m}^{-2}\text{s}^{-1}$, $50\pm 5\%$ humidity. 11-week-old *in vitro* grown plant samples were used for analysis (Figure 1b).

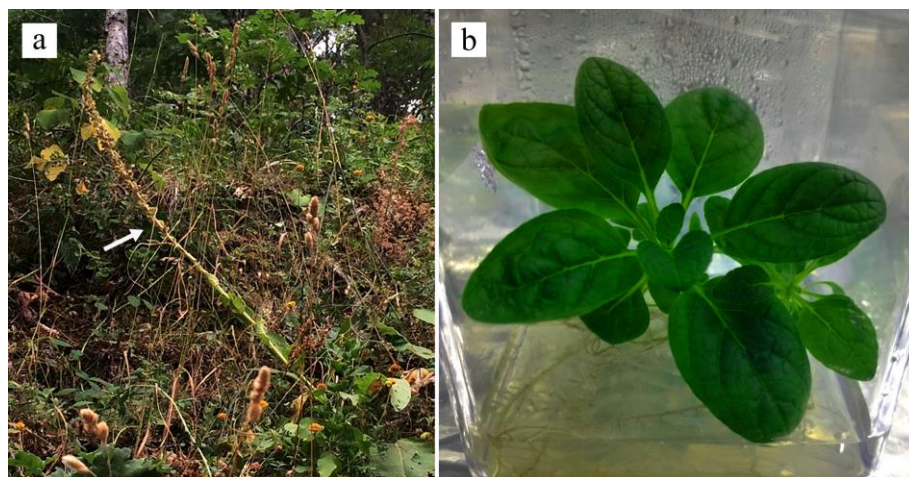


Figure 1: a) Field-grown plant, b) 11-week-old *in vitro* grown plant of *V. scamandri*

Table 1: The information of the localities that field-grown plants are collected

No	Locality	Altitude (m)	Latitude Longitude
1	Çırpılar Village, Bayramiç	625	39°47'26.4" N 26°53'48.2" E
2	Çırpılar Village, Bayramiç	675	39°47'03.2" N 26°53'57.5" E
3	Evciler Village, Bayramiç	800	39°45'19.7" N 26°51'08.2" E

Extraction of plants

The field-grown plants from three different localities and 11-week-old *in vitro* grown plant samples were ground using a mechanical crusher under aseptic conditions after being dried at room temperature. 15 grams of the weighed plant material was then soaked in 150 mL of distilled water for 12 h. For *in vitro* plant extraction, dried (at 50°C for 5 days) tissue powders (1 g) of plant were dissolved separately in 20 mL of 80% (v/v) distilled water overnight on a rotary shaker at room temperature. The extracts were filtered using Whatman filter paper no. 1 and the extracts were stored in sterile screw-capped bottles at 4°C (Dülger and Hacıoğlu, 2008).

Methods of antimicrobial activity

Three different methods were employed to compare the antimicrobial activities of the plant samples. In the antimicrobial activity experiments, a total of eight microorganisms were used, including Gram-negative (*Acinetobacter*

baumanii ATCC 19606, *Escherichia coli* NRRL B-3704, *Proteus vulgaris* ATCC 13315, *Pseudomonas aeruginosa* ATCC 27853), Gram-positive bacteria, and *Candida albicans* yeast culture.

Disc diffusion method

The experiments conducted using the disk diffusion method (Bauer et al., 1966) utilized Mueller Hinton Agar (MHA) as the standard growth medium. The revitalization of test bacteria involved inoculating a loopful of bacterial culture into Brain Heart Infusion Broth (BHI) for 24 h of incubation at $37\pm 0.1^\circ\text{C}$, while for yeast culture, Malt Extract Broth (MEB) was used at $30\pm 0.1^\circ\text{C}$ for the same duration. Following the 24-h period, the diameters of inhibition zones formed around the disks were measured. Additionally, disks solely soaked in the solvent were used as negative controls, while standard antibiotic disks [Penicillin (P10), Nystatin (NYS 100)] were utilized as positive controls (CLSI, 2006).

Minimal inhibition (MIC) and minimal microbicidal concentration (MMC) methods

The Minimum Inhibitory Concentration (MIC) values of plant extracts were determined using the microdilution method (Wikler, 2006). For the determination of inhibitory doses in serial dilutions of plant extracts (20, 15, 10, 5, 2.5, 1.25 mg/mL), 96-well microplates were employed on cultures that had been revitalized. Bacterial cultures were incubated at $37\pm 0.1^\circ\text{C}$, while yeast culture was incubated at $30\pm 0.1^\circ\text{C}$ for 24 h, and the first well showing no turbidity was identified as the MIC. Measurements were conducted in triplicate, and the MIC values were determined using a microplate reader device at a wavelength of 550 nm.

From wells where the dilution resulting in the MIC and above showed no visible growth, 10 μL inoculation was made onto MHA plates for bacterial cultures incubated at $37\pm 0.1^\circ\text{C}$ and onto yeast cultures at $30\pm 0.1^\circ\text{C}$ for 24 hours using the drop plate method. The extract concentration where no visible growth was observed in the Petri dish was considered as the Minimum Bactericidal Concentration (MBC) for bacteria and Minimum Fungicidal Concentration (MFC) for yeast cultures.

RESULTS AND DISCUSSION

The findings of disk diffusion, MIC, and MMC of the water extract from four different samples of the same species (3 field-grown plants and 1 *in vitro* grown plant) are presented in Tables 2 and 3, respectively.

Table 2: Disc diffusion results of *V. scamandri* field grown and *in vitro* extracts

Test Cultures	Extracts				Control antibiotics	
	V1	V2	V3	V4	P10	NY100
Gram (-)						
<i>A. baumannii</i>	6,00	6,00	6,00	6,00	12,0	ND
<i>E. coli</i>	7,00	6,00	6,00	6,00	16,0	ND
<i>P. vulgaris</i>	6,00	6,00	6,00	6,00	13,0	ND
<i>P. aeruginosa</i>	15,00	12,00	6,00	6,00	8,0	ND
Gram (+)						
<i>S. haemolyticus</i>	10,00	6,00	6,00	6,00	14,0	ND
<i>S. aureus</i>	6,00	6,00	6,00	12,00	15,0	ND
<i>B. subtilis</i>	10,00	8,00	8,00	6,00	14,0	ND
Yeast						
<i>C. albicans</i>	6,00	6,00	6,00	6,00	ND	16,0

V1: location no 1; V2: location no 2; V3: location no 3; V4: *in vitro* grown plant of *V. scamandri*; *Numbers indicate the diameters of inhibition zones.

P10: Penicillin (10 µg/disc); NY100: Nystatin (100 µg/disc);

The antagonistic effects of field-grown from three different locations and *in vitro* grown plant samples of *V. scamandri* against eight different test cultures using the disk diffusion method are presented in Table 2. The plant samples collected from Çirpılar village (V1) exhibited antibacterial activity against *P. aeruginosa* and *S. haemolyticus*, the plant samples collected from Çirpılar village (V2) against *P. aeruginosa* and *B. subtilis*, the plant samples collected from Evciler village (V3) against *B. subtilis*, and *in vitro* grown plant samples (V4) only against *S. aureus*. None of which showed antifungal activity against *C. albicans*. However, it was noted that compared to the control antibiotic (P10), the plant extracts collected from different altitudes in Çirpılar village (V1 and V2) demonstrated higher antibacterial activity against the *P. aeruginosa* bacterial culture (Table 2).

Table 3: MIC and MMC results of *V. scamandri* field grown and *in vitro* grown plant extracts

Test Cultures	Antimicrobial Test Methods									
	MIC				Control antibiotics		MMC			
	V1	V2	V3	V4	S10	NY100	V1	V2	V3	V4
<i>A. baumannii</i>	5,0	5,0	5,0	5,0	2,0	ND	5,0	5,0	5,0	5,0
<i>E. coli</i>	5,0	5,0	5,0	5,0	4,0	ND	5,0	5,0	5,0	5,0
<i>P. vulgaris</i>	5,0	5,0	5,0	5,0	4,0	ND	5,0	5,0	5,0	5,0
<i>P. aeruginosa</i>	1,25	2,5	5,0	5,0	1,0	ND	1,25	5,0	5,0	5,0
<i>S. haemolyticus</i>	2,5	5,0	5,0	5,0	5,0	ND	5,0	5,0	5,0	5,0
<i>S. aureus</i>	5,0	5,0	5,0	2,5	4,0	ND	5,0	5,0	5,0	5,0
<i>B. subtilis</i>	2,5	5,0	5,0	5,0	4,0	ND	5,0	5,0	5,0	5,0
<i>C. albicans</i>	5,0	5,0	5,0	5,0	ND	2,5	5,0	5,0	5,0	5,0

S10: Streptomycin (10 µg/disc)

MIC values ranging between 1.25-5.0 µg/mL against all tested bacterial and yeast cultures were determined for the four different extracts. However, it was observed that the MIC values of plant collected from Çırpılar village (V1) extract against *S. haemolyticus* and *B. subtilis*, as well as *in vitro* grown plant extract (V4) against *S. aureus*, were higher than the MIC value of the comparative antibiotic (Table 3).

The MMC values against the test cultures for the four different extracts, except for the 1.25 µg/mL value obtained for the plant collected from Çırpılar village (V1) extract against *P. aeruginosa* bacteria, were measured at 5.0 µg/mL (Table 3).

There have been numerous antimicrobial activity studies encompassing *Verbascum* species in the literature, especially including *V. speciosum*, *V. mucronatum*, and *V. thapsus* (Sener and Dulger, 2009; Amin et al., 2015; Dülger et al., 2015; Ghasemi et al., 2015; Anil et al., 2016). There are no studies of this scope with the endemic plant species *V. scamandri*, which is our study material, and our research is the first to compare *in vitro* specimens with different localities.

Dülger and Dülger (2018) examined the antibacterial activity of methanol extract from *V. antinori* against *S. aureus* ATCC 6538P, *P. vulgaris* ATCC 8427, *K. pneumoniae* UC57, *M. luteus* CCM 169, *E. coli* ATCC 11230, *L. monocytogenes* ATCC 15313, *B. cereus* ATCC 7064, and *P. aeruginosa* ATCC 27853 bacteria, reporting its effectiveness against Gram-positive bacteria. They also noted that the zone diameters obtained against *S. aureus* ATCC 6538P, *B. cereus* ATCC 7064, *L. monocytogenes* ATCC 15313, and *M. luteus* CCM 169

bacteria were higher than those of comparative antibiotics, measuring 22.6 mm, 20.4 mm, 14.2 mm, and 17.4 mm, respectively.

Similarly, in our study, we detected antibacterial effects on Gram-positive bacteria akin to Dülger and Dülger (2018). However, the notably high antagonistic relationship observed against *P. aeruginosa* ATCC 27853 Gram-negative bacteria differs from their study.

In their study, Özcan et al. (2010) reported that *V. antiochium* plant did not exhibit antimicrobial effects against *E. coli* and *C. albicans* strains. Amin et al. (2015) observed antimicrobial activity of *V. sinuatum* plant extracts against test microorganisms other than *P. aeruginosa* and *C. albicans*. Additionally, Morteza-Semnani et al. (2012) indicated the effectiveness of *V. thapsus* plant against *B. subtilis* PTCC 1023, *S. aureus* PTCC 1112, *S. typhi* PTCC 1639, *P. aeruginosa* PTCC 1074, and *Aspergillus niger* PTCC 5011, while reporting no antagonistic effect against *E. coli* PTCC 1330 and *C. albicans* PTCC 5027 cultures. These studies generally suggest that the *Verbascum* species investigated are effective against Gram-positive bacteria but ineffective against certain Gram-negative bacteria and *C. albicans* strains.

However, contrary to these findings, some other studies on *Verbascum* plant species, such as those by Sener and Dulger (2009), Noori et al. (2012), Dülger et al. (2015), and Ghasemi et al. (2015), have reported the effectiveness of these species, especially against Gram-negative bacteria like *E. coli* and *C. albicans* yeast culture.

Our findings, particularly the high antagonistic effect against Gram-negatives, different from the literature, are thought to stem from the use of a different *Verbascum* species in our study, leading to differences in active compounds and variations in the geographical origin of the samples.

The varied results obtained from *V. scamandri* plant samples from different localities, all belonging to the same species but demonstrating different outcomes on the same test microorganisms, are believed to result from the locality of collection, ecological conditions, seasonal variations, and whether the samples were field-grown or *in vitro* grown. Additionally, while higher antimicrobial activity was generally detected in field samples compared to those *in vitro* germinated and grown plant samples, noteworthy antagonistic activity against the *S. aureus* bacterium was observed in the *in vitro* grown plant samples.

ACKNOWLEDGEMENTS

We thank Prof. Dr. Ersin KARABACAK, Department of the Biology, Çanakkale Onsekiz Mart University, Çanakkale, Türkiye for the identification of the species in the field study.

REFERENCES

- Akdemir, Z., Kahraman, Ç., Tatlı, I.I., Akkol, E.K., Süntar, I., and Keles, H. (2011). Bioassay-guided isolation of anti-inflammatory, antinociceptive and wound healer glycosides from the flowers of *Verbascum mucronatum* Lam. *Journal of Ethnopharmacology*, 136(3), 436-443.
- Akdemir, Z., Tatlı, I.I., Bedir, E., and Khan, I.A. (2004). Neolignan and phenylethanoid glycosides from *Verbascum salviifolium* Boiss. *Turkish Journal of Chemistry*, 28, 621-628.
- Alsan S. (1999). Yarının Antibiyotikleri. *Tübitak Bilim ve Teknik Dergisi*, 376.
- Amin, J.N, Batool, M., and Abu-hadid, M.M. (2015). Screening antibacterial and antifungal activities and evaluation of exhaustive extractions yields for *Verbascum sinuatum* L. *International Research Ayurveda Pharmacy*, 6, 105-110.
- Anil, S., Dosler, S., and Mericli, A.H. (2016). Chemical Composition and Antimicrobial Activity of *Verbascum caesareum*. *Chemistry of Natural Compounds*, 52(1), 125-126.
- Arrif, S., Lavaud, C., Benkhaled, M. (2008). Iridoids from *Verbascum dentifolium*. *Biochemical Systematics and Ecology*, 8, 669-673.
- Bauer A.W., Kirby W.M., Sherris J.C., and Turck M. (1966). Antibiotic Susceptibility Testing by a Standardized Single Disk Method. *American Journal of Clinical Pathology*, 45, 493-496.
- Boğa, M., Ertaş, A., Haşimi, N., Demirci, S., and Abdullah, M. (2016). Phenolic profile, fatty acid and essential oil composition analysis and antioxidant, anti-Alzheimer and antibacterial activities of *Verbascum flavidum* extracts. *Chiang Mai Journal of Science*, 43, 1090-1101.
- Brownstein, K.J., Gargouri, M., Folk, W.R., and Gang, D.R. (2017). Iridoid and phenylethanoid/phenylpropanoid metabolite profiles of *Scrophularia* and *Verbascum* species used medicinally in North America. *Metabolomics*, 13, 133.
- CLSI, (2006). Clinical and Laboratory Standards Institute. Methods for Dilution Antimicrobial Susceptibility Tests for Bacteria That Grow Aerobically; Approved Standard-Seventh Edition. M07- A7, Villanova, PA, USA.
- Dülger B., and Hacıoğlu N. (2008). Antimicrobial Activity of Some Endemic *Verbascum* and *Scrophularia* Species from Turkey. *Asian Journal of Chemistry*, 20, 3779-3785.
- Dülger, B., and Dülger, B. (2018). Antibacterial Activity of *Verbascum antinori*. *Konuralp Medical Journal*, 10(3), 395-398.
- Dülger, G., Tutenocaklı, T., and Dulger, B. (2015). Antimicrobial potential of the leaves of common mullein (*Verbascum thapsus* L., Scrophulariaceae)

- on microorganisms isolated from urinary tract infections. *Journal of Medicinal Plants Studies*, 3(2), 86-89.
- Erdoğan, E.A. (2014). Lamiaceae Familyasına Ait Bazı Bitkilerin Uçucu Yağ İçeriklerinin Belirlenmesi, Antimikrobiyal ve Antimutajenik Aktivitelerinin Araştırılması. Doktora Tezi, Mersin Üniversitesi, Türkiye.
- Farnsworth N.R., Akerev O., and Bingel A.S. (1985). Medicinal Plants in Therapy. *Bulletin of the World Health Organization*, 63, 9865-9871.
- Faydaoğlu E., and Sürücüoğlu M.S. (2011). Geçmişten Günümüze Tıbbi ve Aromatik Bitkilerin Kullanılması ve Ekonomik Önemi. Kastamonu Üniversitesi, *Orman Fakültesi Dergisi*, 11(1), 52-67.
- Georgiev, M., Alipieva, K., Orhan, I., Abrashev, R., Denev, P., and Angelova, M. (2011). Antioxidant and cholinesterases inhibitory activities of *Verbascum xanthophoeniceum* Griseb. and its phenylethanoid glycosides. *Food Chemistry*, 128, 100-105.
- Ghasemi, F., Rezaei, F., Araghi, A., and Tabari, M.A. (2015). Antimicrobial Activity of Aqueous-Alcoholic Extracts and the Essential Oil of *Verbascum thapsus* L. *Jundishapur Journal of Natural Pharmaceutical Products*, 10(3).
- Ghorbani, A. (2005). Studies on pharmaceutical ethnobotany in the region of Turkmen Sahra, north of Iran:(Part 1): general results. *Journal of ethnopharmacology*, 102(1), 58-68.
- Hacıoğlu Doğru, N., Demir, N., and Yılmaz, Ö. (2021). Three species of *Verbascum* L. from Northwest Anatolia of Turkey as a source of biological activities. *Turkish Journal of Analytical Chemistry*, 3(1), 19-26.
- Halimi, M., and Nasrabadi, M. (2018). Isolation and identification macrocyclic spermine alkaloid (protoverbine) from *Verbascum speciosum*. *Iranian Chemical Communication*, 6, 143-147.
- Heywood, V.H. (1993). Flowering plants of the world. Oxford University Press.
- Huber-Morath, A. (1971). Die Türkischen *Verbasceen* (pp. 8-35). Zürich: Kommissionsverlag von Gebrüder Fretz AG.
- Huber-Morath, A. (1978). *Verbascum* L. Editör P. H. Davis, *Flora of Turkey and the East Aegean Islands, Vol VI* (pp. 461-603). Edinburgh: Edinburgh University Press.
- IUCN, International Union for Conservation of Nature. (2012). IUCN Red List categories and criteria: Version 3.1.
- Kahraman, C., Tatli, İ., Kart, D., Ekizoglu, M., and Akdemir, Z. (2018). Structure elucidation and antimicrobial activities of secondary

- metabolites from the flowery parts of *Verbascum mucronatum* lam. *Turkish Journal of Pharmaceutical Sciences*, 15, 231-237.
- Karavelioğulları, F.A., Yüce, E., and Başer, B. (2014). *Verbascum duzgunbabadagensis* (Scrophulariaceae), a new species from eastern Anatolia, Turkey. *Phytotaxa*, 181 (1), 47-53.
- Mihailović, V., Kreft, S., Benković, E.T., Ivanović, N., and Stanković, M.S. (2016). Chemical profile, antioxidant activity and stability in stimulated gastrointestinal tract model system of three *Verbascum* species. *Industrial Crops and Products*, 89, 141-151.
- Morteza-Semnani, K., Saeedi, M., and Akbarzadeh, M. (2012). Chemical Composition and Antimicrobial Activity of the Essential Oil of *Verbascum thapsus* L. *Journal of Essential Oil Bearing Plants*, 15(3), 373-379.
- Murashige, T., and Skoog, F. (1962). A revised medium for rapid growth and bioassays with tobacco tissue cultures. *Physiologia Plantarum*, 15(3), 473-497.
- Murbeck, S. (1925). Monographie der Gattung *Celsia*. *Acta Universitatis Lundensis*, 22(1), 1-20.
- Murbeck, S. (1933). Monographie der Gattung *Verbascum*. *Acta Universitatis Lundensis*, 29(2), 1-630.
- Noori, M., Malayeri, B., Moosaei, M., Pakzad, R., and Piriye, M.H. (2012). Effects of heavy metals on the antibacterial properties of *Verbascum speciosum* Schard. *Revista Científica UDO Agrícola*, 12(2), 463-471.
- Nykmukanova, M.M., Mukazhanova, Z.B., Kabdysalym, K., Eskalieva, B.K., and Beyatli, A. (2019). Flavonoids from *Verbascum marschallianum* and *V. orientale*. *Chemistry of Natural Compounds*, 55, 937-938.
- Özcan, B., Yilmaz, M., and Caliskan, M. (2010). Antimicrobial and Antioxidant Activities of Various Extracts of *Verbascum antiochium* Boiss. (Scrophulariaceae). *Journal of Medicinal Food*, 1147-1152.
- POWO (2023). Plants of the World Online. *Verbascum* L. retrieved on April 13. <https://powo.science.kew.org/taxon/urn:lsid:ipni.org:names:30049308-2>.
- Prakash, V., Rana, S., and Sagar, A. (2016). Studies on antibacterial activity of *Verbascum thapsus*. *Journal of Medicinal Plants Studies*, 4(3), 101-103.
- Saeidi, K., and Lorigooini, Z. (2017). Determination of mucilage content of mullein (*Verbascum songaricum*) populations. *Journal of Pharmaceutical Sciences and Research*, 9, 2641-2643.

- Sener, A., and Dulger, B. (2009). Antimicrobial activity of the leaves of *Verbascum sinuatum* L. on microorganisms isolated from urinary tract infection. *African Journal of Microbiology Research*, 3(11), 778-781.
- Sher, H. (2011). Ethnoecological evaluation of some medicinal and aromatic plants of Kot Malakand agency, Pakistan. *Scientific Research and Essays*, 6(10), 2164-2173.
- Shinwari, Z. K., and Gilani, S.S. (2003). Sustainable harvest of medicinal plants at Bulashbar Nullah, Astore (Northern Pakistan). *Journal of Ethnopharmacology*, 84(2-3), 289-298.
- Tatlı, İ.İ., and Akdemir, Z. (2004). Chemical constituents of *Verbascum* L. Species. *FABAD Journal of Pharmaceutical Sciences*, 29, 93-107.
- Turker, A.U., and Camper, N.D. (2002). Biological activity of common mullein, a medicinal plant. *Journal of Ethnopharmacology*, 82(2-3), 117-125.
- Wikler, M.A. (2006). Methods for Dilution Antimicrobial Susceptibility Tests for bacteria That Grow Aerobically. *Clinical & Laboratory Standards Institute*, 61-64.
- Zhao, Y.L., Wang, S.F., Li, Y., He, Q.X., Liu, K.C., Yang, Y.P., and Li, X.L. (2011). Isolation of chemical constituents from the aerial parts of *Verbascum thapsus* and their antiangiogenic and antiproliferative activities. *Archives of Pharmacal Research*, 34(5), 703-707.

Chapter 8

Determination the antimicrobial activities of *Verbascum hasbenlii* Aytac & H. Duman, an endemic species of Türkiye

Nurşen ÇÖRDÜK¹

Ebru CAMBAZ²

İlke KARAKAŞ³

Nurcihan HACIOĞLU DOĞRU⁴

1- Assoc. Prof. Dr.; Çanakkale Onsekiz Mart University, Faculty of Sciences, Department of Biology. nursencorduk@comu.edu.tr ORCID: 0000-0001-8499-4847

2- Çanakkale Onsekiz Mart University, School of Graduate Studies, Department of Biology. ebrucmbzz@gmail.com ORCID: 0000-0001-7301-9288

3- Lect.; Çanakkale Onsekiz Mart University, Vocational School of Health Services, Pharmacy Services Program. ilke.karakas@comu.edu.tr ORCID:0000-0001-6596-0879

4- Prof. Dr.; Çanakkale Onsekiz Mart University, Faculty of Sciences, Department of Biology. nurcihan.n@gmail.com ORCID: 0000-0002-5812-9398

INTRODUCTION

In the universe, all living organisms, including plants, animals, and humans, maintain a delicate balance with one another. Mythology often depicts plants as a precious gift from the gods to humanity. This enduring relationship has given rise to the field of ethnobotany and studies the relationship between people and plants. Plants produce vital compounds as part of their metabolic processes, such as essential oils, alkaloids, tannins, and more, which have served as natural remedies for various ailments over time. Today, many medicinal products are derived from natural plant products, which contain this primary and secondary metabolites that plants produce as defense mechanisms (Faydaoğlu and

Sürücüoğlu, 2011). The World Health Organization (WHO) notes that approximately 80% of the global population, around 4 billion people, have utilized herbal medicine as their primary healthcare approach. Moreover, a significant portion of today's prescription drugs contains plant-derived active components, reflecting the historical significance of plant-based remedies (Farnsworth et al., 1985).

Antibiotics, either originating from microorganisms or chemically synthesized, have played a crucial role in treating pathogenic microorganisms by either halting their growth or eradicating them. Since the discovery of the first antibiotic, Penicillin, thousands of antibiotics have been discovered for use in treatment or clinical settings. However, the progress in the field of antibiotics has led to a pressing global health concern: antibiotic resistance. In addition, antibiotics can cause side effects such as allergic reactions, teratogenic effects, drug residue accumulation in food, endotoxic shock, and disruption of natural flora, which pose significant health risks (Alsan, 1999).

The genus *Verbascum* L. (including the genus *Celsia* L.) within the Scrophulariaceae family encompasses ~459 species (natural and hybrid) in Europe, Asia, and Northeast Africa (POWO, 2023). Türkiye stands as one of the richest countries in this genus, hosting ~250 species, and about 80% of these species are endemic to the country (Kaynak et al. 2006; Bani et al. 2010, Karavelioğulları et al. 2012; 2015; Çeçen 2015, Çıngay and Karavelioğulları 2016). In addition, *Verbascum* genus is known for its richness in species and the presence of numerous phytochemical compounds, which have been utilized in traditional medicine. This genus is extensively employed in industrial sectors such as pharmaceuticals and cosmetics. Through classes of secondary metabolites such as iridoids (Arrif et al., 2008), phenylethanoids (Brownstein et al., 2017), flavonoids (Nykjukanova et al., 2019), neolignan glycosides (Akdemir et al., 2004), saponins (Kahraman et al., 2018), spermine alkaloids (Halimi and Nasrabadi, 2018), mucilage (Saeidi and Lorigooini, 2017), essential oils, and fatty acids (Boğa et al., 2016). Thanks to their secondary metabolites, *Verbascum* species have been reported to be used in the treatment of various conditions such as wounds (Rajbhandari et al., 2009), migraine (Grieve 1995), asthma (Kay, 1978), and earache (Lans et al., 2007). This is attributed to their antimicrobial (Hacıoğlu Doğru et al., 2021), antioxidant, and antiproliferative activity (Amin et al., 2020), as well as their anti-inflammatory and antinociceptive (Diker et al., 2019), anti-inflammatory and hepatoprotective effects (El Gizawy et al., 2019), antihyperlipidemic (Aboutabl et al., 1999), immunomodulatory (Klimek et al., 1994), anti-carcinogen activity (Zhao et al., 2011), and wound healing properties (Selseleh et al., 2020). *Verbascum*

hasbenlii Aytac & H. Duman (sect. *Bothrosperma* Murb.) is an local endemic species distributed in Çanakkale-Çan (B1), Türkiye (Aytaç and Duman, 2012). *V. hasbenlii* is grows on large boulders in metamorphic rocks, a biennial to perennial plant species, with long multicellular eglandular to glandular hairs throughout and 15-30 cm tall (Aytaç &Duman, 2012). According to IUCN criteria, it is classified under the Critical (CR) category (IUCN, 2001).

The aim of this study was to determine the comparative antimicrobial activities of *V. hasbenlii* samples collected from field-grown and *in vitro* growing.

MATERIAL AND METHODS

Plant materials

Verbascum hasbenlii plants and seeds were collected from Çanakkale-Çan province during the vegetation period (Figure 1a). The gathered field-grown plants were dry at room temperature.

The seeds of the species underwent a 20-minute treatment with 5% sodium hypochlorite followed by three washes with sterile distilled water. These surface-sterilized seeds were then placed onto Murashige and Skoog (MS: Murashige and Skoog, 1962) basal nutrient medium supplemented with 3% sucrose and 0.7% phytoagar. These cultured seeds were left for *in vitro* germination in a plant growth chamber maintained at 25±2 °C and 50±5% humidity in darkness. Following germination, a photoperiod of 16 h of light and 8 h of darkness was applied, maintaining a light intensity of 72 µmol m⁻²s⁻¹. The plants were regularly transferred to fresh MS nutrient medium every 4 weeks as they grew. Plants grown *in vitro* for a duration of 13 weeks were utilized for analysis (Figure 1b).

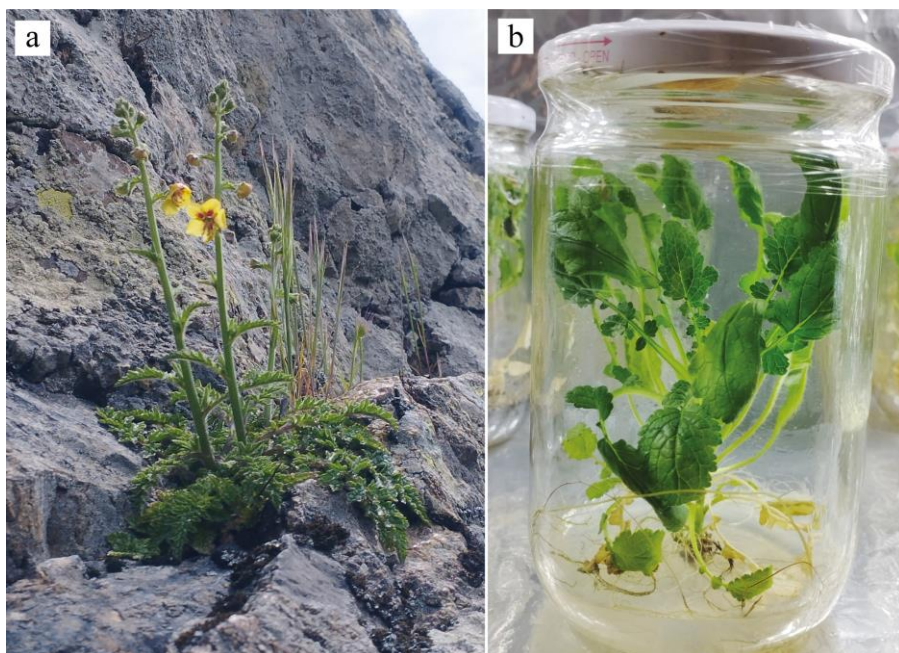


Figure 1: a) Field-grown plant, b) 13-week-old *in vitro* growing plant of *V. hasbenlii*

Extraction of plants

The field-grown plants and 13-week-old *in vitro* grown plant samples were ground using a mechanical crusher under aseptic conditions after being dried at room temperature. 15 grams of the weighed plant material was then soaked in 150 mL of distilled water for 12 h. For *in vitro* plant extraction, dried (at 50°C for 5 days) tissue powders (1 g) of plant were dissolved separately in 20 mL of 80% (v/v) distilled water overnight on a rotary shaker at room temperature. The extracts were filtered using Whatman filter paper no. 1 and the extracts were stored in sterile screw-capped bottles at 4°C (Dülger and Hacıoğlu, 2008).

Methods of Antimicrobial Activity

Three different methods were employed to compare the antimicrobial activities of the plant samples. In the antimicrobial activity experiments, a total of eight microorganisms were used, including Gram-negative (*Acinetobacter baumannii* ATCC 19606, *Escherichia coli* NRRL B-3704, *Proteus vulgaris* ATCC 13315, *Pseudomonas aeruginosa* ATCC 27853), Gram-positive bacteria, and *Candida albicans* yeast culture.

Disc diffusion method

The experiments conducted using the disk diffusion method (Bauer et al., 1966) utilized Mueller Hinton Agar (MHA) as the standard growth medium. The revitalization of test bacteria involved inoculating a loopful of bacterial culture into Brain Heart Infusion Broth (BHI) for 24 h of incubation at $37\pm 0.1^{\circ}\text{C}$, while for yeast culture, Malt Extract Broth (MEB) was used at $30\pm 0.1^{\circ}\text{C}$ for the same duration. Following the 24-h period, the diameters of inhibition zones formed around the disks were measured. Additionally, disks solely soaked in the solvent were used as negative controls, while standard antibiotic disks [Penicillin (P10), Nystatin (NYS 100)] were utilized as positive controls (CLSI, 2006).

Minimal inhibition (MIC) and minimal microbicidal concentration (MMC) methods

The Minimum Inhibitory Concentration (MIC) values of plant extracts were determined using the microdilution method (Wikler, 2006). For the determination of inhibitory doses in serial dilutions of plant extracts (20, 15, 10, 5, 2.5, 1.25 mg/mL), 96-well microplates were employed on cultures that had been revitalized. Bacterial cultures were incubated at $37\pm 0.1^{\circ}\text{C}$, while yeast culture was incubated at $30\pm 0.1^{\circ}\text{C}$ for 24 h, and the first well showing no turbidity was identified as the MIC. Measurements were conducted in triplicate, and the MIC values were determined using a microplate reader device at a wavelength of 550 nm.

From wells where the dilution resulting in the MIC and above showed no visible growth, 10 μL inoculation was made onto MHA plates for bacterial cultures incubated at $37\pm 0.1^{\circ}\text{C}$ and onto yeast cultures at $30\pm 0.1^{\circ}\text{C}$ for 24 hours using the drop plate method. The extract concentration where no visible growth was observed in the Petri dish was considered as the Minimum Bactericidal Concentration (MBC) for bacteria and Minimum Fungicidal Concentration (MFC) for yeast cultures.

RESULT AND DISCUSSION

Significantly high antimicrobial activities were observed against all test cultures except for *P. aeruginosa*, with both natural and *in vitro* extracts of *V. hasbenlii* according to the disk diffusion method and the disk diffusion, MIC and MMC findings of the water extract obtained from field grown and *in vitro* plant samples of *V. hasbenlii* species are given in Table 1, respectively. Field grown plant extract (VH1) showed high antagonistic effects against *A.*

baumannii, *P. vulgaris*, and *S. aureus*, while *in vitro* grown plant extract (VH2) exhibited this effect against *E. coli* and *P. vulgaris*, surpassing the control antibiotic P10. The MIC values of Field grown plant extract (VH1) and *in vitro* grown plant extract (VH2) varied between 0.3125–5.0 µg/mL for all tested bacteria and yeast cultures. However, except for *A. baumannii* and *P. aeruginosa* test bacteria, MIC values were higher than the comparative antibiotics S10 and NY100 for all cultures. MMC values against test cultures ranged between 0.3125–5.0 µg/mL for both extracts (Table 1).

Table 1. Disc diffusion results of *V. hasbenlii* field grown and *in vitro* extracts

Test Cultures	Antimicrobial Activities							
	Disc Diffusion		Control antibiotics		MIC/MMC		Control antibiotics	
	VH1	VH2	P10	NY100	VH1	VH2	S10	NY100
<i>A. baumannii</i>	14,00	10,00	12,0	ND	2,5/2,5	2,5/5,0	2,0	ND
<i>E. coli</i>	13,00	16,00	16,0	ND	0,625/2,5	1,25/2,5	4,0	ND
<i>P. vulgaris</i>	20,00	25,00	13,0	ND	0,3125/0,3125	0,15625/0,3125	4,0	ND
<i>P. aeruginosa</i>	7,00	8,00	8,0	ND	5,0/5,0	5,0/5,0	1,0	ND
<i>S. haemolyticus</i>	10,00	10,00	14,0	ND	2,5/2,5	2,5/2,5	5,0	ND
<i>S. aureus</i>	16,00	12,00	15,0	ND	1,25/1,25	2,5/5,0	4,0	ND
<i>B. subtilis</i>	12,00	11,00	14,0	ND	2,5/5,0	2,5/5,0	4,0	ND
<i>C. albicans</i>	13,00	14,00	ND	16,0	1,25/2,5	1,25/1,25	ND	2,5

VH1: field grown; VH2: *in vitro* grown plant of *V. hasbenlii*. *Numbers indicate the diameters of inhibition zones. P10: Penicillin (10 µg/disc); NY100: Nystatin (100 µg/disc); S10: Streptomycin (10 µg/disc).

Despite numerous studies on antimicrobial activity encompassing *Verbascum* genus members in the literature, no research on this specific endemic *V. hasbenlii* plant species was found, possibly due to its local endemic nature (Şener and Dülger 2009; Akdemir et al., 2011; Amin et al., 2015; Dülger et al., 2015; Ghasemi et al., 2015; Anil et al., 2016).

Dülger and Dülger (2018) examined the antibacterial activity of methanol extract of *V. antinori* against *S. aureus* ATCC 6538P, *P. vulgaris* ATCC 8427, *K. pneumoniae* UC57, *M. luteus* CCM 169, *E. coli* ATCC 11230, *L. monocytogenes* ATCC 15313, *B. cereus* ATCC 7064, and *P. aeruginosa* ATCC 27853 bacteria, reporting effectiveness against Gram-positive bacteria. Additionally, they noted zone diameters of 22.6 mm, 20.4 mm, 14.2 mm, and 17.4 mm, respectively, for *S. aureus* ATCC 6538P, *B. cereus* ATCC 7064, *L.*

monocytogenes ATCC 15313, and *M. luteus* CCM 169, which were higher compared to reference antibiotics. Contrary to Dülger and Dülger (2018), although antagonistic effects against Gram-positives were observed in our study, particularly noteworthy was the higher antibacterial activity against Gram-negatives compared to the reference antibiotic. Hence, our findings differ in this aspect.

Özcan et al. (2010) reported no antimicrobial effect of *V. antiochium* on *E. coli* and *C. albicans* strains in their study, whereas Amin et al. (2015) observed antimicrobial activity of *V. sinuatum* plant extracts against test microorganisms excluding *P. aeruginosa* and *C. albicans*. Morteza-Semnani et al. (2012) found *V. thapsus* effective against *B. subtilis* PTCC 1023, *S. aureus* PTCC 1112, *S. typhi* PTCC 1639, *P. aeruginosa* PTCC 1074, and *Aspergillus niger* PTCC 5011, but without antagonistic effects on *E. coli* PTCC 1330 and *C. albicans* PTCC 5027 cultures. These studies generally indicated effectiveness of the tested *Verbascum* species against Gram-positive bacteria, inefficacy against some Gram-negatives, and *C. albicans*. However, contrary to these data, certain studies reported effectiveness of *Verbascum* species, including *E. coli* and *C. albicans* cultures (Şener and Dülger, 2009; Dülger et al., 2015; Ghasemi et al., 2015).

Our study, focusing on *V. hasbenlii*, a locally endemic species different from other *Verbascum* species in the literature, suggests that the observed variations in antagonistic activity might stem from habitat, ecology, seasonal collection of the plant, altitude, and similar conditions. Furthermore, the high antagonistic activity obtained from both the field grown and *in vitro* samples of this species indicates its potential as a valuable source for medical research.

REFERENCES

- Aboutabl, E.A., Goneid, M.H., Soliman, S.N., Selim, A. A., (1999). Analysis of certain plant polysaccharides and study of their antihyperlipidemic activity. *Al-Azhar Journal of Pharmaceutical Sciences*, 24, 187- 195.
- Akdemir, Z., Kahraman, Ç., Tatlı, I.I., Akkol, E.K., Süntar, I., Keles, H., 2011. Bioassay-guided isolation of anti-inflammatory, antinociceptive and wound healer glycosides from the flowers of *Verbascum mucronatum* Lam. *Journal of Ethnopharmacology*, 136(3): 436-443. <https://doi.org/10.1016/j.jep.2010.05.059>
- Akdemir, Z., Tatlı, I.I., Bedir, E., and Khan, I.A. (2004). Neolignan and phenylethanoid glycosides from *Verbascum salviifolium* Boiss. *Turkish Journal of Chemistry*, 28, 621-628.
- Alsan S. (1999). Yarının Antibiyotikleri. *Tübitak Bilim ve Teknik Dergisi*, 376.
- Amin J.N, Batool M., Abu-hadid M.M., 2015. Screening Antibacterial and Antifungal Activities and Evaluation of Exhaustive Extractions Yields for *Verbascum sinuatum* L. *International Research Ayurveda Pharmcy*, 6: 105-110.
- Amin, J.N, Batool, M., and Abu-hadid, M.M. (2015). Screening antibacterial and antifungal activities and evaluation of exhaustive extractions yields for *Verbascum sinuatum* L. *International Research Ayurveda Pharmcy*, 6, 105-110.
- Anil S., Dosler S., Mericli A.H., 2016. Chemical Composition and Antimicrobial Activity of *Verbascum caesareum*. *Chemistry of Natural Compounds*, 52 (1): 125-126.
- Arrif, S., Lavaud, C., Benkhaled, M. (2008). Iridoids from *Verbascum dentifolium*. *Biochemical Systematics and Ecology*, 8, 669-673.
- Aytaç Z., and Duman H. (2012). *Verbascum hasbenlii* (Scrophulariaceae), a new species from Turkey. *Turkish Journal of Botany*, 36,322-327.
- Bani, B., Adıguzel, N. and Karavelioğulları, F.A. (2010) A new species (*Verbascum turcicum* sp. nov., Scrophulariaceae) from South Anatolia, Turkey. *Annales Botanici Fennici*, 47: 489-492.
- Bauer A.W., Kirby W.M., Sherris J.C., Turck M., 1966. Antibiotic Susceptibility Testing by a Standardized Single Disk Method. *Am. J. Clin. Pathol.*, 45: 493-496.
- Boğa, M., Ertaş, A., Haşimi, N., Demirci, S., and Abdullah, M. (2016). Phenolic profile, fatty acid and essential oil composition analysis and antioxidant, anti-Alzheimer and antibacterial activities of *Verbascum flavidum* extracts. *Chiang Mai Journal of Science*, 43, 1090-1101.

- Brownstein, K.J., Gargouri, M., Folk, W.R., and Gang, D.R. (2017). Iridoid and phenylethanoid/phenylpropanoid metabolite profiles of *Scrophularia* and *Verbascum* species used medicinally in North America. *Metabolomics*, 13, 133.
- Çeçen, Ö., Karavelioğulları, F.A. Ayvaz, Ü. (2015) *Verbascum misirdalianum* (Scrophulariaceae), a new species from central Anatolia, Turkey. *Phytotaxa*, 217(1), 96-99.
- Çingay, B. and Karavelioğulları, F.A. (2016) A new species of *Verbascum*, *V. nihatgoekyigitii* (Scrophulariaceae), from southeastern Anatolia, Turkey. *Phytotaxa*, 269, 287-293.
- CLSI, 2006. Clinical and Laboratory Standarts Institute. Methods for Dilution Antimicrobial Susceptibility Tests for Bacteria That Grow Aerobically; Approved Standard-Seventh Edition. M07- A7, Villanova, PA, USA.
- Diker, N. Y., Kahraman, C., Kupeli Akkol, E., Karaoglu, M. T., Comoglu, T., Akdemir, Z. S. and Tatli Cankaya, I. I. (2019). The evaluation of sterile solutions of Ilwensisaponin A and C from *Verbascum pterocalycinum* var. *mutense* Hub.-Mor. On antiviral, antinociceptive and anti-inflammatory activities. *Saudi Pharmaceutical Journal*, 27(3), 432-436.
- Dülger B., Dülger B., 2018. Antibacterial Activity of *Verbascum antinori*. *Konuralp Medical Journal*, 10 (3): 395-398.
- Dülger B., Hacıoğlu N., 2008. Antimicrobial Activity Of Some Endemic *Verbascum* And *Scrophularia* Species From Turkey. *Asian Journal of Chemistry*, 20: 3779-3785
- Dülger G., Tutenocakli T., Dulger B., 2015. Antimicrobial Potential of The Leaves of Common Mullein (*Verbascum thapsus* L., Scrophulariaceae) on Microorganisms Isolated from Urinary Tract Infections. *Journal of Medicinal Plants Studies*, 3 (2): 86-89.
- El Gizawy, H., Hussein, M.A., and Abdel-Sattar, E. (2019) Biological activities, isolated compounds and HPLC profile of *Verbascum nubicum*. *Pharmaceutical Biology*, 57(1), 485-497.
- Farnsworth N.R., Akerev O., and Bingel A.S. (1985). Medicinal Plants in Therapy. *Bulletin of the World Health Organization*, 63, 9865-9871.
- Faydaoğlu E., and Sürücüoğlu M.S. (2011). Geçmişten Günümüze Tıbbi ve Aromatik Bitkilerin Kullanılması ve Ekonomik Önemi. Kastamonu Üniversitesi, *Orman Fakültesi Dergisi*, 11(1), 52-67.
- Ghasemi F., Rezaei F., Araghi A., Tabari M.A., 2015. Antimicrobial Activity of Aqueous-Alcoholic Extracts and the Essential Oil of *Verbascum thapsus* L. *Jundishapur Journal of Natural Pharmaceutical Products*, 10 (3): 1-5.
- Grieve MA (1995) *A modern herbal*. Barnes and Noble Books, New York

- Hacıoğlu Doğru, N., Demir, N., and Yılmaz, Ö. (2021). Three species of *Verbascum* L. from Northwest Anatolia of Turkey as a source of biological activities. *Turkish Journal of Analytical Chemistry*, 3(1), 19-26.
- Halimi, M., and Nasrabadi, M. (2018). Isolation and identification macrocyclic spermine alkaloid (protoverbine) from *Verbascum speciosum*. *Iranian Chemical Communication*, 6, 143-147.
- IUCN (2001). IUCN Red List Categories and Criteria, version 3.1-Gland and Cambridge: IUCN Survival Commission.
- Kahraman, C., Tatlı, İ., Kart, D., Ekizoglu, M., and Akdemir, Z. (2018). Structure elucidation and antimicrobial activities of secondary metabolites from the flowery parts of *Verbascum mucronatum* lam. *Turkish Journal of Pharmaceutical Sciences*, 15, 231-237.
- Karavelioğulları, F.A. (2012) *Verbascum* L. In: Güner, A., Aslan, S., Ekim., T., Vural, M. and Babaç, M.T. (Eds.) *Türkiye Bitkileri listesi (Damarlı Bitkiler)*. Nezahat Gökyiğit Botanik Bahçesi ve Flora Araştırmaları Derneği Yayını, İstanbul, pp. 850–870.
- Karavelioğulları, F.A. (2015) *Verbascum ibrahim-belenlii* (Scrophulariaceae), a new species from East Anatolia, Turkey. *Phytotaxa* 212: 246–248.
- Kay, M. (1978). Medical botany: Plants affecting man's health. Walter H. Lewis and memory P. F. Elvin-Lewis. *Medical Anthropology Newsletter*, 10(1), 15-16.
- Kaynak, G., Daşkın, R., Yılmaz, O. and Erdoğan, E. (2006) *Verbascum yurtkurianum* (Scrophulariaceae) a new species from north West Anatolia, Turkey. *Annales Botanici Fennici*, 43, 456-459.
- Klimek B, Stepien H. (1994). Effect of some constituents of mullein (*Verbascum* sp.) on proliferation of rat splenocytes *in vitro*. *European Journal of Pharmaceutical Sciences*, 2, 123.
- Lans, C., Turner, N., Khan, T., Brauer, G., & Boepple, W. (2007). Ethnoveterinary medicines used for ruminants in British Columbia, Canada. *Journal of Ethnobiology and Ethnomedicine*, 3, 11.
- Murashige, T., and Skoog, F. (1962). A revised medium for rapid growth and bioassays with tobacco tissue cultures. *Physiologia Plantarum*, 15(3), 473-497.
- Nykmukanova, M.M., Mukazhanova, Z.B., Kabdysalym, K., Eskalieva, B.K., and Beyatli, A. (2019). Flavonoids from *Verbascum marschallianum* and *V. orientale*. *Chemistry of Natural Compounds*, 55, 937-938.

- Özcan B., Yılmaz M., Caliskan M., 2010. Antimicrobial and Antioxidant Activities of Various Extracts of *Verbascum antiochium* Boiss. (Scrophulariaceae). *Journal of Medicinal Food*, 1147-1152.
- Plants of the World Online. *Verbascum* L. Retrieved April 13, 2023, from <https://powo.science.kew.org/taxon/urn:lsid:ipni.org:names:30049308-2>
- Saeidi, K., and Lorigooini, Z. (2017). Determination of mucilage content of mullein (*Verbascum songaricum*) populations. *Journal of Pharmaceutical Sciences and Research*, 9, 2641-2643.
- Selseleh, M., Nejad Ebrahimi, S., Aliahmadi, A., Sonboli, A., & Mirjalili, M. H. (2020). Metabolic profiling, antioxidant, and antibacterial activity of some Iranian *Verbascum* L. species. *Industrial Crops and Products*, 153, 112609.
- Şener A., Dulger B., 2009. Antimicrobial Activity of the Leaves of *Verbascum sinuatum* L. on Microorganisms Isolated from Urinary Tract Infection. *African Journal of Microbiology Research*, 3 (11): 778-781.
- Wikler M.A., 2006. Methods for Diltion Antimicrobial Susceptibility Tests for bacteria That Grow Aerobically, *Clinic Lab stand Ins*, 61-64.
- Zhao, Y.-L., Wang, S.-F., Li, Y., He, Q.-X., Liu, K.-C., Yang, Y.-P., & Li, X.-L. (2011). Isolation of chemical constituents from the aerial parts of *Verbascum thapsus* and their antiangiogenic and antiproliferative activities. *Archives of Pharmacal Research*, 34(5), 703–707.

Chapter 9

IMPORTANT ORGANOCATALYTIC INTRAMOLECULAR FRIEDEL-CRAFTS ALKYLATION REACTIONS IN THE LAST DECADE

Tülay YILDIZ¹

*1- Doç.Dr.; Istanbul University-Cerrahpaşa, Engineering Faculty,
Chemistry Department. Organic Chemistry Division, 34320 Avcılar-
Istanbul/Türkiye
tulayyil@iuc.edu.tr. ORCID ID: <https://orcid.org/0000-0001-5857-2480>.*

INTRODUCTION

With many years of experience, one of the most crucial methods in organic synthesis is the Friedel–Crafts alkylation (FCA) of aromatic compounds. These days, FCA is a crucial synthetic step in many research-based syntheses as well as in industrial processes related to bulk chemicals. FCA reaction continues to be one of the easiest methods for functionalizing aromatic compounds and obtaining multi-aromatic rings. The writers of this chapter present an overview of studies applying this reaction intramolecularly and organocatalytically. In the constrained space of this chapter, a thorough assessment of the literature is quite difficult. Therefore we have made an effort to maintain an equitable and representative sample size with a range of substrate structures, electrophiles and donors, and organocatalysts. The syntheses have been chosen from the most recent literature published in the last decade. The FCA reaction's properties and organocatalysts used are included in this chapter. Here, there is no consideration has been given to simple alkylations of aromatic compounds. Rather, we have selected instances when a significant portion of the molecule or functionalized groups are added, enabling additional alteration on the alkyl chain. Especially

we focused on the synthesis of ring structures using intramolecular FCA reaction.

Catalytic intramolecular FCA and its mechanism

Traditional FCA reagents (AlCl_3 , H_2SO_4 , H_3PO_4 , alkyl, and acyl chlorides) are very corrosive chemicals, affected by moisture, and difficult to work with (Başpınar Küçük et al., 2017). Therefore, unlike classical reagents, new reagents, and reaction methods have been discovered in recent years to eliminate these disadvantages. For this purpose, instead of classical acid catalysts, more moderate Lewis acids and organic Bronsted acids or organocatalysts, which are the subject of this book chapter, have begun to be used. Alcohol or alkene derivatives have begun to be preferred instead of the classical reagents of the FCA reaction (Başpınar Küçük et al., 2019; Küçük, 2015). The possible mechanism of this reaction is given in Figure 1.

Intramolecular FCA of appropriate alcohols or alkenes is one of the most effective ways to produce cyclic compounds. Because new methods have lately started to appear in the literature on arylation employing an FCA procedure. In particular, arylation without the use of metals has gained a lot of popularity since it circumvents the drawbacks of organometallic chemistry, which include high costs, the use of hazardous compounds, and difficulty in purification (Shirakawa et al., 2010; Yanagisawa et al., 2008). By using inexpensive and less hazardous catalysts and gentle reaction conditions, these new techniques have opened up new possibilities (Deng et al., 2007; Hashmi et al., 2006; X. Zhang et al., 2009). Nowadays, π -activated alcohols or alkenes have expanded more and more in the chemical field as opposed to organohalides, which are more poisonous and require hard conditions (Bandini & Tragni, 2009; Muzart, 2008).

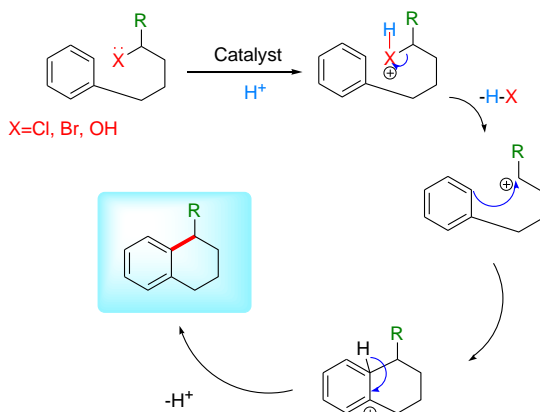


Figure 1: General mechanism of catalytic intramolecular FCA.

Intramolecular FCA studies conducted in recent years

A study in 2013, it was developed a new method to create tetraline and indoline rings using the intramolecular FCA method (Begouin et al., 2013). In this method, high degrees of regio- and diastereoselectivity were achieved when diastereomeric mixes of benzyl carbinols were treated with a catalytic quantity of $\text{Ca}(\text{NTf}_2)_2/\text{Bu}_4\text{NPF}_6$ to produce the corresponding tetralin or indane in good yields (Figure 2).

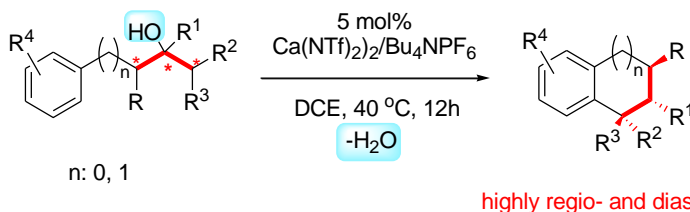


Figure 2: The intramolecular FCA method developed by Begouin et al.

In another study, for the enantioselective synthesis of highly functionalized cyclohepta[b]indoles with high enantioselectivity (up to 96% ee), a novel technique was developed in 2013 (Dange et al., 2013). The method achieves good yields and stereoselectivity by combining an extremely effective double Friedel-Crafts reaction sequence with an enantioselective organocatalytic Michael addition in a single pot.

When asymmetric FCA reactions were examined, indole and pyrroles were frequently used as substrates due to their strong reactivity (J. W. Zhang et al., 2015). Following this strategy, Zhang et al. developed olefin cross-metathesis/asymmetric intramolecular Friedel-Crafts alkylation of pyrrole derivatives by chiral phosphoric acid (Figure 3).

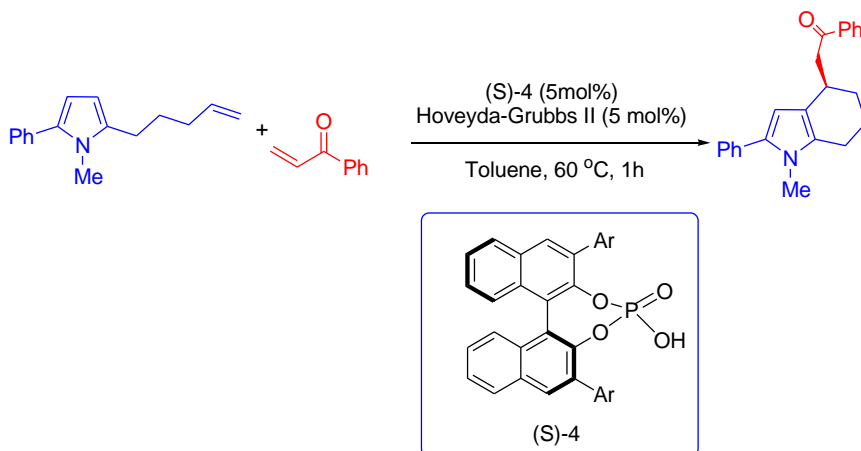


Figure 3: *The intramolecular FCA method developed by Zhang et al.*

Yıldız and Küçük in 2017, using the intramolecular FCA reaction, an effective organocatalytic technique established for the production of novel substituted 9-arylxanthenes starting from diarylcarbinol compounds containing an arenoxy group (Yildiz & Küçük, 2017). In this work, for the first time, several organic Brønsted acids were investigated as catalysts in the intramolecular Friedel–Crafts alkylation reaction. Within fifteen minutes at room temperature, N-triflylphosphoramidate supported the synthesis of many new substituted 9-arylxanthenes in excellent yields (Figure 4).

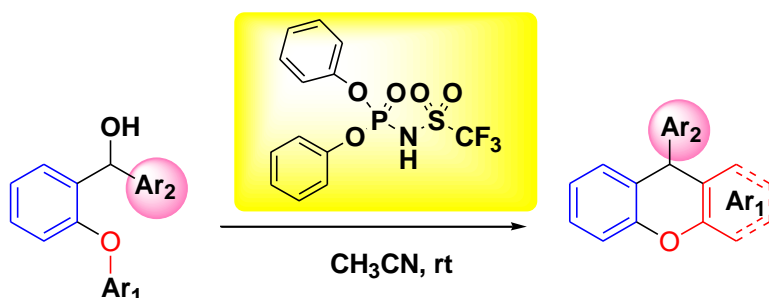


Figure 4: *The intramolecular FCA method developed by Yıldız et al.*

In another study published in 2017, the synthesis of dihydrocoumarins was carried out enantioselectively using organocatalytic FCA followed by lactonization reactions (Y. L. Zhao et al., 2017). Using only 2.5 mol% of a quinine-derived squaramide catalyst in this study, which used naphthols and 3-trifluoroethylidene oxindoles as starters, the products had excellent enantio- and diastereo-selectivities (up to 98% ee, >20:1 d.r.) and high efficiency (up to 99%) has been achieved (Figure 5).

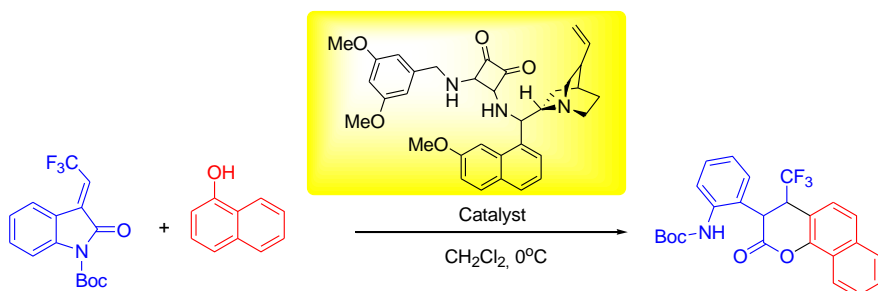


Figure 5: *The intramolecular FCA and Lactonization of naphthols with 3-trifluoroethylidene oxindoles via organocatalysis*

Then in 2018, through a catalyst-free Domino Mannich and intramolecular FCA reactions of N arylamines with paraformaldehyde and electron-rich olefins, a useful and efficient method was developed to construct diversely substituted 1,2,3,4-tetrahydroquinolines in good yields (Castillo et al., 2018). The key intermediates in this process are the formation of N-aryl-N-alkylmethyleneiminium ions, which serve as the necessary intermediates to afford the target products (Figure 6).

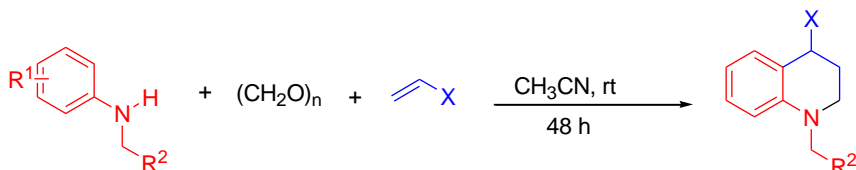


Figure 6: The intramolecular FCA method developed by Castillo et al.

In this study, it was demonstrated that some of the substituted 1,2,3,4-tetrahydroquinolines obtained have the strongest activity against many cancer cell lines according to anticancer in vitro experiments. For this reason, the intramolecular FCA reaction has a very important place in the synthesis of new cyclic systems of biological importance.

Intramolecular FCA reaction has also been widely used for the synthesis of thioxanthene derivatives. Because thioxanthene rings are used as medicine, especially in the treatment of neurological diseases. In one of these studies, some novel substituted thioxanthenes were synthesized using N-triflylphosphoramidate as organocatalysis (Yildiz, 2018). This new methodology made it possible to produce novel substituted thioxanthenes without the need for inert reaction conditions or protection, and they may find applications in pharmaceutical chemistry as bioactive chemicals (Figure 7).

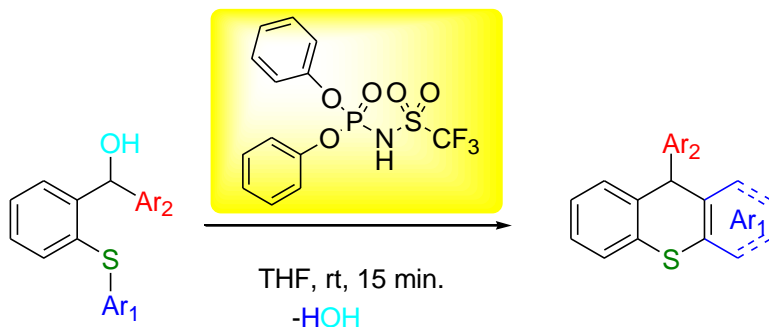


Figure 7: Synthesis of new thioxanthenes using the intramolecular FCA.

In 2019, the synthesis of some heterocyclic motives containing nitrogen through an organocatalytic tandem using intramolecular FCA was developed (Rabasa-Alcañiz et al., 2019). This entire procedure occurred under Brønsted acid catalysis and resulted in the formation of final products with moderate to good yields. Enantioselective attempts at implementing the tandem protocol utilized chiral (*R*)-BINOL-derived *N*-triflyl phosphoramides. After the initial optimization experiments, it was exhibited that the tandem method gave moderate levels of enantioselectivity (Figure 8).

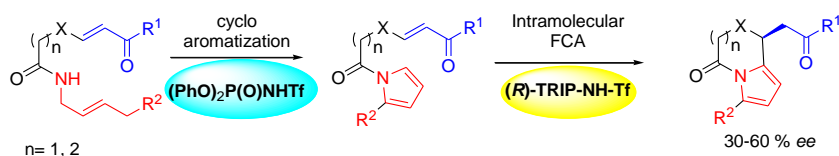


Figure 8: Synthesis of indolizinones and pyrrolo-azepinone derivatives via the intramolecular FCA.

In a separate investigation, Lanke et al. revealed a diastereoselective process involving the ring opening of non-donor-acceptor cyclopropanes through an intramolecular Friedel-Crafts alkylation, leading to the generation of functionalized dihydronaphthalene scaffolds featuring quaternary carbon stereocenters (Lanke et al., 2019). They illustrated that the transformation occurs via a specific bond cleavage at the most alkylated carbon center while maintaining the configuration entirely (Figure 9).

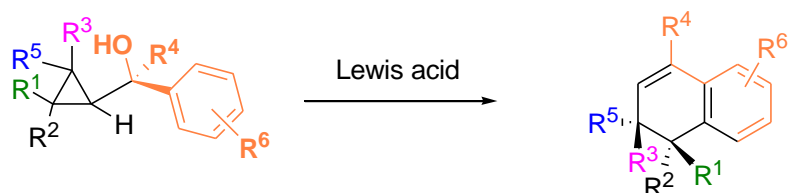


Figure 9: The intramolecular FCA method developed by Lanke et al.

In another study, the synthesis of stereoselectively 9-vinyl substituted unsymmetrical xanthenes and thioxanthenes was achieved using intramolecular FCA and a Lewis acid catalyst (Prajapati et al., 2020). In this reaction, π -activated 2-allylic alcohols were chosen as a different starting point and they performed a successful ring closing reaction under mild reaction conditions (Figure 10).



Figure 10: The intramolecular FCA method developed by Prajapati et al.

In an article by Bryant et. al. in 2021, they a highly enantioselective intramolecular cyclization of these systems by a Friedel–Crafts-type 1,4–addition employing an organocatalyst with a large silyl protecting group (Bryant et al., 2021). They also demonstrate that heat increases reaction yield almost entirely without compromising enantioselectivity. Good enantioselectivities (up to 94%) were obtained for bicyclic resorcinols. This study is quite important, as the organocatalytic intramolecular transformation of resorcinol derivatives has not been encountered before (Figure 11).

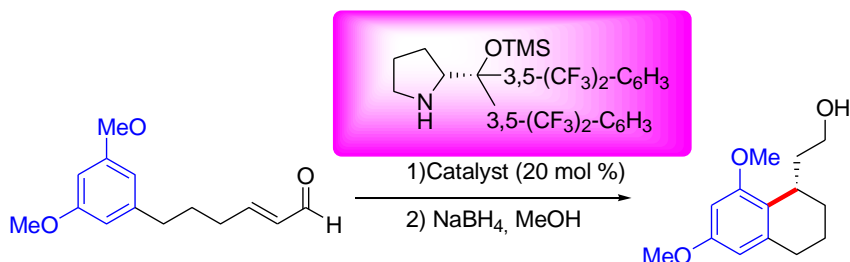


Figure 11: The intramolecular FCA method developed by Bryant et al.

In another study published in 2021, bromination/intramolecular FCA methods were combined using CBr_4 and a suitable base to synthesize some indole derivatives (L. Zhao et al., 2021). Unlike the intramolecular cross-dehydrogenative coupling reaction of the same substrates, in this study, only an oxidant of the same equivalent value was used instead of a transition metal. This method achieved indole synthesis under environmentally friendly and temperate conditions (Figure 12). According to the authors, the reactions may occur in a straightforward one-pot process in tandem with intramolecular FCA and bromination.

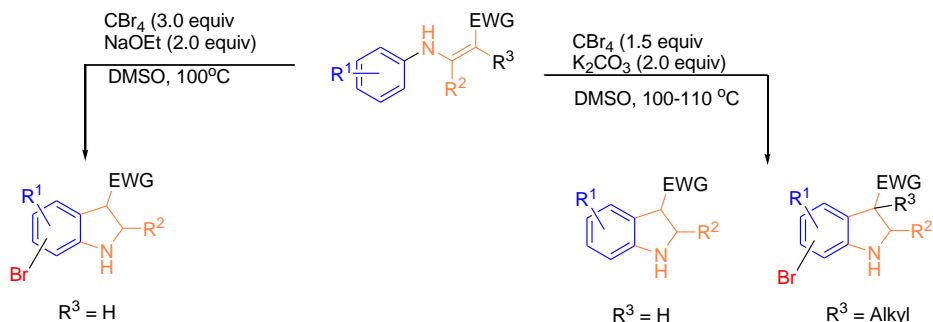


Figure 12: The Bromination/intramolecular FCA method developed by L.Zhao et al. in 2021.

3-Chloro-2-oxo-N,3-diarylpropanamides have a structure that is very suitable for forming a new C-C bond via intramolecular FCA to synthesize hydroxyindolin-2-ones compounds. Mamedov et. al. performed optimization studies of this reaction using TFA as an organocatalyst and obtained very good yields under mild conditions (Mamedov et al., 2022). As a result of the reactions, anti and syn-diastereomeric mixtures were easily separated by column chromatography with a majority of the former occurring (Figure 13).

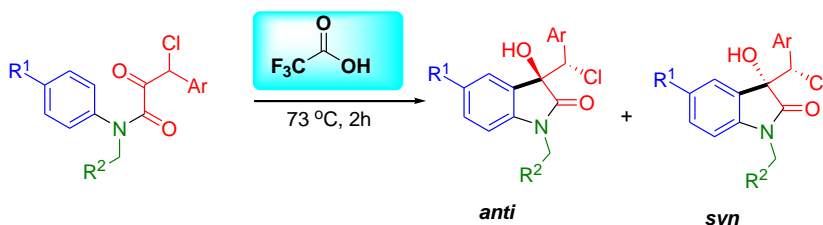


Figure 13: The intramolecular FCA of 3-Chloro-2-oxo-N,3-diarylpropanamides.

Oxidative carbene-catalyzed intramolecular FCA reaction of indoles has also been used to synthesize spirocyclic indolene compounds in a report (Breuers et al., 2022). According to the report, the process is initiated by adding indole intramolecularly to an α,β -unsaturated acyl azolium that is produced in situ. An appropriate external nucleophile traps the cyclized indolenine with an acyl azolium functionality, preventing it from reacting efficiently via direct acylation with the α,β -unsaturated acyl azolium (Figure 14).

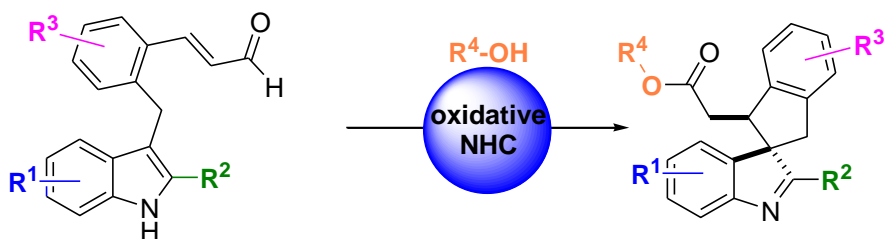


Figure 14: The synthesis of spirocyclic indolenes by intramolecular FCA.

Another study reported a Brønsted acid-catalyzed intramolecular FCA reaction using isoindolinone-derived propargyl alcohols and external aromatic nucleophiles for the synthesis of spiroisoindolinone indenes (Topolovčan et al., 2022). In the reaction, spiroins have been synthesized chemoselectively and regioselectively in moderate to high yields using a wide range of substrates (Figure 15).

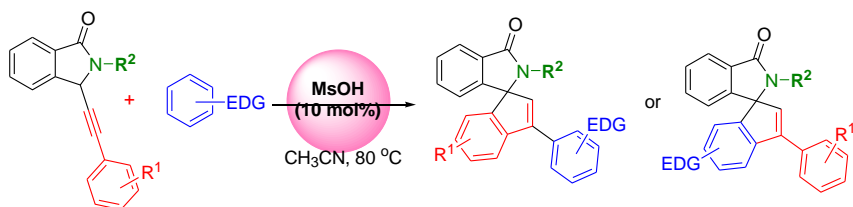


Figure 15: The synthesis of spirocyclic indolenes by Brønsted acid-catalyzed intramolecular FCA.

In another Brønsted acid-catalyzed intramolecular FCA reaction, tertiary allylic alcohols were added to indoles (Wakefield et al. 2022). In this study, substituted indoles were obtained by intramolecular FCA reaction of allylic alcohols, which synthesized using a two-step procedure, in the presence of phosphoric acid (Figure 16).

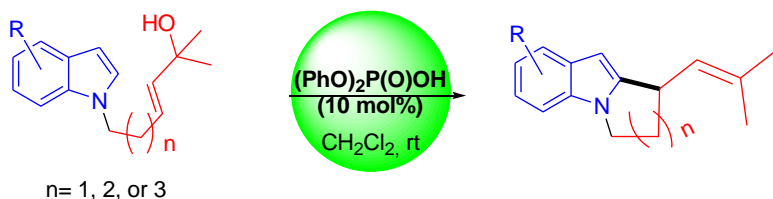


Figure 16: The intramolecular FCA of allylic alcohols.

REFERENCES

- Bandini, M., & Tragni, M. (2009). π -Activated alcohols: An emerging class of alkylating agents for catalytic Friedel-Crafts reactions. *Organic and Biomolecular Chemistry*, 7(8), 1501–1507. <https://doi.org/10.1039/b823217b>
- Başpınar Küçük, H., Banu Salt, Z., Mataracı Kara, E., Sayık Mehan, A., & Yusufoglu, A. S. (2019). Synthesis of novel 1,2,3-thiadiazoles and 1,2,3-selenadiazoles as new antimicrobial agents. *Phosphorus, Sulfur and Silicon and the Related Elements*, 194(9), 903–908. <https://doi.org/10.1080/10426507.2019.1576676>
- Başpınar Küçük, H., Yaşa, H., Yıldız, T., & Yusufoglu, A. S. (2017). Detailed studies on the reduction of aliphatic 3-, 4-, 6-, and 13-oximino esters: Synthesis of novel isomeric amino esters, oximino alcohols, and amino alcohols. *Synthetic Communications*, 47(22), 2070–2077. <https://doi.org/10.1080/00397911.2017.1364768>
- Begouin, J. M., Capitta, F., Wu, X., & Niggemann, M. (2013). Diastereoselective synthesis of indanes and tetralins via intramolecular Friedel-Crafts reaction. *Organic Letters*, 15(6). <https://doi.org/10.1021/ol400341p>
- Breuers, C. B. J., Daniliuc, C. G., & Studer, A. (2022). Oxidative N-Heterocyclic Carbene-Catalyzed Intramolecular Friedel-Crafts Alkylation of Indoles for the Synthesis of Spirocyclic Indolenines. *Organic Letters*, 24(29), 5314–5318. <https://doi.org/10.1021/acs.orglett.2c01927>
- Bryant, L. A., Shankland, K., Straker, H. E., Johnston, C. D., Lees, N. R., & Cobb, A. J. A. (2021). Enantioselective Organocatalytic Synthesis of Bicyclic Resorcinols via an Intramolecular Friedel–Crafts-Type 1,4-Addition: Access to Cannabidiol Analogues. *Advanced Synthesis and Catalysis*, 363(16), 4067–4074. <https://doi.org/10.1002/adsc.202100647>
- Castillo, J. C., Jiménez, E., Portilla, J., Insuasty, B., Quiroga, J., Moreno-Fuquen, R., Kennedy, A. R., & Abonia, R. (2018). Application of a catalyst-free Domino Mannich/Friedel-Crafts alkylation reaction for the synthesis of novel tetrahydroquinolines of potential antitumor activity. *Tetrahedron*, 74(9), 932–947. <https://doi.org/10.1016/j.tet.2017.12.049>
- Dange, N. S., Hong, B. C., Lee, C. C., & Lee, G. H. (2013). One-pot asymmetric synthesis of seven-membered carbocycles cyclohepta[b]indoles via a sequential organocatalytic Michael/double Friedel-Crafts alkylation reaction. *Organic Letters*, 15(15). <https://doi.org/10.1021/ol4016749>
- Deng, X., Liang, J. T., Liu, J., McAllister, H., Schubert, G., & Mani, N. S.

- (2007). A practical synthesis of enantiopure 7-alkoxy-4-aryl-tetrahydroisoquinoline, a dual serotonin reuptake inhibitor/histamine H₃ antagonist. *Organic Process Research and Development*, *11*(6), 1043–1050. <https://doi.org/10.1021/op700183q>
- Hashmi, A. S. K., Schwarz, L., Rubenbauer, P., & Blanco, M. C. (2006). The condensation of carbonyl compounds with electron-rich arenes: Mercury, thallium, gold or a proton? *Advanced Synthesis and Catalysis*, *348*(6), 705–708. <https://doi.org/10.1002/adsc.200505464>
- Küçük, H. B. (2015). Practical synthesis of 2,5-disubstituted 1,3-dioxolane-4-ones and highly diastereoselective cis-2,5-disubstituted 1,3-dioxolane-4-ones from α -hydroxy acids catalyzed by N-triflylphosphoramidate. *Tetrahedron Letters*, *56*(41), 5583–5586. <https://doi.org/10.1016/j.tetlet.2015.08.046>
- Lanke, V., Zhang, F. G., Kaushansky, A., & Marek, I. (2019). Diastereoselective ring opening of fully-substituted cyclopropanes: Via intramolecular Friedel-Crafts alkylation. *Chemical Science*, *10*(41), 9548–9554. <https://doi.org/10.1039/c9sc03832a>
- Mamedov, V. A., Galimullina, V. R., Kadyrova, S. F., Rizvanov, I. K., & Latypov, S. K. (2022). A concise synthesis of indolin-2-ones via direct acid-catalyzed intramolecular Friedel-Crafts alkylation of 3-chloro-N-(substituted)-2-oxo-N,3-diarylpropanamides. *Tetrahedron Letters*, *99*. <https://doi.org/10.1016/j.tetlet.2022.153797>
- Muzart, J. (2008). Gold-catalysed reactions of alcohols: isomerisation, inter- and intramolecular reactions leading to C-C and C-heteroatom bonds. In *Tetrahedron* (Vol. 64, Issue 25, pp. 5815–5849). <https://doi.org/10.1016/j.tet.2008.04.018>
- Prajapati, A., Kumar, M., Thakuria, R., & Basak, A. K. (2020). Stereoselective synthesis of 9-vinyl substituted unsymmetrical xanthenes and thioxanthenes. *Tetrahedron Letters*, *61*(37), 152347. <https://doi.org/10.1016/j.tetlet.2020.152347>
- Rabasa-Alcañiz, F., Sánchez-Roselló, M., Fustero, S., & Del Pozo, C. (2019). Tandem Organocatalytic Cycloaromatization/Intramolecular Friedel-Crafts Alkylation Sequence for the Synthesis of Indolizinones and Pyrrolo-azepinone Derivatives. *Journal of Organic Chemistry*, *84*(17), 10785–10795. <https://doi.org/10.1021/acs.joc.9b01314>
- Shirakawa, E., Itoh, K. I., Higashino, T., & Hayashi, T. (2010). Tert-butoxide-mediated arylation of benzene with aryl halides in the presence of a catalytic 1,10-phenanthroline derivative. *Journal of the American Chemical Society*, *132*(44), 15537–15539.

- <https://doi.org/10.1021/ja1080822>
- Topolovčan, N., Degač, M., Čikoš, A., & Gredičak, M. (2022). Chemoselective and Regioselective Synthesis of Spiroisindolinone Indenes via an Intercepted Meyer-Schuster Rearrangement/Intramolecular Friedel-Crafts Alkylation Relay. *Journal of Organic Chemistry*, 87(5), 3712–3717. <https://doi.org/10.1021/acs.joc.1c02647>
- Yanagisawa, S., Ueda, K., Taniguchi, T., & Itami, K. (2008). Potassium t-butoxide alone can promote the biaryl coupling of electron-deficient nitrogen heterocycles and haloarenes. *Organic Letters*, 10(20), 4673–4676. <https://doi.org/10.1021/ol8019764>
- Yildiz, T. (2018). Synthesis of new thioxanthenes by organocatalytic intramolecular Friedel–Crafts reaction. *Synthetic Communications*, 48(17), 2177–2188. <https://doi.org/10.1080/00397911.2018.1482351>
- Yildiz, T., & Küçük, H. B. (2017). An organocatalytic method for the synthesis of some novel xanthene derivatives by the intramolecular Friedel-Crafts reaction. *RSC Advances*, 7(27), 16644–16649. <https://doi.org/10.1039/c6ra27094h>
- Wakefield1, B.H., Barnes, R., Brown, T., Jones, A.M., Knotts, V.A., Martinetti, C. Brønsted Acid Catalyzed Intramolecular Friedel-Crafts Addition of Tertiary Allylic Alcohols to Indoles. *Journal of the South Carolina Academy of Science*, [s. l.], v. 20, n. 1, p. 6–9, 2022.
- Zhang, J. W., Liu, X. W., Gu, Q., Shi, X. X., & You, S. L. (2015). Enantioselective synthesis of 4,5,6,7-tetrahydroindoles via olefin cross-metathesis/intramolecular Friedel-Crafts alkylation reaction of pyrroles. *Organic Chemistry Frontiers*, 2(5). <https://doi.org/10.1039/c5qo00034c>
- Zhang, X., Rao, W., Sally, & Chan, P. W. H. (2009). Iron(III) chloride-catalysed direct nucleophilic α -substitution of Morita-Baylis-Hillman alcohols with alcohols, arenes, 1,3-dicarbonyl compounds, and thiols. *Organic and Biomolecular Chemistry*, 7(20), 4186–4193. <https://doi.org/10.1039/b908447a>
- Zhao, L., Qiu, C., Zhao, L., Yin, G., Li, F., Wang, C., & Li, Z. (2021). Base-promoted, CBr₄-mediated tandem bromination/intramolecular Friedel-Crafts alkylation of N-aryl enamines: a facile access to 1H- And 3H-indoles. *Organic and Biomolecular Chemistry*, 19(24), 5377–5382. <https://doi.org/10.1039/d1ob00731a>
- Zhao, Y. L., Lou, Q. X., Wang, L. S., Hu, W. H., & Zhao, J. L. (2017). Organocatalytic Friedel–Crafts Alkylation/Lactonization Reaction of Naphthols with 3-Trifluoroethylidene Oxindoles: The Asymmetric Synthesis of Dihydrocoumarins. *Angewandte Chemie - International*

Edition, 56(1), 338–342. <https://doi.org/10.1002/anie.201609390>

Chapter 10

Faunistic and floristic diversity around the marble quarries in the vicinity of Lake Yarışlı (Burdur, Türkiye)

Ümit KEBAPÇI¹

Neslihan BALPINAR²

1- Prof. Dr.; Burdur Mehmet Akif Ersoy Üniversitesi Fen Edebiyat
Fakültesi Biyoloji Bölümü. kebapci@gmail.com ORCID No: 0000-
0003-4991-3356

2- Doç. Dr.; Burdur Mehmet Akif Ersoy Üniversitesi Fen Edebiyat
Fakültesi Biyoloji Bölümü. botanistneslihan@gmail.com ORCID No:
0000-0002-4469-8629

INTRODUCTION

Due to its location at the crossroads of three floristic regions and continents, the climatic diversity and undulated topography enabling different microclimatic features, relatively elevated levels of biological diversity and richness have been recorded for various organism groups in Türkiye.

Within the Mediterranean ecoregion borders, Burdur Province lies in the southwestern corner of the country within Lakes Region (named after the lakes occupying tectonic depressions to the north of Taurus Mountains) and exhibits a transient climatic character between Mediterranean and continental climates (Kaplan and Örucü, 2019). Due to climatic factors and anthropogenic pressure, almost all lakes in Burdur area are in a drying up process (Taş and Akpınar, 2021; Tulan Işıldar and Yalçınır Ercoşkun, 2021), some of which like Lake Akgöl have become seasonal lakes. Surface levels of the spring fed alkaline lake Yarışlı varies greatly though the year due to changes in the evaporation-rainfall balance (Anonymous, 2013). Being among the smallest natural lakes of Burdur (Aksoy et al., 2019), it is hence more vulnerable to anthropogenic factors like pollution, land erosion and habitat destruction.

Marble mining activity in Burdur province has developed significantly since early 90s, bringing Burdur the top rank nationwide in marble and travertine production (Yılmaz, 2019). Currently, more than half of the licensed quarries are concentrated in small area between lakes Burdur and Yarışlı, two different marble types produced around the latter is commercially favored due to appearance and

quality (Yılmaz and Caran, 2019). Therefore, Lake Yarışlı is amongst the most suitable locations to monitor biotic and other environmental impacts of marble mining.

Marble mining industry causes a variety of environmental problems such as pollution, erosion, habitat fragmentation and biodiversity loss (Demira and Güngör, 2013). Open mining practices widely applied as well in Burdur, depending on the scale and size of the area, involve clearing top soil and plant cover (Demir and Güngör, 2013). Furthermore, increased noise pollution and human traffic levels cause spatiotemporal avoidance and behavioral shifts among wildlife.

Biodiversity loss has now become a global problem, with the rise in the global population and destruction of natural or protected areas in quality and quantity. To understand and minimize the effects of various activities on the biodiversity, monitoring studies and inventories should be performed around protected areas. Following study aims to present findings of a brief faunal and floral survey of the close proximity of a marble mining area.

STUDY AREA

Vertebrate fauna and flora of a mining area to the south of Lake Yarışlı (Yeşilova, Burdur) were investigated in 2013. Lake Yarışlı is an alkaline lake situated in a tectonic depression forming an endorrheic (closed) basin, fed by karstic springs and Gençali stream (only flowing in winters) (Yılmaz et al., 2019) and having greatly changing lake levels within a year (Aksoy et al., 2019; Yılmaz, 2019; Yılmaz et al., 2019), from a full extent during winters to almost the drying point in some summers.

To the east and south, there is a steep valley divides between the site and rocky mountain slopes, while to west there are low hills covered with dense maquis shrubland and in the north and northwest direction lies the transformed agricultural land below the site.

METHODOLOGY

To sample from as different habitat pieces as possible, 8 collection spots were selected on the way to a random mining area and peripheral areas. The plant specimens lacking organs such as flowers, fruits, or leaves providing characters that can be used for reliable identification due to the factors like grazing or season, also the plants growing outside the periphery of mining area or the road were not taken into consideration.

The faunal inventory was based on interviews with local people, direct observations, and additional material (feathers, traces, sound recording, scat analysis etc.) from likewise immediate surroundings of the study area.

VEGETATION AND FLORA

Limestone rocks (Triassic Dutdere formation) covering much of the area provide a variety of habitats with rich flora. A homogenous secondary forest dominated by a single species, kermes oak (*Quercus coccifera* L.) characterize the study area. Even though grazing risk poses a lesser threat in the active mining areas, effects of overgrazing below the study area and pastures in the forest clearings around it are clearly seen.

Less elevated areas surrounding Lake Yarışlı have been transformed into cultivated land. Forest is the dominant vegetation type in the elevated terrain where the marble quarries are located, formed mainly by the kermes oak (*Quercus coccifera* L.), along with sparse groups of juniper (*Juniperus excelsa* M. Bieb.) and interspersed cade (*Juniperus oxycedrus* L. subsp. *oxycedrus*).

Clearings along the road to the site from the main road junction has a bushy maquis type vegetation mixed with the kermes oak. Western Anatolian endemic *Crocus biflorus* Miller subsp. *crewei* (Hook. F.) B.Mathew found in this habitat is a new record for the region.

Table 1: The seed plant taxa determined from the study area.

No.	Plant taxon
1	<i>Juniperus oxycedrus</i> L. subsp. <i>oxycedrus</i>
2	<i>Juniperus excelsa</i> M. Bieb.
3	<i>Berberis crataegina</i> DC.
4	<i>Alyssum linifolium</i> Steph. ex Willd. var. <i>linifolium</i> Steph. ex Willd.
5	<i>Linum tenuifolium</i> L.
6	<i>Erodium cicutarium</i> (L.) L Herit.
7	<i>Alhagi pseudalhagi</i> (M. Bieb.) Desv.
8	<i>Astragalus angustifolius</i> Lam. subsp. <i>pungens</i> (Willd.) Hayek
9	<i>Sedum album</i> L.
10	<i>Sanguisorba minor</i> Scop. subsp. <i>minor</i>
11	<i>Scabiosa argentea</i> L.
12	<i>Scorzonera cana</i> (C.A. Mey.) Hoffm. var. <i>jacquiniana</i> (W. Koch) Chamb.
13	<i>Crupina vulgaris</i> Cass.
14	<i>Cichorium intybus</i> L.
15	<i>Picnomon acarna</i> (L.) Cass.
16	<i>Cyclamen coum</i> Mill. var. <i>coum</i>
17	<i>Verbascum</i> sp.
18	<i>Salvia viridis</i> L.
19	<i>Teucrium polium</i> L.
20	<i>Phlomis bourgaei</i> Boiss.
21	<i>Sideritis libanotica</i> Labill. subsp. <i>linearis</i> (Bentham) Bormm
22	<i>Lamium amplexicaule</i> L.
23	<i>Acantholimon acerosum</i> (Willd.) Boiss. Var. <i>acerosum</i>
24	<i>Origanum onites</i> L.
25	<i>Euphorbia rigida</i> M. Bieb.
26	<i>Quercus coccifera</i> L.
27	<i>Ornithogalum comosum</i> L.
28	<i>Crocus biflorus</i> Miller subsp. <i>crewei</i> (Hooker Fil.) Mathew
29	<i>Brachypodium pinnatum</i> (L.) P. Beauv.
30	<i>Bromus hordeaceus</i> L. subsp. <i>hordeaceus</i>
31	<i>Cynodon dactylon</i> (L.) Pers.
32	<i>Festuca arundinacea</i> Schreber subsp. <i>arundinacea</i>
33	<i>Catapodium rigidum</i> (L.) C. E. Hubbard
34	<i>Poa annua</i> L.

The slopes on the southern and eastern directions is covered with a sparse *Juniperus excelsa* forest. The two juniper species can be encountered individually amongst the degraded shrubland even close to the mining area.

The mining areas themselves devoid of any vegetation growth, while leaves and stems of surrounding vegetation is observed to be covered with a layer of dust.

In pastures and clearings formed within maquis, several shrub or bush species exemplified by *Berberis crataegina* DC, *Verbascum* sp., *Alhagi pseudalhagi* M. Bieb. and seldom *Picnomon acarna* can be seen.

Rock vegetation is common and represented by species typical for the region like *Astragalus angustifolius* Lam. subsp. *pungens* (Willd.) Hayek, *Cyclamen coum* Miller var. *coum*, and *Sedum album* L.

According to the findings of our excursions, 34 seed plant taxa and 1 fern species (*Asplenium ceterach* L.) have been determined (Table 1), none of which are threatened according to Red Data Book of Turkish Plants (Ekim et al., 2000).

A flora listing of 350 plant taxa from 72 families has been compiled from the entire lake basin (Anonymous, 2013), among which endemic *Verbascum pyroliforme* subsp. *dudleyanum* (Hub.-Mor.) Karavel. & Aytaç, *Bolanthus minuartioides* (Jaub. & Spach) Hub.-Mor., *Hedysarum pestalozzae* Boiss., *Ballota nigra* L. subsp. *anatolica* P. H. Davis, *Micromeria cristata* (Hampe) Griseb. subsp. *phrygana* P. H. Davis were reported to occur in the lake surroundings. Southern shores of the lake are characterized with a halophytic vegetation dominated by *Juncus heldreichianus* Marsson ex Parl. subsp. *orientalis* Snog. (Anonymous, 2013). Aquatic flora was described as rich by Özçelik et al. (2014b). Common reed (*Phragmites australis* (Cav.) Trin. Ex Steudel) and southern cattail (*Typha domingensis* Pers.) are found in groups on the shores of the lake (Özçelik et al., 2014b).

There is no previous direct flora study of marble mining areas in Lake Yarıışlı and other similar areas. Our relatively smaller list is devoid of aquatic and mesic species, and restricted to a much smaller area. Even though it has been reported that marble mines threaten local plants especially narrow endemic species (Özçelik et al., 2014b), to understand direct or indirect effects on the flora which shows some consistency in the area according to our observation future studies are needed.

OVERVIEW OF THE VERTEBRATE FAUNA

Rather uniform rocky and shrubby character of study site provides a limited habitat diversity. Constant noise during the daytime radiated from densely spaced quarries, network of busy roads surrounding them, and the limited food availability are the limiting factors to the foraging behavior and daily activity of animals as direct observations could only be made at a distance to quarry site.

According to our findings 1 amphibian, 6 reptile, 28 bird and 5 mammal (sub)species inhabit the study area (Tables 2 to 4). The species numbers are highly likely to increase with inclusion of more sites, increasing the radius of study or number of excursions to the site.

Amphibians and reptiles

The only amphibian species in the fully terrestrial habitat is the common variable toad. Unlike the birds and mammals, avoiding the study site during daytime, reptiles can commonly be found among the bush cover and on rocks, or under stones near the site. The blotched snake record is based on an anecdotal evidence. One lizard species, *Anatololacerta ibrahimi* is endemic to Taurus range and Burdur sets the western limit of its distribution (Bellati et al. 2015; Karakasi et al., 2021).

Table 2: The amphibian and reptile species determined from the study area.

No.	Vernacular name	Scientific name
1	Variable toad	<i>Bufo taurus</i> (Pallas, 1771)
2	Greek tortoise	<i>Testudo graeca ibera</i> Pallas, 1814
3	Snake-eyed lizard	<i>Ophisops elegans macrodactylus</i> Berthold, 1842
4	Baran's rock lizard	<i>Anatololacerta ibrahimi</i> (Eiselt and Schmidtler, 1986)*
5	European snake-eyed skink	<i>Ablepharus kitaibelii</i> Bibron & Bory St. Vincent, 1833
6	Caspian snake	<i>Dolichophis caspius</i> (Gmelin, 1789)
7	Blotched snake	<i>Elaphe sauromates</i> (Pallas, 1811)

*Endemic

In a previous study focused on the herpetofauna of Lakes Region (Ege et al., 2015), in addition to Baran's rock lizard and snake-eyed lizard, and two species restricted to the springs connected to the lake, Beyşehir frog *Pelophylax caralitanus* and European pond turtle *Emys orbicularis*, 3 further regionally common reptile species (*Trachylepis aurata*, *Stellagama stellio* and *Eirenis modestus*) were found from three localities near the lake. The halotolerant dice snake, *Natrix tessellata*, was determined to occur in the lake area along with the Beyşehir frog and European pond turtle in an other inventory study (Öztürk and Tavuç, 2022).

In a thesis study on the ornithofauna of the lake, Dut (2007) reported Beyşehir frog (as marsh frog) and European pond turtle (as Caspian turtle), dice snake, variable toad, starred agama, snake-eyed lizard, and greek tortoise to occur in the lake area as well.

Although threatened by organic wastes (Anonymou 2013; Özçelik et al., 2014b), impacts of marble mining to springs feeding the lake are largely unknown. Along with the endangered Beyşehir frog and European pond turtle, two Burdur endemic fish species *Anatolichthys fontinalis* (Akşiray, 1948) and *Pseudophoxinus ninae* Freyhof and Özuluğ, 2006 inhabit these springs as well (Anonymous, 2013). As some of the newer quarries are in closer proximity of the lake, this issue should be investigated in the future.

Birds

The steep cliffs and agricultural lands surrounding the area possess particular ornithological importance, serving as nesting and foraging grounds.

Table 3: The bird species determined from the study area.

No.	Vernacular name	Scientific name
1	Ruddy shelduck	<i>Tadorna ferruginea</i> (Pallas, 1764)
2	White stork	<i>Ciconia ciconia</i> (Linnaeus, 1758)
3	Golden eagle	<i>Aquila chrysaetos</i> (Linnaeus, 1758)
4	Eurasian sparrowhawk	<i>Accipiter nisus</i> (Linnaeus, 1758)
5	Long-legged buzzard	<i>Buteo rufinus</i> (Cretzschmar, 1827)
6	Eurasian kestrel	<i>Falco tinnunculus</i> Linnaeus, 1758
7	Rock dove	<i>Columba livia</i> Gmelin, 1789
8	Eurasian collared dove	<i>Streptopelia decaocto</i> (Frivaldszky, 1838)
9	Eurasian scops owl	<i>Otus scops</i> (Linnaeus, 1758)
10	Little owl	<i>Athene noctua</i> (Scopoli, 1769)
11	Eurasian hoopoe	<i>Upupa epops</i> Linnaeus, 1758
12	Red-backed shrike	<i>Lanius collurio</i> Linnaeus, 1758
13	Eurasian jay	<i>Garrulus glandarius</i> (Linnaeus, 1758)
14	Hooded crow	<i>Corvus cornix</i> Linnaeus, 1758
15	Common raven	<i>Corvus corax</i> Linnaeus, 1758
16	Coal tit	<i>Parus ater</i> (Linnaeus, 1758)
17	Great tit	<i>Parus major</i> Linnaeus, 1758
18	Crested lark	<i>Galerida cristata</i> (Linnaeus, 1758)
19	Eurasian crag martin	<i>Ptyonoprogne rupestris</i> (Scopoli, 1769)
20	Barn swallow	<i>Hirundo rustica</i> Linnaeus, 1758
21	Lesser whitethroat	<i>Sylvia curruca</i> (Linnaeus, 1758)
22	Eastern olivaceous warbler	<i>Iduna pallida</i> (Hemprich & Ehrenberg, 1833)
23	Western rock nuthatch	<i>Sitta neumayer</i> Michahelles, 1830
24	Common blackbird	<i>Turdus merula</i> Linnaeus, 1758
25	Eurasian chaffinch	<i>Fringilla coelebs</i> Linnaeus, 1758
26	European goldfinch	<i>Carduelis carduelis</i> (Linnaeus, 1758)
27	Common linnet	<i>Linaria cannabina</i> (Linnaeus, 1758)
28	Corn bunting	<i>Emberiza calandra</i> Linnaeus, 1758

Ravens and possibly ruddy shelducks nest in the distant rocks above the site. Even though diurnal passage migrants and summer visitors preferring open habitats could use the site temporarily, this seems unlikely due to poor habitat quality parameters and the noise.

Most species are observed by the agricultural lands along way to the site. The doubtful record of the golden eagle, previously unrecorded from the lake area, is based on anecdotal evidence of former occurrence and nesting on high cliffs above the study site.

Previous studies on ornithofauna of the lake (Dut, 2007; Öztürk and Tavuç, 2022) or the lake basin (Anonymous, 2013) give varying numbers of species counts: Dut (2007) reports 98 species, Öztürk and Tavuç (2022) mentions 34 species, while in an inventory study combining all available literature data, a record of 141 species in total were given for the whole basin (Anonymous, 2013).

Lake Yarışlı holds important numbers of bird species like flamingo, lapwing and avocet in different periods of the year. Rocky islets and cliffs to the east of the lake serve as breeding grounds for several avian taxa. 141 species determined from the endorheic lake basin, including 50 waders and 9 diurnal raptors, are composed of 52 resident, 46 wintering, 34 summer visitor and 9 passage migrant species, 104 of which are protected under Bern convention. Wintering white headed duck (*Oxyura leucocephala*) and the passage migrant Egyptian vulture (*Neophron percnopterus*) are the two threatened bird species of the lake area listed as endangered (EN) status according to risk categories of IUCN. The ruddy shelduck (*Tadorna ferruginea*), common shelduck (*Tadorna tadorna*) and mallard (*Anas platyrhynchos*) are the most frequently observed bird species during the winter season. Iconic non-breeding visitor flamingo (*Phoenicopterus roseus*) can be seen across the year in varying numbers (Anonymous, 2013).

Mammals

It is notable to mention that the fauna list consists of highly adaptable small to moderate sized species (Yavuz et al., 2011; Yılmaz, 2019). Traces, scat samples and other indirect evidence were obtained from agricultural land below the study site. Presence of the fox and weasel is based on anecdotal evidence.

Tablo 4: The mammal species determined from the study area.

No.	Vernacular name	Scientific name
1	European hare	<i>Lepus europaeus</i> Pallas, 1778
2	East European vole	<i>Microtus mystacinus</i> (de Filippi, 1865)
3	Anatolian blind mole-rat	<i>Nannospalax xanthodon</i> (Nordmann, 1840)
4	Least weasel	<i>Mustela nivalis</i> Linnaeus, 1766
5	Red fox	<i>Vulpes vulpes</i> (Linnaeus, 1758)

In a thesis study on the ornithofauna of the lake, Dut (2007) reported red fox, Anatolian squirrel (*Sciurus anomalus anomalus*) (as red squirrel) and southern white-breasted hedhehog (*Erinaceus concolor* Martin, 1838) (as European hedhehog) to occur in the lake area.

A previous study based on the phototrap method records 12 mammal species around marble sites near lakes Burdur and Yarıřlı (Yılmaz, 2019). Among these, six species (European hare, wild boar, Eurasian lynx, gray wolf, red fox and golden jackal) were selected as target species. European hare is noticeable with the highest detection rate and extensive use of marble sites due to lack of hunting pressure. Presence of potential prey (hare) seems to attract carnivores to marble sites which even though restrict their activity due to human activity, preferring nocturnal or crepuscular activity around the marble sites, showing lesser activity and population size in marble sites as compared to the control area. However, contrastingly, adaptive carnivore golden jackal show a markedly higher activity in human dominated areas, where it is known to adopt a scavenging lifestyle. Despite decreased hunting pressure, excessive grazing pressure observed in the marble sites, responded by lesser habitat use of marble sites by the wild boar. Habitat fragmentation and destruction seem to be the most significant impacts of marble quarries on the mammal populations, implicated as well by virtual absence of the lynx around Lake Yarıřlı even though it exists around Lake Burdur sites having a higher habitat integrity in small numbers (Yılmaz, 2019).

CONCLUSION

In Burdur area, aside from the environmental aspect, human-centered adverse effects like overuse of ground water supplies, loss of aesthetic and recreational value, as well as problems concerning public and crop health due to dust cloud have been reported (Kaya et al., 2015). Loss of the forest cover as an indirect effect of open mining also causes land erosion, also problems involving access to clean water, pollution, and flood control (Özmiş and Tolunay, 2017). However, to develop mitigation strategies and gain public support for possible restrictions, detailed documentation of impacts marble industry is required necessarily.

Lakes in Burdur area and surrounding vegetation provide many ecosystem services, and bear cultural significance for the local people (Özçelik and Balabanlı, 2005). Under climate change and the increasing demand for natural resources, sustainable use and protection of water sources especially has become essential, yet regulations and legislations fall behind to handle the problem or fail to balance the economical growth and sustainability. Due to feasibility of potential quarries are understudied, the rate of leftover mining sites are fairly high in the area (Yılmaz and Caran, 2019). Such areas are not replanted nor restored, as opposed to legislations (Özçelik et al., 2014a), therefore renewability of ecosystems is not possible. Avoidance of regulations would also trigger several after-effects like land erosion and pollution. Public perception of the lakes in Burdur has been negatively affected by the drying process (Ceylan and Bulut, 2019), and seasonal drying of the lake is often viewed as complete drying, which in turn is misconceived and associated with uselessness. Therefore, to protect the lake biodiversity, education of Burdur people is of critical importance. We expect our findings will contribute to the future biodiversity and habitat management studies in the Burdur area.

REFERENCES

- Aksoy, T., Sarı, S., and Çabuk, A. (2019). Determination of Water Index with Remote Sensing within Wetland Management Context, Lakes Region. *GSI Journals Serie B: Advancements in Business and Economics*. 1(2), 35-48 [In Turkish].
- Anonymous (2013). *Lake Yarışlı Wetland Subbasin Biodiversity Study*. Burdur: Ministry of Forest and Water Works, General Directorate of Nature Protection and National Parks [In Turkish].
- Bellati, A., Carranza, S., Garcia-Porta, J., Fasola, M., and Sindaco, R. (2015). Cryptic diversity within the Anatololacerta species complex (Squamata: Lacertidae) in the Anatolian Peninsula: evidence from a multi-locus approach. *Molecular phylogenetics and evolution*, 82A, 219–233. doi: 10.1016/j.ympev.2014.10.003
- Ceylan, S., and Bulut, I. (2019). Tourism pressure, protection and sustainability at Salda Lake which is special environmental protection area. *Turkish Geographical Review*, 73, 79-89. doi: 19.17211/tcd.637091 [In Turkish].
- Demir, B.G. and Güngör, N. (2013). Marble Mining and Environment. *Journal of Istanbul Aydın University*, 20, 7-14 [In Turkish].
- Dut, E. (2007). Ornithofauna of Lake Yarışlı. Süleyman Demirel University Graduate School of Applied and Natural Sciences, Biology Department, MSc Thesis [In Turkish].
- Ege, O., Yakın, B.Y., and Tok, C.V (2015). Herpetofauna of the Lake District around Burdur. *Turkish Journal of Zoology*, 39(6), 1164-1168.
- Ekim, T, Koyuncu, M, Duman, H., Aytaç, Z., and Adıgüzel, N. (2000). *Red Data Book of Turkish Plants, Pteridophyta*. Ankara: TTKD and Van Yüzüncü Yıl University Press [In Turkish].
- Kaplan, A., and Örucü, Ö.K. (2019). Determination of Tourism Potential in Terms of Landscape Values of Burdur Lake and Its Surroundings. *Journal of Architecture Sciences and Applications*, 4(2), 105-121 [In Turkish].
- Karakasi, D., Ilgaz, Ç, Kumlutaş, Y., Candan, K., Güçlü, Ö., Kankılıç, T., Beşer, N., Sindaco, R., Lymberakis, P., and Nikos Poulakakis, N. (2021). More evidence of cryptic diversity in Anatololacerta species complex Arnold, Arribas and Carranza, 2007 (Squamata: Lacertidae) and re-evaluation of its current taxonomy. *Amphibia-Reptilia*, 42(2), 201–216.
- Kaya, L. G., Yücedağ, C., and Duruşkan, Ö. (2015). Environmental Investigation in Burdur Lake Basin. *The Journal of Graduate School of Natural and Applied Sciences of Mehmet Akif Ersoy University*, 6(1), 6-10 [In Turkish].
- Özçelik, H., and Balabanlı, C. (2005). Medicinal and Aromatic Plants in Burdur Province, Lake Burdur Example. *I. Burdur Symposium, 16-19th Nov. 2005*.

- Proceedings, Vol. 2* (pp. 1127-1136). Burdur: Mehmet Akif Ersoy University [In Turkish].
- Özçelik, H., Çinbilgel, I., Koca A., and Muca, B. (2014a). Effects of Marble Quarries on Burdur Region Flora. *National Symposium on Marble and Stone Quarry Reparation Techniques*, 18-20th September 2014 (pp. 191-204). Isparta [In Turkish].
- Özçelik, H., Çinbilgel, I., Tavuç, İ., Bebekli, Ö., Muca, B., and Koca, A. (2014b). Biodiversity Protection and Monitoring Affairs in Terrestrial and Aquatical Ecosystems of Burdur Province. *SDU Journal of Science*, 9 (2), 12-43 [In Turkish].
- Özmiş, M., and Tolunay, A. (2017). Determining the Economic Value of Erosion Control Services and Willingness to Payment Trends of Society at Burdur Region. *Süleyman Demirel University Journal of Natural and Applied Sciences*, 21(1), 99-112 [In Turkish].
- Öztürk, Y., and Tavuç, İ. (2022). Bird Species and Red List Category in Important Wetlands of Burdur Province. *Düzce University Faculty of Forestry Journal of Forestry*, 18(2), 472-489 [In Turkish].
- Taş, M. K., and Akpınar, E. (2021). Detection of Level Changes In Lakes in Burdur Basin With Geographical Information Systems (GIS) and Remote Sensing (RS). *Eastern Geographical Review*, 26(46): 37-54 [In Turkish].
- Tulan Işıldar, H., and Yalçiner Ercoşkun, Y. (2021). Sustainability and Resilience in Göller Yöresi (Lakes Region). *Journal of Management Theory and Practices Research*, 2(2), 89-116 [In Turkish].
- Yavuz, M., Öz, M., and Albayrak, İ. (2011). Ecological preferences of the east european vole *Microtus levis* (Rodentia: Cricetidae) in the West Mediterranean Region at eleven new localities. *Ekoloji*, 20(81), 30 – 36.
- Yılmaz, M., and Caran, Ş. (2019). Investigation on Geological Features and Environmental Impact of Marble Areas Around Yarışlı Lake (Burdur). *Journal of Sustainable Engineering Applications and Technological Developments*, 2(1), 57-66 [In Turkish].
- Yılmaz, T. (2019). Investigation of the Effects of Marble Quarries on Wildlife with Phototrap Method. Burdur Mehmet Akif Ersoy University Graduate School of Natural and Applied Sciences, MSc Thesis [In Turkish].
- Yılmaz, T., Berberoğlu, E., and Gülle, İ. (2019). *Nature of Burdur*. Burdur: VI Regional Directorate, Ministry of Agriculture and Forestry [In Turkish].

Chapter 11

The Role of Supramolecular Design in the Progress of Gas Sensing Performance with Nano Thin Films by Calix[4]arene Macrocycle: SPR Detection for the Excellent VOC Molecule Recognition

Erkan HALAY^{1,2}

Yaser AÇIKBAŞ³

Rifat ÇAPAN⁴

¹*Assoc. Prof. Dr. ; Usak University, Department of Chemistry, Scientific Analysis Technological Application and Research Center.
erkan.halay@usak.edu.tr ORCID No: 0000-0002-0084-7709*

²*Assoc. Prof. Dr. ; Usak University, Banaz Vocational School, Department of Chemistry and Chemical Processing Technologies, Chemical Tecnology Programme. erkan.halay@usak.edu.tr ORCID No: 0000-0002-0084-7709*

³*Assoc. Prof. Dr. ; Usak University, Faculty of Engineering, Department of Materials Science and Nanotechnology Engineering.
yaser.acikbas@usak.edu.tr ORCID No: 0000-0003-3416-1083*

⁴*Prof. Dr. ; Balikesir University, Faculty of Science, Department of Physics.
rcapan@balikesir.edu.tr ORCID No: 0000-0003-3222-9056*

ABSTRACT

The versatility of synthetic organic chemistry has been making it possible for the materials to be arranged such that those can be integrated to the various sensors and similar electronics. In this context, calix[4]arenes have been extensively employed as a such type of molecules that could be arranged thanks to their capacity to act as preorganization platforms. Under favor of superior electronic and optical properties they gain in this way, significant interest has been achieved in sensing applications, in room temperature gas sensors, in particular. Aside from the applications in ion/molecular sensors along with ion extraction fields, calix[4]arenes as cavity-shaped ligands offer incomparable potentiality for making contact with such guest gaseous species. Measurement of

organic vapors demonstrated by surface plasmon resonance technique (SPR) using calix[4]arene analogs as coating materials have been reviewed in this paper. The adsorption and so sensor capability of those calix[4]arene host species against particularly benzene and toluene vapors as guest species have been criticized. Lastly, the future development potentiality of calix based nano thin film SPR sensors from the point of structure and performance is discussed. As an output of those results and discussions, the importance of the SPR technique has been obviously validated for the application of surface-adsorbed analytes interaction with sensing material-dielectric interface.

Keywords: Calix[4]arenes; Surface Plasmon Resonance; Nano Thin Films; Volatile Organic Compounds; Chemical Sensor.

INTRODUCTION

Since the function of a sensor has been well known as providing information about our biological, chemical and physical environment, an exponential ascent has been observed on the sensor research and accordingly active researcher numbers for almost half a century. Chemical sensors that compose of a physical transducer and a chemically selective layer, are responsible for providing data about their environment (Joo ve Brown, 2008:638). These sensors' operating logic is that their electrical properties/responses change as a result of being affected by the presence of liquid or gaseous species in the chemical environment. As a sensor material, those devices have been fabricated from metals, solid electrolytes, classical semiconductors, insulators and catalytic materials (Adhikari ve Majumdar, 2004:699). Because chemical and physical properties of organic materials can be regulated by various modifications through the special needs, those organic compounds attain much more importance in the design of such sensors.

Within this scope, as organic molecular materials, calixarenes have been prevalently used for the diversity of sensors in organic electronics domain. The changeable/arrangeable electronic distribution arising from atomic and/or molecular substitution within this organic skeleton enables perfectible optical, chemical and electrical properties (Bozkurt ve Halay, 2020:131647; Kumar vd., 2019:9657). Concordantly, relevant host molecules have been classified as compounds that require versatile investigation (Makarov vd., 2023:319). To put it more explicitly, crown-shaped calixarenes involve a central cavity along with chemically active sites for manipulating molecular structure in order to meet the need of respective applications (Mourer vd., 2023:6954; Song vd., 2014:2344; Sanchez vd., 2007:10697). Thus, a vast number of calixarene derivatives can be synthesized by incorporating various substituents both at upper and lower rims of

this three dimensional bowl-shaped skeleton as reported in the literature (Uttam vd., 2023:254; Guo vd., 2021:213560; Durmaz vd., 2018:1389). Besides, in order to understand the structure-activity-properties relationship, considerable efforts have been made for designating their potential applications in the field of chemical sensors. The delocalized electrons existence in the macrocycle along with aromatic character and powerful optical absorption make this supramolecular structure a convenient sensing material in various chemical sensing type including resistive, optical as well as acoustic gas sensors (Abd Karim vd., 2023:734; Halay vd., 2019:2521).

Gas sensors, generally categorized under the branch of chemical detectors, stand out as crucial components of smart detection systems. In recent years; since smaller, cost-efficient, and higher performance sensors having low power consumption and long lifetime are essential for gas sensing applications, those sensors have been continuing to draw attention in broad spectrum of such applications as in the environmental science, medical field, automotive and spacecraft industry, public security, chemical quality control and indoor/outdoor air quality monitoring systems (Mirzaei vd., 2018). Various parameters such as response/recovery time, resolution, reversibility, reproducibility, accuracy and precision along with sensitivity and selectivity as classical ones are considered for the evaluation of the performance of those gas sensors (Nazemi vd., 2019:1285; Acikbas vd., 2015:99; Acikbas vd., 2016:470; Acikbas vd., 2016:18; Büyükkabasakal vd., 2019:9097).

Out of which, having major advantages such as ability of operation by using minimum power at room temperature, giving fast responses and minimal drift and performing in real-time monitoring without gas sample consuming should be thought for the preferring of optical gas sensors (Yang vd., 2021:143; Khan vd., 2020:111782; Hodgkinson ve Tatam, 2013:012004; McDonagh vd., 2008:400). Rather than some common optical techniques such as FTIR and UV-Vis spectrophotometry along with ellipsometry, SPR technique, as one of the oldest techniques for optical gas sensing applications, have magnificent advantages (Gahlot vd., 2022:1619). Because SPR is sensitive to the changes about the surface refractive index of materials, this SPR phenomenon has attracted extreme attention. Due to their such features like rapid detection, high stability and sensitivity, ease of sample preparation, being non-destructive and capability of room temperature operating, SPR based sensors exhibit extensive application framework with the fields like environmental monitoring, biomarker detection, medical diagnostics and food allergen screening (Kumar vd., 2022:15661; Zhang vd., 2022:2200009; Roh vd., 2011:1565). While these SPR sensors deal with the refractive index of the analyte molecule directly contacting metallic

grating/surface, SPR sensors containing this metallic grating reveal their performance based upon the permittivity of the metal used. Accordingly, gold have been used as an SPR active surface (Chaudhary vd., 2023:1012).

As a matter of course, an optimized sensing layer is required for the application by SPR technique based gas sensing. Therefore, optimization in terms of fabrication of suitable selected material is crucial in sensor development. At this point, nano structured thin films have been being in the centre of attention owing to their unique features like very small grain size and high surface/volume ratio that both enhancing the sensor performance even at room temperature by facilitating surface interactions with the target gas analyte (Shah vd., 2023:478). Besides exhibiting their great potential usage in the sensor field, those thin films have also found certain applications in numerous fields such as detectors, molecular electronic devices, switching devices, surface coating, optical signal processing and nonlinear optics. The perfectly organized molecular thin films having specific properties and attentive molecule alignment are the basic requirements for such sensor applications, along with a substrate having good stability against thermal and chemical changes (Hussain vd., 2018:e01038). In other words, the related applications require thin film deposition on a solid substrate. Within this scope, several techniques have been used to deposit thin films on solid substrates such as spin-coating, chemical vapor deposition, electrochemical deposition, layer by layer, adsorption and the Langmuir-Blodgett (LB) techniques (Guaus ve Torrent-Burgues, 2022:139145). As the composition of thin film and its distinctive features such as surface morphology along with crystal structure size designate the optical/electrical performance, the LB technique is one of the most popular and useful methods for the nano thin film fabrication among those different methodologies (Malik ve Tripathi, 2013:235). In addition to a wide variety of surface characterization techniques can be used to examine the structure of films created with this technique, it is also a practical method that provides a way of obtaining well-ordered mono/multilayer films on various solid substrates and creates the carefully controlled final supramolecular architectures of organized molecular assemblies that allows the studies of physical phenomena on a molecular level as in above mentioned areas (Li vd., 2022:6761).

In conclusion, for the last quarter-century, a vast number of studies about gas sensing technology that constituted several branches of detection methods have been carried out while some of them have been in the spotlight due to their prospective applications along with distinctive operation principle and convenient fabrication methods. We hope that this review providing the recent

advancements made for SPR sensors along with potential applications based future progress would be directive and shed light upon many forthcoming works.

THE HARMFUL VOLATILE ORGANIC COMPOUNDS (VOCs)

Volatile organic compounds (VOCs) are also known as compounds that cause air pollution and are emitted into indoor air from materials used in daily life such as cigarettes, solvents, paints and thinners, adhesives, dry cleaning fluids, wood protective coatings, photocopiers and printing machines, printers, air fresheners and pesticides. Indoor furniture, cleaning materials, and even cooking can produce these pollutants. The effects of exposure to volatile organic compounds vary depending on several important factors such as the type of volatile organic compounds, the amount and the duration of exposure. Long or short-term exposure to high concentrations of some volatile organic compounds can lead to certain diseases and serious irreversible effects. VOCs commonly found in indoor environments are classified as aliphatics, olefins, aromatics, halogenated hydrocarbons, terpenes and others.

The information about the VOCs (benzene and toluene) selected within the scope of this study is briefly described below.

Benzene

Benzene with chemical formula C_6H_6 and molecular weight 78.1 is colourless and odourless. It is volatile as it has a vapor pressure of 100 mmHg at 26 °C. It is partially soluble in water (Paustenbach vd., 1993:177). The acute and chronic effects of benzene have been studied by many researchers. According to the results of a study conducted on 330 workers exposed to benzene, benzene metabolites were found to be abundant in their blood and urine samples (Kotb vd., 2013:411). Studies have shown that benzene, like various aromatic hydrocarbons, is carcinogenic. When benzene is taken in high doses and in a short time, it results in death. Low level exposure causes adverse effects such as dizziness, drowsiness, heart rhythm disturbances (Akal, 2013:112).

Toluene

With the chemical formula $C_6H_5CH_3$, toluene is soluble in water and has a moderate vapor pressure. Sources where toluene is released into the indoor or outdoor environment include motor vehicles, jets, oil refineries, rubber and paint manufacturing industries, varnishes and tobacco smoke (Reyna and Lee, 2015:1). It is a compound that can be found in various products used in households at an average rate of 12%. Toluene exposure causes various health problems in the eyes, respiratory system and skin. In case of exposure to small amounts, the

central nervous system is suppressed, and memory loss may occur. Symptoms such as headache, fatigue, dizziness, abdominal pain and even coma can be observed (Çomunoğlu vd., 2009:33).

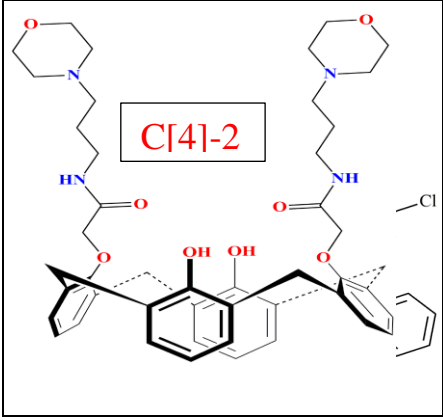
CALIX[4]ARENE-BASED CHEMICAL SENSOR MATERIALS

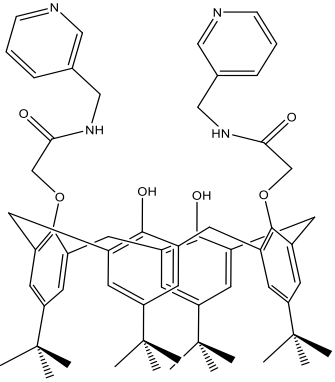
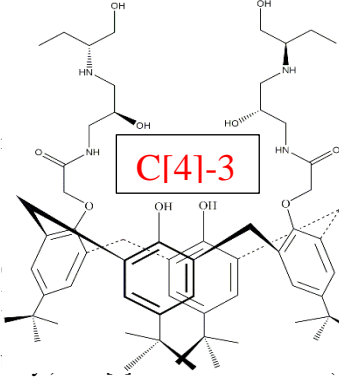
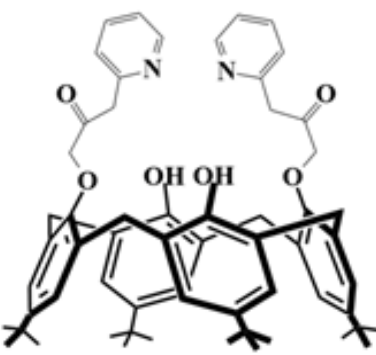
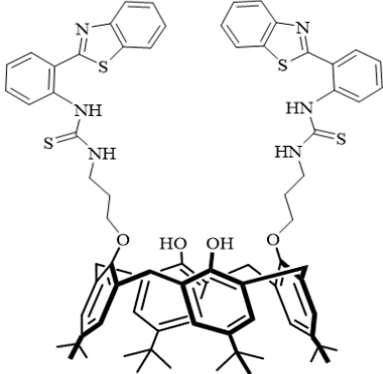
Calixarenes are macrocyclic compounds usually obtained under base catalysis of formaldehyde and p-alkyl phenols. The name was coined by D. Gutsche and is derived from the Latin word "calyx" meaning "vase" due to its vase-like structure. Calixarenes have been synthesized by two general methods. One is the synthesis based on the long and multi-step Hayes and Hunter method. The other is the base-catalyzed condensation of formaldehyde and phenol synthesized by the Zinke-Cornforth method. The vase-like structures of calixarenes are widely used to obtain the central molecules of the formed medium. Calixarene derivatives can also form complexes with cations or neutral molecules. Calixarene is a good carrier for anion, neutral and cation molecules due to its ring structure, easy derivatization and ability to form molecular gaps of different volumes. Due to this feature of calixarene, they have a wide range of applications (Hahn vd., 2006:2519).

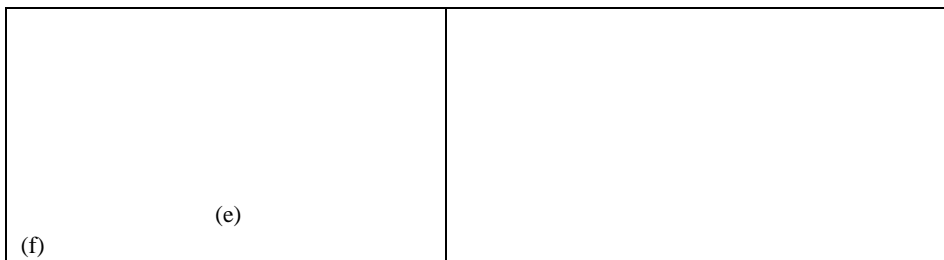
Calixarenes are converted into suitable carriers using the production of nano thin film methods such as spin coating and Langmuir-Blodgett (LB) thin film technique. Calixarenes are converted into monolayer polymeric carrier materials to form membranes. The phases of these membranes can be changed by looking at the permeability ratio and molecular voids (Brake vd., 1993:65).

Table 1 shows some of the calix[4]arene-based materials in the literature that are preferred for developing chemical sensor elements.

Table 1. Some calix[4]arene-based materials used to develop chemical sensor elements.

	<p>Chemical structure of (a) 25,27(Dipropylmorpholinoacetamido)- 26,28-dihydroxycalix[4]arene molecule (Acikbas vd., 2017:77),</p> <p>(b) The C[4]-1 calix[4]arene molecule (Halay vd., 2019:2521).</p>
---	--

<p>(b)</p>	<p>(a)</p>
 <p>(c)</p>	 <p>axlix[4]arene xy-3-[[1R)-]asetamide (tert- ikbas vd., 2021:14).</p> <p>(d)</p>
	 <p>ene molecule]arene-thiour (Bozkurt vd., 2022:629)</p>



SURFACE PLASMON RESONANCE (SPR) TECHNIQUE

SPR is one of the spectroscopic methods used to measure the thickness and refractive index of thin films on metal surfaces. Figure 1 shows a symbolic presentation of the SPR measurements. The thickness of LB films and their weakly bound molecular interactions with organic vapors can be studied with the sensitivity of SPR (Laurinavichyute VD., 2017:1552). That is, the layer-by-layer production of thin films is controlled in relation to the angle shift in the SPR curve of the molecules attached to the substrate. On the other hand, the thickness of the thin film is kept constant and exposed to organic vapors and the molecular interactions are analysed in relation to the reflected light changes recorded in the photodetector.

The light intensity reflected of the metal-thin film structure is recorded as a function of the incident angle in the form of an SPR curve. Surface plasmons (SPs) are waves that have their maximum intensity at the interface and decay exponentially at a penetration depth of the order of 200 nm from the phase boundary (Özbek vd., 2011:235). SPs are not excited directly at air-metal interfaces because momentum matching conditions are not met. Therefore, it becomes necessary to use a prism coupling setup to excite SPs. The most commonly used setup in SPR imaging experiments is the Kretschmann configuration shown in Figure 2. A thin metal surface (usually a 50 nm thick gold surface) is placed in direct contact with the prism. The lost light wave generated at the prism-metal interface during total internal reflection is used to excite SPs on the metal surface. This energy loss is observed as a sharp attenuation of reflectivity known as the surface plasmon resonance effect. At the angles at which this occurs, the refractive index of the medium in contact with the metal surface of the SPR sensor changes very sensitively. Molecular interactions that cause a change in the refractive index, or an increase in molecular mass, change the intensity of the sensor material and hence the angle of incident light, which translates into a response signal in the detector. This change causes a shift in the minimum of the resonance angle in the SPR graph. For thin films with linearly increasing thickness, the change in the resonance angle increases in direct

proportion. From this data, the thickness of the transferred layers can be determined. Since SPR imaging can monitor the amount and distribution of molecules transferred to a metal surface in real time, its use for the determination of the manufacturability of thin film monolayers is quite common (Capan vd., 2015:129).

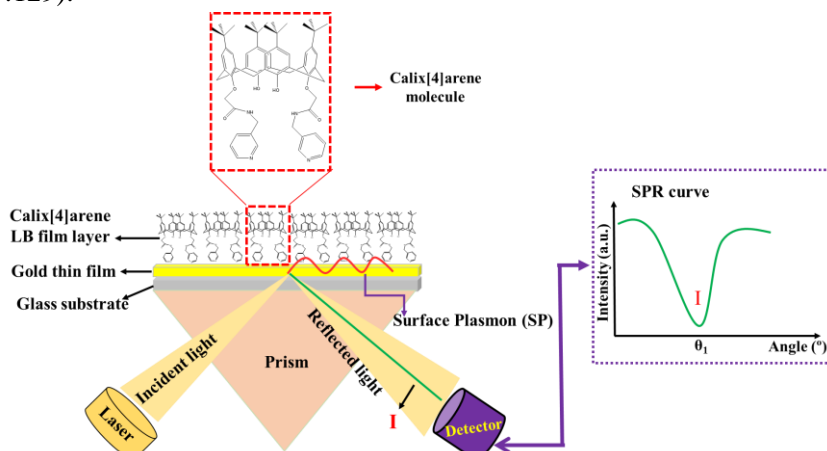


Figure 1. A schematic presentation of the SPR measurements.

SPR Kinetic Measurements

A schematic representation of the gas cell for SPR kinetic measurements is given in Figure 2. When the sensor surface is organized to contain selective receptors for specific chemicals or biomolecules, the structure of the newly formed material can be applied in chemical and biochemical sensor fields. SPR spectroscopy is one of the main optical techniques used today for the development of low-cost and high-resolution chemical and biochemical optical sensors (Homola vd., 1999:3). If binding to target molecules occurs, the refractive index changes, leading to a change in the SPR angle, which can be monitored in real time by detecting the difference in the intensity of the reflected light. SPR sensing has been receiving increasing attention in the scientific community due to its advantages of real-time monitoring and remarkable sensitivity.

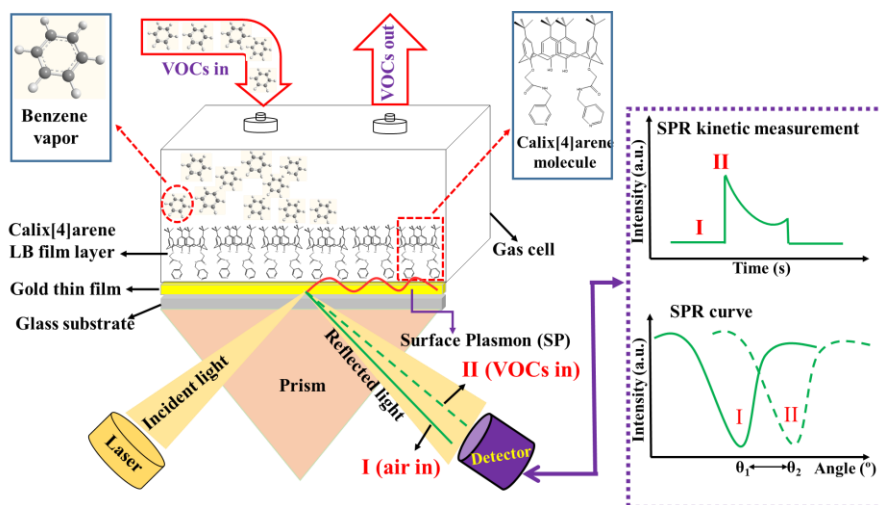


Figure 2. A symbolic presentation of SPR gas kinetic measurements.

Figure 3 shows the comparison of the response of thin film sensors produced from C[4]-1, C[4]-2 and C[4]-3 materials in the literature to benzene vapor. Nano thin films of three different calix[4] materials were fabricated by LB thin film technique. In this context, the response of the developed C[4]-1, C[4]-2 and C[4]-3 LB thin film chemical sensors against some aromatic hydrocarbons (benzene and toluene) was investigated by SPR optical technique. All response values (reflected light intensity) were recorded as a function of time. In Figure 3, the reflected light intensity ratios of the y-axis are presented as a normalized response by the formula given below.

$$\text{Normalised Response (\%)} = \frac{\Delta I}{I_0} \times 100 \quad (1)$$

Here, ΔI represents the difference between the reflected intensity (I) measured at any time and the initial reflected intensity (I_0) measured at $t=0$.

During the first 120 seconds, there is fresh air in the environment of the chemical sensor (gas sensor cell). Between 121st second and 240th second, benzene vapor exists in the cell. Benzene vapor was allowed to remain in the cell for 120 seconds and the responses were recorded over time. Between 121st and 125th seconds, it is thought that a rapid increase in the reflected light intensity ratio is observed due to the molecules of benzene vapor trying to attach to the thin film sensor. This is known as "adsorption" in gas kinetic measurements. After 125. seconds, the adsorption process gives way to diffusion. In this process, the vapor molecules diffuse into the thin film sensor and cause the thin films to swell. At 240 seconds, fresh air was introduced into the gas cell to test whether the reflected light intensity would return to approximately its initial value, and fresh air was allowed to remain in the environment for 120 seconds. It can be

seen that after air is introduced, the three thin film sensors return to approximately the initial reflected intensity ratio. The response values $[(\Delta I/I_0) \times 100]$ of C[4]-1, C[4]-2 and C[4]-3 based LB thin film sensors to benzene vapor were determined as 96.18 %, 71.18 % and 48.77 %, respectively.

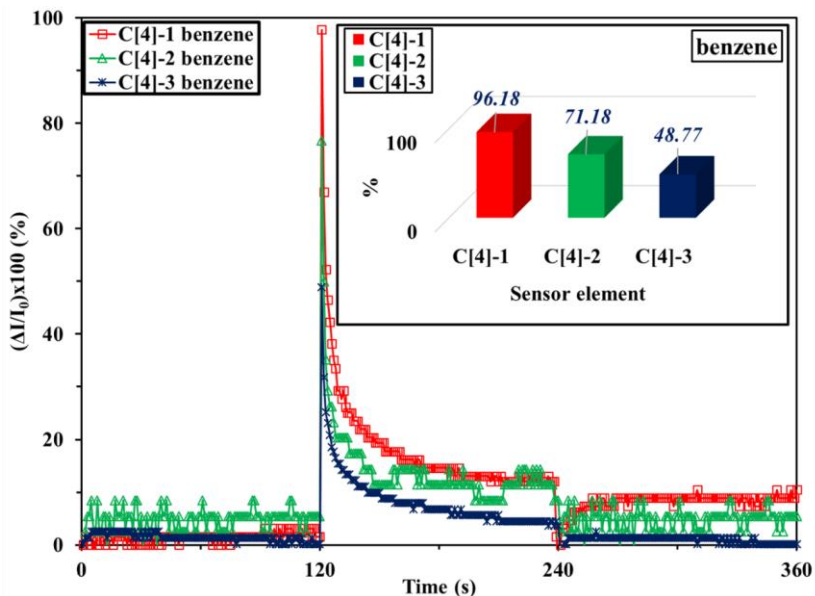


Figure 3. The comparison of the responses of C[4]-based LB thin film sensors to benzene vapor.

A similar experimental process was performed by exposing C[4]-1, C[4]-2 and C[4]-3 LB thin film chemical sensors to toluene vapor. The response values $[(\Delta I/I_0) \times 100]$ of C[4]-1, C[4]-2 and C[4]-3 based LB thin film sensors against toluene vapor, whose interaction graphs are given in Figure 4, were determined as 93.52 %, 50.42 % and 78.45 % respectively.

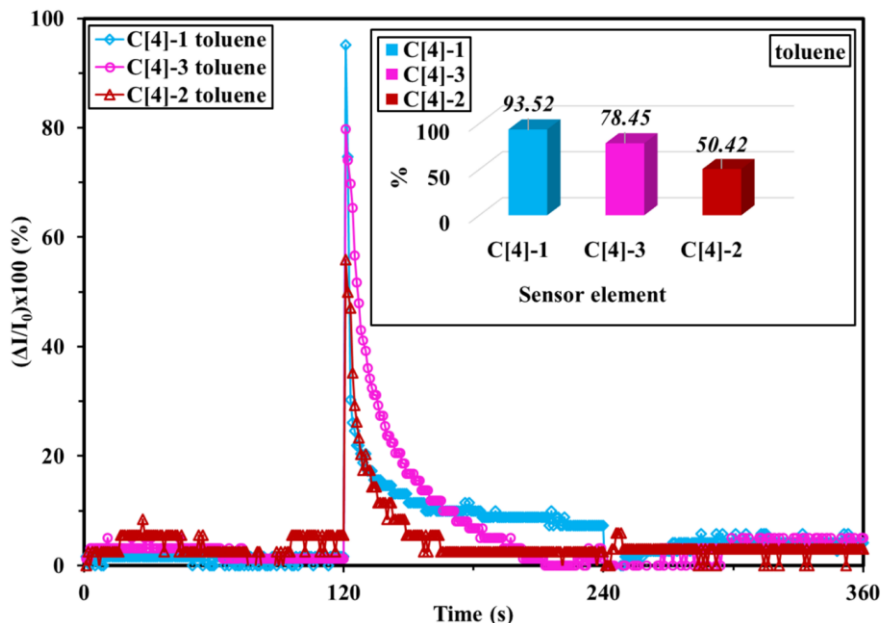


Figure 4. The comparison of the responses of C[4]-based LB thin film sensors to toluene vapor.

CONCLUSIONS

In this review, the sensitivity of some macrocyclic (C[4]-1, C[4]-2 and C[4]-3) calix[4]arene materials to some aromatic hydrocarbons using SPR technique was reviewed and compared. When the response values of C[4]-1, C[4]-2 and C[4]-3 LB thin film chemical sensors to benzene and toluene vapors were compared; i) C[4]-1 LB thin film sensor showed the highest response to benzene and toluene vapors compared to other C[4]-based LB thin film sensors, ii) C[4]-2 LB thin film sensor showed higher response to benzene (71.18 %) and relatively lower response to toluene vapor (50.42 %), iii) C[4]-3 LB thin film sensor showed lower response to benzene (48.77 %) and relatively higher response to toluene vapor (78.45 %). It can be concluded that the preference of C[4]-based materials in the development of LB thin film sensors and their sensitivity to some aromatic carbon vapors are considered promising for use as sensor elements in chemical sensor applications at the room temperature.

References

- Abd Karim, N. F. N., Supian, F. L., Musa, M., Ayop, S. K., Azmi, M. S. M., Yazid, M. D., ve Yi, W. Y. (2023). Calixarene derivatives: A mini-review on their synthesis and demands in nanosensors and biomedical fields. *Mini-Reviews in Medicinal Chemistry*, 23(6), 734-745.
- Acikbas, Y., Capan, R., Erdogan, M., Yukruk, F. (2015). Characterization and organic vapor sensing properties of Langmuir-Blodgett film using perylendiimide material, *Res. Eng. Struct. Mat.* 2, 99–108.
- Acikbas, Y., Dogan, G., Erdoğan, M., Çapan, R., Soykan, C. (2016). Organic vapor sensing properties of copolymer Langmuir-Blodgett thin film sensors, *J. Macromol. Sci. Part A*, 53(8), 470–474.
- Acikbas, Y., Cankaya, N., Çapan, R., Erdoğan, M., Soykan, C. (2016). Swelling behavior of the 2-(4-methoxyphenylamino)-2-oxoethyl methacrylate monomer LB thin film exposed to various organic vapors by quartz crystal microbalance technique, *J. Macromol. Sci. Part A*, 53(1), 18-25.
- Acikbas, Y., Bozkurt, S., Halay, E., Capan, R., Guloglu, M.L., Sirit, A., Erdogan, M. (2017). Fabrication and characterization of calix[4]arene LangmuireBlodgett thin film for gas sensing applications, *J. Inclusion Phenom. Macrocycl. Chem.* 89, 77-84.
- Acikbas, Y., Zeybek, N., Ozkaya, C.,Guloglu, M. L., Sirit, A., Erdogan, M., Capan, R., Bozkurt, S., (2021). Optical and organic vapor properties of Calix[4]arene based macrocyclic Langmuir-Blodgett thin films. *Journal of Optoelectronics And Advanced Materials*, 23(1-2), 14-21.
- Adhikari, B., ve Majumdar, S. (2004). Polymers in sensor applications. *Progress in Polymer Science*, 29(7), 699-766.
- Akal, D. (2013). İç Ortam Hava Kirliliği ve Çalışanlara Olumsuz Etkileri. *Çalışma Dünyası Dergisi*, 1(1), 112-119.
- Ariga, K., Yamauchi, Y., Mori, T., ve Hill, J. P. (2013). 25th Anniversary article: What can be done with the Langmuir-Blodgett method? Recent developments and its critical role in materials science. *Advanced Materials*, 25(45), 6477-6512.
- Bozkurt, S., ve Halay, E. (2020). Synthesis, application and AIE properties of novel fluorescent tetraoxocalix[2]arene[2]triazine: The detection of a hazardous anion, cyanate. *Tetrahedron*, 76(46), 131647.
- Bozkurt, S., Durmaz, M., Erdogan, M., Ozkaya Erdogan, C., Capan, R., Acikbas Y. (2022). The bisbenzothiazole-p-tert-butylcalix[4]arene-thiourea Langmuir–Blodgett thin films: preparation, optical properties, swelling

- dynamics and gas sensing properties via host–guest principles. *J. Inclusion Phenom. Macrocycl. Chem.*, 102, 629-636.
- Brake, M., Böhmer, V., Krämer, P., Vogt, W., Wortmann, R. (1993). O-Alkylated p-Nitrocalix[4]arenes, Syntheses, LB-Monolayers and NLO-Properties, *Supramolecular Chemistry*, 2, 65-70.
- Büyükkabasakal, K., Acikbas, S. C., Deniz, A., Acikbas, Y., Capan, R., Erdogan, M. (2019). Chemical sensor properties and mathematical modeling of graphene oxide langmuir-blodgett thin films, *IEEE Sensors Journal*, 19(20), 9097-9104.
- Capan, R., Göktas, H., Özbek, Z., Sen, S., Özel M. E., F. Davis. (2015). Langmuir–Blodgett thin film for chloroform detection. *Appl. Surf. Sci.*, 350, 129–134.
- Chaudhary, V. S., Kumar, D., Pandey, B. P., ve Kumar, S. (2023). Advances in photonic crystal fiber-based sensor for detection of physical and biochemical parameters-A review. *IEEE Sensors Journal*, 23(2), 1012-1023.
- Çomunoğlu, N., Doğan Ekici, I., Eren, B., Türkmen, N., Fedakar, R., Çöloğlu, S. (2009). Toluene Bileşiklerinin Toksik Etkilerinin 4 Otopsi Olgusu Üzerinden Değerlendirilmesi. *Adli Tıp Dergisi*, 23(1), 33-43.
- Durmaz, M., Halay, E., ve Bozkurt, S. (2018). Recent applications of chiral calixarenes in asymmetric catalysis. *Beilstein Journal of Organic Chemistry*, 14, 1389-1412.
- Gahlot, A. P. S., Paliwal, A., ve Kapoor, A. (2022). Theoretical and experimental investigation on SPR gas sensor based on ZnO/polypyrrole interface for ammonia sensing applications. *Plasmonics*, 17(4), 1619-1632.
- Guaus, E., ve Torrent-Burgues, J. (2022). Characterization of modified solid electrodes with organized thin films of a tetra-substituted zinc phthalocyanine. *Thin Solid Films*, 747, 139145.
- Guo, C., Sedgwick, A. C., Hirao, T., ve Sessler, J. L. (2021). Supramolecular fluorescent sensors: An historical overview and update. *Coordination Chemistry Reviews*, 427, 213560.
- Hahn, M-S., Taite, L-J., Moon, J.J., Rowland, M.C., Ruffino, K.A., West, J.L. (2006). Photolithographic patterning of polyethylene glycol hydrogels. *Biomaterials*, 27, 2519–2524.
- Halay, E., Acikbas, Y., Capan, R., Bozkurt, S., Erdogan, M., ve Unal, R. (2019). A novel triazine-bearing calix[4]arene: Design, synthesis and gas sensing affinity for volatile organic compounds. *Tetrahedron*, 75(17), 2521-2528.
- Hodgkinson, J., ve Tatam, R. P. (2013). Optical gas sensing: A review. *Measurement Science and Technology*, 24(1), 012004.

- Homola, J., Yee, S. S., ve Gauglitz, G. (1999). Surface plasmon resonance sensors: Review. *Sensors & Actuators: B. Chemical*, 54(1-2), 3-15.
- Hussain, S. A., Dey, B., Bhattacharjee, D., ve Mehta, N. (2018). Unique supramolecular assembly through Langmuir-Blodgett (LB) technique. *Heliyon*, 4(12), e01038.
- Joo, S., ve Brown, R. B. (2008). Chemical sensors with integrated electronics. *Chemical Reviews*, 108(2), 638-651.
- Khan, S., Le Calve, S., ve Newport, D. (2020). A review of optical interferometry techniques for VOC detection. *Sensors and Actuators A: Physical*, 302, 111782.
- Kotb, M.A., Ramadan, H.S., Shams El-Din, R., Motaweh, H.A., Shehata, R.R., El-Bassiouni, E.A. (2013). Changes in Some Biophysical and Biochemical Parameters in Blood and Urine of Workers Chronically Exposed To Benzene. *European Scientific Journal*, 9 (24), 411-422.
- Kumar, R., Sharma, A., Singh, H., Suating, P., Kim, H. S., Sunwoo, K., Shim, I., Gibb, B. C., ve Kim, J. S. (2019). Revisiting fluorescent calixarenes: From molecular sensors to smart materials. *Chemical Reviews*, 119(16), 9657-9721.
- Kumar, V., Raghuwanshi, S. K., ve Kumar, S. (2022). Recent advances in carbon nanomaterials based SPR sensor for biomolecules and gas detection-A review. *IEEE Sensors Journal*, 22(16), 15661-15672.
- Laurinavichyute, V.K., Nizamov, S., Mirsky, V.M. (2017). The role of anion adsorption in the effect of electrode potential on surface plasmon resonance response. *Chem. Phys. Chem.*, 18 (12), 1552-1560.
- Li, N., Zhao, T., Bian, P., Liu, S., Ma, J., Liu, B., ve Jiao, T. (2022). Gas-responsive and self-powered visual composite Langmuir-Blodgett films for ultrathin gas sensors. *Langmuir*, 38(21), 6761-6770.
- Makarov, E., Iskhakova, Z., Burilov, V., Solovieva, S., ve Antipin, I. (2023). Synthesis of functional (thia)calix[4]arene derivatives using modular azide-alkyne cycloaddition approach. *Journal of Inclusion Phenomena and Macrocyclic Chemistry*, 103(9-10), 319-353.
- Malik, S., ve Tripathi, C. C. (2013). Thin film deposition by Langmuir Blodgett technique for gas sensing applications. *Journal of Surface Engineered Materials and Advanced Technology*, 3(3), 235-241.
- McDonagh, C., Burke, C. S., ve MacCraith, B. D. (2008). Optical chemical sensors. *Chemical Reviews*, 108(2), 400-422.
- Mirzaei, A., Kim, J.-H., Kim, H. W., ve Kim, S. S. (2018). Resistive-based gas sensors for detection of benzene, toluene and xylene (BTX) gases: A review. *Journal of Materials Chemistry C*, 6(16), 4342-4370.

- Mourer, M., Regnouf-de-Vains, J.-B., ve Duval, R. E. (2023). Functionalized calixarenes as promising antibacterial drugs to face antimicrobial resistance. *Molecules*, 28(19), 6954.
- Nazemi, H., Joseph, A., Park, J., ve Emadi, A. (2019). Advanced micro- and nano-gas sensor technology: A review. *Sensors*, 19(6), 1285.
- Özbek, Z., Çapan, R., Göktaş, H., Şen, S., İnce, F. G., Özel, M. E., Davis, F. (2011). Optical parameters of calix[4]arene films and their response to volatile organic vapors. *Sensors & Actuators: B. Chemical*, 158, 235-240.
- Ozkaya, C., Capan, R., Erdogan, M., Bayrakci, M., Ozmen, M., Acikbas Y. (2020). Fabrication of picoline amide-based calix[4]arene Langmuir-Blodgett thin film for volatile organic vapor sensing application. *Mol. Cryst. Liq. Cryst.* 710 (1) 49–65.
- Ozkaya Erdogan, C., Capan, R., Acikbas Y., Ozmen, M., Bayrakci, M. (2022). Sensor application of pyridine modified calix[4]arene Langmuir-Blodgett thin film. *Optik*. 265, 169492.
- Paustenbach, D.J., Bass, R.D., Price, P. (1993). Benzene Toxicity and Risk Assessment, 1972-1992: Implications ofr Future Regulation. *Environmental Health Perspectives Suttlements*, 101, 177-200.
- Reyna, M., Lee, J. S. (2015). Toluene. *Texas Commission On Environmental Quality*, 1-14.
- Roh, S., Chung, T., ve Lee, B. (2011). Overview of the characteristics of micro- and nano-structured surface plasmon resonance sensors. *Sensors*, 11(2), 1565-1588.
- Sanchez, A., Jimenez, R., Ternero, F., Mesa, R., Pinero, C. A., Muriel, F., ve Lopez-Cornejo, P. (2007). Rigidity and/or flexibility of calixarenes. Effect of the p-sulfonatocalix[n]arenes (n = 4, 6, and 8) on the electron transfer process $[\text{Ru}(\text{NH}_3)_5\text{pz}]^{2+} + \text{Co}(\text{C}_2\text{O}_4)_3^{3-}$. *Journal of Physical Chemistry B*, 111(36), 10697-10702.
- Shah, A. Y., Choudhury, S., ve Betty, C. A. (2023). Reliable liquified petroleum gas sensing at room temperature by nanocrystalline SnO₂ thin film deposited by Langmuir–Blodgett method. *Applied Physics A: Materials Science & Processing*, 129(7), 478.
- Song, M., Sun, Z., Han, C., Tian, D., Li, H., ve Kim, J. S. (2014). Calixarene-based chemosensors by means of click chemistry. *Chemistry-An Asian Journal*, 9(9), 2344-2357.
- Uttam, B., Polepalli, S., ve Rao, C. P. (2023). Synthetic strategies for the functionalization of upper or lower rim of supramolecular calix[4]arene platform. *Arkivoc*, 2022(6), 254-279.

- Yang, T., Chen, W., ve Wang, P. (2021). A review of all-optical photoacoustic spectroscopy as a gas sensing method. *Applied Spectroscopy Reviews*, 56(2), 143-170.
- Zhang, S., Han, B., Zhang, Y.-N., Liu, Y., Zheng, W., ve Zhao, Y. (2022). Multichannel fiber optic SPR sensors: Realization methods, application status, and future prospects. *Laser & Photonics Reviews*, 16(8), 2200009.

Chapter 12

A Review Exploring Biological Activities Of *N*-Sulfonyl Hydrazones (From 2013 To 2023)

Belma HASDEMİR¹

Tülay YILDIZ²

¹Doç.Dr.; İstanbul University-Cerrahpaşa, Engineering Faculty, Chemistry Department. b.hasdemir@iuc.edu.tr ORCID No: 0000-0002-1071-1127

²Doç.Dr.; İstanbul University-Cerrahpaşa, Engineering Faculty, Chemistry Department. tulayyil@iuc.edu.tr ORCID No: 0000-0001-5857-2480

1. INTRODUCTION

Hydrazone group, an important moiety richly found in medicinal molecules, plays a critical role in drug design strategy and functions as bioactive scaffolds due to their various biological and chemotherapeutic activities (Biliz et al., 2023; Hasdemir, 2022; Şenkardeş et al., 2016). Over the past ten years, sulfonyl hydrazones in particular have gained a lot of attention because of their broad-spectrum bioactivities. Sulfonyl hydrazones, defined as non-classical isosteres of acylhydrazones and containing a special structural part (SO₂NHN-C-), are widely used in medicine and agriculture, especially against microbial infections, due to their ability to bind well to the active sites of organisms. Apart from these attributes, sulfonyl hydrazones are among the class of compounds that have been widely employed in recent times for the identification of novel molecules with biological significance because of their capacities like antitumors. (Yang et al., 2021), antioxidant (Karaman et al., 2016; Kurşun Aktar et al., 2020), analgesic (Oliveira et al., 2012), antiurease (Arshia et al., 2019), antidepressant (Oliveira et al., 2011), activity against Alzheimer's disease (Fernandes et al., 2017), insecticidal activity (Wang et al., 2014) and inhibiting the activity of enzymes (Aktar et al., 2014). Figure 1 shows some *N*-sulfonyl hydrazones with various biological properties.

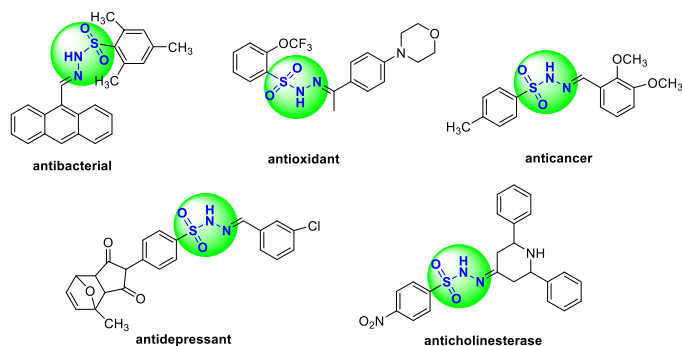


Figure 1. Some *N*-sulfonyl hydrazones with biological properties

The synthesis of sulfonyl hydrazones typically involves a condensation reaction between sulfonyl hydrazides and aldehydes or ketones. The reaction takes place with the addition of glacial acetic acid in a protic or aprotic solvent (such as ethanol, methanol, THF)(Başaran, 2023; Bilen et al., 2022; Shaaban et al., 2020).

This work reviews the studies on the biological activities of *N*-sulfonyl hydrazones in the last decade.

2. BIOLOGICAL ACTIVITIES

Antibacterial and antifungal activity

Nowadays, death rates are increasing rapidly as a result of the increase in hospital infections caused by microorganisms resistant to antibiotics. Unregulated drug sales and access, as well as unregulated drug usage, are the causes of this resistance's formation. As a result, the pharmaceutical industry is focusing on creating new antimicrobial drugs that do not yet have the defense mechanisms established by bacteria. For example, small molecule organic molecules such as oximes, diols, amino alcohols, hydrazones, and sulfonyl hydrazones are very important compounds due to their biological activity (Başpınar Küçük et al., 2017; Hasdemir et al., 2018; Popiołek, 2021). In this context, synthesizing new sulfonyl hydrazones, which is our research topic, is extremely important for the development of new drug candidates with better antibacterial effects and expected to be less toxic.

In 2013, Aslan and Karacan synthesized a series of sulfonyl hydrazone compounds to obtain new antimicrobial agents (Figure 2). The synthesized substances were tested for their antifungal potential against yeasts and efficiency against various bacteria. The authors found that all compounds showed strong inhibition against all strains tested. Compound **4** exhibited

detectable efficacy against selected bacteria. Except for *E. coli*, compound **3** exhibited good action against all tested bacteria. (Aslan & Karacan, 2013).

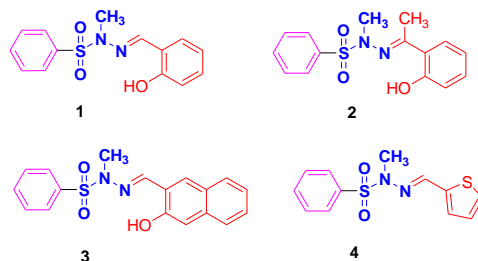


Figure 2. New aromatic sulfonyl hydrazones as antimicrobial agents

Özbek et al. (2013) prepared various metal (Cu(II), Ni(II), Pt(II), and Pd(II)) complexes of the sulfonylhydrazone compound they synthesized (Figure 3). They tested the antibacterial efficacy of the complexes they prepared against several bacteria. According to research on antibacterial activity, The compounds with the highest activity against all bacteria were Pt(II) and Pd(II) complexes (Özbek et al., 2013).

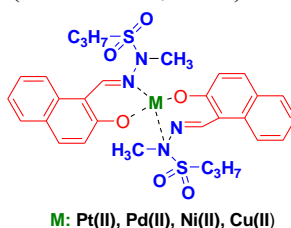


Figure 3. Structure of sulfonylhydrazone complexes

In another study, Gündüzalp and co-workers synthesized aromatic/heteroaromatic sulfonylhydrazone derivatives (Figure 3). The antibacterial characteristics of the obtained compounds were assessed against various microorganisms. The activity results showed that the sulfonylhydrazones had weak activity against the microorganism at the concentration studied. However, compound **10** showed better activity against all microorganisms compared to the other compounds. *Staphylococcus aureus* was found to be the most affected bacterium against compound **10**. However, fungicidal screening of compound **6** showed that the compound had less activity against fungi (*Candida albicans*) (Gündüzalp et al., 2014).

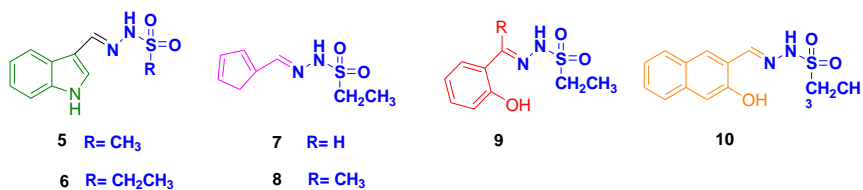


Figure 4. The structure of the aromatic/heteroaromatic sulfonylhydrazones

Bhat et al. investigated the antibacterial efficacy of several novel arylsulfonylhydrazones (**11a-f**) against both Gram-positive and Gram-negative microorganisms (Figure 5). It was discovered that compounds **11a** and **11c**, with MIC values of 3.12 and 6.25 mg/mL, respectively, inhibited the development of *E. faecalis*. Additionally, against the *S. aureus* strain, all of the compounds were found to be somewhat active (Bhat et al., 2018).

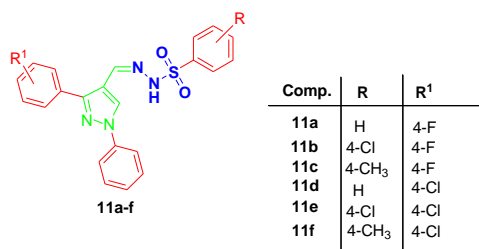


Figure 5. Substituted *N'*-[4-(4-aryl)-1-phenyl-1*H*-pyrazol-3-yl]methyldene-benzenesulfonylhydrazones

In 2021, sulfonyl hydrazone derivatives containing heteroatoms were synthesized and their antimicrobial properties were investigated by Celebioğlu et al. All compounds were found to have antimicrobial activity against *E. coli* and *S. aureus* bacteria. Compound **13** demonstrated the highest efficacy against *S. aureus* and *E. coli*, with concentration values of $831.4 \pm 143.3 \mu\text{g/mL}$ and $703.2 \pm 187.3 \mu\text{g/mL}$, respectively (Celebioğlu et al., 2021).

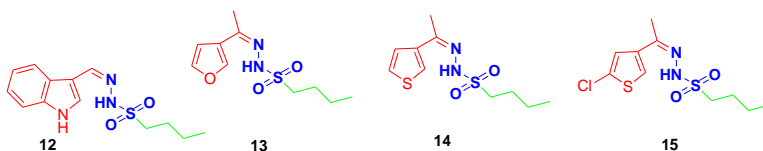


Figure 6. Heteroatom-containing sulfonyl hydrazone derivatives

The antibacterial activity of N'-(substituted arylmethylidene)-4-nitrobenzenesulfonylhydrazide derivatives synthesized by Şenkardeş et al was examined against some bacteria species (Figure 7). It was discovered that every obtained compound had extremely potent antibacterial action against the tested microorganisms. (*E. coli*, *S. aureus*, Methicillin resistant *S. aureus*, *P. aeruginosa*, *E. faecalis* and *K. pneumoniae*) with MIC values ranging from 6.25 to 25 µg/mL. The best inhibitory effect (MIC 6.25 µg/ml) was observed against *P. aeruginosa* (Şenkardeş et al., 2021).

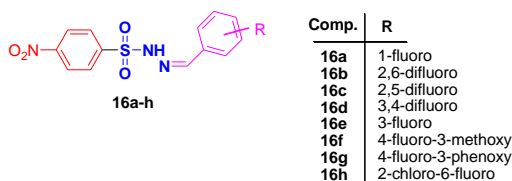


Figure 7. Synthesized N'-(substituted arylmethylidene)-4-nitrobenzene sulfonylhydrazide derivatives

In another study, Popiołek and colleagues synthesized a series of sulfonyl hydrazone-derived compounds and tested their antibacterial activity against a variety of bacteria *in vitro* (Figure 8). Additionally, research was done on its antifungal activity against yeasts. However, it was discovered that none of the substances examined had any effect on Gram-negative fungi or bacteria. According to the findings of the *in vitro* bioactivity study, compound **17x** showed a strong bactericidal effect against the bacteria tested (Popiołek et al., 2021).

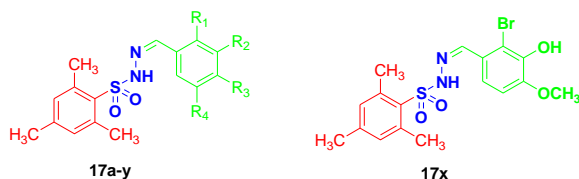


Figure 8. Synthesized 2,4,6-trimethylbenzenesulfonyl hydrazone derivatives

Yu and colleagues examined the antibacterial activities of a series of new sulfonyl hydrazone-derived compounds they synthesized against several bacteria (*Xoo*, *Xoc*, and *Xac*) (Figure 9). When tested against the specified bacteria, the majority of the compounds were shown to have good antibacterial

activity. In particular, compounds **18g**, **18i**, **18j**, and **18l** exhibited very strong inhibitory effects against *Xoo* (Yu et al., 2021).

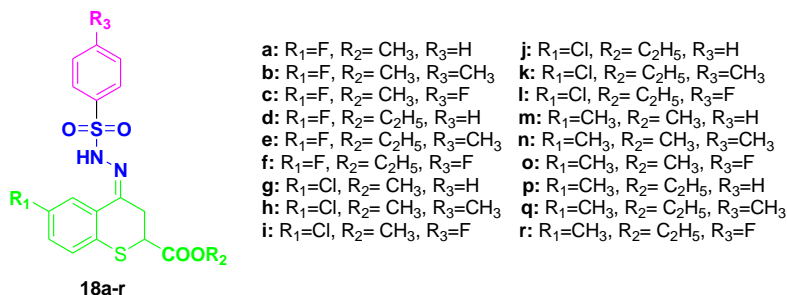


Figure 9. New sulfonamide derivatives with a 100% inhibition rate against *Xoo*

In 2022, Aloe emodin-conjugated sulfonamide hydrazones as new types of antibacterial agents were synthesized by Deng et al (Figure 10). Bioassay results revealed that some of the target molecules performed better than *aloe emodin* and clinical norfloxacin in inhibiting bacterial growth. Compound **19a** exhibited the strongest antibacterial effect (MIC = 0.5 µg/mL) on *S. aureus* out of all the compounds tested (Deng et al., 2022).

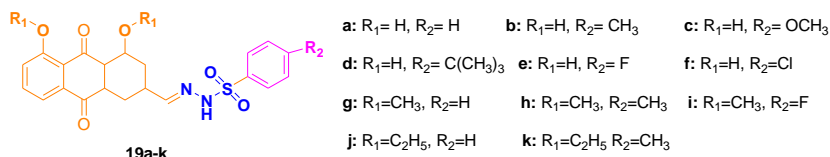


Figure 10. Novel aloe emodin-conjugated sulfonamide hydrazones as antibacterial agents

In another study, Angelova and colleagues used *Mycobacterium tuberculosis* strain H37Rv to evaluate the antimycobacterial activities of the new sulfonamide hydrazone compounds they synthesized (Figure 11). Among the tested compounds, **20g** and **20k** were found to be the most active compounds with MIC values of 0.0763 and 0.0716 M, respectively, and were similarly active as INH against *M. tuberculosis* H37Rv (Angelova et al., 2022).

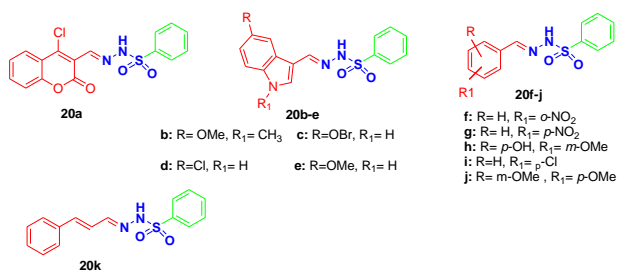


Figure 11. Synthesized *N*-substituted sulfonyl hydrazones

In a study by Aydin et al., the antifungal properties of the produced new sulfonyl hydrazones were examined against standard strains and clinical isolates of planktonic *Candida* species (Figure 12). All compounds were observed to decrease the development of planktonic cells in the examined species of *Candida* (Aydin et al., 2023).



Figure 12. New sulfonyl hydrazones as antifungal agents

In another study, the synthesis involved creating compound **22** (Figure 13). The antimicrobial potential of the synthesized compound was assessed. Minimum inhibitory concentrations (MIC) were evaluated against a wide range of microorganisms (Gram-positive bacteria, Gram-negative bacteria, drug-resistant bacteria, and various *Candida* species). The obtained compound showed effectiveness on *S. aureus* strains. MIC value against *S. aureus* strains was 125 µg/mL. The compound exhibited antifungal activity against a variety of *Candida* species. The highest antifungal effect was observed on *C. albicans* and *C. parapsilosis* with an MIC of 31.2 µg/mL (Doğan et al., 2023).

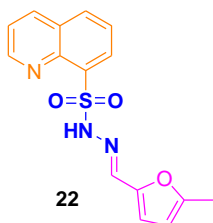


Figure 13. Structure of (E)-*N'*-((5-nitrofuran-2-yl)methylene)quinoline-8-sulfonohydrazide

Anticancer activity

Cancer has been a leading cause of death worldwide since the beginning of the twenty-first century. Cancer can develop in various organs and systems of the body. It occurs when one or more cells in a certain tissue deviate from their normal characteristics and start proliferating uncontrollably. Uncontrolled cell proliferation is a hallmark of cancer, leading to the formation of tumors and the potential spread of cancer cells to other parts of the body (metastasis). Treating and managing cancer involves substantial healthcare costs, and the disease can also lead to indirect economic consequences, such as lost productivity and increased healthcare expenditure. Today, new cancer cases and death rates are constantly reported and are predicted to increase by approximately 50% over the next two decades (Sung et al., 2021). Chemotherapy is a popular cancer treatment because of its impact on tumor cells. However, several anticancer medications that are clinically available have harmful side effects (Hait & Lebowitz, 2019). Consequently, it is crucial to create novel anticancer drugs with the appropriate level of efficacy and low toxicity. In recent years, sulfonyl hydrazones, which have been widely accepted for the design and identification of many biologically active compounds, have been implicated as important compounds with anticancer activity. This pharmacological property is due to the structural properties of sulfonyl hydrazones, which can participate in various biomolecular targets and elicit multiple interactions.

Several heterocyclic sulfonyl hydrazones were created and their anticancer effects against HepG-2 cancer cells were assessed in a 2018 study (Figure 14). The data obtained showed that the synthesized compounds had a certain inhibitory activity on HepG-2 cells. The data obtained showed that the synthesized compounds had a certain inhibitory activity on HepG-2 cells. Among the compounds tested, compound **23i** was determined to be the compound with the best activity, with IC_{50} of 7 of 2.95 $\mu\text{mol/L}$, 69.56 $\mu\text{mol/L}$, and 50.62 $\mu\text{mol/L}$ at 24 hours, 48 hours, and 72 hours, respectively (Wei et al., 2018).

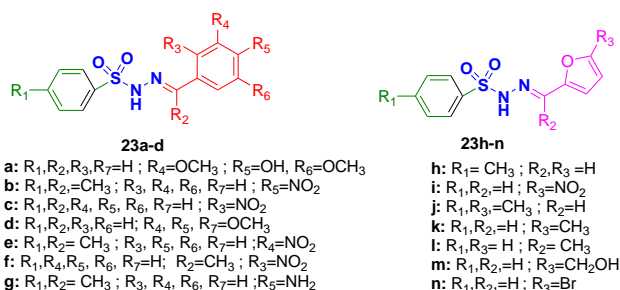


Figure 14. Synthesized aromatic heterocyclic sulfonyl hydrazones

In 2020, the synthesis of several sulfonyl hydrazone compounds as new anticancer agents was achieved (Figure 15). The cytotoxic activity of all obtained compounds was assessed against L929 mouse fibroblast cell lines, PC3 prostate cancer, and MCF-7 breast cancer. **24k** was shown to have the greatest anticancer activity among the investigated compounds, with IC₅₀ values in PC3 and MCF 7 cell lines of 1.38 μM and 46.09 μM, respectively. Additionally, this compound was seen to show the highest selectivity index values (Şenkardeş et al., 2020).

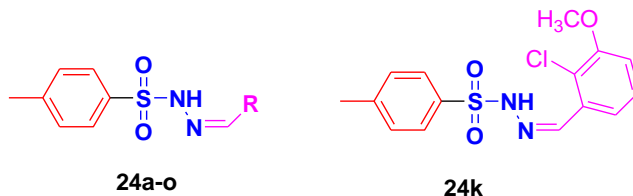


Figure 15. Structure of N'-[(2-chloro-3-methoxyphenyl) methylidene]-4-methylbenzenesulfonylhydrazide

By employing the MTT assay with cisplatin as a positive control, the cytotoxic properties of novel sulfonyl hydrazone derivatives produced by Yang et al. were evaluated against MCF-7 cells (breast cancer), U87 cells (human glioma), and A549 cells (lung cancer). It was found that most of the compounds showed no or moderate cytotoxicity on the cancer cells examined. In contrast, compound **25** was determined to have significant cytotoxic activity (IC₅₀=14.35 μM) on MCF-7 cells (Figure 16). Moreover, this compound appeared to have a lower cytotoxic effect on MCF-10A cells (human normal breast) than cisplatin (Yang et al., 2021).

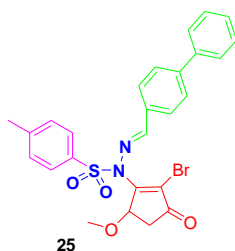


Figure 16. (E)-N-2(5H)-furanonyl sulfonyl hydrazone compound with the highest cytotoxic activity

In a study in 2022, novel sulfonyl hydrazone derivatives and their Pd(II) complexes were synthesized (Figure 17). The synthesized compounds were evaluated for their cytotoxic activity against human breast adenocarcinoma (MDA-MB-231) and human lung epithelium (Beas-2B). According to the activity results, it was determined that compound **26** had more anticancer activity than the Pd(II) complex **28**, but the anticancer activity of compound **27** was less than the Pd(II) complex **29**. Studies on healthy tissue showed that compound **27** killed healthy cells at all concentrations, while the others did not cause much damage. Based on the data obtained, it is predicted that compound **26** and its complex **28**, which exhibited the highest cytotoxic activity, can be used as potential anticancer drugs against human breast adenocarcinoma MDA-MB-231 cells (Güzin Aslan, 2022).

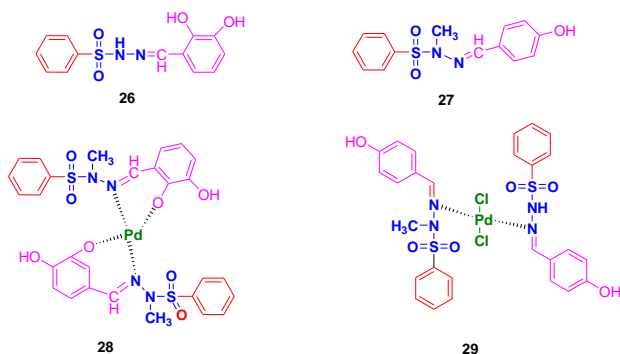


Figure 17. The structure of novel sulfonyl hydrazone derivatives and their Pd(II) complexes

Antioxidant capacity and enzyme inhibition activity

The balance between the body's antioxidant systems and free radicals is important in maintaining the health of the organism. Excessive production of reactive oxygen species (ROS) elicits oxidative stress, which can cause fatal damage to living cell structures. Oxidative stress is also closely associated with diseases such as cancer, neurodegenerative, cardiovascular, inflammatory, and autoimmune, as well as diseases such as diabetes, Alzheimer's, and Parkinson's. In recent years, with the increase in oxidation-related diseases, free radicals formed in the human body have become a serious health problem. For this reason, today, studies on the discovery of new antioxidant agents attract the intense attention of researchers and the number of studies on this subject is increasing (Biliz et al., 2024; Hasdemir et al., 2019; Sokmen et al., 2014; Yaşa et al., 2019). Therefore, the synthesis of new hydrazide-hydrazones combined with the sulfonamide group to increase pharmacological activities is of great interest.

In 2016, Karaman et al. synthesized new sulfonyl hydrazones containing piperidine ring and investigated their antioxidant capacity and anticholinesterase activities (Figure 18). For the determination of the antioxidant capacity of the compounds, b-carotene-linoleic acid, DPPH free radical scavenging, ABTS cation radical scavenging, and Cupric reducing antioxidant capacity (CUPRAC) assays were used. The experimental results showed that compound **30** had the highest lipid peroxidation inhibitory activity and also exhibited better DPPH scavenging activity than standard BHT. Besides, compound **31** was defined to show the best ABTS scavenging test. In the CUPRAC assay, compound **34** was found to show better activity than the standard antioxidant α -tocopherol among the tested compounds. Acetylcholinesterase (AChE) and butyrylcholinesterase (BChE) inhibitory activity studies revealed that compound **32** had the best AChE activity while compound **33** showed the highest BChE activity (Karaman et al., 2016).

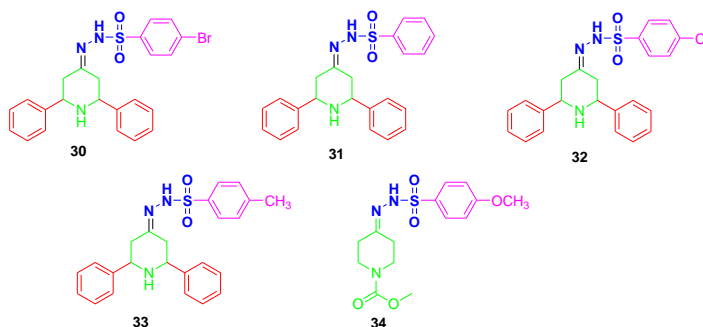


Figure 18. Sulfonyl hydrazones bearing piperidine ring

In 2017, researchers Rajput et al. synthesized novel sulfonyl hydrazone compounds including carvacrol, thymol, and eugenol derivatives, and screened them for antioxidant capacity using a DPPH assay (Figure 19). Among the tested compounds, eugenol derivatives (**37a** and **37b**) exhibited excellent antioxidant activity similar to standard BHT, while thymol (**36a** and **36b**) and carvacrol derivatives (**35a** and **35b**) showed a decrease in the percentage of antioxidant activity (Rajput et al., 2017).

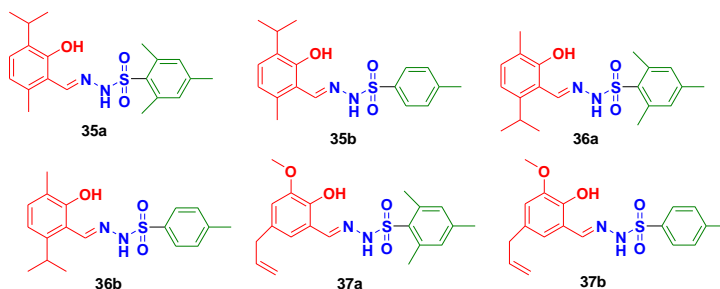


Figure 19. New sulfonyl hydrazone derivatives containing carvacrol, thymol and eugenol moiety

In a study by Fernandes et al., 15 new sulfonyl hydrazone compounds synthesized were evaluated for their ability to inhibit AChE (Acetylcholinesterase), which is used as a drug for the treatment of Alzheimer's disease (Figure 20). The IC_{50} values of all tested compounds were determined to be in the range of 0.64-51.09 μ M. Among all the compounds, compound **38m** was found to have the lowest IC_{50} ($IC_{50} = 0.64 \mu$ M) value. Additionally, due to the similarity of 6d to the drug used in treatment (donepezil), it can be thought that the compound may have appropriate oral absorption and brain penetration (Fernandes et al., 2017).

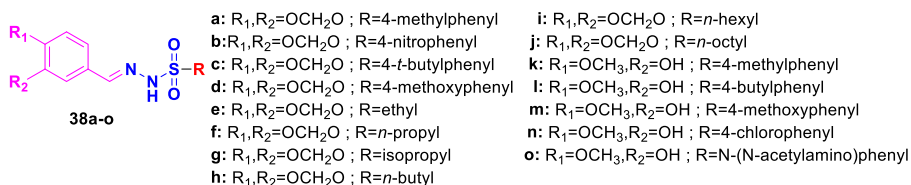


Figure 20. Synthesized novel sulfonyl hydrazones as inhibitor AChE

In another study conducted in 2017, various sulfonyl hydrazones containing a 3-formylchromone moiety were synthesized and examined for their MAO-A and MAO-B (monoamine oxidase) inhibitory effects (Figure 21). It was discovered that compound **39** ($IC_{50} = 1.12 \pm 0.02 \mu\text{M}$) was the most potent MAO-B inhibitor. Furthermore, compound **40** ($IC_{50} = 0.33 \pm 0.01 \mu\text{M}$) was found to be the MAO-A inhibitor with the highest activity. (Abid et al., 2017).

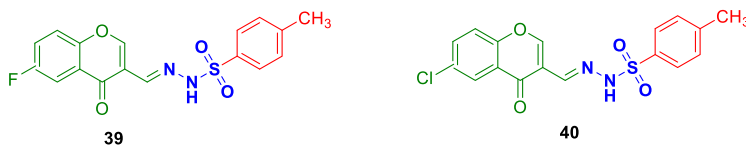


Figure 21. Synthesized sulfonyl hydrazones derived from 3-formylchromone

In 2020, Aktar et al. synthesized sulfonyl hydrazones **41a-j** and investigated their antioxidant and anticholinesterase activities (Figure 22). In the anticholinesterase activity results, it was determined that compounds **41a** ($IC_{50} = 11.51 \pm 0.48 \mu\text{M}$), **41h** ($IC_{50} = 10.16 \pm 0.80 \mu\text{M}$), and **41j** ($IC_{50} = 16.39 \pm 0.22 \mu\text{M}$) inhibited AChE (acetylcholinesterase), whereas compounds **41a-d** ($IC_{50} =$ range from $25.25 \pm 0.20 \mu\text{M}$ to 41.68 ± 1.00) and **41g-j** ($IC_{50} =$ range from $16.52 \pm 0.80 \mu\text{M}$ to 43.07 ± 0.19) inhibited BChE (butyrylcholinesterase) more than galantamine. β -Carotene-linoleic acid, DPPH free radical scavenging, ABTS cation radical scavenging, and CUPRAC assays were used to determine the in vitro antioxidant activity of the synthesized compounds. Compounds **41a** ($IC_{50} = 18.26 \pm 0.58 \mu\text{M}$), **41d** ($IC_{50} = 18.04 \pm 0.59 \mu\text{M}$), **41e** ($IC_{50} = 18.27 \pm 0.33 \mu\text{M}$), **41h** ($IC_{50} = 13.77 \pm 0.12 \mu\text{M}$), **41i** ($IC_{50} = 19.23 \pm 0.68 \mu\text{M}$), and **41j** ($IC_{50} = 10.08 \pm 0.25 \mu\text{M}$) showed the highest lipid peroxidation inhibitory activity. In the DPPH assay, compounds **38** ($IC_{50} = 24.68 \pm 1.33 \mu\text{M}$), **41b** ($IC_{50} = 30.72 \pm 0.84 \mu\text{M}$), **41d-j** ($IC_{50} =$ range from $16.83 \pm 1.04 \mu\text{M}$ to $29.61 \pm 0.87 \mu\text{M}$) exhibited significant scavenging activity. Compounds **41a** ($IC_{50} = 12.55 \pm 2.44 \mu\text{M}$), **41h** ($IC_{50} = 20.82 \pm 1.85 \mu\text{M}$), and **41j** ($IC_{50} = 15.29 \pm 1.92 \mu\text{M}$) showed superior cation radical scavenging activity compared to the other compounds in the ABTS experiment. In the CUPRAC assay, compounds **41a** ($IC_{50} = 23.36 \pm 0.03 \mu\text{M}$), **41h** ($IC_{50} = 37.35 \pm 0.01 \mu\text{M}$), and **41j** ($IC_{50} = 28.78 \pm 0.03 \mu\text{M}$) were found to have higher cupric-reducing antioxidant capacity than the others. Compounds **41h**

and **41j** were shown to have extremely strong antioxidant activity overall. (Aktar et al., 2020).

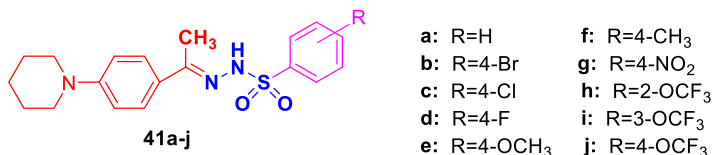


Figure 22. Novel sulfonyl hydrazones as antioxidant and anticholinesterase agents

A study achieved in 2020 aimed to develop and synthesize new aryl sulfonyl hydrazone compounds capable of inhibiting metallo- β -lactamases (Figure 23). The results showed that most synthesized compounds exhibited promising inhibitory activity in vitro. Additionally, the examined compounds not only demonstrated enhanced antibiotic activity but also had a notable impact on resensitizing a resistant strain of *K. pneumoniae* to specific antibiotics. The in vivo experiments further support the potential therapeutic application of these compounds, showing improved survival rates and complete bacterial clearance in infected rats when combined with meropenem and the MBL inhibitor **42m**. This information suggests that these compounds may hold promise as effective strategies in treating infections caused by antibiotic-resistant bacteria (Shaaban et al., 2020).

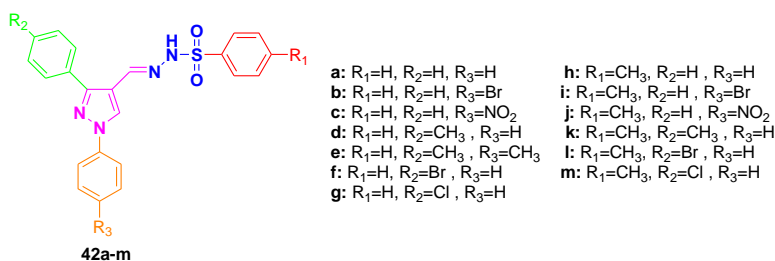
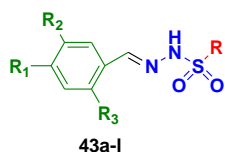


Figure 23. New aryl sulfonyl hydrazone derivatives as promising metallo- β -lactamases inhibitors

A study conducted by Bilen et al. in 2022 involves the synthesis of sulfonylhydrazone compounds (**43a-1**) using the green chemistry method (Figure 24). The focus of the research was to examine the inhibitory efficacy of these compounds on AChE and BChE enzymes. The results showed that all

tested compounds inhibited AChE and BChE enzymes. A comparison of IC₅₀ values revealed that compound **43f** had the best inhibition effect on the AChE enzyme with an IC₅₀ value of 5.27 ± 0.05 μM. Similarly, compound **43i** exhibited the best inhibition effect on the BChE enzyme with an IC₅₀ value of 12.29 ± 1.47 μM. These findings indicate that compounds **43f** and **43i**, both containing butyl groups, have remarkable inhibitory effects on both AChE and BChE enzymes (Bilen et al., 2022).



- | | |
|---|--|
| <p>a: R= ethyl, R₁= NO₂ , R₂,R₃=H
 b: R= propyl, R₁= NO₂ , R₂,R₃=H
 c: R= butyl, R₁= NO₂ , R₂,R₃=H
 d: R= ethyl, R₁= NH₂ , R₂,R₃=H
 e: R= propyl, R₁= NH₂ , R₂,R₃=H
 f: R= butyl, R₁= NH₂ , R₂,R₃=H</p> | <p>g: R= ethyl, R₁= H , R₂=Cl, R₃=OH
 h: R= propyl, R₁= H , R₂=Cl, R₃=OH
 i: R= butyl, R₁= H , R₂=Cl, R₃=OH
 j: R= ethyl, R₁= OCH₃ , R₂=H, R₃=OH
 k: R= propyl, R₁= OCH₃ , R₂=H, R₃=OH
 l: R= butyl, R₁= OCH₃ , R₂=H, R₃=OH</p> |
|---|--|

Figure 24. Structure of sulfonylhydrazone compounds with alkyl derivatives

Several new sulfonyl hydrazone compounds were obtained by Aktar et al., and they were then tested for their ability to inhibit several enzymes, including urease, tyrosinase, and anticholinesterase (Figure 25). Antioxidant activities of the compounds were determined using β-carotene–linoleic acid, ABTS*⁺ cation activity, DPPH radical scavenging activity, and CUPRAC tests. Compound **44h** exhibited the highest antioxidant activity compared to other compounds in the β-carotene–linoleic acid and ABTS*⁺ cation activity tests. Compounds **44c-h** were identified as the most active compounds in the DPPH radical scavenging activity analysis. These compounds showed significantly better activity than BHT (Butylated Hydroxytoluene), which was used as the standard drug. Compounds **44c-h** demonstrated much better activity than α-tocopherol (vitamin E, α-TOC), which was used as the standard drug, in the CUPRAC activity test. These compounds were identified as the most active in this particular test. Compound **44h**, while demonstrating lower activity than the standard drug galantamine, stood out as the most active compound among the others in inhibiting acetylcholinesterase (AChE). Compounds **44c-h** were identified as the most active compounds in the butyrylcholinesterase (BChE) activity test. These compounds exhibited significantly better activity compared to the standard drug galantamine. Compounds **44h**, **44e**, and **44d** showed the best tyrosinase inhibitory activity values. The inhibitory concentrations (IC₅₀ values) for these compounds were reported as 9.75 μM, 13.18 μM, and 16.29 μM, respectively. Compounds **44h**, **44d**, and **44e** demonstrated excellent urease inhibitory activity. The IC₅₀ values for these

compounds were reported as 14.20 μM , 19.07 μM , and 23.73 μM , respectively (Aktar et al., 2022).

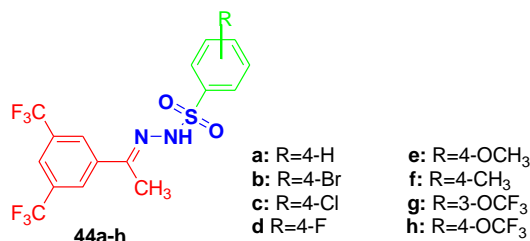


Figure 25. Novel sulfonyl hydrazone compounds

In another investigation, fifteen novel aryl sulfonyl hydrazones were synthesized, and their inhibitory and antioxidant properties were assessed. (Figure 26). The antioxidant capacities of the substances were tested by FRAP and DPPH methods. Compounds **47a**, **47b**, and **47c** were identified as exhibiting good antioxidant activity. When the inhibitory effects of the obtained compounds against AChE were examined, compounds **45d** (10.39 μM), **47b** (10.81 μM), **48b** (12.92 μM), and **47a** (12.93 μM) were found to have strong inhibitory effects against AChE (Demirci et al., 2023).

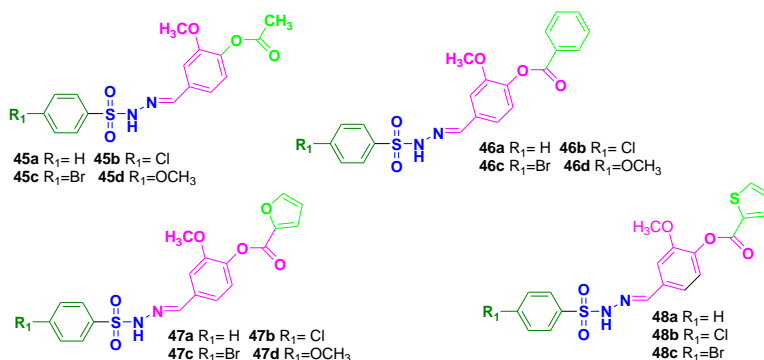


Figure 26. New arylsulfonyl hydrazone derivatives

In another study performed in 2023, new sulfonylhydrazone compounds derived from N'-(4-diethylamino) salicylaldehyde were synthesized (Figure 27). It was noted that the inhibitory effects on AChE were stronger compared to BChE for the tested compounds. The anti-BChE activity of the **49b** was lower than its AChE inhibition. Similarly, the anti-BChE activity of the **49a**

was lower than its AChE inhibition, indicating a preference for inhibiting AChE over BChE. When examining the inhibition activity against acetylcholinesterase (AChE), the compound **49b** demonstrated the best inhibitory activity with an IC_{50} value of $9.549 \pm 0.75 \mu\text{M}$. Compound **49c** exhibited potency close to the best inhibitor of the BChE enzyme (Ozmen et al., 2023).

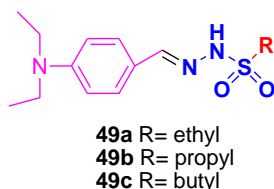


Figure 27. Novel sulfonylhydrazones derived from N'-(4-diethylamino) salicylaldehyde

Başaran synthesized a series of new sulfonyl hydrazones as target molecules to examine acetylcholinesterase (AChE) and butyrylcholinesterase (BChE) inhibition and antioxidant activities *in vitro* (Figure 28). AChE assay was conducted to test the inhibitory activities of various molecules (concentrations ranging from $0.14 \pm 0.25 \mu\text{M}$ to $84.81 \pm 1.09 \mu\text{M}$). All tested molecules exhibited higher inhibition activities against AChE compared to the reference drug rivastigmine. Compound **51f** ($60.14 \pm 0.25 \mu\text{M}$) demonstrated the strongest inhibitory action against AChE among the compounds examined, while compound **50a** ($84.81 \pm 1.09 \mu\text{M}$) showed the least effective inhibition against AChE. The inhibitory efficiency of investigated compounds on BChE was determined to range from $70.11 \pm 0.67 \mu\text{M}$ to $93.60 \pm 0.47 \mu\text{M}$. Comparing the studied compounds to galanthamine and rivastigmine, the former demonstrated more potent inhibitory effects against BChE. Against BChE, compound **50f** demonstrated the most effective inhibition, with an IC_{50} value of $70.11 \pm 0.67 \mu\text{M}$. Four distinct assays were utilized to ascertain the antioxidant capabilities of the investigated molecules: β -carotene bleaching, DPPH free radical scavenging, ABTS cation radical decolorization, and CUPRAC antioxidant capacity tests. In the β -carotene-linoleic acid assay, compound **51f** ($54.11 \pm 1.67 \mu\text{M}$) exhibited the highest level of activity among all the examined molecules, outperforming the reference compounds. Compound **51f** ($64.73 \pm 0.54 \mu\text{M}$) demonstrated the most activity in the DPPH assay when compared to BHT. Compound **51a-f** was shown to be at least two times more active than other compounds **50a-f** in the ABTS test. Compound

51f ($26.58 \pm 0.76 \mu\text{M}$) had the most similar action to α -tocopherol among the compounds examined. In the CUPRAC experiment, compound **50f** ($59.75 \pm 0.64 \mu\text{M}$) was determined to show higher activity than the standard compound α -TOC ($40.69 \pm 0.83 \mu\text{M}$). Compounds **50a-f** had weaker antioxidant activities compared to compounds **51a-f** (Başaran, 2023).

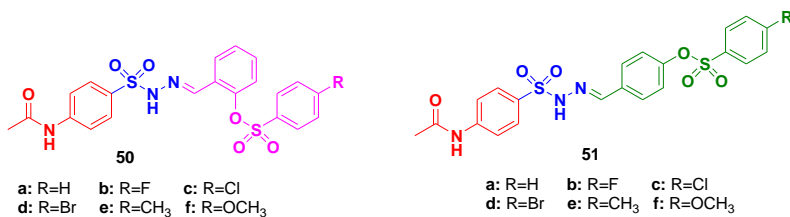


Figure 28. Structure of target sulfonyl hydrazone molecules

References

- Abid, S. M. A., Younus, H. A., Al-Rashida, M., Arshad, Z., Maryum, T., Gilani, M. A., ... Iqbal, J. (2017). Sulfonyl hydrazones derived from 3-formylchromone as non-selective inhibitors of MAO-A and MAO-B: Synthesis, molecular modelling and in-silico ADME evaluation. *Bioorganic Chemistry*, 75, 291–302. doi:10.1016/j.bioorg.2017.10.001
- Aktar, B. S. K., Sıcak, Y., Tatar, G., & Oruç-Emre, E. E. (2022). Synthesis, Antioxidant and Some Enzyme Inhibition Activities of New Sulfonyl Hydrazones and their Molecular Docking Simulations. *Pharmaceutical Chemistry Journal*, 56(4), 559–569. doi:10.1007/s11094-022-02674-3
- Angelova, V. T., Pencheva, T., Vassilev, N., K-Yovkova, E., Mihaylova, R., Petrov, B., & Valcheva, V. (2022). Development of New Antimycobacterial Sulfonyl Hydrazones and 4-Methyl-1,2,3-thiadiazole-Based Hydrazone Derivatives. *Antibiotics*, 11(5), 562. doi:10.3390/antibiotics11050562
- Arshia, Begum, F., Almandil, N. B., Lodhi, M. A., Khan, K. M., Hameed, A., & Perveen, S. (2019). Synthesis and urease inhibitory potential of benzophenone sulfonamide hybrid in vitro and in silico. *Bioorganic & Medicinal Chemistry*, 27(6), 1009–1022. doi:10.1016/j.bmc.2019.01.043
- Aslan, H. G., & Karacan, N. (2013). Aromatic sulfonyl hydrazides and sulfonyl hydrazones: antimicrobial activity and physical properties. *Medicinal Chemistry Research*, 22(3), 1330–1338. doi:10.1007/s00044-012-0104-0
- Aydin, M., Ozturk, A., Duran, T., Ozmen, U. O., Sumlu, E., Ayan, E. B., & Korucu, E. N. (2023). In vitro antifungal and antibiofilm activities of novel sulfonyl hydrazone derivatives against *Candida* spp. *Journal of Medical Mycology*, 33(1), 101327. doi:10.1016/j.mycmed.2022.101327
- Başaran, E. (2023). Synthesis, antioxidant, and anticholinesterase activities of novel <sc>N</sc>-arylsulfonyl hydrazones bearing sulfonate ester scaffold. *Journal of the Chinese Chemical Society*, 70(7), 1580–1590. doi:10.1002/jccs.202300151
- Başpınar Küçük, H., Yaşa, H., Yıldız, T., & Yusufoglu, A. S. (2017). Detailed studies on the reduction of aliphatic 3-, 4-, 6-, and 13-oximino esters: Synthesis of novel isomeric amino esters, oximino

- alcohols, and amino alcohols. *Synthetic Communications*, 47(22), 2070–2077. doi:10.1080/00397911.2017.1364768
- Bhat, M., Poojary, B., Kumar, S. M., Hussain, M. M., Pai, N., Revanasiddappa, B. C., & Kullaiyah, B. (2018). Structural, crystallographic, Hirshfeld surface, thermal and antimicrobial evaluation of new sulfonyl hydrazones. *Journal of Molecular Structure*, 1159, 55–66. doi:10.1016/j.molstruc.2018.01.041
- Bilen, E., Özdemir Özmen, Ü., Çete, S., Alyar, S., & Yaşar, A. (2022). Bioactive sulfonyl hydrazones with alkyl derivative: Characterization, ADME properties, molecular docking studies and investigation of inhibition on choline esterase enzymes for the diagnosis of Alzheimer's disease. *Chemico-Biological Interactions*, 360, 109956. doi:10.1016/j.cbi.2022.109956
- Biliz, Y., Hasdemir, B., Başpınar Küçük, H., Zaim, M., Şentürk, A. M., Müdüroğlu Kırmızıbekmez, A., & Kara, İ. (2023). Novel *N*-Acyl Hydrazone Compounds as Promising Anticancer Agents: Synthesis and Molecular Docking Studies. *ACS Omega*, 8(22), 20073–20084. doi:10.1021/acsomega.3c02361
- Biliz, Y., Hasdemir, B., Küçük, H. B., Yıldırım, S., Kocabaş, F., & Kartop, R. A. (2024). Synthesis of new pyrazolidines by [3+2] cycloaddition: Anticancer, antioxidant activities, and molecular docking studies. *Journal of Molecular Structure*, 1295, 136813. doi:10.1016/j.molstruc.2023.136813
- Celebioglu, H. U., Erden, Y., Hamurcu, F., Taslimi, P., Şentürk, O. S., Özmen, Ü. Ö., ... Gulçin, İ. (2021). Cytotoxic effects, carbonic anhydrase isoenzymes, α -glycosidase and acetylcholinesterase inhibitory properties, and molecular docking studies of heteroatom-containing sulfonyl hydrazone derivatives. *Journal of Biomolecular Structure and Dynamics*, 39(15), 5539–5550. doi:10.1080/07391102.2020.1792345
- De Oliveira, Kely N, Souza, M. M., Cunha Sathler, P., Magalhães, U. O., Rodrigues, C. R., Castro, H. C., ... Nunes, R. J. (2012). Sulphonamide and Sulphonyl-hydrazone Cyclic Imide Derivatives: Antinociceptive Activity, Molecular Modeling and In Silico ADMET Screening. *Arch Pharm Res*, 35(10), 1713–1722. doi:10.1007/s12272-012-1002-1
- de Oliveira, Kely Navakoski, Costa, P., Santin, J. R., Mazzambani, L., Bürger, C., Mora, C., ... de Souza, M. M. (2011). Synthesis and antidepressant-like activity evaluation of sulphonamides and

- sulphonyl-hydrazones. *Bioorganic & Medicinal Chemistry*, 19(14), 4295–4306. doi:10.1016/j.bmc.2011.05.056
- Demirci, Y., Kalay, E., Kara, Y., Güler, H. İ., Can, Z., & Şahin, E. (2023). Synthesis of Arylsulfonyl Hydrazone Derivatives: Antioxidant Activity, Acetylcholinesterase Inhibition Properties, and Molecular Docking Study. *ChemistrySelect*, 8(29). doi:10.1002/slct.202301474
- Deng, Z., Yadav Bheemanaboina, R. R., Luo, Y., & Zhou, C.-H. (2022). Aloe emodin-conjugated sulfonyl hydrazones as novel type of antibacterial modulators against *S. aureus* 25923 through multifaceted synergistic effects. *Bioorganic Chemistry*, 127, 106035. doi:10.1016/j.bioorg.2022.106035
- Doğan, Ş. D., Özcan, E., Çetinkaya, Y., Han, M. İ., Şahin, O., Bogojevic, S. S., Gündüz, M. G. (2023). Linking quinoline ring to 5-nitrofuranyl moiety via sulfonyl hydrazone bridge: Synthesis, structural characterization, DFT studies, and evaluation of antibacterial and antifungal activity. *Journal of Molecular Structure*, 1292, 136155. doi:10.1016/j.molstruc.2023.136155
- Fernandes, T. B., Cunha, M. R., Sakata, R. P., Candido, T. M., Baby, A. R., Tavares, M. T., ... Parise-Filho, R. (2017). Synthesis, Molecular Modeling, and Evaluation of Novel Sulfonylhydrazones as Acetylcholinesterase Inhibitors for Alzheimer's Disease. *Archiv Der Pharmazie*, 350(11). doi:10.1002/ardp.201700163
- Gündüzalp, A. B., Özmen, Ü. Ö., Çevrimli, B. S., Mamaş, S., & Çete, S. (2014). Synthesis, characterization, electrochemical behavior, and antimicrobial activities of aromatic/heteroaromatic sulfonylhydrazone derivatives. *Medicinal Chemistry Research*, 23(7), 3255–3268. doi:10.1007/s00044-013-0907-7
- Güzin Aslan, H. (2022). New sulfonyl hydrazones and their Pd(II) complexes: synthesis and cytotoxic activities in the MDA-MB-231 cell line. *Chemical Papers*, 76, 1413–1421. doi:10.1007/s11696-021-01928-w
- Hait, W. N., & Lebowitz, P. F. (2019). Moving upstream in anticancer drug development. *Nature Reviews Drug Discovery*, 18(3), 159–160. doi:10.1038/d41573-018-00006-3
- Hasdemir, B. (2022). Recent Studies on The Antimicrobial and Anticancer Activities of Hydrazide-Hydrazones. In F. Özbaş Gerçeker, H. Akgül, & H. Baba (Eds.), *International Research in*

- Science and Mathematics* (first edition, pp. 215–239). İzmir: Serüven Publishing. Retrieved from https://www.seruvenyayinevi.com/Webkontrol/uploads/Fck/Sciencearalik2022_4.pdf
- Hasdemir, B., Sacan, O., Yasa, H., Kucuk, H. B., Yusufoglu, A. S., & Yanardag, R. (2018). Synthesis and elastase inhibition activities of novel aryl, substituted aryl, and heteroaryl oxime ester derivatives. *Archiv Der Pharmazie*, 351(2). doi:10.1002/ARDP.201700269
- Hasdemir, B., Yaşa, H., & Akkamaş, Y. (2019). Synthesis and antioxidant activities of novel *N*-aryl (and *N*-alkyl) γ - and δ -imino esters and ketimines. *Journal of the Chinese Chemical Society*, 66(2), 197–204. doi:10.1002/jccs.201800126
- Karaman, N., Oruç-Emre, E. E., Sıcak, Y., Çatıkkaş, B., Karaküçük-İyidoğan, A., & Öztürk, M. (2016). Microwave-assisted synthesis of new sulfonyl hydrazones, screening of biological activities and investigation of structure–activity relationship. *Medicinal Chemistry Research*, 25(8), 1590–1607. doi:10.1007/s00044-016-1592-0
- Kurşun Aktar, B. S., Sıcak, Y., Tok, T. T., Oruç-Emre, E. E., Yağlıoğlu, A. Ş., İyidoğan, A. K., ... Demirtaş, I. (2020). Designing heterocyclic chalcones, benzoyl/sulfonyl hydrazones: An insight into their biological activities and molecular docking study. *Journal of Molecular Structure*, 1211, 128059. doi:10.1016/j.molstruc.2020.128059
- Özbek, N., Alyar, S., Alyar, H., Şahin, E., & Karacan, N. (2013). Synthesis, characterization and anti-microbial evaluation of Cu(II), Ni(II), Pt(II) and Pd(II) sulfonylhydrazone complexes; 2D-QSAR analysis of Ni(II) complexes of sulfonylhydrazone derivatives. *Spectrochimica Acta Part A: Molecular and Biomolecular Spectroscopy*, 108, 123–132. doi:10.1016/j.saa.2013.01.005
- Özmen Özdemir, Ü., Begül Altuntas, A., Balaban Gündüzalp, A., Arslan, F., & Hamurcu, F. (2014). New aromatic/heteroaromatic propanesulfonylhydrazone compounds: Synthesis, physical properties and inhibition studies against carbonic anhydrase II (CAII) enzyme *Spectrochimica Acta Part A: Molecular and Biomolecular Spectroscopy*. *Spectrochimica Acta Part A:*

- Molecular and Biomolecular Spectroscopy*, 128, 452–460.
doi:10.1016/j.saa.2014.02.049
- Ozmen, U. O., Tuzun, B., Bilen Ayan, E., & Cevrimli, S. (2023). Eco-friendly and potential colin esterase enzyme inhibitor agent sulfonyl hydrazone series: Synthesis, Bioactivity Screening, DFT, ADME properties, and Molecular Docking study. *Journal of Molecular Structure*, 1286, 135514.
doi:10.1016/j.molstruc.2023.135514
- Popiołek, Ł. (2021). The bioactivity of benzenesulfonyl hydrazones: A short review. *Biomedicine & Pharmacotherapy*, 141, 111851.
doi:10.1016/j.biopha.2021.111851
- Popiołek, Ł., Szeremeta, S., Biernasiuk, A., & Wujec, M. (2021). Novel 2,4,6-Trimethylbenzenesulfonyl Hydrazones with Antibacterial Activity: Synthesis and In Vitro Study. *Materials*, 14(11), 2723.
doi:10.3390/ma14112723
- Rajput, J. D., Bagul, S. D., & Bendre, R. S. (2017). Synthesis, biological activities and molecular docking simulation of hydrazone scaffolds of carvacrol, thymol and eugenol. *Research on Chemical Intermediates*, 43(11), 6601–6616. doi:10.1007/s11164-017-3007-3
- Şenkardeş, S., Han, M. İ., Kulabaş, N., Abbak, M., Çevik, Ö., Küçükgül, İ., & Küçükgül, Ş. G. (2020). Synthesis, molecular docking and evaluation of novel sulfonyl hydrazones as anticancer agents and COX-2 inhibitors. *Molecular Diversity*, 24(3), 673–689. doi:10.1007/s11030-019-09974-z
- Şenkardeş, S., Kaushik-Basu, N., Durmaz, İ., Manvar, D., Basu, A., Atalay, R., & Küçükgül, Ş. G. (2016). Synthesis of novel diflunisal hydrazide–hydrazones as anti-hepatitis C virus agents and hepatocellular carcinoma inhibitors. *European Journal of Medicinal Chemistry*, 108, 301–308.
doi:10.1016/j.ejmech.2015.10.041
- Şenkardeş, S., Kıymacı, M. E., Kale, K., Kozanoğlu, İ. M., Kaşkatepe, B., & Küçükgül, Ş. G. (2021). Synthesis, structural elucidation and biological activities of some novel sulfonyl hydrazones as antibacterial agents. *Journal of Research in Pharmacy*, 25(2), 135–141. doi:10.29228/jrp.4
- Shaaban, M. M., Ragab, H. M., Akaji, K., McGeary, R. P., Bekhit, A.-E. A., Hussein, W. M., ... Bekhit, A. A. (2020). Design, synthesis, biological evaluation and in silico studies of certain aryl sulfonyl

- hydrazones conjugated with 1,3-diaryl pyrazoles as potent metallo- β -lactamase inhibitors. *Bioorganic Chemistry*, 105, 104386. doi:10.1016/j.bioorg.2020.104386
- Sokmen, B. B., Hasdemir, B., Yusufoglu, A., & Yanardag, R. (2014). Some Monohydroxy Tetradecanoic Acid Isomers as Novel Urease and Elastase Inhibitors and as New Antioxidants. *Applied Biochemistry and Biotechnology*, 172(3), 1358–1364. doi:10.1007/s12010-013-0595-2
- Sung, H., Ferlay, J., Siegel, R. L., Laversanne, M., Soerjomataram, I., Jemal, A., & Bray, F. (2021). Global Cancer Statistics 2020: GLOBOCAN Estimates of Incidence and Mortality Worldwide for 36 Cancers in 185 Countries. *CA: A Cancer Journal for Clinicians*, 71(3), 209–249. doi:10.3322/CAAC.21660
- Wang, Y., Yu, X., Zhi, X., Xiao, X., Yang, C., & Xu, H. (2014). Synthesis and insecticidal activity of novel hydrazone compounds derived from a naturally occurring lignan podophyllotoxin against *Mythimna separata* (Walker). *Bioorganic & Medicinal Chemistry Letters*, 24(12), 2621–2624. doi:10.1016/j.bmcl.2014.04.074
- Wei, D.-C., Pan, Y., Wang, H., Xu, W.-J., Chen, C., Zheng, J.-H., & Cai, D. (2018). Synthesis of substituted aromatic heterocyclic sulfonyl hydrazone compounds and in vitro anti-hepatoma activity: preliminary results. *European Review for Medical and Pharmacological Sciences*, 22, 4720–4729.
- Yang, K., Yang, J.-Q., Luo, S.-H., Mei, W.-J., Lin, J.-Y., Zhan, J.-Q., & Wang, Z.-Y. (2021). Synthesis of N-2(5H)-furanonyl sulfonyl hydrazone derivatives and their biological evaluation in vitro and in vivo activity against MCF-7 breast cancer cells. *Bioorganic Chemistry*, 107, 104518. doi:10.1016/j.bioorg.2020.104518
- Yaşa, H., Hasdemir, B., & Erken, Ö. (2019). β -Amino Carbonyl Compounds from Iodine-Catalyzed Three Component Mannich Reactions and Evaluation of Their Antioxidant Activity. *Organic Preparations and Procedures International*, 51(6), 537–546. doi:10.1080/00304948.2019.1677443
- Yu, L., Chi, J., Xiao, L., Li, J., Tang, Z., Tan, S., & Li, P. (2021). Novel Thiochromanone Derivatives Containing a Sulfonyl Hydrazone Moiety: Design, Synthesis, and Bioactivity Evaluation. *Molecules*, 26(10), 2925. doi:10.3390/molecules26102925

Chapter 13
**HEAVY METAL CONTAMINATION: PROCESSES,
DISTRIBUTION AND ENVIRONMENTAL IMPACTS**

Kadriye URUÇ PARLAK

*Prof. Dr.; Ağrı İbrahim Çeçen Üniversitesi Fen Edebiyat Fakültesi
Moleküler Biyoloji ve Genetik Bölümü
uruckadriye@gmail.com ORCID NO: 0000-0002-1474-1868*

Heavy metals are characterized by a molecular weight ranging between 63.5 and 200.6 g/mol, a density exceeding 5 g/cm³, and natural occurrence in metalloids and metal groups (Ozyigit, 2016). In biological terms, heavy metals refer to pollutants with the potential to cause contamination, toxicity, or ecotoxicity in the environment, exhibiting toxic and harmful effects even at low concentrations due to their high densities (Yerli, 2020). Notable metals in this category include nickel (Ni), lead (Pb), chromium (Cr), cadmium (Cd), copper (Cu), iron (Fe), mercury (Hg), cobalt (Co) and zinc (Zn), totaling approximately 70 metals (Duffus, 2002; Yerli, 2020). Despite not meeting the heavy metal definition based on specific gravity and atomic number, boron and arsenic are considered heavy metals due to their highly toxic effects (Yerli, 2020).

Heavy metals are typically found in soil, either bound to soil particles, forming organic compounds, attaching to mineral structures, existing in molten chelate compound structures, or in various forms as integrated solids or ions in solutions (Yerli, 2020; Jaishankar et al., 2020). These elements are commonly present in the Earth's crust as stable compounds in carbonate, silicate, and sulfur forms or bound within silicates (Jaishankar et al., 2014).

Biological systems categorize heavy metals into essential and non-essential based on their roles (Can et al., 2021). Essential heavy metals are vital for life and should be present in organisms at very low concentrations, whereas non-essential heavy metals do not have recognized biological roles in living organisms (Can et al., 2021; Ozyigit, 2021). Heavy metals such as zinc, copper, iron, manganese, molybdenum, and nickel act as micronutrients for plants as long as they do not exceed permissible limits (Yerli, 2020). Additionally, some heavy metals play significant roles in human and animal metabolisms when their threshold values are not exceeded, contributing to processes such as growth, development, stress resistance, and the biosynthesis and functions of biomolecules like carbohydrates, enzymes, hormones,

chlorophyll, nucleic acids, and secondary metabolites (Can et al., 2021). An example of an essential heavy metal is copper, which serves as an indispensable component in red blood cells and plays a crucial role in numerous oxidation-reduction processes in both animals and humans. Conversely, non-essential heavy metals can impact psychological structures even at very low concentrations, leading to health problems; mercury, binding to sulfur enzymes, is a prime example in this group (Bakar et al., 2009).

However, essential heavy metals may vary for different organism groups such as plants, animals, and bacteria (Ozyiğit, 2016). Recent studies have shown, for example, that chromium, while toxic to plants, is necessary for glucose metabolism in humans (Sharma et al., 2020). Another example is nickel, which is toxic to plants but is an essential element for animals (Yerli, 2020).

The accumulation of heavy metals in the environment occurs due to two main reasons: natural causes and anthropogenic causes. Table 1 schematically presents the different sources and industries where heavy metals are used and disposed of in the environment (Siegel, 2002).

Table 1. Heavy metals in industry: their sources and purposes (Roosmini et al., 2006)

Industry	Heavy metal	Function
Painting	Hg, Zn, Pb, Cr, Cd, Co, Ni	Raw material for painting
Textile	Zn, Pb, Cr, Cd, Ni	Raw material for painting
Metal coating	Zn, Pb, Cr, Cu, Ni	Raw material for processing
Pulp and paper	Zn, Pb, Cd	additive
Printing	Pb, Cd	Raw material for tint/color
Pubber	Cr, Ni, As	Catalyst additive
Leather	Zn, Pb, Cr	additive

The natural accumulation of heavy metals is dependent on various factors such as mineral weathering, erosion, volcanic activities, and forest fires (Siegel, 2002; Çelebi and Gök, 2018). Human activities leading to the accumulation of heavy metals include urbanization, technological advancements, power plants, iron and steel industry, cement production, thermal, glass manufacturing, industrial activities and wastes, waste nuclear

liquids, organic materials, petroleum derivatives, synthetic agricultural fertilizers, detergents, radioactivity, pesticides, inorganic salts, and synthetic organic chemicals (Çelebi and Gök, 2018).

Heavy metals possess the characteristic of being highly resistant to degradation and indestructible in the environments where they are present. Additionally, their propensity for bioaccumulation renders them highly hazardous. Consequently, the environmental pollution they cause leads to significant adverse effects on ecosystems. These adverse effects can easily transfer from one ecosystem to another through direct or indirect pathways (Ozyigit, 2021; Bakar and Baba, 2009). Heavy metals reaching the atmosphere can settle and mix with soil or water sources. They can reach plants from the soil, entering the human and animal bodies upon contact with soil. Furthermore, heavy metals can enter the human body or animals through the food chain, reaching humans through plants that serve as a food source for animals. Heavy metals can contaminate surface water sources such as lakes, rivers, and streams and can also pollute underground water sources by seeping through the soil. Waters with high concentrations of heavy metals, when used in agricultural areas, become a source of various negative impacts on plants, animals, and humans (Yerli, 2020).

The toxic effects of heavy metals depend on factors such as the chemical form of the metal, its biological availability, the route of exposure, the action and metabolism of the metal, interactions with other metals, the acute and chronic effects of the metal, the target region where its toxic effects are demonstrated, and cellular physiological processes (such as respiration and photosynthesis) and genetic adaptations (Patra et al., 2004). The toxicity mechanisms of heavy metals involve blocking functional groups of important molecules, extracting essential ions from cellular regions, or displacing them, denaturing or inactivating enzymes, disrupting the membrane integrity of cells and organelles, and inducing toxic effects by causing the formation of free radicals (Patra et al., 2004; Mallick, 2004).

Although heavy metals exhibit varying effects on the atmosphere, soil, plants, water, and living organisms, their comprehensive assessment should take into account the overall negative impacts, including atmospheric pollution, disruption of soil structure, reduction in plant yield, degradation of water quality, and threats to the health of living organisms (Yerli, 2020; Jaishankar et al., 2020).

Effects of Heavy Metals on Soils

Activities associated with heavy metal pollution hinder or alter the physical, chemical, and biological development of soils, negatively impacting soil ecosystems. This adverse effect can easily propagate throughout ecosystems (Yerli, 2020).

The entry of heavy metals into the soil occurs through various means such as contaminated atmosphere, application of waste sludge through dry and wet storage, use of polluted waters for irrigation, disposal of solid waste into the soil, and the use of pesticides and phosphorus fertilizers containing heavy metals. Soils, plants, and residences located near high-traffic roads are subject to heavy metal contamination (Çelebi and Gök, 2018).

Heavy metals, by forming highly complex structures in the soil, enhance the toxicity of living structures. Heavy metals that adversely affect soil microorganism activity lead to the disruption of soil fauna. Soil activities such as nitrification, soil respiration, enzyme activity, and organic matter mineralization are negatively affected in soils with disturbed biological activity. Consequently, soils become less productive, and their properties change, reflecting in reduced plant yield and quality (Yerli, 2020). The most commonly found heavy metals in the soil are arsenic, mercury, zinc, cadmium, chromium, lead, and nickel (Wuana and Okieimen, 2011).

Various materials such as wastewater used in irrigation or applied treatment sludges can cause changes in soil pH through plant activities. Studies have shown that the use of wastewater for irrigation lowers soil pH, and this can be attributed to ammonium nitrification and the oxidation of different organic compounds (Yerli, 2020; Khurana and Singh, 2012). The decrease in soil pH is associated with an increase in heavy metal toxicity, as this increase is related to the lower attraction force of metal ions compared to hydrogen ions (Singh and Agrawal, 2012; Khurana and Singh, 2012). Accordingly, it is possible to say that heavy metal toxicity is higher in acidic soils. Additionally, organic matter in the soil can influence the movement of heavy metals in the soil by altering soil pH. The decrease in soil pH resulting from the mineralization of organic matter is a significant factor in heavy metal toxicity. The application of treatment sludges to the soil and the use of wastewater in irrigation may reduce heavy metal toxicity due to the increased cation exchange capacity of the soil (Singh and Agrawal, 2012). In the case of using treatment sludge or wastewater, an increase in soil pH due to the dissolution of lime with decreasing soil pH, an increase in calcium content in the soil, and consequently an increase in aggregation and a decrease in soil

lime content can change the interaction of heavy metals in the soil (Singh and Agrawal, 2012).

Fertilizers applied to the soil can influence soil organic matter content, cation exchange capacity and pH, potentially causing heavy metal toxicity or immobilization of heavy metals in the soil (Yerli, 2020; Singh and Agrawal, 2012). The increase in heavy metal mobility and increased uptake by plants have been indicated with the increase in soil acidity due to acid rain, where soils are exposed to more oxygen and temperature through various interventions (Seven et al., 2008; Yerli et al., 2019). Additionally, interventions applied to the soil result in the conversion of organic carbon, an indicator of soil fertility, into carbon dioxide in soils exposed to more oxygen and temperature (Yerli et al., 2019). The carbon dioxide, upon combining with two hydrogen atoms, forms a weak acid called carbonic acid (H_2CO_3). Carbonic acid, causing a decrease in soil pH, can enhance the mobility of heavy metals in the soil, thereby increasing the uptake of heavy metals by plants (Seven et al., 2008; Yerli et al., 2019). Due to the difficulty in remediation and the conversion of heavy metals into forms that plants cannot absorb, heavy metal pollution holds distinct importance from other soil pollutants (Yerli, 2020; Yerli et al., 2019).

Effects of Heavy Metals on Water

The aquatic environment, forming a part of the ecosystem, has become one of the most heavily polluted areas compared to air and soil due to being the receptor for used waters and other wastes. Pollutants that disturb the natural balance can be categorized as organic matter, petroleum derivatives, industrial wastes, synthetic agricultural detergents, fertilizers, pesticides, synthetic organic chemicals, inorganic salts, radioactivity and waste heat. Based on this classification, heavy metals are included in industrial wastes and certain pesticides, thereby posing a threat to ecological balance (Siegel, 2002).

One of the significant causes of natural heavy metal pollution in river sources is the solid matter (sediment) and organic substances entering the waters as a result of soil erosion. Inorganic substances, such as heavy metals and metal compounds, present in excessive amounts in sediment, are considered potential pollutants. These potential pollutants can threaten the health of humans and aquatic organisms and, consequently, human health (Ozyigit, 2021; Bakar and Baba, 2009).

The toxicity of heavy metals depends on factors such as pH, dissolved oxygen, temperature, the volume of the solution relative to the size of the fish, the frequency of solution renewal, other substances in the solution, and

synergistic effects. Among these, the pH of the water can be the most critical factor. Freshwaters are slightly less buffered than seawater, and the effects of heavy metal toxicity can be observed in these treated freshwater systems. Heavy metals are believed to be more toxic in distilled and soft waters compared to hard and alkaline waters (Can et al., 2021).

Toxic substances such as boron and heavy metals in wastewater can accumulate in the soil depending on the climate and soil properties of the region. They can be taken up by plants or exist in the water in dissolved form. Heavy metals, known for their strong toxic effects even in small amounts, are found in polluted waters in the forms of metals, cations, salts, and partially anions. These substances can both hinder the self-purification of polluted waters and limit the use of treated waters for irrigation and the use of treated sludge as fertilizer (Jaishankar et al., 2014).

Effects of Heavy Metals on Plants

The primary non-mobile organisms affected by environmental pollution, particularly heavy metal pollutants, are plants (Ozyiğit, 2016). The accumulation of heavy metals in plants occurs through the uptake of these metals from soil and water sources, as well as through particulate matter of heavy metals present in the atmosphere. The heavy metals absorbed by plants can hinder or alter the physiological activities of the plant, ultimately leading to the death of the plant in advanced stages. Therefore, the accumulation of heavy metals in plants is a significant factor that greatly influences plant yield and quality (Okçu and Tozlu., 2009).

With the accumulation of heavy metals in the soil, plants are unable to obtain the essential nutrients they need from the soil. In other words, heavy metals impede the uptake of essential nutrients by plants. Plants exposed to heavy metals exhibit shorter stem lengths and root, a reduced number of leaves and a smaller leaf area due to the deficiency of essential nutrients (Yerli, 2020; Mengoni et al., 2009). The adverse effect of heavy metals on root length is caused by the inhibition of cell division and proliferation of plant root cells due to oxidative damage, disruption of cell membrane structures, and damage to the epidermal cells that make up the root surface (Yerli, 2020; Mengoni et al., 2009).

Due to their toxic effects, heavy metals disrupt plant physiology by affecting germination, development, stomatal movements, water absorption and transport, transpiration, protein synthesis, and plant tissues and organs. Heavy metal toxicity reduces alpha and beta amylase activities in seeds, preventing the sugar activity necessary for the development of the embryo and

thereby inhibiting seed germination (Ibrahim et al., 2013). Plants exposed to heavy metals show changes similar to mutations in the DNA structure, as well as decreases in RNA, soluble protein, and sugar content (Yerli, 2020; Ibrahim et al., 2013). When heavy metals become free ions and become part of the plant structure, they cause plasma hardening, protein precipitation, increased respiration intensity, and indirectly reduce oxygen consumption in the cell (Yerli, 2020). The effect of heavy metals, which causes changes in chloroplast structure, leads to a decrease in chlorophyll content in the plant. Heavy metals affect the stomatal conductivity of the plant, hindering the continuity of photosynthesis and reducing water consumption by closing stomata (Ibrahim et al., 2013), thereby decreasing yield and quality. With increasing heavy metal toxicity, even if there is water in the soil, the plant becomes unable to absorb water. As the water in the leaves decreases, stomata close, membrane systems are damaged due to increased leaf temperature, and cell death occurs (Yerli, 2020).

Effects of Heavy Metals on Human Health

Humans are exposed to heavy metals from the water they drink to the air they breathe, but 90% of the chemical contamination in their bodies comes from their diet. While some heavy metals are necessary for metabolic activities in the human body, they can have adverse effects on health at high concentrations, leading to diseases such as cancer, Alzheimer's, atherosclerosis, Parkinson's and even causing death. This is because heavy metals accumulate in the body by binding to lipid metabolism or protein structures (Dixit et al., 2015).

Heavy metals affect mental, neurological, and hormonal activities, thereby negatively influencing human behavior. Heavy metals impact various systems in the body, including the circulatory system, toxin elimination systems, energy production systems, hormonal system, immune, enzymes, nervous, stomach, reproductive and excretory systems. Additionally, heavy metals induce allergic reactions, genetic changes, the death of both harmful and beneficial bacteria, and tissue damage (Yerli, 2020). The systems affected by heavy metals and their damages are shown in Table 2.

Table 2. Heavy Metal Types and Their Impact on Human Health (Fahimirad and Hatami, 2017)

Pollutants	Major sources	Effect on human health	Permissible levels (mg/L)
As	Pesticides, fungicides, metal smelters	Bronchitis, dermatitis, poisoning	0.02
Cd	Welding, electroplating, pesticides, fertilizer	Renal dysfunction, lung disease, lung cancer, bone defects, kidney damage, bone marrow	0.06
Pb	Paint, pesticides, smoking, automobile emission, mining, burning of coal	Mental retardation in children, development delay, fatal infant encephalopathy, chronic damage to nervous system, liver, kidney damage	0.1
Mn	Welding, fuel addition, ferromanganese production	Inhalation or contact damage to central nervous system	0.26
Hg	Pesticides, batteries, paper industry	Tremors, gingivitis, protoplasm poisoning, damage to nervous system, spontaneous abortion	0.01
Zn	Refineries, brass manufacture, metal plating	Damage to nervous system, dermatitis	15
Cr	Mine, mineral sources	Damage to nervous system, irritability	0.05
Cu	Mining, pesticide production, chemical industry	Anemia, liver and kidney damage, stomach irritation	0.1

SOME HEAVY METALS AND THEIR EFFECTS

Arsenic

Arsenic, a non-essential element for living organisms, is naturally present on Earth. Due to human activities such as industrial processes, combustion of fossil fuels, use of chemical fertilizers, and disposal of municipal and industrial waste, arsenic can be found in surface and groundwater, agricultural areas, and within plant structures (Ozyiğit, 2016). Plants exposed to arsenic experience inhibited growth and development, leading to the eventual death of the plant. Arsenic induces various physiological disorders in plants (Dixit et al., 2015). Arsenic causes oxidative stress in plants, resulting in reduced yield and quality. Increased levels of arsenic lead to tissue damage due to cell inhibition (Yerli, 2020). Arsenic damages chloroplast membranes, adversely affecting photosynthesis (Cicik., 2003).

In humans, arsenic exposure can cause liver enlargement, anemia, brown spots on the skin, and various skin diseases. High levels of arsenic have been associated with bone and respiratory system cancers (Kocaoba, 2018).

Lead

Lead, the first metal known to humanity, is a significant heavy metal that harms the environment due to human activities (Akbal and Reşorlu, 2015). Lead exists in both inorganic and organic forms, with the inorganic form present in atmospheric particles and the organic form exhibiting volatile characteristics, allowing it to easily enter food items, soil, and water sources (Ozyiğit, 2016). Consequently, lead has a considerable impact on air pollution. Although lead is used in various industries such as cosmetics, petroleum, jewelry, and agricultural pesticides, the major source of environmental pollution is attributed to exhaust emissions from motor vehicles (Yerli, 2020). Therefore, soils near highways with heavy traffic contain high levels of lead. Soluble lead in the soil can be washed away and enter underground water, causing contamination of water sources. The soluble form of lead in the soil can be converted into an inert form by microorganisms, other heavy metals, organic matter, and compounds present in the soil (Çelebi and Gök., 2018).

Exceeding the threshold value in the human body, lead that enters the bloodstream can spread to bones and other organs, causing damage to the kidneys, brain, and nervous system (Akbal and Reşorlu, 2015).

Cadmium

Cadmium is a highly harmful heavy metal whose quantity has significantly increased in recent years. Cadmium generally forms complexes with zinc and, due to its size being close to that of calcium, can enter the bloodstream along with calcium pumps in the intestines. Cadmium also possesses inhibitory properties against zinc reactions. Cadmium accumulates in the kidneys, disrupting their function and causing various diseases. Another aspect relevant to fish is its use as a building block along with calcium in bones (Dixit et al., 2015). Cadmium, by replacing calcium over time, makes bones fragile. Cadmium also leads to reproductive disorders, infertility, and negatively affects neural communication. Cadmium is particularly spread to the environment and humans through smoking (Akbal and Reşorlu, 2015).

Mercury

Mercury is mostly used in the paint, jewelry, cosmetic, electronic, and agricultural industries. Its transition to the soil causes reactions with clay and organic matter or forms insoluble structures, leading to sedimentation (Ozyiğit, 2016). Therefore, the likelihood of mercury entering water sources and plant structures is lower compared to other heavy metals. However, this does not eliminate its danger to humans and animals. Elemental mercury, entering the plant structure, undergoes partial oxidation and, when combined

with inorganic salts, proteins, and alkalies, exhibits a toxic effect on protoplasm, causing the death of plants (Yerli, 2020). Additionally, mercury entering tissues blocks the oxygen supply mechanism, hindering vital activities in plants (Kocaoba, 2018). In humans, high levels of mercury are known to cause kidney damage, nerve system destruction, miscarriages during pregnancy, and abnormalities in infants (Yerli, 2020; Akbal and Reşorlu, 2015). Chronic mercury poisoning leads to gum inflammation, tremors, and psychological disorders (Yerli, 2020).

Copper

Copper, essential at many stages of life, is a necessary element for plants, but high concentrations exhibit toxic effects in plants. Copper plays a significant role in enzyme activity, carbohydrate and lipid metabolism, DNA and RNA production, and the formation of resistance against diseases and pests (Kocaoba, 2018). High concentrations of copper induce toxicity in plants, adversely affecting protein synthesis, nutrient absorption, membrane stability, and respiration (Can et al., 2021). By entering chloroplasts, copper alters their structure and reduces chlorophyll levels (Siegel, 2002). Decreased chlorophyll levels can result in chlorosis in plants. Copper poisoning causes the loss of root properties, negatively affecting the water balance in plants.

Although copper is a fundamental building block for hair, skin, bones, and some internal organs, elevated levels of copper can result in a deceleration of growth and development, graying of hair, a reduction in body temperature, and potential brain damage.

Zinc

Zinc is utilized in diverse industries, including metal alloy production, paint, cosmetics, plastic manufacturing, and mining. It readily infiltrates the soil through industrial wastewater, sewage, and acid rain (Kocaoba, 2018). Although an essential nutrient for living organisms, zinc exhibits toxic effects after exceeding certain levels. Involved in plant metabolism, zinc plays a role in the formation of carbohydrates, proteins, and phosphates, as well as enzyme activity (Yerli, 2020). High levels of zinc result in delayed growth and premature aging of plants (Dixit et al., 2015). Toxic levels of zinc lead to diminished shoot development, adverse impacts on chlorophyll synthesis, chlorosis in young leaves, and a decline in both root and stem development. This is a consequence of inhibited mitotic division in the roots (Kocaoba, 2018).

Zinc levels exceeding 3 mg/L in water cause numerous health problems, including ulcers, edema in the lungs, irritation in mucous membranes and respiratory pathways (Can et al., 2021). Moreover, a study conducted on laboratory animals has identified the carcinogenic effect of zinc (Yerli, 2020).

References

- Mengoni, A., Gonnelli, C., Galardi, F., Gabbriellini, R., Bazzicalupo, M. (2009), Genetic diversity and heavy metal tolerance in populations of *Silene paradoxa* L. (Caryophyllaceae): a random amplified polymorphic DNA analysis, *Molecular Ecology*, 1319-1324.
- Akbal, A., Reşorlu, H. (2015), Ağır Metallerin Kemik Doku Üzerine Toksik Etkileri, *Türk Osteoporoz Dergisi*, 21(1), 30-33.
- Bakar, C., Baba, A. (2009), Metaller ve İnsan Sağlığı: Yirminci Yüzyıldan Bugüne ve Geleceğe Miras Kalan Çevre Sağlığı Sorunları, 1. Tıbbi Jeoloji Çalışmayı
- Can, H., Ozyigit, I.I., Can, M., Hocaoglu-Ozyigit, A., Yalcin, I.E. (2021), Environment-based impairment in mineral nutrient status and heavy metal contents of commonly consumed leafy vegetables marketed in Kyrgyzstan: a case study for health risk assessment, *Biological Trace Element Research*, 199(3), 1123-1144.
- Cicik, B. (2003), Bakır-Çinko Etkileşiminin sazın karaciğer, solungaç ve kas dokularındaki metal birikimi üzerine etkileri, *Ekoloji Çevre Dergisi*, 48, 32-36.
- Çelebi, H., Gök, G. (2018), Topraklarda otoyol ve trafik kaynaklı ağır metal kirliliğinin değerlendirilmesi, *Pamukkale Univ Muh Bilim Derg*, 24(6), 1169-1178.
- Dixit, R., Wasiullah Malaviya D., Pandiyan, K., Singh, U., Sahu, A. (2015), Bioremediation of Heavy Metals from Soil and Aquatic Environment: An Overview of Principles and Criteria of Fundamental Processes, *Sustainability*, 7(2), 2189–2212.
- Duffus, J.H. (2002), Heavy metals a meaningless term?, (IUPAC Technical Report), *Pure and Applied Chemistry*, 74(5), 793-807.
- Fahimirad, S., Hatami, M. (2017), Heavy Metal-Mediated Changes, M. Ghorbanpour and A. Varma (eds.), *Medicinal Plants and Environmental Challenges in Growth and Phytochemicals of Edible and Medicinal Plants*, Springer International Publishing
- Ibrahim, Z.M., Ghazi, S.M., Nabawy, D.M. (2013), Alleviation of heavy metals toxicity in waste water used for plant irrigation, *International Journal of Agronomy and Plant Production*, 4(5), 976-983.
- Jaishankar, M., Tseten, T., Anbalagan, N., Mathew, B.B. (2014), Toxicity, mechanism and health effects of some heavy metals, *Interdisciplinary Toxicology*, 7(2), 60–72.
- Khurana, M.P.S., Singh, P. (2012), Waste water use in crop production: a review, *Resources and Environment*, 2(4), 116-131

- Kocaoba, S. (2018), Besinlerle Alınan Ağır Metaller ve Canlılar Üzerine Etkisi, Editör: Arısoy M, Besin Kirliliği ve İnsan Sağlığına Olan Etkileri, 1. Baskı, 25-37.
- Mallick, N. (2004), Copper- Induced Oxidative Stress in the Chlorophycean Microalga *Chlorella vulgaris*: Response of the Antioxidant System, *J. Plant Physiol*, 161: 591- 597.
- Okçu, M., Tozlu, E., (2009), Ağır Metallerin Bitkiler Üzerine Etkileri, *Alınteri Ziraî Bilimler Dergisi*, 17(2), 14-26.
- Ozyigit, I.I. (2021), Heavy Metals in Agricultural Soils; Origins, Distribution and Effects, *Ereğli Tarım Bilimleri Dergisi*, 1(1), 46-71.
- Patra, M., Bhowmik, N., Bandoadhyay, A. (2004), Comparison of mercury, lead and arsenic with respect to genotoxic effects on plant systems and the development of genetic tolerance, *Environmental And Experimental Botany*, 52, 199-223.
- Roosmini, D., Rachmatiah, I., Suharyanto, Soedomo, Agus., Hadisantosa, F. (2006), Biomarker as an Indicator of River Water Quality Degradation, *PROC. ITB Eng. Science Vol. 38 (2)*, 114-122.
- Seven, T., Can, B., Darende, B.N., Ocak, S. (2008), Hava ve Toprakta Ağır Metal Kirliliği, *Ulusal Çevre Bilimleri Araştırma Dergisi*, 1(2), 91-103.
- Sharma, A., Kapoor, D., Wang, J., Shahzad, B., Kumar, V., Bali, A.S, Yan, D. (2020), Chromium bioaccumulation and its impacts on plants: an overview, *Plants*, 9(1), 100.
- Siegel, F.R. (2002), *Environmental Geochemistry of Potential Toxic Metals*, Verlag Berlin Heidelberg, New York.
- Singh, A., Agrawal, M. (2012), Effects of Waste Water Irrigation on Physical and Biochemical Characteristics of Soil and Metal Partitioning in *Beta vulgaris* L. *Agr. Research*, 1(4), 379-391.
- Wuana, R.A., Okieimen, E.F. (2011), Heavy Metals in Contaminated Soils: A Review of Sources, Chemistry, Risks and Best Available Strategies for Remediation. *International Scholarly Research Network ISRN Ecology*, 1-20.
- Yerli, C. (2020), Ağır Metallerin Toprak, Bitki, Su ve İnsan Sağlığına Etkileri, *Türk Doğa ve Fen Dergisi*, 9(Özel), 103-114.
- Yerli, C., Şahin, Ü., Çakmakçı, T., Tüfenkçi, Ş. (2019), Effects of Agricultural Applications on CO2 Emission and Ways to Reduce, *Turkish Journal of Agriculture Food Science and Tech.*, 7(9), 1446-1456.

Chapter 14

Major Members of the Reactive Oxygen Species (ROS): Formations & Specific Reactions

Mustafa ÖZYÜREK

*Istanbul University-Cerrahpaşa, Faculty of Engineering, Department of Chemistry,
Analytical Chemistry Division, 34320 Avcılar - Istanbul, Turkey
Email: mozyurek@iuc.edu.tr; ORCID No: 0000-0001-5426-9775*

1. REACTIVE OXYGEN SPECIES

Molecular oxygen (O_2) contains two unpaired electrons in a different π^* antibonding orbitals. These electrons are at the minimum energy level when they are in parallel spin and different orbitals. The electronic configuration of triplet oxygen (3O_2 ; relatively inert) is given in Fig. 1. According to the definition of radical, oxygen is a molecule with a 'diradical' structure. However, the reactivity of oxygen is very low, contrary to what is expected. In order for oxygen, which has a diradical structure, to react with any molecule, the molecule to which it can react must have a similar structure. But electron donors to oxygen usually have a pair of electrons with opposite spins in a suitable orbital. Therefore, the tendency of O_2 to react is limited. This is called "spin limitation". In the case of supplying electrons or energy to O_2 , the spin limitation disappears and other types of reactive oxygen species (ROS) are formed. With the transfer of a single electron to O_2 , a superoxide anion radical ($O_2^{\bullet-}$) is formed. The resulting $O_2^{\bullet-}$ is more reactive than oxygen. Solvated electron can be easily created by radiolysis of H_2O [1].

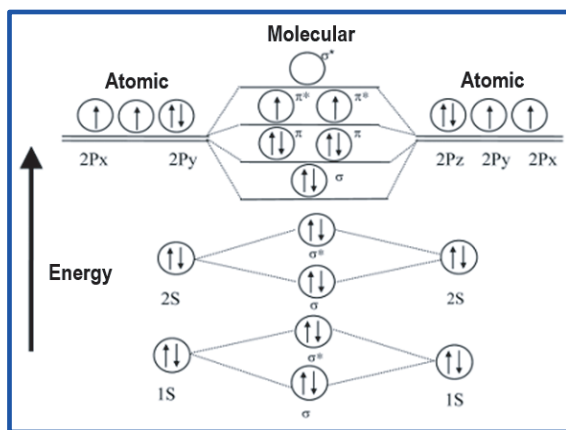


Fig. 1. Electronic configuration of triplet oxygen.



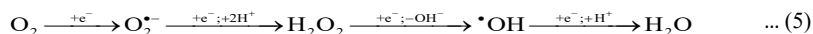
Many free radicals that occur have the activity to form new radicals. As a result of chain reactions, new free radicals are formed. A neutral molecule, H_2O_2 , is formed by the addition of an electron to the $O_2^{\bullet-}$ (Eq. 2).



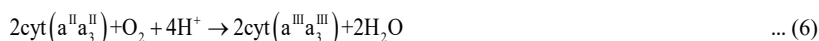
As a result of the addition of an electron to H₂O₂ (Eq. 3), •OH is formed and finally reduced to the OH⁻ ion or H₂O (Eq. 4).



Finally, major members of ROS are formed by single electron transfer steps from O₂ to H₂O (Eq. 5).



The reduction of O₂ to two molecules of H₂O occurs by transferring 4 electrons. The transfer can take place gradually with single-electron transfer steps in the form of the formation of intermediate radical species or by transferring 4 electrons in a single step. The best-known 4-electron transfer reaction takes place in mitochondrial membranes between 2 molecules of cytochrome a-a₃ and O₂ (Eq. 6) [2].



The standard reduction potentials of ROS are given in Table 2. •OH has the highest reduction potential amongst ROS (2310 mV) [3]. This radical is a very powerful oxidant and electrophilic radical. The electron uptake rate is on the order of 10⁹~10¹⁰ M⁻¹s⁻¹ [4]. The electrophilic •OH₂ gives a reaction of addition with aromatic compounds or double bonds. The standard reduction potential of the O₂•⁻ is 940 mV, while the protonated hydroperoxyl radicals of the superoxide anion are 1060~1500 mV [5].

Table 1. Standard reduction potentials of major members of ROS [3,5].

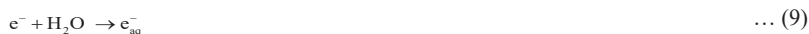
Half reactions	Standard reduction potentials (mV)
O ₂ , H ⁺ / HO ₂ •	- 460
O ₂ / O ₂ • ⁻	- 330
H ₂ O ₂ , H ⁺ / H ₂ O, •OH	320
O ₂ • ⁻ , H ⁺ / H ₂ O ₂	940
HO ₂ •, H ⁺ / H ₂ O ₂	1060 ~ 1500
•OH, H ⁺ / H ₂ O	2310

2. HYDROXYL RADICAL

2.1. Formation of •OH (*in vitro*)

2.1.1. Radiolysis of H₂O

The process of formation of •OH by radiolysis of H₂O, is given in Eq.s 7-9 [1]. This radical and e_{aq}⁻ in equivalent concentrations are formed in this process.



As a result of the reaction of the solvated electron with N₂O, this radical is also formed:



2.1.2. Photo-Fenton reaction

The photochemically occurring reactions of the •OH include the photolysis of phthalimide hydroperoxides [6] (Fig. 2). Phthalimide hydroperoxides dissolve in very little H₂O, but also have not been studied very well in cellular systems.

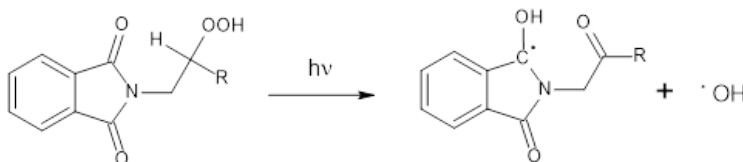
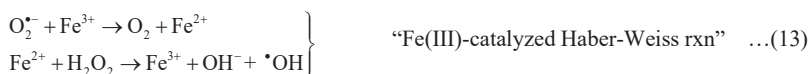
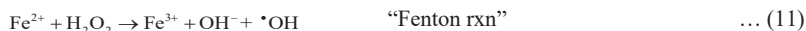


Fig. 2. Photolysis of phthalimide hydroperoxides.

2.1.3. Fenton and Fenton-type reactions

There is a single-electron transfer in the formation of •OH from H₂O₂. The electron-donors can be a transition metal ion of biological importance (Fe²⁺ and Cu⁺) [7] or a radical that donate an electron, such as O₂^{•-}.





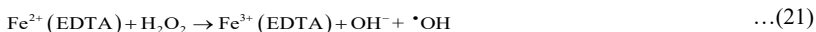
2.1.4. Organic Fenton reaction

This radical can be produced in the presence of H₂O₂ with tetrachlorohydroquinone (TCHQ). This reaction is also called the "Organic Fenton" reaction because of independency of the metal ion. By the autooxidation of TCHQ, the tetrachlorosemiquinone radical (TCSQ•) is formed (Eq.15). This radical replaces the Fe(II) ion in the classical Fenton reaction, producing a •OH [8].



2.1.5. Indirect formation

O₂^{•-} reduces Fe(III) or Cu(II) and then indirectly forms •OH as a result of the Fenton reaction with H₂O₂. However, many organic molecules can also reduce these metal ions *in vivo*. These reducing compounds are: thiols (GSH, cysteamine) (Eq. 16), NADH (Eq. 17) and ascorbate (AH⁻) (Eq. 18-20).



2.2. Reactions of •OH

2.2.1. Reaction of •OH with deoxyribose

•OHs formed by Fenton-type reactions or radiolysis degrade/attack sugar deoxyribose (2-deoxy-D-ribose: DR) and malondialdehyde (MDA)-like compounds are formed by heating at low pH. These compounds are determined as a result of the reaction with thiobarbituric acid (TBA) yielding a pink product (λ₅₃₂) [9]. Although DR degradation is a frequently used method in the determination of •OH, this degradation has not been observed to be specific for •OHs. DR degradation by Fe³⁺-catalyzed Haber-Weiss reaction in phosphate-buffered media and in

the presence of EDTA is inhibited by some $\cdot\text{OH}$ scavenger compounds (Fig. 3). However, DR degradation by DMSO is not inhibited in the absence of EDTA [10].

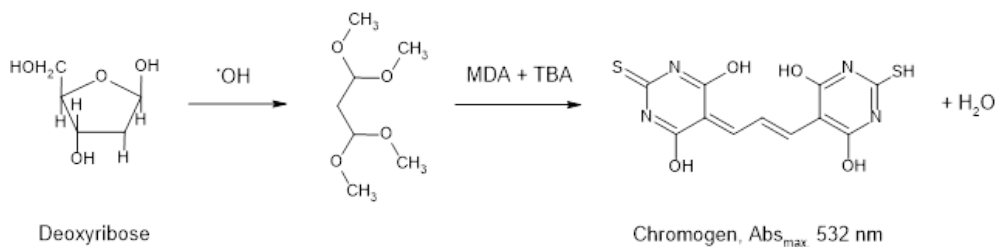
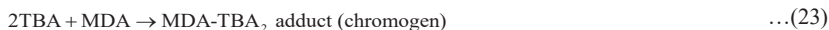


Fig. 3. Mechanism of deoxyribose assay.

2.2.2. Aromatic hydroxylation

Hydroxycyclohexadienyl radical, which is formed by the addition of $\cdot\text{OH}$ s to the aromatic ring in the aromatic hydroxylation process, can take part in different radical reactions (Fig. 4). These reactions are: oxidation, reduction, dimerization, dysmutation, dehydration and reaction with O_2 .

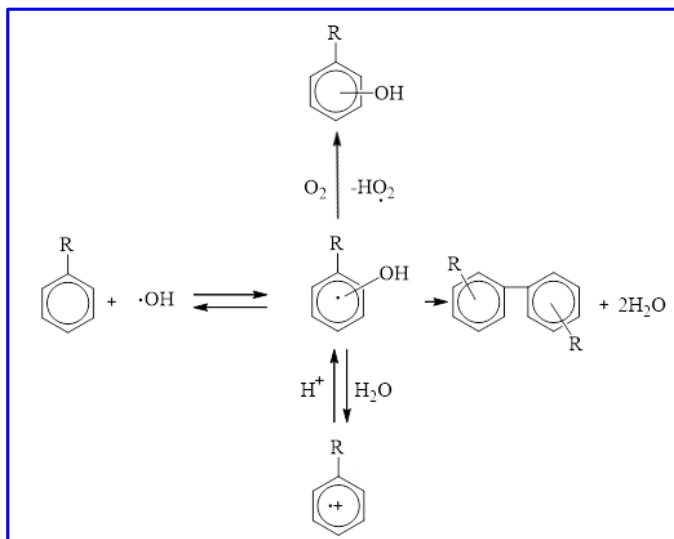


Fig.4. Aromatic hydroxylation [11].

3. SUPEROXIDE ANION RADICAL

3.1. Formation of $O_2^{\bullet-}$ (*in vitro*)

3.1.1. Radiolysis of aqueous solutions



This radiolysis reaction can be generally used by the oncologists to increase in the killing of tumor cells using radiation technique [1].

3.1.2. Ooxidation of metal ions

Many metal ions (Ag^+ , Cd^{2+} , Co^{2+} , and Fe^{2+}) react with O_2 to form the $O_2^{\bullet-}$ [12]. Amongst these metal ions, Fe^{2+} -EDTA and Cu^+ ions are very important in biological systems.



3.1.3. Oxidation of radicals

O_2 reacts with some radicals in two different ways to form the $O_2^{\bullet-}$:

(i) by a direct transfer of e or

(ii) as an intermediate product $O_2^{\bullet-}$ during the formation of the peroxy radical (ROO^{\bullet}).

These radicals undergo secondary reactions such as lipid peroxidation, which are of particular biological importance. The most important source of $O_2^{\bullet-}$ in organisms is the oxidation of semiquinon-type radicals (Fig.5) and this reaction in the electron transfer chain occurs in the mitochondria [13].

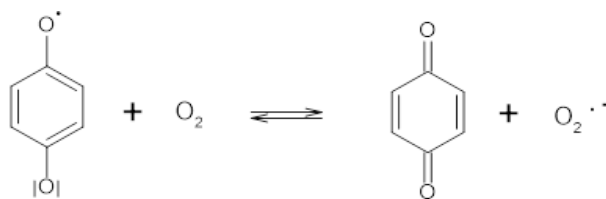
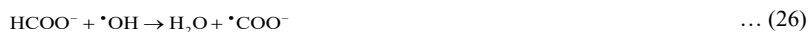


Fig.5. Oxidation of semiquinon-type radicals.

The formation of $O_2^{\bullet-}$ is not important only in normal metabolism, but also in the certain xenobiotics metabolism of (drugs such as adriamycin and mitomycin C, *etc.*) from systems containing a quinone ring. This type of many reactions have been used in pulse radiolysis. The

format radical ($\bullet\text{COO}^-$) is also used as a one-electron donor. This anionic radical can be formed by radiolysis of aqueous formate solution (Eq.s 26,27) [1].



Another radically toxic herbicide of biological importance and capable of giving an electron to O_2 is the paraquat cationic radical (1,1'-dimethyl-4,4'-bipyridylium: $\text{PQ}^{\bullet+}$) [14]:

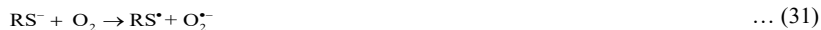


3.1.4. Oxidation of organics

Polyhydroxyaromatics (pirogallol, 6-hydroxydopamine:HODA *etc.*) can easily react with O_2 by donating their H-atoms [15,16]. The first step in these reactions is the oxidation of the semiquinone radical ($\text{SQ}\bullet$). HODA can spontaneously react with O_2 , but this autooxidation reaction is inhibited by superoxide dismutase (SOD). HODA, causes selective degeneration of nerve terminals in the central nervous system.



As a result of the autooxidation of thiols (RS^-), $\text{O}_2^{\bullet-}$ are formed [17].



Another method of forming the $\text{O}_2^{\bullet-}$ is the autooxidation of TBHQ [18].



3.1.5. Reaction with singlet oxygen

$\text{O}_2^{\bullet-}$ was formed as a result of oxidation of electron-rich compounds (tetramethylphenylenediamine:TMPD) with singlet oxygen ($^1\text{O}_2$) [19].



3.1.6. Enzymatic formation by the X-XO system

The xanthine-xanthine oxidase (X-XO) is one of the most widely used methods of producing $\text{O}_2^{\bullet-}$. In the X-XO reaction (Fig.6), O_2 acts as an electron acceptor, and as a result of the reaction, $\text{O}_2^{\bullet-}$ and H_2O_2 are slowly formed in the second step.

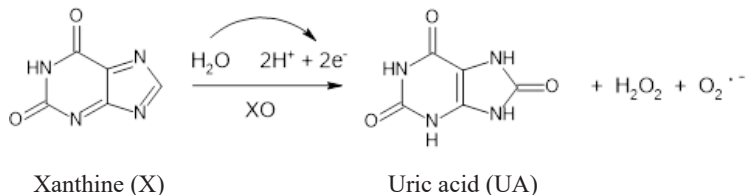
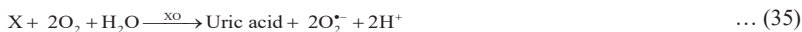
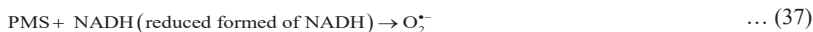


Fig.6. Enzymatic formation $O_2^{\bullet-}$ by the X-XO system.

3.1.7. Formation by the PMS-NADH system

The phenazine metasulfate-nicotinamide dinucleotide (PMS-NADH) method, which is a method of producing $O_2^{\bullet-}$ by a non-magnetic way (which does not contain enzyme inhibition that can cause interference effect), has a wide range of uses [20].

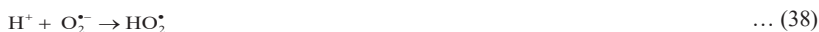


3.2. Reactions of $O_2^{\bullet-}$

3.2.1. Redox and nucleophilic properties

The main chemical properties of the $O_2^{\bullet-}$:

i.) $O_2^{\bullet-}$ has a basic character.



pK_a values of the conjugated acid of $O_2^{\bullet-}$ (HO_2^{\bullet}) is 4.8. Accordingly, at neutral pH, $O_2^{\bullet-}$ is in its non-protonated form.

ii.) $O_2^{\bullet-}$ is a nucleophile.

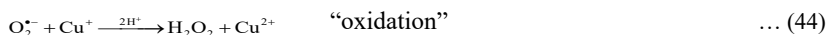


iii.) Due to its radicalic characteristic, it gives the typical reactions of a radical.



$O_2^{\bullet-}$ can act as a reductant or oxidant. An example of the reaction in which $O_2^{\bullet-}$ acts both as a reductant and oxidant is the disproportionation reaction of $O_2^{\bullet-}$ to H_2O and O_2 .



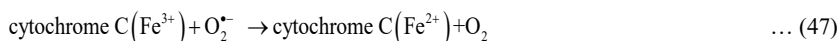


In the Haber-Weiss reaction of iron-catalysis, the reduction of metal ions demonstrates an important step [21] (Eq. 13).

Another examples of $\text{O}_2^{\bullet -}$ reactions are the reduction of methemoglobin (metHb) and oxidation of oxyhemoglobin (HbO_2) [22]:



The reducing property of $\text{O}_2^{\bullet -}$ makes it easier to identify this radical. McCord and Fridovich [23] determined $\text{O}_2^{\bullet -}$ with a change in absorbance, which is formed by milk XO, by the redox reaction between cytochrome C and $\text{O}_2^{\bullet -}$. SOD also inhibits this reaction.



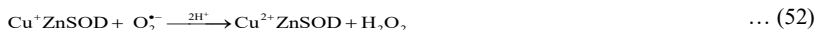
According to Liochev and Fridovich [24], *in vitro* $\text{O}_2^{\bullet -}$ reacts as a reductant (Haber-Weiss reaction in iron-catalysis), while *in vivo* $\text{O}_2^{\bullet -}$ reacts as an oxidant apart from the separation of iron from ferritin with $\text{O}_2^{\bullet -}$.

Due to the basic property of the $\text{O}_2^{\bullet -}$, three different dismutation reactions take place [25]:



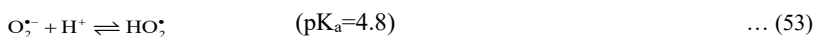
The spontaneous dismutation reaction occurs most rapidly at pH 4.8. The non-protonated form of $\text{O}_2^{\bullet -}$ is very slowly dismuted due to the electrostatic repulsion of 2 negative charges [25]. When the rate constant of the uncatalyzed dismutation reaction is compared with the SOD-catalyzed dismutation reaction, the rate constant of the uncatalyzed dismutation reaction is of the second order and the SOD-catalyzed reaction is of the first order. This result shows that the half-life of SOD-catalyzed reactions is independent of the $\text{O}_2^{\bullet -}$ concentration.

The catalytic dismutation reaction with Cu-ZnSOD occurs in two single-electron transfer steps [26].



3.2.2. Addition of hydrogen to $\text{O}_2^{\bullet-}$

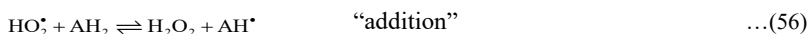
$\text{O}_2^{\bullet-}$ and perhydroxyl radical (HO_2^{\bullet}) exists in equilibrium together and the reactivity of the $\text{O}_2^{\bullet-}$ is largely dependent on pH..



HO_2^{\bullet} acts as an oxidant by abstracting protons from many compounds (catechol, hydroquinone, α -tocopherol, linoleic acid).



It is unlikely that protons will be added directly to $\text{O}_2^{\bullet-}$. Two-step process including addition of protons:



4. HYDROGEN PEROXIDE

4.1. Formation of H_2O_2 (*in vivo*)

In the organism, H_2O_2 is formed as a result of the enzymatic reduction of O_2 by two electrons or by the reactions of enzymatic (SOD) and non-enzymatic dismutation of $\text{O}_2^{\bullet-}$. Reactions to the formation of H_2O_2 in metabolism:



H_2O_2 is not reactive because it does not contain unpaired electrons in its structure. H_2O_2 causes the formation of $\bullet\text{OH}$, which is very reactive in the presence of metal ions such as iron and copper with its oxidizing property (Fenton reaction).

H₂O₂ reacts specifically with iron in proteins to form reactive iron species with high levels of oxidation. Iron in this form has very strong oxidizing properties and can initiate radical reactions such as protein and lipid peroxidation in cell membranes and deterioration of DNA chains. •OH is also formed as a result of the reaction of H₂O₂ with the O₂•⁻ (Haber-Weiss reaction).

Due to its oxidizing properties, H₂O₂ formed in biological systems must be removed from the environment. This removal is carried out by the important antioxidant cellular enzymes such as catalase (CAT) and glutathione peroxidase (GSH-Px). Catalase is an enzyme found in the cells of plants, animals and aerobic bacteria. This enzyme effectively decomposes H₂O₂ into O₂ and H₂O.



4.2. Reactions of H₂O₂

4.2.1. Reaction of H₂O₂ with Cu⁺

Cu(I) is associated with H₂O₂ produce •OH in a similar way to the Fenton reaction (Eq. 14).

Another mechanism involving two-electron transfer is as follows:



Cu_{aq}^{III}, decomposes in H₂O to form the •OH:



4.2.2. Reaction of H₂O₂ with Cu²⁺

Since many transition metals are often present in the high oxidation step (Fe³⁺, Cu²⁺), these metal ions must be reduced before the Fenton reaction in order to act/used as Fenton catalysts.

The cell components such as ascorbic acid, NADPH, NADH, and thiol compounds can perform this reduction *in vivo*. Halliwell *et al.* [27] examined DNA damage caused by the (Fe³⁺-H₂O₂) and (Cu²⁺+H₂O₂) systems in the presence or absence of ascorbic acid. Damage on the basis of DNA was assessed by measuring typical hydroxylation products such as thymine/cytosine glycol, 8-hydroxyguanine and 8-hydroxyadenine. It reacts with ascorbic acid and H₂O₂ to form an •OH, resulting in •OHs attack DNA site-specific.



Oxygen paradox; It is due to the fact that aerobic organisms cannot do without O₂, and at the same time, O₂ is a reactive species. Major members of ROS (\bullet OH, O₂ \bullet^- and H₂O₂) that inevitably occur as a result of the donation of electrons to O₂ from various substrates in the respiratory chain are responsible for O₂ toxicity. Because these species attack target molecules (DNA, proteins, lipids *etc.*) in the cell. Recently, the importance of preventing damage to biological macromolecules by ROS in living organisms has been better recognized. In this sense, the formation of these major ROS species and their *in vivo* and *in vitro* reactions need to be well examined.

REFERENCES

- [1] I.G. Draganic, Z.D. Draganic. The radiation chemistry of water, Academic Press, New York, 1979.
- [2] A. Naqui, B. Chance, E. Cadenas. Reactive oxygen intermediates in biochemistry, Annual Review of Biochemistry, 55 (1986) 137–166.
- [3] E. Choe, D.B. Min. Chemistry and reactions of reactive oxygen species in foods, Journal of Food Science, 70 (2005) 142–159.
- [4] B. Halliwell, J.M.C. Gutteridge. Free radicals in biology and medicine. 3rd ed. New York: Oxford Univ. Press, 2001.
- [5] D.B. Min, J.M. Boff. Lipid oxidation of edible oil. In: Akoh CC, Min DB, editors. Food lipids. 2nd editors. New York: Marcel Dekker. (2002) 335–64.
- [6] S. Matsugo, J. Saito. Photochemical cleavage of N- (hydroperoxyalkyl) phthalimides by intramolecular energy transfer, Tetrahedron Letters, 32 (1991) 2949–2950.
- [7] M.K. Eberhardt, G. Ramirez, E. Ayala. Does the reaction of Cu⁺ with H₂O₂ give OH radicals? A study of aromatic hydroxylation, Journal of Organic Chemistry, 54 (1989) 5922–5926.
- [8] B. Zhu, N. Kitrossky, M. Chevion. Evidence for production of hydroxyl radicals by pentachlorophenol metabolites and hydrogen peroxide: A metal – independent organic Fenton reaction, Biochemical and Biophysical Research Communications, 270 (2000) 942–946.
- [9] B. Halliwell, J.M.C. Gutteridge. Formation of a thiobarbituric-acid-reactive substance from deoxyribose in the presence of iron salts. The role of superoxide and hydroxyl radicals, FEBS Letters, 128 (1981) 347–352.
- [10] C.C. Winterbourn, H.C. Sutton. Iron and xanthine oxidase catalyze formation of an oxidant species distinguishable from OH: comparison with the Haber-Weiss reaction, Archives of Biochemistry and Biophysics, 244 (1986) 27–34.
- [11] M.K. Eberhardt. Homolytic aromatic hydroxylations via radiolysis of aqueous solutions and via metal ion - oxygen systems, Reviews Heteroatom Chemistry, 4 (1991) 1-26.
- [12] R.M. Sellers, M.G. Simic. Pulse radiolysis study of the reactions of some reduced metal ions with molecular oxygen in aqueous solution, Journal of American Chemical Society, 98 (1976) 6145–6150.

- [13] Y.A. Ilan, G. Czapski, D. Meisel. The one-electron transfer redox potentials of free radicals. I. The oxygen/superoxide system, *Biochimica et Biophysica Acta*, 430 (1976) 209–224.
- [14] J.A. Farrington, M. Ebert, E.J. Land, K. Fletcher, Bipyridilium quaternary salts and related compounds. V. Pulse radiolysis studies of the reaction of paraquat radical with oxygen. Implications for the mode of action of bipyridil herbicides, *Biochimica et Biophysica Acta*, 314 (1973) 372–381.
- [15] S. Marklund, G. Marklund. Involvement of the superoxide anion radical in the autoxidation of pyrogallol and a convenient assay for superoxide dismutase, *European Journal of Biochemistry*, 47 (1974) 469–474.
- [16] R.E. Heikkila, G. Cohen. 6-Hydroxydopamine: evidence for superoxide radical as an oxidative intermediate, *Science*, 181 (1973) 456–457.
- [17] H.P. Misra. Generation of superoxide free radical during the autoxidation of thiols, *Journal of Biological Chemistry*, 249 (1974) 2151–2155.
- [18] B. Bergmann, J.K. Dohrman, R. Kahl. Formation of the semiquinone anion radical from tert-butylquinone and from tert-butylhydroquinone in rat liver microsomes, *Toxicology*, 74 (1992) 127–133.
- [19] I. Saito, T. Matsuura. Formation of superoxide ion via oneelectron transfer from organic electrondonors to singlet oxygen, in *Oxygen Radicals in Chemistry and Biology*, W. Bors, M. Saran, and D. Tait, eds., Walter de Gruyter, Berlin 1984, p. 535.
- [20] J. Robak, R.J. Grylewski. Flavonoids are scavengers of superoxide anions, *Biochemical Pharmacology*, 37 (1988) 837–841.
- [21] J.D. Rush, B.H.J. Bielski. Pulse radiolytic study of the reaction of perhydroxyl/superoxide $O_2^{\cdot-}$ with iron(II) iron(III) ions. The reactivity of $HO_2^{\cdot}/O_2^{\cdot-}$ with ferric ions and its implications on the occurrence of the Haber-Weiss reaction, *Journal of Physical Chemistry*, 89 (1985) 5062–5066.
- [22] H.C. Sutton, P.B. Roberts, C.C. Winterbourn. The rate of reaction of superoxide radical ion with oxyhemoglobin and methemoglobin, *Biochemical Journal*, 155 (1976) 503–510.
- [23] J.M. Mccord, I. Fridovich. The reduction of cytochrome c by milk xanthine oxidase, *Journal of Biological Chemistry*, 243 (1968) 5753–5760.
- [24] S.I. Liochev, I. Fridovich. The role of $O_2^{\cdot-}$ in the production of $\bullet OH$: in vitro and in vivo, *Free Radical Biology & Medicine*, 16 (1994) 29–33.
- [25] B.H.J. Bielski, A.O. Allen. Mechanism of the disproportionation of superoxide radicals, *Journal of Physical Chemistry*, 81 (1977) 1048–1050.
- [26] E.M. Fielden, P.B. Roberts, R.C. Bray, D.J. Lowe, G.N. Mautner, G. Rotilio, L. Calabrese. Mechanism of action of superoxide dismutase from pulse radiolysis and electron paramagnetic resonance. Evidence that only half the active site functions in catalysis, *Biochemical Journal*, 139 (1974) 49–60.
- [27] B. Halliwell, O.I. Aruoma. DNA damage by oxygen-derived species: its mechanisms and measurement in mammalian systems, *FEBS Letters*, 281 (1991) 9–19.

Bimultipliers of R-algebroids

Gizem Kahrıman ^{*1}

ABSTRACT. In this paper we give generalization of the notion of the bimultiplication algebra by defining multipliers of an R-algebroid. Firstly we introduce the set denoted with $Bim(M)$, bimultipliers of an R-algebroid M , then we prove that this set is an R-algebroid called multiplication R-algebroid by defining operations on this set. By using this multiplication R-algebroid $Bim(M)$, for an R-algebroid morphism $A \rightarrow Bim(M)$, we obtain that this morphism gives the R-algebroid action. Then we examine some of the properties associated with this action.

KEYWORDS: R-Algebroid, Bimultiplier

1. INTRODUCTION

In group theory, it is well known that the action of a group on another group is determined by the automorphism group. The action of a group A on a group B is given by the homomorphism $A \rightarrow Aut(B)$. Any extension of group A and group B is also related to a homomorphism $A \rightarrow Aut(B)$. In algebra case, the action of an algebra on another is related to the multiplication algebra. In algebraic extension, the outer product takes place. The concept of multiplication algebra is defined by MacLane S. [1]. In [2], using multiplication algebras, Ege U. and Arvası Z., introduce actor crossed modules of commutative algebras and use it to generalise some aspects from commutative algebras to crossed modules of commutative algebras. [13], [14].

R-algebroids were especially studied by Mitchell in [3, 4, 5] and by Amgott in [6]. Mitchell gave a categorical definition of R-algebroids. Mosa on the other hand, introduced crossed modules of R-algebroids and proved their equivalence to special double algebroids with connections in [7]. Then Akca İ.İ. and Avcıođlu O. studied on crossed modules of R-algebroids in [8], [9],[10], [11] and [12].

In this paper, firstly we introduce the set denoted $Bim(M)$ of multipliers of an R-algebroid M , then we prove that this set is an R-algebroid called multiplication R-algebroid by defining operations on this set. By using this multiplication R-algebroid $Bim(M)$, we define an R-algebroid morphism $A \rightarrow Bim(M)$, and obtain that this morphism gives the R-algebroid action. Then we examine some of the properties associated with this action.

Throughout this paper R will be a fixed commutative ring.

1.1. Preliminaries. Most of the following data can be found in [3, 4, 5].

Definition 1.1. *A category of which each homset has an R-module structure and of which composition is R-bilinear is called an R-category. A small R-category is called an R-algebroid. Moreover, if we omit the axiom of the existence of identities from an R-algebroid structure then the remaining structure is called a pre-R-algebroid.*

Note that every R-algebroid is a pre-R-algebroid and every R-algebra is an R-algebroid with one object.

Remark 1. *Throughout this paper for any pre-R-algebroid A we adopt the following notational assumptions:*

1: $Ob(A)(= A_0)$ and $Mor(A)$ are the object and morphism sets of A , respectively, and A is said to be over A_0 .

2: $s, t : Mor(A) \rightarrow A_0$ are the source and target functions. Thus, s_a and t_a are the source and target of each $a \in Mor(A)$, respectively, and a is said to be from s_a to t_a .

3: $a \in A$ means that $a \in Mor(A)$ and if $a, a' \in A$ with, of all morphisms from x to y is denoted by $A(x, y)$.

4: The zero morphism of any homset $A(x, y)$ is denoted by $0_{A(x,y)}$, or only by 0 if there is no ambiguity.

5: The identity morphism on any $x \in A_0$, if exists, is denoted by 1_x , or only by 1 if there is no ambiguity.

Definition 1.2. An R -linear functor between two R -categories is called an R -functor and an R -functor between two R -algebroids is called an R -algebroid morphism. Moreover, an assignment between two pre- R -algebroids satisfying all axioms of an R -functor except for the identity preservation axiom is called a pre- R -algebroid morphism.

Definition 1.3. Let A be a pre- R -algebroid and $I = \{I(x; y) \subset A(x; y) : x, y \in A_0\}$ be a family of R -submodules. If $ab, ba' \in I$ for all $b \in I$, $a, a' \in A$ with $ta = sb, tb = sa'$ then I is called a two-sided ideal of A .

Definition 1.4. Let A and N be two pre- R -algebroids with the same object set A_0 . A family of maps defined for all $x, y, z \in A_0$ as

$$\begin{array}{ccc} N(x, y) \times A(y, z) & \longrightarrow & N(x, z) \\ (n, a) & \mapsto & n^a \end{array}$$

is called a right action of A on N if the conditions

1. $n^{a_1+a_2} = n^{a_1} + n^{a_2}$
2. $(n_1 + n_2)^a = n_1^a + n_2^a$
3. $(n^a)^{a'} = n^{aa'}$
4. $(n'n) = n'n^a$
5. $r \cdot n^a = (r \cdot n)^a = n^{r \cdot a}$

and the condition $n^{1_{tn}} = n$, whenever 1_{tn} exists, are satisfied for all $r \in R$, $a, a', a_1, a_2 \in A$, $n, n', n_1, n_2 \in N$ with compatible sources and targets.

A left action of A on N is defined similarly, only with a side difference. Moreover, if A has a right and a left action on N and if $({}^a n)^{a'} = {}^a(n^{a'})$ for all $n \in N, a, a' \in A$ with $ta = sn, tn = sa'$ then A is said to have an associative action on N or to act on N associatively.

Corollary 1.5. Given two pre- R -algebroids A and N with the same object set

- i. if A has a left action on N then ${}^0_{A(x, sn)} n = 0_{A(x, tn)}$ and ${}^{-a} n = {}^a(-n) = -{}^a n$,
- ii. if A has a right action on N then $n^{0_{A(tn, y)}} = 0_{A(sn, y)}$ and $n^{-a'} = (-n)^{a'} = -n^{a'}$ for all $n \in N, a, a' \in A, x, y \in A_0$ with $ta = sn, tn = sa'$.

Definition 1.6. Let M is an R -Algebroid, for all $m, m', m'' \in M$, with $t(m) = s(m')$ and $t(m'') = s(m)$

$$\text{Ann}_M M = \{m \in M : mm' = 0, m''m = 0, m', m'' \in M\}$$

is called Annihilator of M R -Algebroid.

Definition 1.7. [7] Let A, M be R -Algebroids with the same object sets and A associative action on M . An R -Algebroid morphism $\eta : M \rightarrow A$ is called crossed module of R -Algebroids if the conditions

$$\begin{array}{l} \text{CM1. } \eta({}^a m) = a\eta(m) \\ \eta(m^{a'}) = \eta(m)a' \\ \text{CM2. } m\eta(m') = mm' = \eta(m) m' \end{array}$$

are satisfied for all $a, a' \in A$, $m, m' \in M$ with $t(a) = s(m)$, $t(m) = s(a') = s(m')$.

2. BIMULTIPLIERS OF AN R -ALGEBROID

In this section, firstly we define the bimultipliers of an R -algebroid M , then we prove that the set of bimultipliers of M is an R -algebroid called multiplication R -algebroid by defining operations on this set. Then by using this multiplication R -algebroid $\text{Bim}(M)$, we define an R -algebroid morphism $A \rightarrow \text{Bim}(M)$, and obtain that this morphism gives the R -algebroid action.

Definition 2.1. Let M is an R -Algebroid and $f, g : M \rightarrow M$ be an R -Linear mappings with identity on object set satisfying the following equations for $m, m' \in M$ with $t(m) = s(m')$,

$$\begin{array}{l} f(mm') = mf(m') \\ g(mm') = g(m)m' \\ f(m)m' = mg(m') \end{array}$$

The pair (f, g) is called bimultipliers of M . Set of all bimultipliers of M are denoted by $\text{Bim}(M)$.

Theorem 2.2. Let $Bim(M)$ be a set of bimultipliers of M . $Bim(M)$ is an R -Algebroid with single object and with the following operations,

$$\begin{aligned}(f, g) + (f', g') &= (f + f', g + g') \\ (f, g) \circ (f', g') &= (f' \circ f, g \circ g') \\ r \cdot (f, g) &= (r \cdot f, r \cdot g)\end{aligned}$$

Proof.

$$\begin{aligned}r \cdot ((f, g) + (f', g')) &= r \cdot (f + f', g + g') \\ &= (r \cdot f + r \cdot f', r \cdot g + r \cdot g') \\ &= r \cdot (f, g) + r \cdot (f', g') \\ \\(r_1 + r_2) \cdot (f, g) &= ((r_1 + r_2) \cdot f, (r_1 + r_2) \cdot g) \\ &= (r_1 \cdot f + r_2 \cdot f, r_1 \cdot g + r_2 \cdot g) \\ &= (r_1 \cdot f, r_1 \cdot g) + (r_2 \cdot f, r_2 \cdot g) \\ &= r_1 \cdot (f, g) + r_2 \cdot (f, g) \\ \\(r_1 r_2) \cdot (f, g) &= (r_1 r_2 \cdot f, r_1 r_2 \cdot g) \\ &= r_1 (r_2 \cdot f, r_2 \cdot g) \\ &= r_1 \cdot (r_2 \cdot (f, g)) \\ \\r \cdot (f, g) \circ (f', g') &= (r \cdot f, r \cdot g) \circ (f', g') \\ &= ((r \cdot f') \circ f, (r \cdot g) \circ g') \\ &= (r \cdot (f' \circ f), r \cdot (g \circ g')) \\ &= r \cdot (f' \circ f, g \circ g') \\ &= r \cdot ((f, g) \circ (f', g')) \\ \\(f, g) \circ r \cdot (f', g') &= (f, g) \circ (r \cdot f', r \cdot g') \\ &= ((r \cdot f') \circ f, g \circ (r \cdot g')) \\ &= (r \cdot (f' \circ f), r \cdot (g \circ g')) \\ &= r \cdot (f' \circ f, g \circ g') \\ &= r \cdot ((f, g) \circ (f' \circ g'))\end{aligned}$$

□

In the case of groups, description of an action is provided by the automorphism group. The action of any group A on itself is given by a homomorphism $A \rightarrow AutA$. In some other algebraic context, automorphism structure is not enough to give an action. The set of automorphisms of an algebra is not usually an algebra. For commutative algebra case is examined by Arvasi Z. and Ege U. [2]. For associative algebra case, bimultiplication algebra $Bim(M)$ of an associative algebra M which is defined by MacLane S. [1] accomplishes role of automorphism group.

Definition 2.3. Let A and M be R -Algebroids with same object we define the set

$$M \underset{t \times s}{\overset{a}{\times}} M = \{(m, m') \in M \times M : t(m) = s(a), t(a) = s(m')\}$$

for an $a \in A$.

Theorem 2.4. Let A and M be R -Algebroids with same object set and $Ann(M) = 0$ or $M^2 = M$. For the maps

$$\begin{aligned}f_a : M &\rightarrow M \\ m &\mapsto f_a(m) = m^a\end{aligned}$$

and

$$\begin{aligned}g_a : M &\rightarrow M \\ m' &\mapsto g_a(m') = {}^a m'\end{aligned}$$

for an $a \in A$ with $(m, m') \in M \underset{t \times s}{\overset{a}{\times}} M$, let $(f_a, g_a) \in Bim(M)$. Then the R -Algebroid morphism

$$\begin{aligned}\phi : A &\rightarrow Bim(M) \\ a &\mapsto \phi(a) = \phi_a = (f_a, g_a)\end{aligned}$$

gives an R -Algebroid action of A on M .

Proof. (i) Since ϕ is an R-algebroid homomorphism, then

$$r \cdot \phi(a) = \phi(r \cdot a) \Rightarrow r \cdot \phi(a) = \phi(r \cdot a)$$

for $a \in A$ and

$$\begin{aligned} r \cdot \phi_a(m, m') &= r \cdot (f_a, g_a)(m, m') \\ &= r \cdot (f_a(m), g_a(m')) \\ &= (r \cdot f_a(m), r \cdot g_a(m')) \end{aligned}$$

$$\begin{aligned} \phi_{r \cdot a}(m, m') &= (f_{r \cdot a}, g_{r \cdot a})(m, m') \\ &= (f_{r \cdot a}(m), g_{r \cdot a}(m')) \end{aligned}$$

for $(m, m') \in M \overset{a}{\times}_s M$. Therefore we get

$$f_{r \cdot a}(m) = r \cdot f_a(m) \Rightarrow m^{r \cdot a} = r \cdot m^a$$

$$g_{r \cdot a}(m') = r \cdot g_a(m') \Rightarrow m'^{(r \cdot a)} = r \cdot (m'^a) = r \cdot a \cdot m' = r \cdot a \cdot m'.$$

(ii) Since ϕ is an R-Algebroid homomorphism, then

$$\phi(a_1 + a_2) = \phi(a_1) + \phi(a_2) \Rightarrow \phi_{a_1+a_2} = \phi_{a_1} + \phi_{a_2}$$

for $a_1, a_2 \in A$ with $s(a_1) = s(a_2), t(a_1) = t(a_2)$ and

$$\begin{aligned} \phi_{a_1+a_2}(m, m') &= (f_{(a_1+a_2)}, g_{(a_1+a_2)})(m, m') \\ \phi_{a_1}(m, m') + \phi_{a_2}(m, m') &= (f_{a_1}(m), g_{a_1}(m')) + (f_{a_2}(m), g_{a_2}(m')) \\ &= (f_{a_1}(m) + f_{a_2}(m), g_{a_1}(m') + g_{a_2}(m')) \end{aligned}$$

for $(m, m') \in M \overset{a}{\times}_s M$.

Therefore we get

$$\begin{aligned} f_{a_1+a_2}(m) &= f_{a_1}(m) + f_{a_2}(m) \Rightarrow m^{a_1+a_2} = m^{a_1} + m^{a_2} \\ g_{a_1+a_2}(m') &= g_{a_1}(m') + g_{a_2}(m') \Rightarrow m'^{a_1+a_2} = m'^{a_1} + m'^{a_2} \end{aligned}$$

(iii) Since $\phi_a = (f_a, g_a) \in \text{Bim}(M)$ for $a \in A$, then,

$$\phi_a((m_1, m'_1) + (m_2, m'_2)) = \phi_a(m_1, m'_1) + \phi_a(m_2, m'_2)$$

and

$$\begin{aligned} \phi_a((m_1, m'_1) + (m_2, m'_2)) &= \phi_a(m_1 + m_2, m'_1 + m'_2) \\ &= (f_a(m_1 + m_2), g_a(m'_1 + m'_2)) \\ &= ((m_1 + m_2)^a, {}^a(m'_1 + m'_2)), \\ \phi_a(m_1, m'_1) + \phi_a(m_2, m'_2) &= (f_a(m_1), g_a(m'_1)) + (f_a(m_2), g_a(m'_2)) \\ &= (m_1^a, {}^a m'_1) + (m_2^a, {}^a m'_2) \\ &= (m_1^a + m_2^a, {}^a m'_1 + {}^a m'_2) \end{aligned}$$

for $(m_1, m'_1), (m_2, m'_2) \in M \overset{a}{\times}_s M, (s(m_1) = s(m_2))$ and $(t(m'_1) = t(m'_2))$ therefore we get

$$(m_1 + m_2)^a = m_1^a + m_2^a$$

and

$${}^a(m'_1 + m'_2) = {}^a m'_1 + {}^a m'_2.$$

(iv) Since $\phi_a = (f_a, g_a) \in \text{Bim}(M)$ for $a \in A$, then

$$\begin{aligned} \phi_a(m_1 m_2, m'_1 m'_2) &= (f_a, g_a)(m_1 m_2, m'_1 m'_2) \\ &= (f_a(m_1 m_2), g_a(m'_1 m'_2)) \\ &= ((m_1 m_2)^a, {}^a(m'_1 m'_2)) \end{aligned}$$

and

$$\begin{aligned} (f_a(m_1 m_2), g_a(m'_1 m'_2)) &= (m_1 f_a(m_2), g_a(m'_1) m'_2) \\ &= (m_1 (m_2^a), ({}^a m'_1) m'_2) \end{aligned}$$

for $(m_1 m_2, m'_1 m'_2) \in M \overset{a}{\times}_s M$ and $t(m_1) = s(m_2), t(m'_1) = s(m'_2)$ therefore we get

$$m_1 m_2^a = m_1 (m_2)^a$$

and

$${}^a m'_1 m'_2 = ({}^a m'_1) m'_2.$$

(v) Since ϕ is an R-Algebroid homomorphism, then

$$\begin{aligned}\phi_{aa'} &= \phi_a \circ \phi_{a'} \\ \phi_{aa'} &= (f_{aa'}, g_{aa'}) \\ \phi_a \circ \phi_{a'} &= (f_a, g_a) \circ (f_{a'}, g_{a'}) \\ &= (f_{a'} \circ f_a, g_a \circ g_{a'})\end{aligned}$$

for $a, a' \in A$ with $t(a) = s(a')$ and

$$\begin{aligned}\phi_{aa'}(m, m') &= (f_{aa'}, g_{aa'})(m, m') \\ &= (f_{aa'}(m), g_{aa'}(m')) \\ &= (m^{aa'}, {}^{aa'}m') \\ (\phi_a \circ \phi_{a'})(m, m') &= (f_{a'} \circ f_a, g_a \circ g_{a'})(m, m') \\ &= ((f_{a'} \circ f_a)(m), (g_a \circ g_{a'})(m')) \\ &= (f_{a'}(f_a(m)), g_a(g_{a'}(m'))) \\ &= (f_{a'}(m^a), g_a({}^a m')) \\ &= ((m^a)^{a'}, {}^{a'}(m'))\end{aligned}$$

for $(m, m') \in M_{t \times_s}^{aa'} M$, therefore we get $m^{aa'} = (m^a)^{a'}$ and ${}^{aa'}m' = {}^a(m')$.

Thus, $\phi : A \rightarrow \text{Bim}(M)$ R-Algebroid morphism induces an R-Algebroid action of A on M. \square

Definition 2.5. Let A be an R-Algebroid. For an R-Algebroid morphism

$$\begin{aligned}\phi : A &\rightarrow \text{Bim}(A) \\ a &\mapsto \phi(a) = (f_a, g_a)\end{aligned}$$

the pair $(f_a, g_a)(a', a'') = (f_a(a'), g_a(a'')) = (a'a, aa'')$ is called inner bimultipliers of A for $(a', a'') \in A_{t \times_s}^a A$. Set of all bimultipliers of A are denoted by $I(A)$ and $I(A) = \text{Im}(\phi)$.

Theorem 2.6. Let M be an R-Algebroid. The kernel of homomorphism

$$\begin{aligned}\phi : M &\rightarrow \text{Bim}(M) \\ m &\mapsto \phi(m) = (f_m, g_m)\end{aligned}$$

is Annihilator of M .

Proof. The annihilator of M is

$$\text{Ann}_M(M) = \{m \in M : f_m(m') = m'm = 0, g_m(m'') = m''m = 0, m', m'' \in M\}.$$

$$\begin{aligned}f_{m_1 m_2}(m') &= m'(m_1 m_2) \\ &= (m' m_1) m_2 \\ &= f_{m_2}(m' m_1) \\ &= f_{m_2}(f_{m_1}(m')) \\ &= (f_{m_2} \circ f_{m_1})(m') \\ g_{m_1 m_2}(m'') &= (m_1 m_2)(m'') \\ &= m_1(m_2 m'') \\ &= g_{m_1}(m_2 m'') \\ &= g_{m_1}(g_{m_2}(m'')) \\ &= (g_{m_1} \circ g_{m_2})(m'')\end{aligned}$$

and

$$\begin{aligned}\phi_{m_1 m_2} &= (f_{m_1 m_2}, g_{m_1 m_2}) \\ &= (f_{m_2} \circ f_{m_1}, g_{m_1} \circ g_{m_2}) \\ &= (f_{m_1}, g_{m_1}) \circ (f_{m_2}, g_{m_2}) \\ &= (\phi_{m_1} \circ \phi_{m_2})\end{aligned}$$

for $(m', m'') \in M_{t \times_s}^{m_1 m_2} M$. Also

$$m \in \text{Ker}\phi \Leftrightarrow \phi_m = (f_m, g_m) = (\mathbf{0}, \mathbf{0})$$

and

$$f_m(m') = \mathbf{0}, g_m(m'') = \mathbf{0} \Leftrightarrow m'm = 0, mm'' = 0 \Leftrightarrow m \in \text{Ann}_M(M)$$

for $(m', m'') \in M_{t \times_s}^m M$. Thus $\text{Ker}\phi = \text{Ann}_M(M)$.

□

Theorem 2.7. Let $I(M)$ be image of $\phi : M \rightarrow Bim(M)$ algebroid homomorphism. $I(M)$ is ideal of $Bim(M)$.

Proof. For $(f_m, g_m) \in I(M)$ and $(f', g') \in Bim(M)$ and $(m', m'') \in M \overset{m}{t} \times_s M$.

$$\begin{aligned}
 I(M) \times Bim(M) &\rightarrow I(M) \\
 ((f_m, g_m), (f', g')) &\mapsto ((f_m, g_m) \circ (f', g')) = ((f' \circ f_m), (g_m \circ g')) \\
 f' f_m(m') &= f'(m' m) \\
 &= m' f'(m) \\
 &= f_{f'(m)}(m') \\
 g_m g'(m'') &= m g'(m'') \\
 &= f_{g'(m'')}(m)
 \end{aligned}$$

and

$$\begin{aligned}
 Bim(M) \times I(M) &\rightarrow I(M) \\
 ((f', g'), (f_m, g_m)) &\mapsto ((f', g') \circ (f_m, g_m)) = ((f_m \circ f'), (g' \circ g_m)) \\
 f_m f'(m') &= f'(m') m \\
 &= g_{f'(m')}(m) \\
 g' g_m(m'') &= g'(m m'') \\
 &= g'(m) m'' \\
 &= g_{g'(m)}(m'')
 \end{aligned}$$

Thus $I(M)$ is ideal of $Bim(M)$.

□

Definition 2.8. Let $I(M)$ be ideal of $Bim(M)$ algebroid,

$$O(M) = Bim(M)/I(M)$$

division algebroid is called the outer multiplication of M algebroid and denoted by $O(M)$.

REFERENCES

- [1] S. Mac Lane , *Extensions and Obstructures for Rings*, *Illinois J. Math.*, 121 , 316-345, 1958
- [2] Z. Arvasi and U. Ege , *Anihilators, Multipliers and Crossed Modules*, *Applied Categorical Structures*, 11:487-506, 2003.
- [3] B. Mitchell , Rings with several objects, *Advances in Mathematics*, 8(1), 1-161, 1972.
- [4] B. Mitchell , *Some applications of module theory to functor categories*, *Bull. Amer. Math. Soc.*, 84, 867-885 , 1978.
- [5] B. Mitchell , *Separable algebroids*, *Mem. Amer. Math. Soc.*, 57, 333, 96 pp (1985).
- [6] Amgott S. M., Separable categories, *Journal of Pure and Applied Algebra*, 40, 1-14 (1986).
- [7] Mosa G.H., Higher dimensional algebroids and crossed complexes, *PhD Thesis, University College of North Wales*, Bangor (1986).
- [8] Avcioglu O., Akça I.I., Coproduct of Crossed A-Modules of R-algebroids, *Topological Algebra and its Applications*, 5, 37-48 (2017).
- [9] Avcioglu O., Akça I.I., Free modules and crossed modules of R-algebroids, *Turkish Journal of Mathematics*, (2018) 42: 2863-2875.
- [10] Avcioglu O., Akça I.I., On generators of Peiffer ideal of a pre-R-algebroid in a precrossed module and applications, *NTMSCI* 5, No. 4, 148-155 (2017).
- [11] Avcioglu O., Akça I.I., On Pullback and Induced Crossed Modules of R-Algebroids, *Commun.Fac.Sci.Univ.Ank.Series A1*, Volume 66, Number 2, Pages 225-242 (2017).
- [12] Akca I.I., Avcioglu O.,Equivalence between (pre)cat¹-R-algebroids and (pre) crossed modules of R-algebroids, *Bull. Math. Soc. Sci. Math. Roumanie Teme* (110) No-3, 2022,267-288.
- [13] Ege Arslan U., Hurmetli S. Bimultiplications and Annihilators of Crossed Modules in Associative Algebras, *Journal of New Theory* 2021.
- [14] Ege Arslan U., On the Actions of Associative Algebras, *Innovative Research in Natural Science and Mathematics*, ISBN:978-625-6507-13-5, 1-15.